Transcriptome profiling of syncytia induced by the beet cyst nematode *Heterodera schachtii* in Arabidopsis roots

A model system to study plant-nematode interactions at a global view

Dissertation

submitted by Mag. rer.nat. Dagmar Elisabeth SZAKASITS

Vienna, December 2009

Supervisor: Priv.-Doz. Dr. Holger Bohlmann

Institute of Plant Protection,

Department of Applied Plant Sciences and Plant Biotechnology (DAPP)

Universität für Bodenkultur Wien

University of Natural Resources and Applied Life Sciences

Vienna, Austria

Acknowledgments

I would like to express my gratitude to my advisor Holger Bohlmann for his support and guidance throughout the work on our nematode project at BOKU.
And I am thankful to all colleagues at the Institute of Plant Protection for their assistance regarding theoretical and practical issues of daily work, especially to Shahid.
My profound thanks to my family and friends for their encouragement to go for this research and their support throughout it.
Last but not least, I am grateful to my friends and co-workers at my current working place for their patience and aid to complete my degree.

The studies were financially supported by grants (NO-NEMA) from the European Union, FWF grants and funding by the Vienna Science and Technology Fund (WWTF), the Austrian Centre of Biopharmaceutical Technology (ACBT), Austrian Research Centres (ARC) Seibersdorf, Baxter AG and Higher Education Commission Pakistan (HEC).

Abstract

Plant-parasitic nematodes are obligate biotrophic pathogens. Their devastating effects on a variety of crop plants cause major economic impacts worldwide. Sedentary endoparasites such as cyst nematodes from the genera *Globodera* and *Heterodera* have evolved very specialized and complex feeding relationships with their hosts. They invade roots as vermiform second-stage juveniles hatched from protective cysts sustaining in the soil and induce the formation of specific feeding cells that become their permanent source of nutrients during all their sedentary stages. To date our knowledge about the processes of feeding cell formation and function is still limited.

For a plant-based approach we therefore used the model plant Arabidopsis as an ideal host for the economically important beet cyst nematode *H. schachtii* to investigate the complex changes at a global view via transcriptome analysis using the Arabidopsis ATH1 GeneChip. We employed microaspiration to harvest pure material from the induced feeding site that starts from a single cell within the vascular cylinder and grows by incorporation of adjacent cells into an enlarged, multicellular syncytium, thereby undergoing drastic morphological and ultrastructural changes. Our analysis showed that between 5 and 15 days after infection the gene expression profile did not differ greatly. However, the combined syncytial tissue (both times points) compared to uninfected control roots revealed that 34.2 % out of a total of 21,138 Arabidopsis genes are differentially expressed, comprising almost balanced portions of up- (18.4 %) and downregulated (15.8 %) genes. Gene ontology analyses showed that genes belonging to categories related to metabolic activity were preferentially upregulated in syncytia. In a principal component analysis we included chip data available from several other root tissues and organs of Arabidopsis. It demonstrated that both transcriptomes of the syncytia are clearly distinct from all other organs including the root.

As the syncytial cell wall undergoes dramatic changes during syncytium formation, we examined the involvement of two entire Arabidopsis gene families coding for cell wall modifying proteins and enzymes in more detail by including several further techniques. Within the expansin and endo-1,4-β-glucanase gene family each two usually shoot-specifically expressed genes are significantly induced in syncytia and

are supposed to play a functional role in cell wall assembly and disassembly processes; i.e. *AtEXPA3* and *AtEXPA1* and *AtCel2* and *KOR3,* respectively.

Two of the most strongly upregulated genes belong to the *MIOX* gene family that are usually pollen-specific. A nematode development assay hinted also towards their important role during syncytium development.

For an efficient production of transgenic plants, we constructed an improved binary *Agrobacterium* vector termed pPZP3425. It derives from the widely used pPZP111 and includes a *gus* gene driven by a strong constitutive promoter and thus can be used for multiple cloning purposes that might help to engineer nematode resistant plants.

Kurzfassung

Pflanzenparasitäre Nematoden (Fadenwürmer) sind obligate biotrophe Pathogene. Sie richten verheerende Schäden an einer Vielfalt von Pflanzen an und verursachen weltweit große ökonomische Verluste. Sedentäre Endoparasiten wie z.b. zystenformende Nematoden der Gattungen *Globodera* und *Heterodera* haben sehr spezialisierte und komplexe Beziehungen zu ihren Wirtspflanzen entwickelt. Die wurmförmigen Larven schlüpfen aus Cysten, die als schützende Hülle in der Erde überdauern, dringen in die Wurzeln ein und induzieren die Bildung von spezifischen Nährzellen. Diese dienen ihnen während aller sedentären Entwicklungsstadien als permanente Nahrungsquelle. Unser Wissen über die der Nährzellenausbildung zugrunde liegenden Prozesse und bezüglich Bekämpfungsmaßnahmen ist immer noch relativ beschränkt.

Daher wurde ein pflanzenseitiger Untersuchungsansatz gewählt, in dem die Modellpflanze Arabidopsis, die eine ideale Wirtspflanze für den wirtschaftlich bedeutenden Rübenzystennematoden *H. schachtii* darstellt, herangezogen, um anhand dieses Modell-Systems die komplexen Veränderungen auf Transkriptom-Ebene zu analysieren. Dazu wurden die aktuellen GeneChips ATH1 der Firma Affymetrix verwendet. Es wurde Mikroaspiration angewandt, um möglichst reines Untersuchungsmaterial von der Infektionsstelle zu gewinnen, welche ausgehend von einer einzelnen Zelle innerhalb des Zentralzylinders durch Eingliederung von benachbarten Zellen wächst. So entsteht ein multizelluläres Synzytium, das drastische morphologische und ultrastrukturelle Veränderungen erfährt. Unsere Analyse zeigte, dass sich die Expressionsprofile von 5 und 15 Tage alten Synzytien nicht stark unterscheiden. Ein Vergleich zwischen Kontrollwurzeln und Synzytien von beiden Infektionszeitpunkten zusammen genommen hat allerdings offen gelegt, dass 34.2 % der insgesamt 21,138 Arabidopsis Gene unterschiedlich exprimiert sind, wobei etwa die eine Hälfte der Gene signifikant aufreguliert (18.4 %) war und die andere abreguliert (15.8 %). Genontologische Analysen haben gezeigt, dass Gene aus Kategorien, die hinsichtlich Metabolismus relevant sind, in Synzytien präferentiell aufreguliert sind. Eine principal component analysis, auch Hauptkomponenten-Analyse genannt, in welcher auch Chip-Daten von diversen anderen Wurzelgeweben und Organen von Arabidopsis integriert wurden, hat gezeigt, dass sich die beiden

Transcriptome der Synzytien klar von denen aller anderen Organe und Wurzelproben unterscheiden.

Da die Zellwand drastischen Veränderungen während der Synzytienbildung unterworfen ist, wurden zwei Genfamilien, die für zellwandmodifizierende Proteine und Enzyme codieren, unter Hinzunahme weiterer Techniken detailierteren Untersuchungen unterzogen. Innerhalb der Familien der Expansine und der Endo-1,4-β-Glukanasen wurden je zwei synzytial induzierte Gene entdeckt, die normalerweise nur sproßspezifisch exprimiert werden und möglicherweise eine funktionale Rolle bei zellwandaufbauenden- und -abbauenden Prozessen spielen; u.zw. die beiden Expansin-Gene *AtEXPA3* und *AtEXPA1* sowie die Glukanasen-Gene *AtCel2* und *KOR3.*

Zwei der am stärksten aufregulierten Gene gehören zur *MIOX* Genfamilie, welche normalerweise pollenspezifisch exprimiert werden. Ähnlich wie bei den Glukanasen wurden auch hier erste Hinweise auf eine wichtige Rolle bei der Entwicklung von Synzytien gefunden.

Zwecks einer effizienten Produktion von transgenen Pflanzen mittels *Agrobakterium* wurde ein verbesserter binärer Vektor namens pPZP3425 konstruiert. Er leitet sich vom weit verbreiteten pPZP111 ab und beinhaltet ein *gus*-Gen, das von einem starken konstitutiven Promoter gesteuert wird. Er kann daher sowohl zur Überexpression von Genen als auch zur Erzeugung von Promotor:*gus* Fusionen verwendet werden und möglicherweise auch dazu beitragen, nematodenresistente Pflanzen zu erzeugen.

Table of Contents

CHAPTER 1

Introduction

(I) Biological importance of nematodes

(I.A) Nematodes in general

Nematodes, or roundworms, are multicellular unsegmented soft-bodied (pseudocoelomate) worms of the phylum Nematoda (Hodda, 2000; Decraemer and Hunt, 2006). Nematodes are ubiquitous and can be found from the sediment of the oceans to high mountains, in a variety of climates (from tropical to polar regions) in almost every ecological niche (Wyss, 1997; Hodda, 2000). Although previously they all were thought to be very alike *Ascaris*, the best known example of the phylum, research of the last years has shown, that they are more diverse. *Caenorhabditis elegans* is widely used as a model organism in molecular biology. However, their body structure is quite uniform and simple, i.e. their overall morphology and neuroanatomy is significantly conserved (Wyss, 1997; Decraemer and Hunt, 2006). Except a few plant-parasitic species of the order Tylenchida, nematodes are generally vermiform shaped. They are thought to be the most abundant multicellular animals with an estimated species range between 10^6 - 10^8 although only 20,000 nematode species are described (Lewis *et al.*, 2004; Decraemer and Hunt, 2006). Unfortunately, species recognition based on morphological traits is a challenging task, even for nematode professionals, since due to their relatively small size detailed insights require high power light microscopy, while on the other hand only few characters are used to classify the bulk of specimen. Hence, several molecular methods of collecting nucleotide sequence data and generating genetic profiles or molecular barcodes were introduced to assess biodiversity of (terrestrial and marine) nematodes, thereby complementing or partly substituting morphological identification by expert classical taxonomists (Powers, 20004*;* Blaxter *et al.*, 2005).

As nematodes depend on moisture for their locomotion, relative humidity in their environment is generally an essential factor for their survival, however, there are

diverse exceptions of nematodes that can survive in anhydrobiosis (Decraemer and Hunt, 2006).

Nematodes are mainly free-living worms, living as bacteriovores, fungivores or algivore-omnivore-predators in terrestrial and aquatic environments (Blaxter *et al.*, 1998; Williamson and Gleason 2003). Furthermore, there are also parasites of animals, invertebrates as well as vertebrates, including nematode species and humans, where they can cause serious health damage and even human death; well known ancient examples are the intestinal worm *Ascaris lumbricoides* and the guinea worm *Dranunculus medinensis* (Decraemer and Hunt, 2006). Other nematodes are parasitic on plants causing many non-specific above-ground symptoms such as leaf chlorosis and patchy, stunted growth (Webster, 1995) and will be discussed in more detail.

(I.B) Plant-parasitic nematodes

Approximately 4,100 described species (Decraemer and Hunt, 2006) are plant-parasites which can exploit a wide range of crop plants such as potato, tomato and sugar beet as important examples for/in Europe. They have a devastating effect on agricultural production by either causing a direct damage to crops or as virus vectors, thereby causing major economic and social impacts worldwide. The international yield loss has been estimated to exceed 10 % annually, corresponding to US $ 125 billion per year (Sasser and Freckman, 1987).

All plant-parasitic nematodes are obligate biotrophic pathogens, i.e. they require living cells as exclusive nutrient source for which they have evolved diverse feeding strategies (Wyss 1997; Hussey and Grundler, 1998; Gheysen and Fenoll, 2002). The most primitive mode of root parasitism is shown by the migratory ectoparasites that remain outside the root and cause relatively little obvious tissue damage with their protrusible stylet, however, they are more dangerous as vectors of several soilborne viruses; e.g. within the order Dorylaimida several species of the two families Trichodoridae and Longidoridae are exclusively belonging to this functional group (Wyss 1997; Hussey and Grundler, 1998; Gheysen and Fenoll, 2002). Another two main functional groups of plant-parasitic nematodes are the sedentary ectoparasites

and migratory endoparasites, the latter entering the root and thereby extensively destroying the tissue along the migration path (Hussey and Grundler, 1998). Economically most important are the sedentary endoparasitic forms, especially the genera *Heterodera, Globodera* (cyst nematodes) and *Meloidogyne* (root-knot-nematodes) within the family *Heteroderidae* that belong to the order Tylenchida and feed on plant roots. They have very specialized and complex feeding relationships with their host plants, which have been studied intensively since their nurse cell structures are relative large and amenable to microscopy and biochemical and molecular analyses (Tytgat *et al.,* 2000; Bird and Bird, 2001).

For the very cosmopolitan genus *Meloidogyne*, whose species are commonly termed **'root-knot nematode(s)**', more than 2,000 plant species are known to serve as host plants; some agronomically important examples are cereals, cotton and a variety of vegetables such as soybean, potato, tomato, and sugar beet. Root-knot nematodes penetrate the root as second-stage juveniles (J2 or larvae L2) which are attracted to the root tips. After entrance near the elongation zone through continuous head rubbings and the following (mainly) non-destructive intercellular migration, i.e. firstly down towards the root apex and after a turn around towards the differentiation zone, the J2 reaches the differentiating vascular cylinder where it induces a feeding site which consists of several giant cells. These cells become multinucleate by repeated mitoses that lack cytokinesis and are surrounded by cortical and pericycle cells that divide and expand, thereby inducing the formation of 'galls' or 'root knots'. The nematodes grow and become saccate and after moulting three times they develop almost exclusively into female adults that reproduce parthenogenetically and deposit their eggs in gelatinous egg sacs. Despite their wide host range, the induced giant cells are commonly formed from parenchymatic cells in all plant host species. (Wyss, 1997; Hussey and Grundler, 1998; Wyss, 2002; Williamson and Gleason, 2003; **Figure 1**).

Cyst nematodes, establish 'syncytia' as typical feeding sites that are distinct from giant calls. The vermiform J2 of the beet cyst nematode *Heterodera schachtii,* the most intensively studied cyst nematode species mainly infecting sugar beet but also cabbage, cauliflower and cruciferous weeds, hatch in the soil stimulated by root exudates. They invade preferably the elongation zone by piercing cells through

continuous vigorous stylet thrusts that are stimulated by root diffusates. Then they migrate intracellulary upwards to the vascular cylinder, thereby disrupting cortical and endodermal cells by further thrusts with their robust stylet (in contrast to the more delicate stylet of root-nematodes), forming a kind of slit to move through. This destructive behaviour is changed to a more exploratory one, once the vascular cylinder is reached. By careful use of their stylet they search for a suitable cell to turn into the initial syncytial cell (ISC). For the next few (6-8) hours, termed the feeding-preparation period, the stylet remains inside the ISC. Afterwards (after retraction and subsequent re-insertion of its stylet) the J2 begins to feed in repeated cycles and becomes sedentary. The ICS undergoes visible changes, starting with an increased cytoplasmatic streaming and enlargement of the nucleus. After 24 hours, cell walls between the ISC and its hypertrophying neighboring cells are partially dissolved, whereby the protoplasts fuse and a syncytium develops. It continuously grows by incorporation of new cells, while the juvenile continues to withdraw nutrients and undergoes further molts inside the root before developing into one of the two sexual dimorph adult stages.

Developing males have two feeding juvenile stages (J2 and J3) and become bottle-like shaped while growing but become vermiform again upon molting to the last juvenile stage J4. After the final molt to the adult stage they emerge trough the larval cuticles and as free-living male adults they start to search for females in the soil.

In contrast, female juveniles keep taking up nutrients till J4 stage, while they assume a bigger lemon-shaped body due to the rapid growth of the reproductive system. Upon the final molt to the adult stage the female ruptures the root and is accessible for mobile males to mate with and food retrieval is resumed. After fertilization of the female the new nematode generation develops within the eggs inside the female body as far as stage J2. When the females die, their translucent cuticle turns brown, hardens, and forms a protective cyst which contains several hundred embryonated eggs that can remain dormant in the soil for many years until attraction by an appropriate host. Thus, syncytia associated with females remain active all lifetime long providing life-sustaining nutrients, whereas syncytia associated with males become already necrotic after the adult male leaves the root (Wyss, 1997; Wyss, 2002*;* Decraemer and Hunt, 2006; Turnerand Janet, 2006; **Figure 1**).

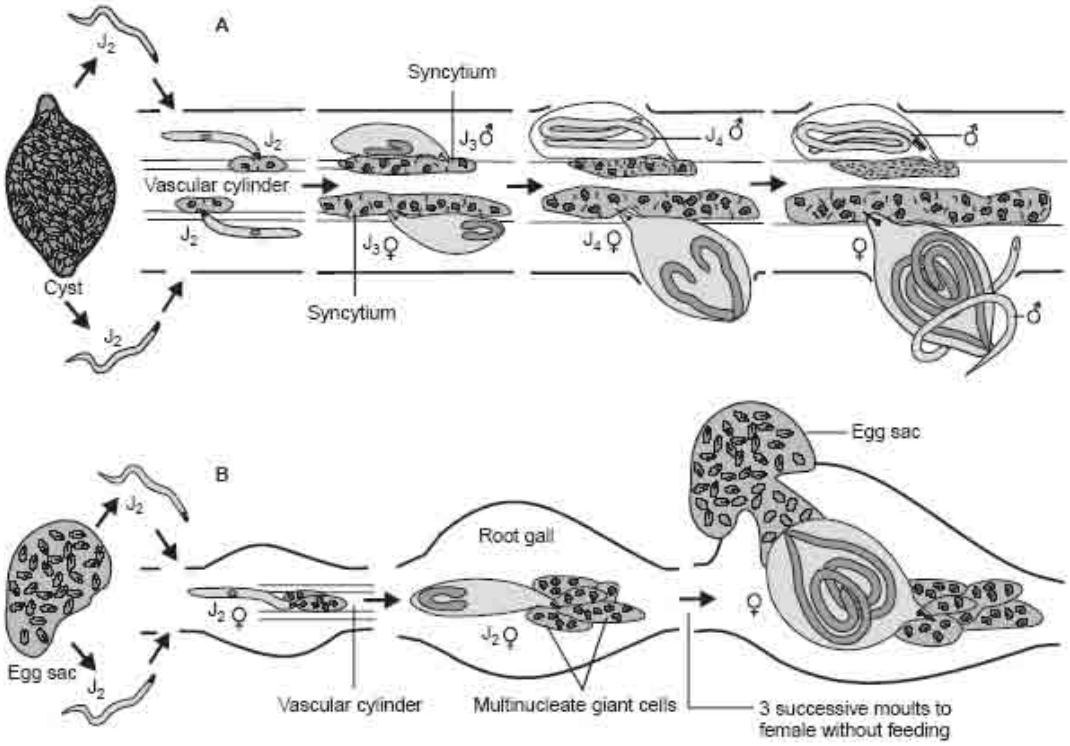

Figure 1: Schematic representation of the life cycles of (A) cyst and (B) root-knot nematodes. J2, J3, J4 are juveniles in the second, third and fourth developmental stages (Jung and Wyss, 1999).

As successful sedentary parasites they necessarily have evolved some refined adaptations enabling them to induce and maintain specialized feeding sites which allow them to feed on until their life cycle can be completed (Burrows, 1992; Hussey and Grundler, 1998). These include a well-developed nervous system and special structures such as a hollow, protrusible stylet in combination with marked morphological and physiological modifications of the pharynx (esophagus). There are three pharyngeal (esophageal) glands, each composed of single large cells producing secretions that are released into the plant tissue through the stylet. They appear to have a crucial role in parasitism, i.e. the two subventral glands are thought to be important for the early stages during invasion and migration and the single dorsal gland for the development and maintenance of the feeding sites, since several proteins and their possible functions could be identified (Jung and Wyss, 1999; Gheysen and Fenoll, 2002; Williamson and Gleason, 2003; Davis *et al.*, 2008). Despite the diverse ontogeny of the two types of multinucleate nematode feeding sites (NFS), i.e. the giant cells of the root-knot nematodes going through acytokinetic mitosis and the syncytium of the cyst nematodes undergoing endoreduplication but

lacking mitosis, the physiological function such as the nutrient supply is supposed to be similar. In order to understand the underlying molecular processes of feeding site induction and development, it helps to use a model system for plant-pathogen interaction that comprises a model nematode and a model host plant.

(I.C) Host cellular responses to cyst nematode parasitism

Arabidopsis thaliana is an ideal host for the cyst nematode *H. schachtii* because the nematode can complete its life cycle on the thin, translucent roots within 5-6 weeks under monoxenic conditions (Sijmons *et al.*, 1991; **Figure 2**) This model system has widely been exploited, for example for observations by means of video enhanced contrast light microscopy.

Figure 2: Infection assay of Arabidopsis roots with *H.* schachtii used as model system. Arabidopsis plants are grown in petri dishes on a modified Knop medium and inoculated with J2 larvae (left). After ~ 15 days females remain with their head attached to the syncytia on which they keep on feeding (right).

The selection of a proper tissue is most important for the later on sessile nematode. Under favourable environmental conditions that are facilitating the development of females, procambial or cambial cells are selected as ICS, whereas in case of future males pericyclic cells within the vascular cylinder are preferably chosen. Then they undergo similar cytological changes. Callose-like material is deposited on the ICS cell wall. After food uptake started, cytoplasmic streaming and cytoplasm density as

well as the nuclear volume increases, while the central vacuole decreases and new small cytoplasmic vacuoles are formed. And within the cytoplasm further organelles are proliferated: free ribosomes, mitochondria, plastids dictyosomes and endoplasmatic reticulum (ER). While inner cell walls are partly degraded, some parts of the outer cell walls of the growing syncytium are thickened sustaining the high osmotic pressure inside (Böckenhoff and Grundler, 1994).
At the beginning of the J3 stage cell wall ingrowths develop, which are different in structure and localisation between the sexes. As compared to females, the ingrowths of males are not only occurring at the interface with xylem elements but are rare and poorly developed, similarly as the male syncytia themselves are usually smaller; they are less hypertrophied, however, comprising more cells. At the end of the male J3 stage - when the male ceases feeding - the syncytia start to degrade gradually, i.e. the number and size of vacuoles increase and the cytoplasm becomes electron translucent and retracted from the cell wall. Female syncytia also collapse gradually at mature status after the completion of egg production (Golinowski *et al.*, 1996; Sobczak *et al.*, 1997; Hussey and Grundler, 1998).

These drastic cellular modifications within the feeding site raise the question of which host genes are essential for the development of the feeding sites? Thus, specific genes may be switched on or switched off or rather be induced or repressed to a certain level in infected cells as compared to non-infected tissue.
As nematode infection results in wounding of plant tissue (during migration and expansion of the feeding site), the plant is supposed to react by switching on defense genes for example. However, downregulation of defense related genes may also occur, suggesting that the nematode is able to actively suppress the defense response. Furthermore, since the morphological changes within the growing feeding site indicate high metabolic activities, it is not surprising that genes which function in metabolic pathways and cell cycle progression are found to be induced in and around feeding sites. Plant cell wall modifying proteins and enzymes may play a crucial role during nematode infection in several regards since after the invasion of the larvae and the selection of an ICS most notably the syncytial cell wall undergoes remarkable changes as mentioned above; i.e. on the one hand the syncytium grows by local cell wall dissolutions to adjacent cells while on the other hand *de novo* cell wall biosynthesis is required due to thickening of the outer cell wall and the

development of cell wall ingrowths that may facilitate the apo-/symplasmic solute exchange as considered in case of secondary wall ingrowths in transfer cells. However, the genetic and molecular background of these processes, including the role of primary and secondary cell wall loosening agents such as expansins and endo-1,4-β-glucanases (EGases; EC 3.2.1.4)., is not well known yet. Expansins have unique 'loosening' effects on plant cell walls and are thought to play a role in cell wall disassembly and thus may also be involved in nematode feeding cell formation. Similarly, plant EGases seem to play a potential role in NFS since they function as cellulolytic enzymes that hydrolyze the 1,4-β glycosidic linkages between glucose residues. Several expansin and glucanase genes have been reported to be activated in NFS (for reviews see e.g. Gheysen and Fenoll, 2002; Williamson and Gleason, 2003).

There is a wide range of molecular approaches to explore the alterations in gene expression at different time points of nematode infection, ranging from gene-by-gene based methods such as diverse reverse-transcription polymerase chain reaction (RT-PCR) techniques and promoter-*β*-glucuronidase (GUS) fusions to genome-wide based techniques such as SAGE and microarraying (see paragraph **II.B** and **II.C**, respectively).

(I.D) Approaches for management of plant-parasitic nematodes

Although the plant-parasitic species represent a minor part within the phylum Nematoda, especially the root-knot and cyst nematodes have a devastating effect on crop plants as they are obligate biotrophs throughout their life, thereby causing a strong metabolic sink within the root tissue and thus a typical stunted growth. They have an evolutionary advantage since they are living mostly underground and in many cases they are furthermore enclosed by plant tissue protecting them from predators and parasitism or they are protected in cysts.

Up to date, plant parasitic nematodes are difficult to combat. Previously, nematicides were intensively used as a control strategy; e.g. in 1982 in the USA 50,000 tonnes of nematicide active ingredient at a cost of more than US $ 1 billion were applied (Landels, 1989). However, besides high costs for the chemicals itself and associated application costs (equipment and labor), the use of agricultural chemicals (e.g. methyl bromide) is restricted nowadays, due to the implied danger to the

environment, i.e. groundwater contamination, toxiticity to other non-target animals including humans and not last because of residues in the food. Similarly, fumigants are highly toxic and environmentally harmful. Soil amendments (e.g. chitin and bone meal) could help to suppress nematode populations and increase crop yield, but like biocontrol strategies they are rarely employed as stand-alone solutions. Another alternative option is crop rotation, however, the use of non-host crops that have natural resistance can be uneconomical. Thus, engineering durable host-plant resistance would provide the best method to control nematode infection since the trait is intrinsic to the plant seed. (Williamson and Gleason, 2003; McCarter, 2009).

(II) Techniques to investigate gene expression

(II.A) From the 'genome' to the 'transcriptome'

In 1900, the rediscovery of Mendel's rules of inheritance based on certain traits in pea plants (*Pisum sativum*) - first published in 1865 by Gregor Mendel - which assume a factor (later on termed 'gene') within a cell being responsible for the heredity of biological traits of an organism, was the hour of birth of genetics and giving Mendel himself the name 'father of modern genetics'. The **'genome'** can be defined as the complete set of genetic information contained in the DNA of an organism (or cell). However, the term 'genome' includes both the genes encoding for protein sequences and also non-coding sequences of the DNA (see below). Although non-coding elements were thought to be just 'junk' or evolutionary residuals for quite a long time, nowadays there is strong evidence that they play an important role in gene regulation.

In general, genomic complexity is proportional to the complexity of the organism. Relatively simple organisms such as bacteria have genomes in the 1-5 megabases range only. For example, *Escherichia coli* as 'the' bacterium of molecular biology contains 4,639,211 base pairs that are coding for 4,288 genes, while genomes of organisms of intermediate complexity such as worms and insects are typically 100-200 Mbs (per haploid chromosome set). The genome of the free-living soil nematode *Caenorhabditis elegans*, extensively used as a model organism of molecular and developmental biology since 1974, was the first multicellular organism whose genome was completely sequenced and published in 1998 (C. elegans Sequencing

Consortium 1998), although the last of the small unknown gaps was finished by October 2002; its sequence of 97 Mbs contains approximately 20,000 genes. The more complex mammalian genomes including mouse (*Mus musculus*) and human are approximately 3,000 Mbs. Hence, for procaryotic genomes the ratio of the number of nucleotide and the number of genes fits very well to the fact that most proteins are consisting of 200 to 500 amino acids, since one may theoretically conclude from these numbers, that a single gene should be comprised of 600-1500 nucleotides. This further leads to the conclusion that there is no or hardly any space between the single genes in prokaryotes.

However, in the course of time accumulating data from DNA sequencing conveyed that in contrast to the procaryotic genome the genome of eucaryotes seem to include a high percentage of non-coding sequences, i.e. highly diverse non-coding sections are included both between genes and also within genes.

The first plant genome to be fully sequenced was that of the model organism *Arabidopsis thaliana*. This was the achievement of an international collaboration called the Arabidopsis Genome Initiative (AGI), which started sequencing in 1996 by using a top-down approach and officially completed in December 2000 by announcing that their five chromosomes comprising 125 Mbs are including approximately 25,500 genes encoding proteins (The Arabidopsis Genome Initiative 2000). The sequencing technique determining the nucleotide order of a given DNA (or protein) fragment has advanced since its introduction of modern DNA sequencing methods in 1977 - the chemical method was developed by Maxam and Gilbert, (Maxam and Gilbert, 1977) and the dideoxy method of Sanger (Sanger *et al.*, 1977) - from manually performed techniques ('For their contributions of base sequences in nucleic acids' Sanger and Gilbert were awarded the 1962 Nobel Prize in Chemistry in 1980, see http://nobelprize.org/) to meanwhile high-volume, automized sequencing methods to gathering a lot of sequence data at lower costs; examples are 454 sequencing (by 454 Life Sciences, a Roche company) based on the pyrosequencing method and the sequencing technology by Solexa/Illumina.

Knowing the complete sequence, however, is only the first step toward characterizing its gene content. Therefore, the DNA sequence must be analyzed in more detail, i.e. not only to distinguish the coding-part from the non-coding part of the genome but to further identify the single genes and their functional background. This includes both experimental and also bioinformatic strategies such as alignments searching for gene

sequences similar to those already identified in other genomes (e.g. by using comparison algorithms such as BLAST (**B**asic **L**ocal **A**lignment **S**earch **T**ool)), and applying software that recognizes gene features such as open reading frames (ORFs), transcription start and termination sites, exon-intron-boundaries etc.

Although each single cell of an organism carries an organism's complete set of DNA sequences in distinct chromosomes, the expression activity for each gene is a quite dynamic and multifactorial process. Thus, the 'genome' of an individual or cell is clearly distinguishable from its **'transcriptome'** which is the complete set of transcripts and their relative levels of expression in a particular cell or tissue type under defined conditions (Gibson and Muse, 2004). And since 'transcription' is the process by which mRNA (messenger RNA) and other RNAs (tRNA, rRNA) are synthesized from a DNA template, the transcriptome can be more simply described as the set of RNA molecules present in a given cell population, which in turn reflects the actively expressed genes at any given time.

The expression levels for each gene are driven physiologically by a combination of genetic and environmental factors. Genetic factors with the potential for determining gene expression activity include non-(protein-)coding regulatory regions such as promoters, enhancers and splice sites within the genomic DNA sequence.

Especially in higher organisms, the relatively low total number of genes can be explained by the important regulatory mechanism of alternative splicing, a post-transcriptional modification by which the coding capacity of a single gene can be expanded by allowing the production of different protein isoforms with probably different functions. Extrapolation for the human gene complement for example led to an estimation that at least 59 % of the genes are alternatively spliced (Lander *et al.*, 2001). Besides, expression levels are also affected by a large number of environmental factors, including diverse abiotic stress factors such as temperature (change)s, light, drought and other signals as well as biotic stress including pathogens leading to changes in the levels of hormones and other signalling substances. Thus, RNA analysis provides information about the genetic potential of an organism and also about changes in the functional state and important hints to gene function can be gleaned from analyzing transcription profiles.

(II.B) Single-Gene Analyses

Traditional methods in molecular biology generally work on a 'one gene in one experiment' basis, investigating expression of one gene at a time. Biologists started measuring transcript abundance on a single gene basis by using **Northern blot** (Alwine *et al.*, 1977) that is a variant of the first blotting technique, i.e. the DNA-based **Southern blot** developed by Southern (1975). Similarly to Southern blotting, the isolated poly-A-mRNA rather than DNA is separated on a gel according to size. Subsequently, it is transferred to a nylon or nitrocellulose filter by capillary or electrolytic blotting and probed with a radioactively or chemically labeled RNA or DNA sequence fragment corresponding to the gene of interest.
Where size differentiation is not relevant, the method can be simplified by blotting the mRNA samples directly onto the filter of an array of small dots or slots; such blots enable simultaneous comparison of expression levels from tens or even hundreds of samples and are less time consuming by taking hours rather than a couple of days.
A further variant of the filter-based blotting technique is to **reverse** the procedure, i.e. blotting a collection of known cDNAs (complementary DNA, i.e. a reverse-transcribed copy of mRNA) to the membrane and hybridizing them with RNA samples (mostly radioactively labeled) specifically extracted from the cell line or tissue of interest. Such **'macroarrays'** (an array being an orderly arrangement of samples) are quite useful for standard molecular laboratories as they are easy to construct and including the analysis step they are also less expensive. But due to technical reasons the spot diameter is usually over 300 µm, which limits the total amount of spots on a single membrane (in most cases customized macroarrays contain a few 100 genes of interest). Thus, meanwhile macroarrays have been faded into the background by so called **'microarrays'** with smaller spot sizes enabling deposition of many more probes on even smaller platforms (see below).

Another popular single-gene analysis method is the **reverse-transcription PCR**. In contrast to the standard PCR technique, where a DNA fragment is repeatedly synthesized by specific primers and DNA polymerase, the RT-PCR reaction starts with one cycle of reverse transcription, i.e. isolated total RNA being the template to be transcribed into single-stranded cDNA by the enzyme reverse transcriptase (RT). If the measurement of product accumulation is not taken at the end of the reaction

(known as *'end-point detection'* in traditional PCR) but during the exponential phase (when ideally every cycle is doubling the product) of the amplification process, the PCR becomes quantitative, thus called **'quantitative reverse-transcription PCR'** or '**real-time reverse-transcription (RT) PCR'** (often denoted as **'qRT-PCR'** though abbreviations for PCR methods vary widely).

In the presence of a fluorescent dye (e.g. ethidium bromide or SYBR GREEN I etc.) that fluorescence only when intercalating with double-stranded DNA the intensity of the signal will increase with the quantity of products; the higher the starting concentration of the template, the lower the number of cycles is takes to cross the threshold value (an observable fluorescence level reached after a certain number of cycles is referred to as the C_T-value), thus allowing DNA concentrations to be quantified. However, since such unspecific dyes also bind to any dsDNA PCR product, including artefacts such as 'primer dimers', the low specificity is a main disadvantage of this technique. Alternatively, the real-time measurement can be based on the property of **fluorescence resonance energy transfer (FRET**, introduced by Cardullo *et al.*, 1988). To this end, more sophisticated but on the other hand quite expensive fluorescent probes that are specific for a particular sequence are utilized. They consist of short single-stranded oligonucleotides attached to a fluorescent dye. Depending on the kind of system, either the emission of the first or the second dye is measured, and correspondingly the couples of dyes are referred to reporter and quencher or donor and acceptor, respectively. The widely used TaqMan assay is the oldest example of the first system (Livak *et al.,* 1995). TaqMan probes are double-labeled fluorogenic oligonucleotides hybridizing to the target PCR product and Taq DNA polymerase, thereby exploiting its 5' to 3' exonuclease activity which increases the distance between the dyes and stops the energy transfer to the quencher; i.e. an increase in reporter fluorescence intensity indicates the progressive cleavage of the probe during proceeding amplification and thus permits quantitative measurements. There are several quantification strategies in real-time RT-PCR. Absolute quantitation approaches generally utilize standard curves (constructed from samples of known concentrations) as references whereas relative quantification strategies are based on comparing the amount of the target sequence to that of a reference sample (housekeeping gene). The comparative C_T method also known as $2^{-\Delta\Delta C}{}_T$ method for example calculates the relative expression ratio based on the differences of the C_T values (Livak and Schmittgen, 2001)

Real-time PCR is currently the most sensitive and accurate technique for detecting one (or a few) gene(s) and there are numerous applications in basic research and also diagnostics. Although meanwhile multiplex PCR (firstly described in 1988 by Chamberlain *et al.*) assays theoretically enable simultaneous amplification of more than one and up to 100 fragments, the throughput of real-time PCR is relatively limited, while the costs for materials and technical equipment are relatively high. Thus, the real-time PCR technique is nowadays mainly used for validating transcriptome analysis results and for determining the expression of a particular gene that changes its activity over time or in response to altered environmental conditions or in response to pathogen attacks.

Another possibility to examine gene expression in a highly specific way is to perform RT-PCR amplification *in situ*, i.e. on fixed tissue or cells. ***In situ* RT-PCR** is a highly specific method for detection of transcripts in the target cells, since the PCR reaction starting with a reverse transcription actually takes place inside the cell and the following detection is performed via hybridization *in situ*. To this end, probes with either radioactive or non-radioactive labels (e.g. biotin or digoxigenin) can be used for hybridization to the target sequence of the fixed sample.

A further way to monitor the location and timing of gene expression is through the use of a reporter gene as a scorable marker. Promoter-driven markers such as chloramphenicol acetyltransferase (CAT), luciferase (*lux*), *β*-galactosidase *(lacZ* gene*), β*-glucuronidase (GUS encoded by the *uidA locus)* and the green fluorescent protein (GFP) are routinely used in plant molecular biology to identify gene expression in transgenic plants. For plant-nematode interactions many promoter:*gfp* constructs as well as promoter:*gus* constructs, which cause with X-gluc as the most common substrate for the histochemical GUS staining a clear blue color at active sites, have been used to study the expression pattern of specific genes in nematode feeding sites.

(II.C) Parallel Analysis of Gene Expression on a genome-wide scale (transcriptome analysis)

Genome-wide methods can be divided into two main classes: (i) **direct analysis** and (ii) **indirect analysis** (for a review see Donson *et al.,* 2002).

(II.C.1) Direct analysis – sequencing and fragment sizing

The first category includes procedures involving *nucleotide sequencing* such as EST sequencing and SAGE on the one hand and *fragment sizing methods* such as **differential display (DD)** and selective fragment amplification (cDNA-AFLP) on the other hand. All these technologies as well as several variants thereof have also been used for transcript profiling of Arabidopsis. The concept of the PCR based fragment sizing methods is to discriminate differences in gene expression levels by transcribing unknown templates to representative cDNA fragments that are subsequently separated on high resolution polyacrylamide gels, finally yielding a band pattern specific for the sample under investigation. Thus, DD and its modifications are relatively simple and cost-effective approaches, theoretically enabling a complete picture of differences in gene expression, where only small amounts of RNA are needed. Further steps of isolating, cloning and finally sequencing of the band of interest may follow in order to identify the corresponding gene. However, as in a DD assay the cDNA is amplified by using arbitrary primers to allow for priming at multiple sites, at the same time they permit production of unspecific amplicons, thereby distorting the result. This is, however, a general problem inherent to arbitrary primed PCR processes. Thus, after the first application of DD in 1992 (Liang and Pardee) and its extensive use in plant research DD methods have lost a lot of their popularity as they are not very accurate in quantitative gene expression profiling.

An improvement of the traditional DD techniques is the **cDNA-amplified fragment length polymorphism analysis** (**cDNA-AFLP**), developed by KeyGene in the Netherlands (Vos *et al.*, 1995; Bachem *et al.*, 1996) that has derived from the widely used genomic DNA-based AFLP mapping technique. The PCR conditions are more stringent since cDNAs are first digested with two restriction enzymes and after ligation of adapters specific primer sets (comprised of the adapter sequence with

nucleotide extension) are used for a final selective amplification, thereby increasing the sensitivity of the analysis. In contrast to the DD technique cDNA-AFLP is a very robust and reproducible method which produces only few false-positive bands**.**

EST sequencing makes use of single sequencing runs of random clones derived from cDNA libraries (Adams *et al*., 1991). The high-throughput automated partial sequencing technology led to a huge worldwide collection of ESTs of various animal and plant species, obtained from diverse cells under a variety of environmental conditions. Now there are millions of ESTs available in diverse private and public databases (e.g. GenBank, see the web page at http://www.ncbi.nlm.nih.gov/dbEST/) that are growing at an exponential rate. Besides serving valuable information about gene discovery, alternative splicing etc., EST projects have provided a major contribution with expression analysis, espec. in Arabidopsis (Höfte *et al.*, 1993; Newman *et al.*, 1994) in recent years.

The development of the **Serial Analysis of Gene Expression method** (**SAGE**) in 1995 (Velculescu *et al*., 1995*),* was an important cost-saving improvement as compared to the EST sequencing method. This is achieved by a protocol that is based on the idea to quantitatively collect very short gene-specific oligonucleotides, 'tags', that are cut out directly from the transcripts present in the sample and further linked together to long serial molecules termed 'concatemers' (containing few 100 up to few kilobases) prior to cloning and the final sequencing step analyzing concatemer by concatemer (further information on SAGE including applications and recent publications is provided on the SAGE web site: http://www.sagenet.org/). The original protocol was developed to elucidate the gene expression differences in human cancer cells (Velculescu *et al.*, 1995) and since then it was intensively used, i.e. first in many human and yeast studies and since the late 1990s also in plant research studies. Meanwhile several improvements were suggested, espec. by changing the restriction enzymes causing an increase of the original tag length of 9 bps (Velculescu *et al.*, 1995) to more than 20 bps counteracting SAGE's main weakness due to the small tag size; although a 9mer can theoretically encode for (4^9, i.e.) 262,144 different genes, which exceeds the number of genes found in Arabidopsis by far. Most notable variants thereof may be **LongSAGE** (Saha *et al.*, 2002) and the most recent **SuperSAGE** (Matsumura *et al.,* 2005) with 21 and 25-27 bp per tag,

respectively, enabling more confident identification of the corresponding gene. The identification of the tags is automated by using SAGE analytical software that delivers a list of all discovered tags and their abundance, i.e. the counts of each particular tag in relation to the total number of all tags found in the SAGE library, thereby providing 'absolute expression levels' in contrast to 'relative expression values' as e.g. in case of microarray assays (see below). Although the patent covering SAGE (TM) technology is owned by Genzyme Molecular Oncology, diverse web-based analysis tools are accessible through SAGEnet (http://www.sagenet.org/) since the method itself is freely available for non-commercial research.

Further analytical steps include identifying the corresponding genes provided the organism's sequence is known due to available EST and/or the whole genome information. However, SAGE is also capable of detecting new genes in cases where a sequence does not match a known gene, which was a very valuable advantage of this method, especially at the time of SAGE's introduction when only a few organisms had been completely sequenced. Since SAGE also has the great advantage to be unbiased by experimental conditions (reference samples, hybridization artifacts etc.), direct comparison of data sets deriving from different experiments is possible, which does not hold true for microarray experiments (see below).

However, with the technical progress massively parallel sequencing came up and the microarray technique was considerably improved. Nowadays large-scale studies do not employ SAGE anymore, since it is much more time-consuming (many more work steps) and cost-intensive as compared to other methods such as microarrays.

During the last years 'next generation' massively parallel sequencing (MPS, also called 'ultra high throughput sequencing'), such as the Supported Oligonucleotide Ligation and Detection system (SOLiD) by Applied Biosystems and Illumina's Genome Analyzer II, has emerged as a technology that is also applicable to transcriptome analysis similar to EST sequencing because of a very high throughput, however, without requiring any traditional cloning (recently reviewed by Wilhelm and Landry, 2009). Compared to microarrays or GeneChips the advantage of the method is that it covers all genes, while the current Arabidopsis ATH1 GeneChip (see chapter **II.C.2**) for instance covers only 60-70 % of the genome. In addition, these massively parallel mRNA sequencing methods are also able to detect alternative splicing, however, the costs per sample are higher as compared to microarraying.

,

(II.C.2) Indirect analysis – microarrays

The second main category of transcriptome analysis methods are based on hybridization of mRNA or cDNA, comprising high density microarraying. Since the late 1990s and early 2000s various kinds of microarrays have attracted tremendous interest among biologists (for an overview see for example the review by Rensink and Buell, 2005).

The microarray technique is based on base-pairing rules and similar to the reverse northern blotting procedure, in that defined DNA fragments affixed to a substrate (preferably termed 'probes' or 'reporters') are interrogated by hybridization to labeled (e.g. with a fluorescent dye), unknown nucleic acid sequences (cDNA) derived from cellular mRNA samples under investigation (preferably termed 'targets'). As the amount of target that sticks to each spot is proportional to the abundance of the specific target in the sample, taking measurements of the signal (e.g. fluorescent) intensities is used for gene expression quantification, i.e. distinct transcript levels are detected by differences in signal intensities.

A first important technical progress as compared to the membrane-based macroarrays (see above) was to use a flat solid surface such as glass or silicon rather than spotting onto filter paper, since these non-porous substrates imply several advantages, as for instance less problems with diffusion (Livshits and Mirzabekov, 1996) and absorption of applied reagents during array fabrication and processing (Schena, 1999). This permits the use of small sample volumes for deposition at a precisely defined location via fine pins or needles, thereby facilitating miniaturization and automation of array fabrication. The diameter of the spots is typically less than 200 µm (in contrast to the sizes of ≥ 300 µm in case of macroarrays described above). Furthermore, in contrast to the filter-based assays, the inherent flatness of the MA format permits true parallelism, which significantly increases in the accuracy of the microarray assay.

There were two groups pioneering the innovation of microarray technology in the early 1990s (Lander, 1999).

(1) spotted cDNA microarrays

The first report on a **cDNA microarray** was published in 1995 at Stanford University School of Medicine, by Patrick Brown and his colleagues, who prepared high density arrays by high-speed robotic printing for measuring differential expression of 45 Arabidopsis genes by means of two-color fluorescence detection (Schena *et al.*, 1995; Schena, 1996). Most early versions of these 'spotted' microarrays as one of the two major microarray technologies relied on PCR amplified cDNA fragments (ESTs). However, in principle any kind of nucleic acid can be used for various applications, also beyond transcriptome studies (e.g. genomic DNA). Besides, long oligonucleotides in the range of 50-80 bp (e.g. arrays from Agilent or Operon) have gained popularity as probes since they have several advantages over cDNAs as most notably they can be designed from ESTs or annotated genome sequences according to specific demands and easily be ordered from a company, thereby replacing the cost- and time-intensive preparation of an amplicon set derived from clones. The oligos are either also spotted or alternatively synthesized such as for example 60mers in case of the Arabidospis 2 oligo array commercialized by Agilent Technologies (Palo Alto, CA, USA) that uses, however, a combination of different fabrication technologies, i.e. ink-jet printing and phosphoramidite chemistry, for in-situ synthesis (Hughes *et al.* 2001; Gibson and Muse, 2004).

For target preparation the extracted mRNA is converted into cDNA and usually labeled either by either radioactivity or fluorescent dyes. In the second case, for an experiment with a typical *two-color microarray* or *two-channel microarray*, two independent RNA samples, i.e. an experimental test and a reference/control sample, are labeled with distinguishable fluorochromes (commonly used is the green Cy3 (emission wavelength of 570 nm) together with the red Cy5 (670 nm)), they are mixed and then hybridized to a single spotted microarray. After a washing step in order to remove unhybridized molecules, a microarray scanner is used to visualize fluorescence of the two fluorophores after excitation with a laser beam of a defined wavelength. Since the fluor's emission is proportional to the level of the specific target in the hybridization solution, the standard approach for quantitative analysis is to compute the ratio of the two signal intensities of the two cell samples, hence

identifying any changes of expression levels as up- or downregulation of an experimental sample relative to the reference sample.

As the developers openly dispensed their knowledge including diverse software for scanning and data analysis (http://cmgm.stanford.edu/pbrown/), this conceptually simple technology of spotted microarrays was widely adopted since it is relative cost-effective and of high flexibility in several regards as mentioned above. They can nowadays be manufactured in different ways, either in-house or from commercial vendors.

(2) short oligonucleotide gene chips

At the same time when the group in Patrick Brown's lab developed their spotted DNA microarrays, Steve Fodor and co-workers worked on the second innovative idea of light-directed high-density spatial synthesis of oligonucleotides on a solid substrate by adapting photolithographic masking techniques used in semiconductor manufacture (Fodor *et al.*, 1991; Fodor *et al.*, 1993; Pease *et al.*, 1994).

In contrast to the spotted 'cDNA microarrays', such short-oligonucleotide arrays are synthesized *in-situ* and based on sequence information. The approach of Affymetrix (http://www.affymetrix.com) was to use sequence information directly to design tiny (1.28 cm x 1.28 cm) arrays of synthetic DNA probes that comprise sets of independent 25-mer oligonucleotides that are synthesized by a sequential nucleotide-addition reaction attaching one nucleotide after the other on a silicon platform with the aid of a mask directing the light (**Figure 3**).

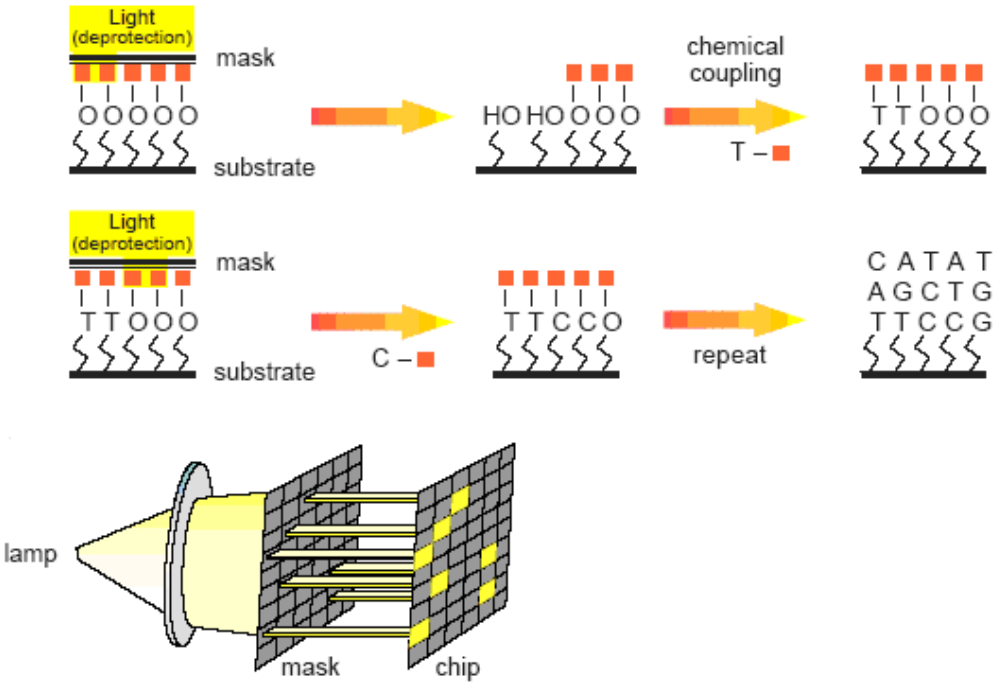

Figure 3: Schematic representation of light-directed oligonucleotide synthesis for the construction of high-density DNA probe arrays such as the Affymetrix GeneChips. A solid support is derivatized with a covalent linker molecule terminated with a photolabile protecting group. Light is directed through a mask to deprotect and activate selected sites, and protected nucleotides couple to the activated sites. The process is repeated, activating different sets of sites and coupling different bases allowing arbitrary DNA probes to be constructed at each site. (Lipshutz *et al*., 1999).

Each probe is serving as a sensitive, unique tag of known or predicted open reading frames. In general, 11-16/20 different probes are selected among all possible oligos in order to control for variation in hybridization efficiency. In contrast to *two-color microarray* these chips are *one-color microarrays* as per chip only one RNA sample can be hybridized after transcription to cDNA or cRNA and following labelling (biotin), thus, requiring the double amount of arrays for an experiment (**Figure 4**).

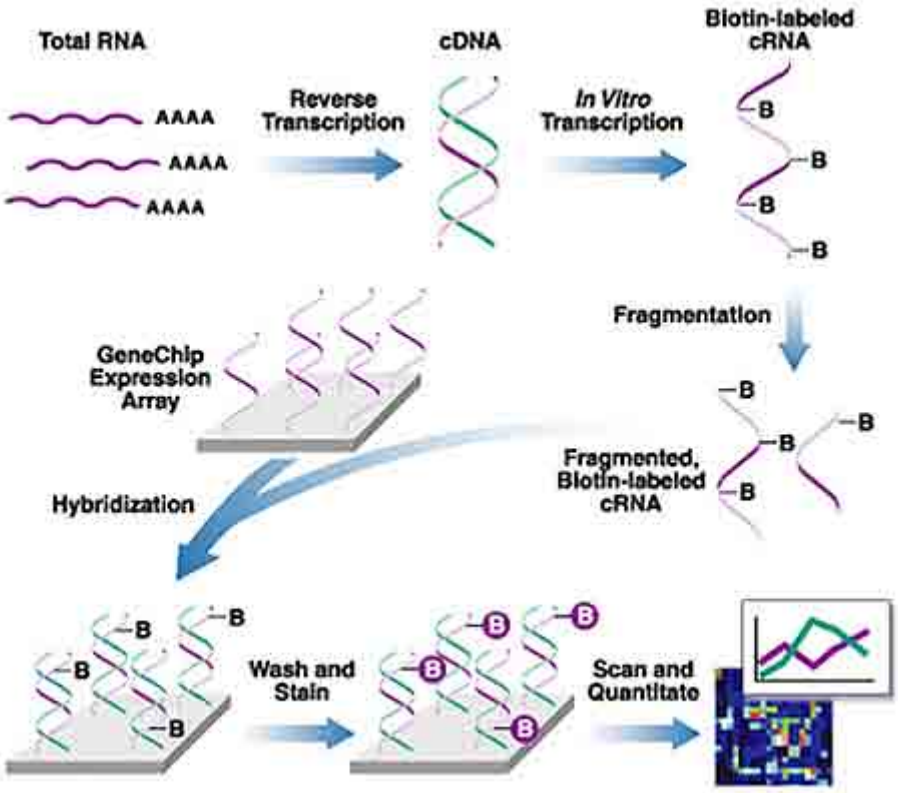

Figure 4: Standard eukaryotic gene expression assay. The basic concept behind the use of GeneChip arrays for gene expression: labeled cDNA or cRNA targets derived from the mRNA of an experimental sample are hybridized to nucleic acid probes attached to the solid support. By monitoring the amount of label associated with each DNA location, it is possible to infer the abundance of each mRNA species represented (http://www.affymetrix.com).

Another key element of their design universally applied to the GeneChips is the Perfect Match (PM)/Mismatch (MM) probe strategy; i.e. for each probe being perfectly complementary to the target sequence there is an adjacent partner probe that is identical except for a single base mismatch in its center, with the intention of measuring non-specific binding (cross-hybridization) because the MM control should not hybridize under high stringency conditions. The expression level of each gene can thus be calculated as a difference between the partner probes using a procedure (Affymetrix® Microarray Suite (MAS)) provided by Affymetrix with their scanning software. However, this approach is not universally agreed upon and thus several alterations and improvements were suggested. Li and Wong (2001) first proposed model-based expression measures and Irizarry *et al.* (2003) proposed a background adjustment step ignoring the MM values, which resulted for example in the algorithm

called robust multi-array analysis (RMA) that has become a popular alternative to the default adjustment provided by Affymetrix. Besides, further adjustments were introduced such as the model based background adjustment by Wu *et al.* (2004) that is available as part of the Bioconductor Project which brings together open-source software (written in the R programming language) and is used for the analysis and comprehension of genomic data. For a review regarding data normalization and quantification of gene expression studies via microarrays see for example Steinhoff and Vingron (2006) and Ahmed (2006).

The first high-density oligonucleotide probe array designed for plants was the **Arabidopsis GeneChip 8k AG**. Besides 40 control probe sets for spiking and negative controls, it contained 8,835 Arabidopsis specific probe sets (each composed of 16 probe pairs per gene) corresponding to approx. 8,100 genes (about 70 % genes with known or predicted function and 30 % predicted genes with matching ESTs or proteins), that, however, covered about one-third of the whole genome only (Zhu and Wang, 2000). With the elucidation of the complete genomic complement of Arabidopsis at the end of the twentieth century (the Arabidopsis Genome Sequencing project was officially completed in late 2000), Affymetrix released in 2003 in collaboration with The Institute for Genomic *Research* (TIGR, http://www.tigr.org) the second generation of GeneChip comprising the whole genome, i.e. the **Arabidopsis ATH1-121501 (25 K) Genome Array**, commonly referred to as ATH1 that was based on the TIGR re-annotation data (Wortman *et al.*, 2003; Redman *et al.*, 2004). Their database (version 2.0, in 2001) contained annotation for 26,155 protein coding genes and 1,296 pseudogenes, while the newer GeneChip design including a reduction of feature size to 18 µm and a reduction in the number of required probes per set (11 per gene) allowed the placement of approx. 22,750 specific genes/probe sets. Therefore, some selection was necessary, thereby giving first preference to genes where there was evidence of expression (cDNA, EST) or secondly strong support by database matches. However, in order to represent as many genes as possible on the ATH1, non-unique probe sets corresponding to (mostly) two ore more highly similar genes were preferably chosen wherever possible, which ultimately resulted in an array representing a total of 23,734 Arabidopsis genes, while 2,411 genes are absolutely missing (for details see Redman *et al.*, 2004). Tremendous technical and analytical progress in the recent years, however, revealed that the original annotations utilized for Affymetrix GeneChip design are significantly different from

newer knowledge and needs to be updated regularly (Dai *et al.*, 2005). TAIR, The Arabidopsis Information Resource (available online via the web site http://www.arabidopsis.org), maintains a database of genetic and molecular biology data for Arabidopsis after taking over the responsibility for annotation updates in 2003 (Wortman *et al.*, 2003).

For classifying genes, TIGR and TAIR as well as other big databases for plant, animal and microbial genomes, use the **Gene Ontology (GO)** established by the Gene Ontology Consortium in 1998 (Ashburner *et al.*, 2000). The GO Consortium is an international collaboration among scientists with the effort to produce dynamic, controlled vocabularies (i.e. ontologies) for describing the roles of genes and their products in any eukaryote. They initiated the GO project after the availability of sequences of entire genomes of the first model organisms (budding yeast *Saccharomyces cerevisiae* in 1996 and *C. elegans* in 1998) had revealed that there are surprisingly high degrees of (sequence) similarities displaying evidence of orthologies, most of them found to play a role in the 'core biological processes' (DNA replication, transcription etc.) common to all eukaryotic cells.
The high degree of observed sequence and functional conservation, i.e. the knowledge that the biological role of a shared protein in one organism can often be transferred to another one, presented a challenge to establish an automated system for comparing annotation among different species, which was based on three discrete, non-overlapping major domains of molecular biology; i.e. the GO project has developed structured ontologies that describe gene products in terms of their associated (i) biological processes, (ii) molecular functions, (iii) and cellular components in a species-independent manner (Ashburner *et al.*, 2000; Gene Ontology Consortium 2004*;* Gibson and Muse, 2004). The output of the GO project as a major bioinformatics initiative is freely available via the GO Web Pages at http://www.geneontology.org.

With rapidly growing interest in microarray technologies in diverse biological fields including medicine (diagnostic purposes) the range of technical solutions and commercially available instruments including a variety of services for producing and analyzing microarray data grew fastly. Since each platform has its advantages and drawbacks (including costs, gene coverage, availabiltiy on the market and quality

etc.), carefull considerations have to be taken already at the starting point of a microarray study when planning the experimental design (e.g. choice of control samples, availability of technical and biological replicates) that strongly influences the statistical power of data analysis afterwards (Gibson and Muse, 2004; Steinhoff C. and Vingron, 2006).

(II.C.2.a) *Statistical analysis of microarray data*

During the last years, various procedures for data preprocessing (e.g. background correction as mentioned above) and normaliziation to remove any bias inherent in each hybridization event (adjusting raw fluorescent intensities for measuring the transcript abundance) were introduced. Similarly, there are also several approaches for further statistical analyses and data mining (Gibson and Muse, 2004; for reviews see e.g. Ahmed, 2006; Steinhoff and Vingron, 2006). Most commonly two different groups of samples are compared for differentially expressed genes, either by using one two-color microarray or two one-color microarrays. Accordingly, a standard approach for comparing gene expression is to calculate the ratio of signal intensities of two samples (Eisen *et al.*, 1998). In the beginnings of microarray analysis, a twofold-change (as determined cut-off value), i.e. two times induction or repression of a test sample relative to a reference sample was commonly considered to indicate a meaningful change in gene expression. Nowadays, however, this is rather used as a preliminary screening method only, while on the other hand assessments of statistical significances are mostly required for yielding profound results (Gibson and Muse, 2004; Ahmed 2006; Steinhoff and Vingron, 2006). A general problem when generating a list of significantly differentially expressed genes by ranking thousands of genes is the need to control for multiple testing because performing many tests at a time increases the number of false positives in genome wide studies. One more recent solution to overcome this problem is to control for the **'false discovery rate'** (**FDR**), being the rate at which significant features are truly null (i.e. a FDR of 5 % for example means that 5 % of genes found to be significantly differentially expressed, are, in fact, false positive, i.e. not differentially expressed). The FDR supports to balance between the number of true and false positives, whereby a measure of statistical significance called q-value is associated with each tested feature, i.e. an adjusted p-value that in contrast measures the significance in terms of the false positive rate (Reimers, 2005; Ahmed, 2006).

The Bioconductor Project mentioned above is only one of a number of freely distributed software packages and of course there are various commercial packages with diverse statistical algorithms available, as for example the computer program GeneSpring (Silicon Genetics, Agilent Technologies, Inc. Headquarters, USA).

(II.C.2.b) *Microarray data mining*

In order to investigate the biological relevance of the genes found to be differentially regulated, it is a useful option to utilize GO with its functional annotation by e.g. testing the abundance *(relative enrichment)* of particular GO subcategories, i.e. whether they are significantly under- or over-represented (with)in a test group of genes (e.g. up-regulated genes) in relation to a reference group (e.g. all significantly expressed genes or total number of genes present on the chip) (Gibson and Muse, 2004; Blüthgen, 2005) or by looking at the preferential regulation in GO categories.

Besides detection of differentially expressed genes on the one hand, pattern recognition could be considered the second broad category of data profiling strategies (Ahmed, 2006). In fact, there are numerous ways of displaying expression data deriving from a huge number of genes represented on a microarray platform, so that our human brain is able to process it. Determining specific patterns can either be done in a supervised or unsupervised approach, however, the two approaches can also be applied combined on a data set. Examples for the first alternative that depend on the presence of variables characterizing the specimen under study are 'support vector machines' (SVMs) and linear discriminants, while in unsupervised approaches no predefined reference vectors are used (Eisen *et al.*, 1998; Ahmed, 2006). These include the widely used clustering algorithms, such as hierarchical and non-hierarchical, in order to identify 'clusters' of genes that share an expression profile across a number of experiments or within a population. Clustering is based on co-expression and thus may also imply co-regulation and in turn lead to the conclusion that the genes may be involved in the same boiological process (Gibson and Muse, 2004). Hierarchical clustering includes so called botton-up and top-down methods and it often employs a 'heat-map' for visualization (introduced for microarray data by Eisen *et al.*, 1998) that is a 2D data matrix (genes and samples) of colors where each cell is colorized based on the expression level in the sample (typically red colors represent increased expression values, green decreased and black is used for intermediate expression levels), thereby giving an overall expression view.

Hence, heat maps help to find similarities across a set of samples (e.g. different times points relative to time 0) (Eisen *et al.*, 1998; Ahmed, 2006). Non-hierarchical methods where data are forced to fit to the number of clusters determined in advance, include e.g. self-organizing maps (SOMs) and k-means clustering being one of the simplest and widely used algorithms. Another exploratory multivariate statistical technique to uncover unkown trends in data is the **pricipal component analysis (PCA)** which is a standard tool in modern data analysis in diverse fields, while it is agnostic to the source of data. PCA is a simple non-parametric mehod for finding patterns in data of high dimension by reducing the number of dimensions - by performing a covariance analysis between factors - with minimal loss of information. Thereby the first principal component accounts for as much of the variability in the data as possible, and each succeeding component accounts for as much of the remaining variability as possible (Pevsne, 2003).

However, one should always keep in mind that independent of the chosen data profiling method, the result should never be considered without including the biological background knowledge of the researcher to avoid biological senseless conclusions!

Outline of the work

Since for sedentary endoparasitic nematodes such as root-knot and cyst forming examples the exploited structure inside the root organ is the only nutrient source to support their development and reproduction, the growth of nematodes and that of their induced feeding sites are intimately connected. Although the obvious transformation from a selected single root cell into a parasitic-specific multicellular feeding site structure has been known for about a century, our knowledge of the underlying mechanisms remains sparse.

The main goal of this thesis was therefore to get an insight into this complexity of plant-nematode-interactions by an interrogation of the transcriptomic changes within the nematode feeding site in the course of time. We utilized an ecotype (Columbia) of the model plant Arabidopsis that is susceptible to the economically important beet cyst nematode H. *schachtii* to investigate the transcriptome of the syncytia that develop inside the small translucent roots. We employed in our transcriptome study the last generation of Affymetrix GeneChips, the Arabidopsis ATH1 array that is widely used by the Arabidopsis community. In contrast to initial transcriptome studies we have performed a localized approach by extracting pure syncytial material excluding any surrounding tissue - via microaspiration - in order to get a clue on localized responses to invading and/or developing nematodes, which may finally help to generate potential targets to combat nematode infection.

The expression profiles of syncytia at 5 and 15 dpi turned out to be quite similar at a global view, however, the syncytial transcriptome as a whole - comprising 34.2 % differentially expressed genes as compared to uninfected control roots - is quite distinct from that of uninfected roots (and other Arabidopsis organs such as flower, leaf, pollen, root and seed). Gene ontology analyses showed clear trends of upregulation of genes that are involved in metabolic activity, which fits to observations of cellular changes inside the developing multinucleate syncytium that supplies a huge amount of nutrients to the sucking nematode **(chapter 2).**

Since the syncytial cell wall also undergoes remarkable changes (fulfilling opposing requirements such as counteracting the increased osmotic pressure inside the syncytium on the one hand and on the other hand remaining flexible to allow expansion and be permeable to facilitate the uptake of nutrients), we took a closer look at the expression profiles of gene families coding for primary and secondary cell wall modulating agents, expansins (comprising 31-32 gene members; **chapter 3)** and

endo-1,4-β-glucanases (comprising 25 members; **chapter 4)**, respectively. In both families some genes were significantly upregulated in syncytia while others were downregulated. After applying additional technical approaches such as several RT-PCR techniques and promoter:*gus* assays, we suppose the two induced expansins *AtEXPA3* and *AtEXPA1,* that are usually shoot-specifically expressed, to be involved in NFS establishment. Similarly, among the EGases further experiments including infections tests with mutants suggest that at least the significantly upregulated *AtCel2* and *KOR3,* both again usually shoot-specific, play an important role during syncytium formation.

The most strongly induced gene was found among the small *MIOX* gene family (comprising 4 members; **chapter 5)**, i.e. the pollen-specific *MIOX5.* Similarly, further experiments to evaluate gene expression and probable function via double mutants indicate that their upregulated expression levels within the NFS may be due to some functional reasons that are currently under further investigation in our lab.

Furthermore, we worked on a general approach of reverse genetics by improving a binary vector that can be easily used in a reproducible transformation system to assess potential effects on plant tissues **(chapter 6).** For this purpose we modified the relatively small, stable binary vector pPZP111 in several regards due to some of its crucial drawbacks for successful *Agrobacterium tumefaciens* transformation. The new binary vector pPZP3425 can be used for selections requiring solely kanamycin and implies a new expression cassette that consists of a strong constitutive promoter (on the basis of 35S CaMV) and the reporter gene *gus*. Both sequence parts can easily be exchanged by any other sequence of interest and thus pPZP3425 can be used for many purposes to identify functional information.

References

Adams, M.D., Kelley, J.M., Gocayne, J.D., Dubnick, M., Polymeropoulos, M.H., Xiao, H., Merril, C.R., Wu, A., Olde, B., Moreno M., R.F., Kerlavage, A.R., McCombie, W.R. and Venter, J.C. (1991) Complementary DNA sequencing: expressed sequence tags and human genome project. Science 252:1651-1656.

Ahmed, F.E. (2006) Expert Rev. Mol. Diagn. 6:535-550.

Alwine, J.C., Kemp, D.J. and Stark, G.R. (1977) Method for detection of specific RNAs in agarose gels by transfer to diazobenzyloxymethyl-paper and hybridization with DNA probes. Proc. Natl. Acad. Sci. U.S.A. 74:5350-4.

Ashburner, M., Ball, C.A., Blake, J.A., Botstein, D., Butler, H., *et al.* (2000) Gene Ontology: tool for the unification of biology. Nature Genetics 25:25-29.

Bachem, C.W.B., van der Hoeven, R.S., de Bruijn, S.M., Vreugdenhil, D., Zabeau, M. and Visser, R.G.F. (1996) Visualization of differential gene expression using a novel method of RNA fingerprinting based on AFLP: analysis of gene expression during potato tuber development. The Plant Journal 9:745-753.

Bird, D.M. and Bird, A.F. (2001) Plant-parasitic Nematodes. In: Parasitic Nematodes: Molecular Biology, Biochemistry And Immunology. Kennedy, M.W. and Harnett, W.. eds.,. CAB International, 139-166.

Blaxter, M.L., De Ley, P., Garey J.R., Liu, L.X., Scheldeman, P., Vierstraete, A., Vanfleteren, J.R., Mackey, L.Y., Dorris, M., Frisse, L.M., Vida, J.T. and Thomas, W.K. (1998) A molecular evolutionary framework for the phylum Nematoda. Nature. 392:71-75.

Blaxter, M., Mann., J., Chapman., T., Thomas., F., Whitton, C., *et al.* (2005) Defining operational taxonomic units using DNA barcode data. Philos Trans R Soc London, Ser B. 360:1935-1943.

Blüthgen, N., Brand. K., Cajavec, B., Swat, M., Herzel, H., *et al.* (2005) Biological profiling of gene groups utilizing Gene Ontology. Genome Inform 16:106-115.

Böckenhoff, A. and Grundler, F.M.W. (1994) Studies on the nutrient uptake by the beet cyst nematode *Heterodera schachtii* by *in situ* microinjection of fluorescent probes into the feeding structures in *Arabidopsis thaliana*. Parasitology 109:249-254.

Burrows, P.R. (1992) Molecular Analysis of the Interactions between Cyst Nematodes and Their Hosts. Journal of Nematology 24:338-342.

Cardullo, R.A., Agrawal, S., Flores, C., Zamecnik, P.C. and Wolf, D.E. (1988) Detection of nucleic acid hybridization by nonradiative fluorescence resonance energy transfer. Proc Natl Acad Sci USA. 85:8790-8794.

Chamberlain, J.S., Gibbs, R.A., Ranier, J.E., Nguyen, P.N. and Caskey, C.T. (1988) Deletion screening of the Duchenne muscular dystrophy locus viamultiplex DNA amplification. Nucleic Acids Research 16:11141-11156.

Dai, M., Wang, P., Boyd, A.D., Kostov, G., Athey, B., Jones, E.G., Bunney, W.E., Myers, R.M., Speed, T.P., Akil, H., Watson, S.J., and Meng, F. (2005) Evolving gene/transcript definitions significantly alter the interpretation of GeneChip data. *Nucleic Acids Res*., **33**, e175.

Davis, E.L., Hussey, R.S., Mitchum, M.G. and Baum ,T.J. (2008) Parasitism proteins in nematode-plant interactions. Current Opinion in Plant Biology 11:360-366.

Decraemer, W. and Hunt, D.J. (2006) Structure and classification. In: Plant Nematology. Perry, R.N. and Moens, M. eds., CABI North American Office, 3-32.

Donson, J., Fang, Y., Espiritu-Santo, G., Xing, W., Salazar, A., Miyamoto, S., Armendarez, V. and Volkmuth, W. (2002) Comprehensive gene expression analysis by transcript profiling. Plant Mol Biol. 48:75-97.

Eisen, M.B., Spellman, P.T., Brown, P.O. and Botstein, D. (1998) Cluster analysis and display of genome-wide expression patterns. Proc Natl Acad Sci U S A 95:14863-14868.

Fodor, S.P., Read, J.L., Pirrung, M.C., Stryer, L., Lu, A.T. and Solas, D. (1991) Light-directed, spatially addressable parallel chemical analysis. Science 251:767 773.

Fodor, S,P., Rava, R.P., Huang, X.C., Pease, A.C., Holmes, C.P. and Adams, C.L. (1993) Multiplexed biochemical assays with biological chips. Nature 364:555-556.

Gene Ontology Consortium (2004) The Gene Ontology (GO) database and informatics resource. Nucleic Acids Research 32:D258-D261.

Gheysen, G. and Fenoll, C. (2002) Gene expression in nematode feeding sites. Annu.Rev.Phytopathol. 40:191-219.

Gibson, G., Muse, S. (2004) A Primer of Genome Science. Sinauer Associates, Sunderland, MA, USA.

Golinowski, W., Grundler, F.M.W., Sobczak, M. (1996) Changes in the structure of *Arabidopsis thaliana* during female development of the plant-parasitic nematode *Heterodera schachtii*. Protoplasma 194:103-116.

Hodda, M. (2000). Nematodes of the Murray-Darling river system and coastal freshwaters of southeastern Australia
http://www.ento.csiro.au/science/nematode.html

Höfte, H., Desprez, T., Amselem, J., Chiapello, H., Caboche, M., Moisan, A., Jourjon, M.F., Charpenteau, J.L., Berthomieu, P., Guerrier, D., *et al.* (1993) An inventory of 1152 expressed sequence tags obtained by partial sequencing of cDNAs from *Arabidopsis thaliana.* Plant J 4:1051-1061.

Hughes, T.R., Mao, M., Jones, A.R., *et al.* (2001) Expression profiling using microarrays fabricated by an ink-jet oligonucleotide synthesizer. Nature Biotechnol 19:342-347.

Hussey, R.S. and Grundler, F.M. (1998) Nematode parasitism of plants. In: The Physiology and Biochemistry of Free-living and Plant-parasitic nematodes. Perry, R.N. and Wright, D.J. eds., CAB International, 213-243.

Irizarry, R.A., Hobbs, B., Collin, F., Beazer-Barclay, Y.D., Antonellis, K.J., Scherf, U. and Speed, T.P. (2003). Exploration, normalization, and summaries of high density oligonucleotide array probe-level data. Biostatistics 4:249-264.

Jung, C. and Wyss, U. (1999) New approaches to control plant parasitic nematodes. Appl Microbiol Biotechnol 51:439-446.

Landels, S. (1989) Fumigants and nematicides. In: Chemical Economics Handbook. Stanford Research Institute International, California.

Lander, E.S. (1999) Array of hope. Nat. Genet. 21:3-4.

Lander, E.S., Linton, L.M., Birren, B., Nusbaum, C., Zody, M.C., Baldwin,J., Devon, K., Dewar, K., Doyle, M., FitzHugh, W. *et al.* (2001) Initial sequencing and analysis of the human genome. Nature 409:860-921.

Lewis, S.A., David J., Chitwood, D.J. and McGawley, E.C. (2004) Nematode Biology, Morphology, and Physiology. In: Encyclopedia of Plant and Crop Science. Robert, M. Goodman, R.M. eds., Taylor & Francis.

Li, C. and WONG, W. (2001) Model-based analysis of oligonucleotide arrays: Expression index computation and outlier detection. Proceedings of the National Academy of Science U S A 98:31-36.

Liang, P. and Pardee, A.B. (1992) Differential display of eukaryotic messenger RNA by means of the polymerase chain reaction. Science 257:967-971.

Lipshutz, R.J., Fodor, S.P.A., Gingeras, T.R. and Lockhart, D.J. (1999) High density synthetic oligonucleotide arrays. Nature Genetics 21:20-24.

Livak, K.J., Flood, S.J., Marmaro, J., Giusti, W. and Deetz, K. (1995) Oligonucleotides with fluorescent dyes at opposite ends provide a quenched probe system useful for detecting PCR product and nucleic acid hybridization. PCR Methods Appl 4:357-362.

Livak, K.J. and Schmittgen, T.D. (2001) Analysis of relative gene expression data using real-time quantitative PCR and the 2(-Delta Delta C(T)). Methods 25:402-408.

Livshits, M.A. and Mirzabekov, A.D. (1996) Theoretical analysis of the kinetics of DNA hybridization with gel-immobilized oligonucleotides. Biophys. J. 71:2795-2801.

Matsumura, H., Ito, A., Saitoh, H., Winter, P., Kahl, G., Reuter, M., Krüger, D.H. and Terauchi, R. (2005) SuperSAGE. Cell Microbiol 7:11-8.

Maxam, A. and Gilbert, W. (1977) A new method of sequencing DNA. In: Proceedings of the National Academy of Sciences U.S.A. 74:560-564.

McCarter, J.P. (2009) Molecular Approaches Toward Resistance to Plant-Parasitic Nematodes. In: Cell Biology of Plant Nematode Parasitism. Berg, R.H. and Taylor, C.G. eds., Springer, 239-269.

Newman, T., DeBruijn, F.J., Green, P., Keegstra, K., Kende, H., Mcintosh, L., Ohlrogge, J., Raikhel, N., Somerville, S., Thomashow, M., Retzel, E., and Somerville, C. (1994) Genes galore: A summary of methods for accessing results from largescale partial sequencing of anonymous Arabidopsis cDNA clones. Plant Physiol. 106:1241-1255.

Pease, A.C., Solas, D., Sullivan, E.J., Cronin, M.T, Holmes, C.P., Fodor, S.P. (1994) Light-generated oligonucleotide arrays for rapid DNA sequence analysis. PNAS 91:5022-5026.

Pevsne, J. (2003) Bioinformatics and functional genomics. John Wiley & Sons eds., Inc. Hoboken, New Jersey.

Powers, T. (2004) Nematode molecular diagnostics: from bands to barcodes. Annu. Rev. Phytopathol. 42:367-383.

Redman, J.C., Haas, B.J., Tanimoto, G. and Town, C.D. (2004) Development and evaluation of an Arabidopsis whole genome Affymetrix probe array. Plant J. 38:545-61.

Reimers, M. (2005) Statistical analysis of microarray data. Addiction Biol. 10:23-35.

Rensink, W.A. and Buell, C.R. (2005) Microarray expression profiling resources for plant genomics. Trends Plant Sci.10:603-609.

Saha, S., Sparks, A.B., Rago, C., Akmaev, V., Wang, C.J., Vogelstein, B., Kinzler, K.W. and Velculescu, V.E. (2002) Using the transcriptome to annotate the genome. Nat Biotechnol 20:508-512.

Sanger, F, Nicklen, S. and Coulson, A.R. (1977) DNA sequencing with chain-terminating inhibitors. Proc Natl Acad Sci U S A. 74:5463-7.

Sasser, J.N. and Freckman, D.W. (1987) A world perspective on nematology: the role of the Society. In: Vistas on Nematology, Veech J.A. and Dickson D.W. eds.,, Hyatssville: Society of Nematologists, 7-14.

Schena, M. (1996) Genome analysis with gene expression microarrays. Bioessays.18:427-31.

Schena M. (1999) DNA Microarrays - a Practical Approach. Oxford University Press.

Schena, M., Shalon, D., Davis, R.W. and Brown, P.O. (1995) Quantitative monitoring of gene expression patterns with a complementary DNA microarray. Science 270: 467-470.

Sijmons, P.C., Grundler, F.M.W., von Mende, N., Burrows, P.R. and Wyss, U. (1991) Arabidopsis thaliana as a new model host for plant-parasitic nematodes. Plant J. 1:245-254.

Sobczak, M., Golinowski, W., and Grundler, F.M.W. (1997) Changes in the structure of *Arabidopsis thaliana* roots induced during development of males of the plant parasitic nematode *Heterodera schachtii*. Europ.J.Plant Pathol. 103:113-124.

Southern, E.M. (1975) Detection of specific sequences among DNA fragments separated by gel electrophoresis. J. Mol. Biol. 98:503-517.

Steinhoff, C. andVingron, M. (2006) Normalization and quantification of differential expression in gene expression microarrays. Brief. Bioinformatics 7:166-177.

Turner, S. and Janet, A.R. (2006) Cyst Nematodes. In: Plant Nematology. Perry, R.N. and Moens, M. eds., CABI North American Office, 91-122.

Tytgat, T., Meutter, J.D., Gheysen, G. and Coomans, A. (2000) Sedentary endoparasitic nematodes as a model for other plant parasitic nematodes. Nematology 2:113-121.

Velculescu, V.E., Zhang, L., Vogelstein, B., Kinzler, K.W. (1995) Serial analysis of gene expression. Science 270:484-487.

Vos. P., Hogers, R., Bleeker, M, Reijans, M., van de Lee, T., Hornes, M., Frijters, A., Pot, J., Peleman, J., Muiper, M. and Zabeau, M. (1995) AFLP: a new concept for DNA fingerprinting. Nucleic Acids Res. 21:4407-4414.

Webster, J.M. (1995) The Host-Parasite Relationships of Plant-Parasitic Nematodes In: Advances in Parasitology. Dawes, B. ed., ACADEMIC PRESS INC., 36:1-31

Wilhelm, B.T. and Landry, J.R. (2009) Transcriptome analysis by strand-specific sequencing of complementary DNA. Methods 48:249-257.

Williamson, V.M. and Gleason. C.A. (2003) Plant-nematode interactions. Current Opinion in Plant Biology 6:327-333.

Wortman, J.R., Haas, B.J., Hannick, L.I., *et al.* (2003) Annotation of the Arabidopsis genome. Plant Physiol 132:461-468.

Wu, Z., Irizarry, R.A., Gentleman, R., Martinez-Murillo, F. and Spencer, F. (2004) A model based background adjustment for oligonucleotide expression arrays. J. Am. Stat. Assoc. 99:909-917.

Wyss, U. (1997) ROOT PARASITIC NEMATODES: AN OVERVIEW. In: Cellular and Molecular Aspects of Plant-Nematode Interactions. Fenoll C., Grundler F.M.W. and Ohl S.A., eds., Dordrecht: Kluwer Academic Publishers, 5-22.

Wyss, U. (2002) Feeding Behaviour of Plant-Parasitic Nematodes. In: The Biology of Nematodes. Lee, D.L. ed., Taylor & Francis, London, 635.

Zhu, T. and Wang, X. (2000) Large-scale profiling of the Arabidopsis transcriptome. Plant Physiol. 124:1472-1476.

CHAPTER 2

The transcriptome of syncytia induced by the cyst nematode *Heterodera schachtii* in Arabidopsis roots

Szakasits, D., Heinen, P., Wieczorek, K., Hofmann, J., Wagner, F., Kreil, D.P., Sykacek, P., Grundler, F.M.W. and Bohlmann, H.

The Plant Journal (2009) 57:771-784.

the plant journal

SOCIETY FOR EXPERIMENTAL BIOLOGY

The Plant Journal (2009) **57**, 771–784 doi: 10.1111/j.1365-313X.2008.03727.x

The transcriptome of syncytia induced by the cyst nematode *Heterodera schachtii* in Arabidopsis roots

Dagmar Szakasits[1], Petra Heinen[1], Krzysztof Wieczorek[1], Julia Hofmann[1], Florian Wagner[2,†], David P. Kreil[3], Peter Sykacek[3], Florian M. W. Grundler[1] and Holger Bohlmann[1,*]

[1]*Institute of Plant Protection, Department of Applied Plant Sciences and Plant Biotechnology, University of Natural Resources and Applied Life Sciences, Vienna, Austria,*

[2]*RZPD German Resource Center for Genome Research, Berlin, Germany, and*

[3]*WWTF Chair of Bioinformatics, Department of Biotechnology, University of Natural Resources and Applied Life Sciences, Vienna, Austria*

Received 9 April 2008; revised 10 July 2008; accepted 23 September 2008; published online 9 December 2008.

[*]For correspondence (fax: +43 1 47654 3359; e-mail holger.bohlmann@boku.ac.at).

[†]Present address: ATLAS Biolabs GmbH, Berlin, Germany.

Summary

***Arabidopsis thaliana* is a host for the sugar beet cyst nematode *Heterodera schachtii*. Juvenile nematodes invade the roots and induce the development of a syncytium, which functions as a feeding site for the nematode. Here, we report on the transcriptome of syncytia induced in the roots of Arabidopsis. Microaspiration was employed to harvest pure syncytium material, which was then used to prepare RNA for hybridization to Affymetrix GeneChips. Initial data analysis showed that the gene expression in syncytia at 5 and 15 days post-infection did not differ greatly, and so both time points were compared together with control roots. Out of a total of 21 138 genes, 18.4% (3893) had a higher expression level and 15.8% (3338) had a lower expression level in syncytia, as compared with control roots, using a multiple-testing corrected false discovery rate of below 5%. A gene ontology (GO) analysis of up- and downregulated genes showed that categories related to high metabolic activity were preferentially upregulated. A principal component analysis was applied to compare the transcriptome of syncytia with the transcriptome of different Arabidopsis organs (obtained by the AtGenExpress project), and with specific root tissues. This analysis revealed that syncytia are transcriptionally clearly different from roots (and all other organs), as well as from other root tissues.**

Keywords: Arabidopsis, plant pathogen, *Heterodera schachtii*, syncytium, transcriptome, Affymetrix GeneChip.

Introduction

Biotrophic plant parasites derive all of their nutrients from living plant tissues. Such a lifestyle has been developed by bacteria, fungi and oomycetes, and animals. All of them face similar problems: to be successful, they have to make intimate contact with their host while avoiding a resistance response, and they have to produce specific structures for the uptake of nutrients, such as the haustoria produced by powdery mildews. Plant parasitic nematodes of the family *Heteroderidae* induce the development of specialized feeding structures in the roots of their host plants, which consist of a syncytial fusion of hypertrophied cells. The syncytia are the only nutrient source for these nematodes, and are thus a severe nutrient sink for the host. The nematodes feed from the syncytium through a feeding tube that is produced at the tip of the stylet during each feeding cycle (Davis *et al.*, 2004; Williamson and Kumar, 2006). The nematodes invade the roots with the help of their stylet, assisted by secretions produced from two subventral pharyngeal gland cells that have been shown to contain cell wall degrading enzymes, such as cellulases and pectinases, as well as a putative expansin (Kudla *et al.*, 2005; Smant *et al.*, 1998; Vanholme

et al., 2004). Having reached the central cylinder, the nematode selects a single cell that is carefully pierced by the stylet. In Arabidopsis, the initial syncytial cells are preferably procambium or pericycle cells within the central cylinder (Golinowski *et al.*, 1996; Sobczak *et al.*, 1997). From this cell the development of the syncytium is initiated through secretions of the nematode, and by a coordinated expression of plant genes. Such plant genes include, for instance, expansins and cellulases, which are important for the degradation of cell walls to incorporate new cells into the growing syncytium (Goellner *et al.*, 2001; Wieczorek *et al.*, 2006, 2008). Cells incorporated into the syncytium undergo drastic changes in structure and activity. The central vacuole is fragmented into many smaller ones and the cells become metabolically active, as indicated by the dense granular cytoplasm, large numbers of mitochondria, ribosomes, and a proliferation of the endoplasmic reticulum (Golinowski *et al.*, 1996; Sobczak *et al.*, 1997). To cope with this high metabolic acivity, the nuclei and nucleoli are enlarged, and contain endoreduplicated DNA (Niebel *et al.*, 1996). Although the syncytium is a plant-derived structure, it is also dependent on the continuous activity of the nematode, because death or artificial removal of the nematode leads to a degradation of the syncytium. How exactly the nematode induces the development of the syncytium is currently unknown, although a few proteins that are produced by the dorsal pharyngeal gland cell that might be involved in this activity have been identified (Jaubert *et al.*, 2002; Vanholme *et al.*, 2004).

The structurally visible drastic changes in cell morphology imply an underlying global change in gene expression. Indeed, a number of genes have been identified that are particularly induced in syncytia or in giant cells, using a variety of methods such as differential display and promoter tagging, as reviewed by Gheysen and Fenoll (2002). During recent years the methodology has shifted towards microarrays and GeneChips, which allow a global view on the changes in gene expression in feeding sites. As a first approach, whole roots or dissected root segments of Arabidopsis roots infected with *Heterodera schachtii* (Puthoff *et al.*, 2003) and soybean roots infected with *Heterodera glycines* (Alkharouf *et al.*, 2006; Ithal *et al.*, 2007a; Klink *et al.*, 2007a) were used. Recently, laser capture microdissection and Affymetrix GeneChips have been used to study the transcriptome of syncytia induced in soybean roots by *H. glycines* (Ithal *et al.*, 2007b; Klink *et al.*, 2007b).

The rather wide host range of the sugarbeet cyst nematode *H. schachtii* has been exploited to use the interaction with *Arabidopsis thaliana* roots as a model system. The translucent roots growing on artificial media have made it possible to study the behavior of this and other nematode species inside the root (Wyss and Grundler, 1992). *H. schachtii* can complete its whole life cycle on Arabidopsis plants *in vitro* within 6 weeks (Sijmons *et al.*, 1991). Now, the availability of microarrays makes it possible to study the transcriptome of feeding sites induced in Arabidopsis roots. Puthoff *et al.* (2003) used the first-generation Affymetrix Arabidopsis GeneChip, which covers ~30% of the genome. They compared whole roots infected with *H. schachtii* or *H. glycines* at 3 days post-infection (dpi) with control roots (Puthoff *et al.*, 2003), and identified 128 and 12 genes, respectively, with altered steady-state mRNA levels after nematode infection.

The second-generation ATH1 Arabidopsis GeneChip, which contains probes covering ~75% of the genome, was used by Hammes *et al.* to study *Meloidogyne incognita* galls on Arabidopsis roots, but only the expression of 1400 genes coding for transport proteins was reported (Hammes *et al.*, 2005). Similarly, Jammes *et al.* studied *M. incognita* galls using the CATMA microarrays, which contain probes for 22 089 genes (Jammes *et al.*, 2005).

Previous reports concerning studies of gene expression in Arabidopsis feeding sites were hampered by the fact that the material used contained not only material from the feeding cells, but also included surrounding tissue. It is thus difficult to differentiate between gene expression in feeding cells and in the surrounding tissue. In studies that used the whole-root system, these expression patterns were even overlain with systemic expression from elsewhere in the root system. To avoid these problems, our approach has been to isolate pure syncytium material by microaspiration, thereby enabling a transcriptome analysis of syncytia alone. In this way, we were able to monitor and analyze the expression of 21 138 genes at different time points during the interaction of *H. schachtii* with Arabidopsis roots. Our results reveal the transcriptome of syncytia, and show that they are clearly different from roots and all other organs.

Results

Syncytia that develop inside the roots can be microaspirated to obtain pure syncytium material, without contaminating root tissues (Juergensen *et al.*, 2003). We have used this technique to obtain material for a transcriptome analysis of syncytia at 5 and 15 dpi.

The development of the syncytium starts from an initial syncytial cell in the central cylinder of the root, selected by the nematode (Golinowski *et al.*, 1996; Wyss and Grundler, 1992). Therefore, the preferred control would have been material from such cells before induction. This was, however, technically impossible. We have therefore used root segments from 12-day-old plants (0 dpi), corresponding to the elongation zone, and have excluded root tips and secondary root primordia.

Total RNA was isolated, amplified, and hybridized to Affymetrix ATH1 GeneChips (as described in detail in Experimental procedures).

Our initial strategy was to analyze the development of the syncytium over time. However, in line with analysis results showing that only a few transcripts were significantly different between syncytia at 5 and 15 dpi, instead of treating the data as a time series, we used a linear model of effects, with one contrast giving the differences between both (combined) syncytia tissues and the controls, and another contrast examining the remaining differences between syncytia at 5 and 15 dpi.

Broad trends in gene expression, in comparison with previously published data sets, were visualized using principal component analysis (PCA).

In an analysis of differential expression, the transcriptome of syncytia was observed to be very different from the control root samples. Table S1 presents the complete results from comparing the syncytium samples (at both 5 and 15 dpi) with controls. A total of 7231 genes (34.2%) were differentially expressed for a false discovery rate cut-off of $q < 5\%$, after correction for the multiple testing of 21 138 genes. Compared with the control, in syncytia 18.4% (3893) of all genes had a higher expression level, and 15.8% (3338) had a lower expression level. The average expression levels, and differences between syncytia and controls, for the 100 most significantly differentially expressed genes, are shown in Figure S1.

Upregulated genes

Table S2 takes an alternative view, showing the list of 100 genes that have the highest increase in expression compared with the controls. Among these upregulated genes, several genes encode proteins that are probably involved in the degradation of cell walls, a process that is important for the expansion of the syncytium: pectate lyase family proteins *At3g27400* and *At4g24780*, as well as expansins ATEXPA6 (*At2g28950*) and ATEXPA1 (*At1g69530*) (Wieczorek *et al.*, 2006). Several other genes code for chloroplast proteins such as glyceraldehyde 3-phosphate dehydrogenase A (*At3g26650*), cytochrome B6-F complex iron-sulfur subunit (*At4g03280*) and several chlorophyll *a*–*b* binding proteins (*At3g54890*, *At5g54270*, *At2g40100*, *At4g10340*, *At1g15820* and *At5g01530*).

Downregulated genes

On the other hand, if we look at the list of genes that showed a strong decrease in expression level, we find two prominent groups of genes (Table S3). One strongly over-represented group comprises genes coding for peroxidases. Among the 3338 downregulated genes were 35 peroxidases, representing an odds ratio of 4.6 (95% confidence interval, CI, 2.8–7.3), $P < 10^{-9}$, Fisher's exact test, compared with the number of peroxidase genes assessed on the chip. The effect was even more pronounced when we focussed on the 100 differentially expressed genes with the strongest decrease in expression. These include 14 peroxidases, corresponding to an odds ratio of 47 (CI 24–89), $P < 10^{-15}$. In contrast, only one gene coding for a (chloroplast) peroxidase was found among the 100 genes with the strongest significant increase in expression (Table S2), a number compatible with the representation of peroxidases on the chip. The second prominent group of genes over-represented are those that code for major intrinsic proteins (MIPs), which include aquaporins (Wallace and Roberts, 2004). Arabidopsis has 35 MIP genes, and nine of them were among the list of 100 genes with a strong decrease in expression level, corresponding to an odds ratio of 73 (CI 29–164), $P < 10^{-12}$. Contingency tables for all tests are provided in the Table S4(a,b).

Highly expressed genes

Genes can also be viewed according to their expression level in the syncytium (Table S5). The most strongly expressed genes typically had only slightly higher expression levels in the syncytia, compared with the control roots. As we go down the list, more and more genes show no significant differences. The genes most strongly expressed included those coding for proteins involved in primary metabolism, such as ribosomal proteins.

Differences between 5- and 15-day-old syncytia

In a comparison of 5- and 15-day-old syncytia, only 22 genes were differentially expressed with a false discovery rate cut-off of $q < 5\%$, after correction for multiple testing. Of these, 19 genes were more highly expressed in 15-dpi syncytia, as compared with 5-dpi syncytia, whereas only three genes were more highly expressed in 5-dpi syncytia than in 15-dpi syncytia (Table S6). Results for all genes are shown in Table S7, and the high degree of similarity of 5- and 15-dpi samples is also reflected in MA plots (Figure S2). Whereas many of the differentially expressed genes have no known function, two of the genes that were more highly expressed in 15-dpi syncytia code for phytosulfokines (Yang *et al.*, 2001).

Validation of GeneChip data

We have already published a detailed expression analysis of expansins (Wieczorek *et al.*, 2006) and endo-1,4-β-glucanases (Wieczorek *et al.*, 2008), in relation to the formation of syncytia induced in Arabidopsis roots by *H. schachtii*. In these studies, the differential expression of 29 and 25 genes, respectively, was validated using *in situ* RT-PCR, RT-PCR, and promoter:*gus* lines. Furthermore, several genes involved in starch metabolism in syncytia have also been validated recently (Hofmann *et al.*, 2008). Therefore, we

Table 1 qPCR validation

Accession number	Function	Chip data-fold change (log_2)		qPCR-fold change (log_2)	
		5-dpi versus ct	15-dpi versus ct	5-dpi versus ct	15-dpi versus ct
At3g63140	Putative mRNA-binding protein	6.3	6.5	–	∞
At5g64080	Lipid transfer protein	5.3	4.5	–	∞
At1g10010	AAP8; amino acid permease	2.9	6.1	–	6.2
At1g22710[a]	AtSUC2; phloemspec. sucrose transporter	−0.6	0.0	−1.5	−1.0
At1g09960[a]	AtSUC4; phloemspec. sucrose transporter	0.8	0.9	−0.9	0.3
At4g05320[b]	UBQ10; polyubiquitin	−0.5	−0.4	−1.1	−0.3
At3g18780[b]	ACT2; actin 2	−1.0	−1.6	−2.3	−1.1
At5g10790[b]	UBP22; ubiquitin-specific protease	−0.4	−0.4	−0.7	−0.6
At1g32900[c]	GBSS1; starch synthase	4.4	6.1	3.6	3.5
At5g24300[c]	SS1; starch synthase	3.7	4.4	2.6	2.6
At3g29320[c]	PHS1; starch phosphorylase	5.2	4.7	2.3	2.1
At5g03650[c]	SBE2; branching enzyme	3.3	4.1	1.2	2.0
At4g39210[c]	APL3; ADP-glc pyrophosphorylase	3.2	3.1	3.3	2.8
At3g46970[c]	PHS2; starch phosphorylase	3.2	3.1	1.7	1.9

The fold change of 5- and 15-dpi syncytia, as compared to control roots, is shown on a log_2 scale. For the first three genes, only one time point was measured via qPCR, whereas for the remaining genes investigated in previous studies ([a]Hofmann *et al.*, 2007; [b]Hofmann and Grundler, 2007; [c]Hofmann *et al.*, 2008), both time points were measured. For both *At3g63140* and *At5g64080* no RNA was detected in the control, making it impossible to calculate a fold change value (indicated by ∞).

have only selected three additional genes for further analysis using qPCR and *in situ* RT-PCR in the present study: *At3g63140* codes for a putative mRNA binding protein (84-fold upregulated, significance rank 40), *At5g64080* codes for a lipid transfer protein (30-fold upregulated, significance rank 1159), and *At1g10010* codes for an amino acid permease (AAP8, 23-fold upregulated, significance rank 259). All three genes showed a strong upregulation in syncytia as compared with roots. Of these, only expression of *At1g10010* was detectable in uninfected control root segments by real-time PCR, but transcripts for all three genes were detected in syncytia (Table 1). As no expression was detected for *At3g63140* and *At5g64080* in control root segments, it was not possible to formally calculate a fold change value. The *in situ* RT-PCR revealed that all genes showed a strong expression in syncytia. *At3g63140* and *At5g64080*, but not *At1g10010*, were found to be slightly expressed in the surrounding tissue. For the last two genes, specific staining was also detected in the phloem of uninfected roots, whereas in control reactions without polymerase only non-specific background staining was found (Figure 1a–i).

Genes involved in syncytium formation and maintenance

In analogy with the procedure described by Jammes *et al.* (2005), we explored the regulation of 'biological processes' and 'molecular functions', and their distribution across 'cellular components', according to the gene ontology classification (GO; http://www.geneontology.org), by comparing their representations in significantly up- and downregulated genes. To this end, for each of the 4278 GO categories used, we compared the prevalence in the 3885 GO annotated significantly upregulated genes, with the prevalence in the same number of downregulated genes (Fisher's exact test with Bonferroni correction). Conversely, its prevalence in the 3331 GO annotated significantly downregulated genes was compared with its prevalence in the same number of upregulated genes (full results in Table S8a,b). Categories of special interest are shown in Figures 2 and 3, and are outlined below. In our comparison of significantly up- and downregulated genes, for the domain 'cellular component', significantly more genes were upregulated for the categories 'chromosome', 'cytoplasm', 'intracellular organelle', 'mitochondrion', 'plastid', and 'ribosome'. Similarly, we found more upregulated genes than downregulated genes belonging to the 'biological process' categories 'biosynthetic process', 'cellular biosynthetic process', 'cellular metabolic process', 'macromolecular biosynthetic process', 'photosynthesis', and 'translation' (Figure 2a). On the other hand, this comparison identified categories of the 'biological process' domain, such as 'defense response', 'response to chemical stimulus', and 'response to hormone stimulus', with a significant over-representation of downregulated genes. Within the 'cellular component' domain, the category 'vacuole' included significantly more genes that were downregulated rather than upregulated (Figure 2b).

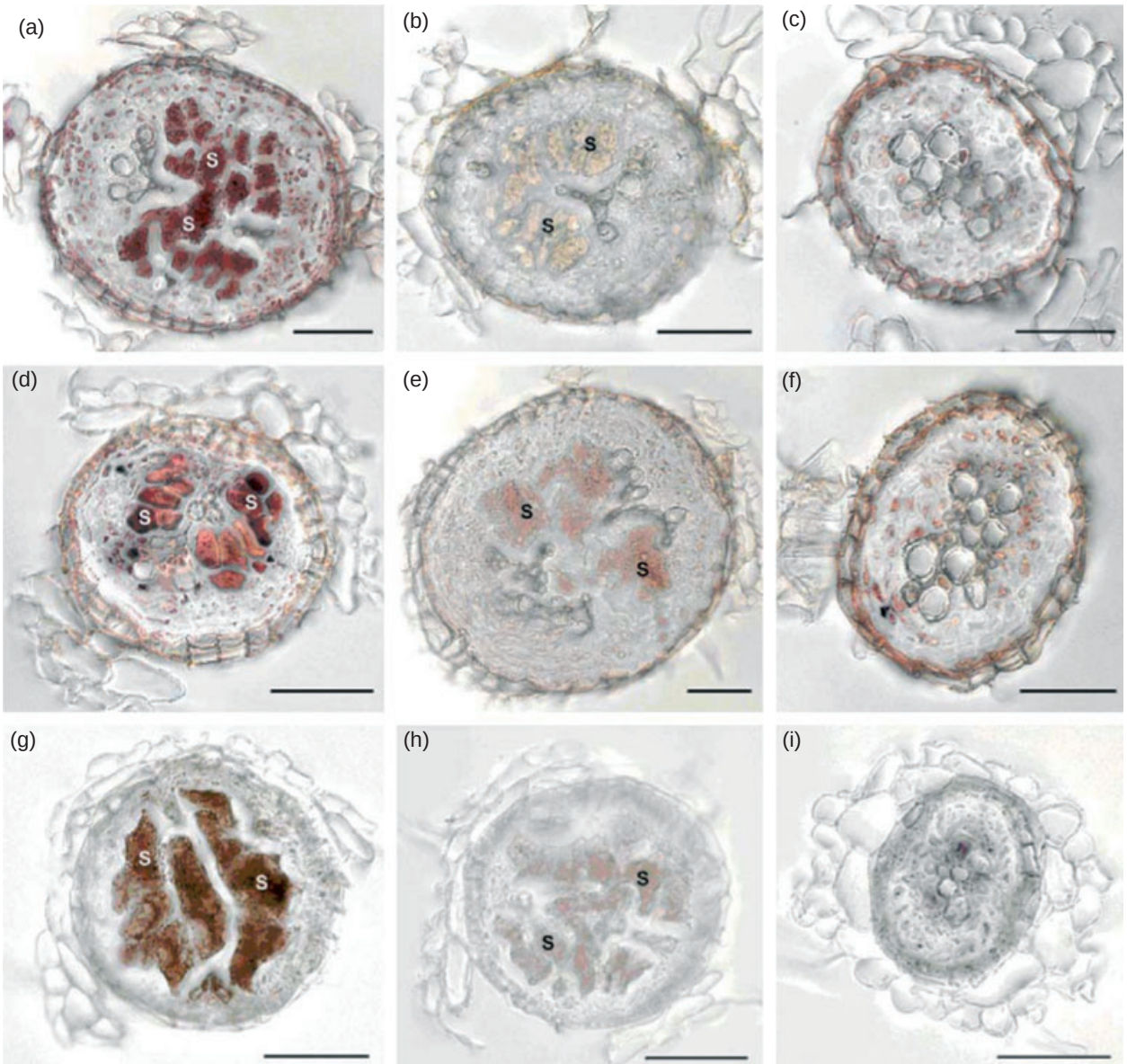

Figure 1. *In situ* RT-PCR analysis of three induced genes.
The expression of *At3g63140*, *At5g64080* and *At1g10010* was analyzed on cross sections of infected (15-dpi syncytia) and uninfected control roots of Arabidopsis (scale bar = 50 μm).
(a) Purple stained transcripts of *At3g63140* are visible within the syncytium (S), and only visible to a small extent in the surrounding tissue outside of the vascular cylinder.
(b) A control reaction for (a) on a syncytium performed without Taq polymerase shows neither specific staining in the infected part of the root (S) nor staining in any other root cells.
(c) Uninfected root sections show no staining of transcripts.
(d) Transcripts of *At5g64080* are mainly stained within the syncytium (S), with some staining in small cells adjacent to the syncytium.
(e) A control reaction for (d) without Taq polymerase on another syncytium shows no specific (purple) staining.
(f) In an uninfected root there is some typical transcript staining visible in the phloem.
(g) For *At1g10010*-specific transcripts, an intensive staining is restricted to cells within the syncytium (S) only.
(h) In a control reaction for (g) excluding Taq polymerase the whole cross-section through a syncytium does not show any specific staining.
(i) In an uninfected root staining of *At1g10010* is restricted to phloem cells.

The transcriptome of syncytia is distinct from that of roots or other organs

We analyzed the tissue-specific expression of the one hundred most strongly induced genes in Genevestigator (Zimmermann *et al.*, 2004) (Table S9), and noted that some strongly induced genes are not root-specific, but are instead expressed in seeds (such as *Pdf2.1*) or pollen (*MIOX4* and *MIOX5*). This is also reflected in a comparison of up- and downregulated genes in the categories 'repro-

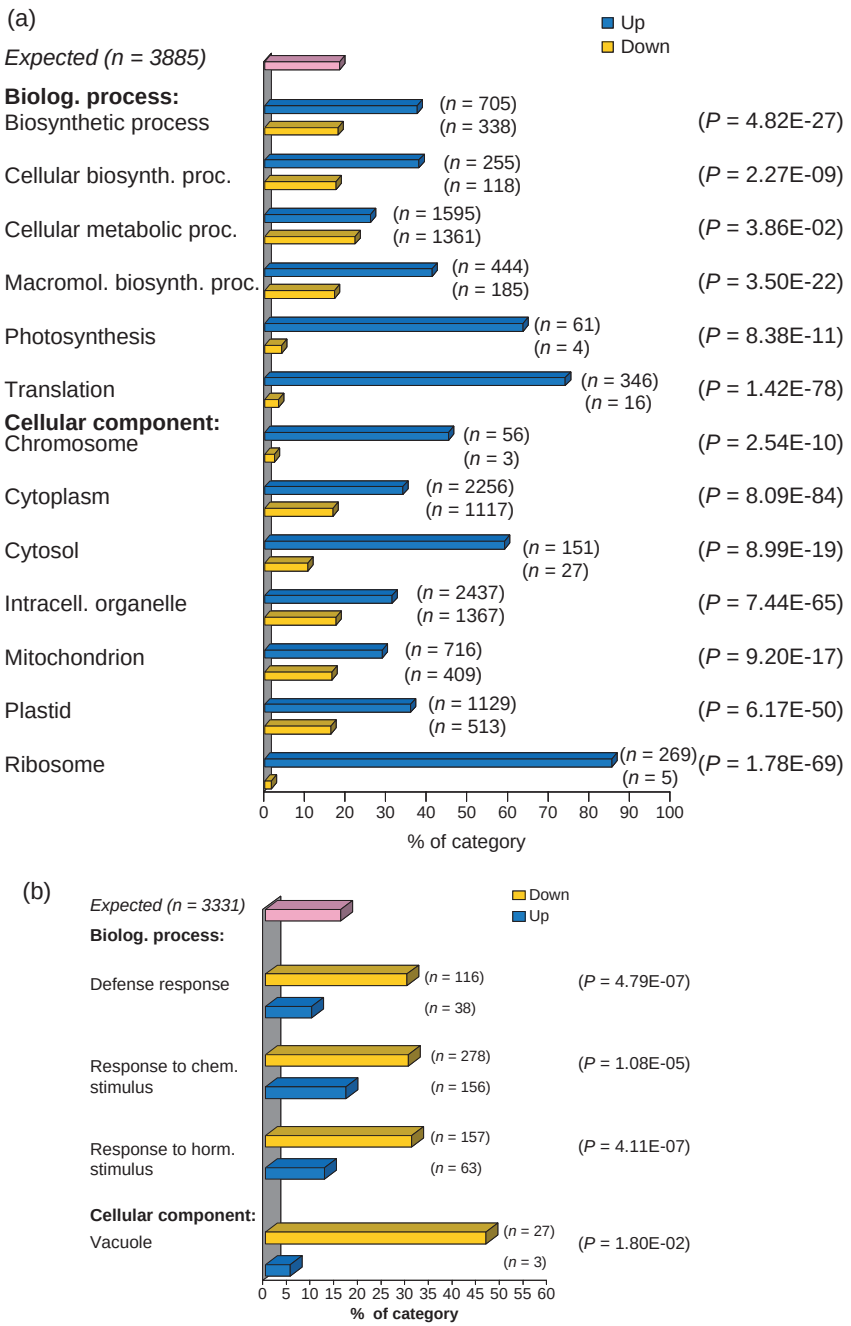

Figure 2. Preferential regulation in gene ontology (GO) categories with relevance to syncytium function.
Preferential regulation of differentially expressed genes for selected GO categories of the two domains 'biological process' and 'cellular component'. The percentage of genes found in the examined subset is shown on the *x*-axis. The first (pink) bar at the top of each panel thus plots the size of the examined gene set (3331 and 3385, respectively) relative to the chip size. This represents the ratio expected on average if the distribution of examined genes across GO categories matched that of all the genes tested on the chip. For each GO category, a pair of bars compares the numbers of repressed genes (yellow) and induced genes (blue), and the *P* value for this comparison is displayed on the right.
(a) Over-representation of upregulated genes compared with downregulated genes for a representative random selection of categories.
(b) Over-representation of downregulated genes compared with upregulated genes in four different subcategories of particular interest.

ductive process' and 'seed development' within the domain 'biological process' (Figure 3), where upregulated genes were significantly over-represented. To examine data with a global view, we compared the transcriptomes of syncytia with the transcriptomes of different Arabidopsis organs (flower, leaf, pollen, root and seed) obtained by the AtGenExpress project (Schmid *et al.*, 2005) by PCA. We also included transcriptome data from a project that used

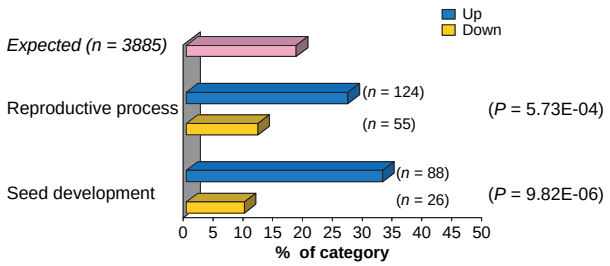

Figure 3. Preferential regulation in gene ontology (GO) categories related to reproduction.
GO categories showing over-representation of upregulated genes compared with downregulated genes within the domain 'biological process'. For details, see Figure 2.

fluorescence-activated cell sorting to isolate specific root tissues (Birnbaum *et al.*, 2003). Whereas the transcriptome of our root samples clustered together with the transcriptomes of whole roots of different stages and different root tissues, the syncytial transcriptomes were clearly separated (Figure 4). The separation on PCA component 1 clearly differentiates syncytia from root tissue. On the other hand, the samples did not cluster with any other organ tissues. Thus, although derived from root cells and inside the root, the transcriptome of the syncytium is clearly different from roots (and all other organs), as well as from other root tissues.

Discussion

A problem in analyzing gene expression in nematode feeding sites is that a plant root can only support a limited number of these feeding sites. Thus, if sampling total roots, the feeding sites will comprise only a small quantity of the root material, and it will therefore not be possible to differentiate gene expression in the syncytia from systemic expression in the root induced through nematode infection. For a thorough analysis it is therefore necessary to isolate pure material from feeding sites. We have used microaspiration of syncytia induced by the cyst nematode *H. schachtii* in Arabidopsis roots to isolate such pure material for a transcriptome analysis with Affymetrix GeneChips. Using the latest generation of Affymetrix Arabidopsis chips (ATH1), together with the current annotation by TAIR (http://www.arabidopsis.org), allowed a clear assessment of expression levels for 21 138 genes (Dai *et al.*, 2005).

Validation

For validation, we have compared the GeneChip results of three genes (*At3g63140, At5g64080* and *At1g10010*) with *in situ* RT-PCR and qPCR (Figure 1a–i and Table 1). It should be noted that for qPCR we are routinely using syncytia that are cut out from the roots, and thus also contain the surrounding root tissues, in comparison with the pure

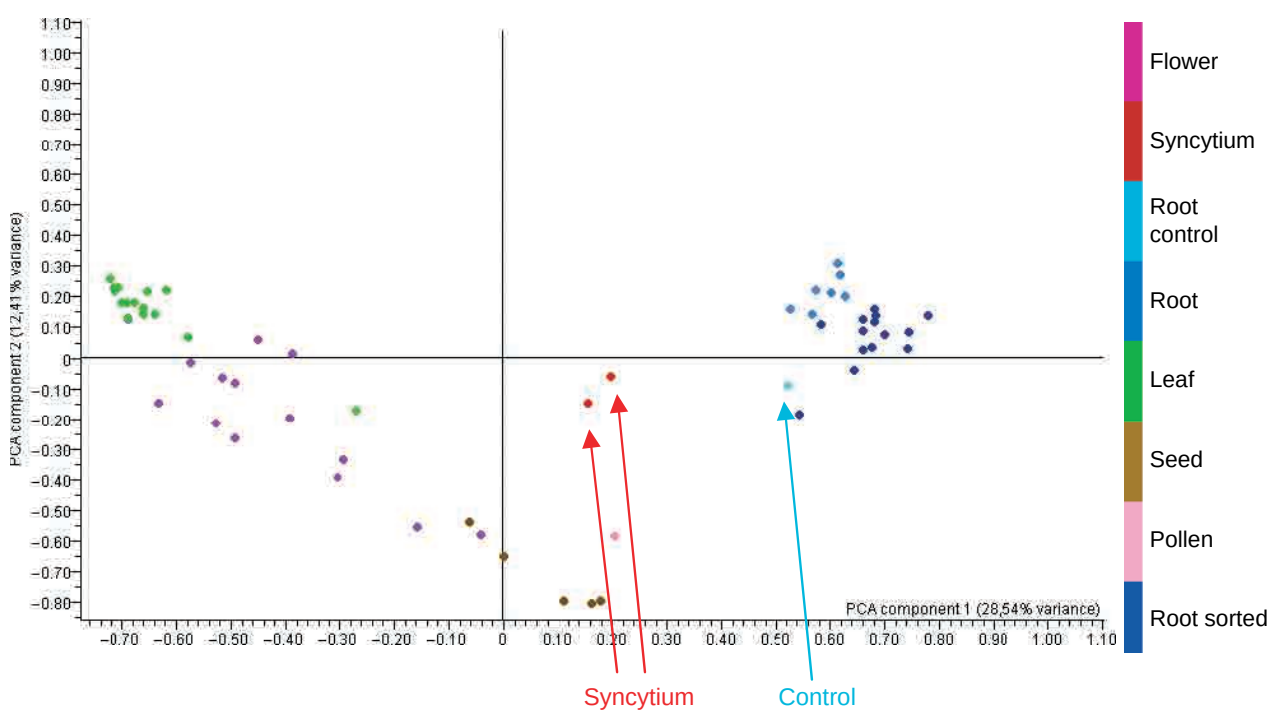

Figure 4. Principal component analysis.
PCA was applied to a total of 185 samples from three different studies. Each dot represents a condition (i.e. a specific tissue type), and colours code for specific plant organs. The control sample for the current study is indicated in turquoise, and the two different infection stages of the syncytium samples at 5 and 15 dpi are shown in red.

syncytium material that was obtained through microaspiration for GeneChip analysis. Expression levels obtained by these methods may therefore show quantitative differences, but the time needed to obtain material through microaspiration precludes their use as a routine method. In addition to the three genes validated in this paper, we have recently published a comprehensive analysis of expansin gene expression in syncytia, in which we have also validated this GeneChip dataset with *in situ* RT-PCR, promoter:*gus* lines, and semi-quantitative RT-PCR (Wieczorek *et al.*, 2006). Furthermore, the expression of endo-1,4-β-glucanases observed in this data set has been validated using *in situ* RT-PCR and qPCR (Wieczorek *et al.*, 2008). In addition, the expression of genes involved in sugar transport and starch metabolism has also been validated (Hofmann *et al.*, 2007, 2008). In all cases examined, the results of the GeneChip analysis were found to be reliable. For reference, we have also included the published qPCR values for these other genes in Table 1.

Cell wall degradation and synthesis in syncytia

Starting from a single initial cell, the syncytium expands by incorporating surrounding cells. The cell walls between these cells are partly degraded. It is known that nematodes produce a range of cell wall degrading enzymes in their gland cells (Vanholme *et al.*, 2004, 2006), which can be secreted through the stylet, but to what extent these enzymes might be involved in the cell wall degradation within the syncytium is not yet known. On the other hand, it is known that plant-derived genes for cell wall degrading enzymes (Goellner *et al.*, 2001), as well as expansin genes (Wieczorek *et al.*, 2006), are upregulated in syncytia. Analysis of the syncytial transcriptome showed that several expansin genes were specifically upregulated (Wieczorek *et al.*, 2006). Genes for putative cell wall degrading enzymes were also upregulated, and some of them were among the most strongly induced (Table S2), such as those coding for pectate lyases and for a β-glucanase (Wieczorek *et al.*, 2008). Thus, it is possible that the degradation of cell walls within the syncytium is solely achieved through endogenous plant proteins, and that the nematode-specific enzymes are only responsible for cell wall degradation and loosening during the passage of the nematodes through the plant root towards the central cylinder.

The formation of syncytia is, on the one hand, accompanied by a degradation of cell walls; on the other hand, cell wall synthesis is also needed, for instance, for producing cell wall ingrowths (Jones and Northcote, 1972; Sobczak *et al.*, 1997) that are commonly found close to the xylem, and for the thickening of the outer cell wall of the syncytium (Golinowski *et al.*, 1996). Cell wall ingrowths are also characteristic for transfer cells, which are thought to facilitate solute transport at the interface between the apoplast and the symplast (Offler *et al.*, 2002). In this regard it is also noteworthy that genes coding for myo-inositol oxygenase (MIOX) (Kanter *et al.*, 2005) were strongly expressed in syncytia. Three of the four Arabidopsis *MIOX* genes are represented on the GeneChip. Of these, *MIOX2* was approximately eightfold upregulated, and *MIOX4* and *MIOX5* were among the most strongly upregulated genes in syncytia (Table S2). The function of these genes in general is not totally clear, but MIOX4 and MIOX5 are otherwise highly expressed in pollen (Table S9). *MIOX* genes are probably involved in the production of UDP-glucuronic acid, an important precursor for several nucleotide sugars used in cell wall biosynthesis, but there are also indications from overexpression studies that they might be involved in the synthesis of ascorbate (Lorence *et al.*, 2004). UDP-glucuronic acid can also be produced through a second pathway, which uses UDP-glucose dehydrogenase, but the corresponding genes are expressed at the same level in syncytia and in control roots. Thus, the *MIOX* genes seem to play an important role for the function of syncytia. This issue is currently under further investigation in our laboratory.

Metabolic activity

For the host plant, the syncytia are sinks of nutrients. Other particularly important sinks are seeds and pollen. It is therefore interesting that genes of the GO categories 'seed development' and 'reproductive process' were preferentially upregulated in syncytia (Figure 3; Table S8a). Seeds and pollen are also characterized by high metabolic activity, with an overexpression of components of protein synthesis and metabolism observed in seeds and pollen (Schmid *et al.*, 2005). The same holds true for syncytia, which are also characterized by high metabolic activity. An examination of gene regulation for the category 'ribosome' of the GO domain 'cellular component' found a strong over-representation of upregulated genes (Figure 2a; Table S8a). Highlighting the biological significance of this observation, many ribosomal genes belong to the most strongly expressed genes (Table S5). Moreover, genes of the GO category 'translation' were preferentially upregulated, indicating a strong increase of protein biosynthesis. The high metabolic activity of syncytia was also reflected in the preferential upregulation of genes within the categories 'biosynthetic process', 'cellular biosynthetic process', 'cellular metabolic process', and 'macromolecule biosynthetic process' (Figure 2a). Although these are clear trends, many other GO categories and gene families have both up- and downregulated members. The expansin gene family is a nice example of this (Wieczorek *et al.*, 2006). High metabolic activity with similar numbers of upregulated and downregulated genes has also been observed for galls induced by the root-knot nematode *M. incognita* in Arabidopsis roots (Jammes *et al.*, 2005).

Transport of nutrients into syncytia

Syncytia are the only source of nutrients for the cyst nematodes throughout their life, and are therefore a severe nutrient sink for the plant. Up to recently, it was thought that syncytia are symplastically isolated, and that sucrose is taken up by the sucrose transporter *Suc2* (Juergensen *et al.*, 2003). Analysis of the transcriptome data presented here gave no indication that the *Suc2* gene was induced in syncytia. *Suc2* was expressed at low levels in both syncytia and control roots. This is in agreement with recent data implying the existence of plasmodesmata between syncytia and the phloem (Hofmann and Grundler, 2006; Hofmann *et al.*, 2007; Hoth *et al.*, 2005). Similarly, many other sugar transporters and sugar-metabolizing enzymes were not strongly induced in our experiment (J. Hofmann, P. Hess, D. Szakasits, A. Blöchl, A. van Bell, H. Bohlmann and F. Grundler, unpublished data).

Contrary to the moderate regulation of sugar transporters, we found a strong upregulation of an amino acid transporter (AAP6; Table S2). A second amino acid transporter of the same group (AAP8) was also upregulated in syncytia, and was among the few genes that were significantly more strongly expressed in 15-dpi syncytia than in 5-dpi syncytia (Table S6). These transporters are proton symporters, and seem to be especially needed for the transport of acidic amino acids (Okumoto *et al.*, 2002). It is not yet known if syncytia have a specific demand for acidic amino acids, or if these transporters might have a different function. The gene coding for AAP6 has been found to be only slightly upregulated in gall segments of Arabidopsis roots infected with *M. incognita* (Hammes *et al.*, 2005). Whether this is caused by a dilution effect of the giant cells with the surrounding material, or if there are fundamental differences between the amino acid transport into syncytia and giant cells, remains an open question. However, it once again highlights the importance of using pure material for a transcriptome analysis of nematode feeding sites.

Suppression of defense responses

Pathogens in general face the problem of coping with defense reactions of their hosts. Bacteria, for instance, produce a variety of effectors for this purpose (Debroy *et al.*, 2004; Jamir *et al.*, 2004). It has recently been shown that these can be delivered through a kind of molecular injection needle, the type-III secretion system, into the host cells (Galan and Wolf-Watz, 2006). By analogy, it can be expected that nematodes use their stylet to deliver effectors into syncytia. A range of different proteins that might act as such has been purified from nematodes *in vitro* (Vanholme *et al.*, 2004), but in most cases there is no clue yet as to their possible functions. Microneedles have been used to demonstrate that a mechanical stimulus comparable with the piercing of the cell wall by a nematode stylet induces defense reactions in plant cells (Gus-Mayer *et al.*, 1998). However, the transcriptome analysis of the syncytia presented in this paper shows that defense gene expression is repressed (Figure 2b), similar to the results obtained for galls induced by the root-knot nematode *M. incognita* in Arabidopsis roots (Jammes *et al.*, 2005). Whether the peroxidase genes, which were among the most strongly downregulated genes (Table S3), are also involved in defense responses, remains an open question.

An exception is the expression of a group of plant defensin genes (for a review see Thomma *et al.*, 2002). *Pdf2.2* and *Pdf2.3* were strongly expressed both in control root segments and in syncytia, and *Pdf2.1* was among the most strongly upregulated genes in syncytia (Table S2). It is not known whether these peptides are taken up by the nematode, although their small size indicates that this might be the case (Böckenhoff and Grundler, 1994). This would imply that at least these defensins have no effect on *H. schachtii* and, probably, other cyst nematodes.

Plastids in syncytia

Arabidopsis plants inoculated with nematodes are routinely grown in Petri dishes in a dark/night cycle to assist the observation and manipulation (such as microaspiration) of the infected plants (Sijmons *et al.*, 1991; Wyss and Grundler, 1992). It has been known for a long time that syncytia formed under these conditions contain chloroplasts (Golinowski *et al.*, 1996; Sijmons *et al.*, 1991). In accordance with these observations, we found that genes coding for chloroplast proteins were among the most strongly upregulated genes (Table S2), and that genes in the GO category 'plastid' were preferentially upregulated (Figure 2a). Furthermore, genes assigned to the GO category 'photosynthesis' were also preferentially upregulated (Figure 2a). Thus, at least under these growth conditions, syncytia contain plastids that seem to perform active photosynthesis. This would, of course, not be possible under natural conditions. We have therefore looked at syncytia from roots kept in the dark after infection. These syncytia have a comparable number of plastids that show a similar fluorescence in confocal microscopy as those from plants kept under a light/dark cycle (D. Szakasits, M. Sobczak and H. Bohlmann, unpublished data). Plastids within the syncytia are known to be different from those found in cells surrounding the syncytia (Golinowski *et al.*, 1996). Hence, our results corroborate that the differentiation of plastids is influenced by the syncytium.

The syncytial transcriptome

We noted that among the most strongly upregulated genes in syncytia were several that are otherwise specifically expressed in pollen or seeds (Table S9). This motivated us

to perform a PCA (Figure 4) to compare the transcriptome data from syncytia with those for different Arabidopsis organs and tissues. A similar approach has been reported for Arabidopsis organs (Schmid *et al.*, 2005), and for Arabidopsis root tissues obtained through cell sorting (Birnbaum *et al.*, 2003). Root tissues and root organs also clustered together in our analysis. In addition, the root control segments used in our work fell into the same cluster. Syncytia, however, were clearly located outside the root cluster, which also agreed with the global differences between syncytium and control root sections (18.4% of all genes analyzed were upregulated in syncytia, and 15.8% were downregulated for $q < 5\%$). Moreover, syncytia did not cluster with any other tissue types, including samples from flowers, leaves, pollen and seeds. This analysis therefore indicated that syncytia, although formed within the root, have a characteristic, unique transcriptional profile that is different from that of any other organ, and also from that of any other root tissue.

In a previous study (Puthoff *et al.*, 2003), a comparison of total roots infected with *H. schachtii* at 3 dpi with control roots identified 116 differentially expressed genes (71 upregulated and 45 downregulated), using the first generation Arabidopsis GeneChip, which covered approximately one third of all genes. There are several possible explanations of why that study has identified a much lower number of genes than our analysis. First, the current GeneChip probes more than twice the number of genes. Second, we have isolated pure syncytium material, and have specifically analyzed the changes within syncytia. Third, the differences in sampling time points might also affect results: syncytium material for this study was obtained at both 5 and 15 dpi. The expression differences between 3- and 5-dpi time points, however, seem to be only marginal (initial, sample count limited comparisons in this laboratory have identified only four genes showing significantly different expression levels; D. Szakasits, D. Kreil and H. Bohlmann, unpublished data).

If we compare the analyses of whole infected roots with those of the aspirated syncytia performed for this study, we find that 56 of the genes (34 up- and 22 downregulated) identified by Puthoff *et al.* (2003) are also differentially regulated in syncytia, for an agreement of almost 50%. The genes only identified by Puthoff *et al.* (2003) are probably genes that are systemically induced or repressed through nematode infection. The fact that no genes coding for ribosomal proteins were found in the Puthoff *et al.* (2003) study provides evidence corroborating this interpretation. Such genes have, however, been shown to be strongly expressed in nematode feeding sites in our analysis, and in other transcriptome studies (Ithal *et al.*, 2007b; Jammes *et al.*, 2005), and are indicative of the high metabolic activity in these feeding sites.

Other laboratories have also reported differences comparing excised infection sites versus syncytium material for transcriptome analysis (Ithal *et al.*, 2007b; Klink *et al.*, 2007b). The second study for instance found only two genes in common between the 77 genes induced in syncytia and the 502 genes induced in infected root samples at 3 dpi. These data also suggest that the majority of induced genes in infected whole root samples (Puthoff *et al.*, 2003) probably represent systemically induced genes.

Recently, laser capture microdissection has been applied to study syncytia induced by *H. glycines* in soybean roots, using Affymetrix GeneChips containing 37 744 probe sets (Ithal *et al.*, 2007b; Klink *et al.*, 2007b). In the first study, 1116 genes were induced at 2 dpi, and 649 genes were suppressed. In the second study, 77 genes were induced and 210 were suppressed at 3 dpi in a compatible interaction, whereas 206 were induced and 63 were suppressed at 8 dpi. Both studies used a –fold change cut-off of 1.5, and a 0.5 and 5% false discovery rate threshold, respectively. At present, it is not clear why more induced and repressed genes were identified in the first study. Whereas some small differences could probably be explained by the difference between the 2- and 3-dpi time points, the fact that the first study identified so many more genes is unexpected, particularly as it used a more stringent statistical cut-off. In addition, the second study identified three times more suppressed than induced genes at 3 dpi, whereas the relationship was completely different and reversed at 8 dpi. We currently have no explanation for this.

Ithal *et al.* identified 1116 upregulated and 649 downregulated genes in syncytia at 2 dpi. As expected, this study also revealed a high metabolic activity in syncytia, as shown by the upregulation of 35 genes coding for ribosomal proteins. These authors also found both up- and downregulated genes within gene families, matching our observations in the present study. Of the 1765 differentially regulated genes, 833 upregulated and 449 downregulated genes had homologs in Arabidopsis (collapsing many-to-one mappings). Expecting few gene expression differences between 3- and 5-dpi samples of syncytia induced by *H. schachtii* in Arabidopsis roots (D. Szakasits, D. Kreil and H. Bohlmann, unpublished data), we compared the gene lists for upregulated or downregulated genes from the Ithal *et al.* (2007b) study with our data. We found that of the 833 Arabidopsis homologs of upregulated soybean genes, 312 were also upregulated in syncytia induced by *H. schachtii* in the Arabidopsis roots. Of the 449 Arabidopsis homologs of downregulated soybean genes, 146 were also downregulated in syncytia induced by *H. schachtii* in Arabidopsis roots.

From a biological point of view, syncytia induced by related nematodes in different hosts should be quite similar in relation to their basic metabolism. This is reflected in the comparison here. The list of homologous genes that were upregulated in both systems includes, for instance, almost all of the genes coding for ribosomal proteins (all except

two). In soybean, eight genes homologous to six Arabidopsis expansin genes were upregulated. Of these, four genes were also upregulated in Arabidopsis syncytia (a 66–75% agreement). A detailed gene-level comparison of the differences between data sets is also likely to highlight the subtle effects of choice of sampling time point and differences in statistical analysis, and would require a comprehensive analysis of Arabidopsis and soybean homologs. Of course, paralogs may have diverged in both function and transcriptional regulation. Considering the many non-unique mappings, a reliable identification of orthologs would thus be part of the challenge. (For instance, the present data bases map seven soybean genes to the same putative peroxidase *At5g05340*.)

Conclusion

Our analysis has identified syncytia as having a characteristic, unique transcriptional profile. The expression of a large range of genes is changed in syncytia, compared with control roots, and the fundamental question that remains to be answered is how the formation of this organ is induced by the nematode. It is generally agreed that proteins secreted by the nematode are involved. Future work will be focused on linking the genes that are up- and downregulated in the syncytium to developmental pathways, and on linking these to the activity of nematode-derived effectors.

Experimental procedures

Plant cultivation

Seeds of Arabidopsis (cv. Columbia) were surface-sterilized for 10 min in 5% (w/v) calcium hypochlorite, submerged for 5 min in 70% (v/v) ethanol and were then washed three times in sterile water (Sijmons *et al.*, 1991). The sterilized seeds were then placed into sterile Petri dishes (∅ 9 cm) on a modified 0.2 concentrated Knop medium supplemented with 2% sucrose (Sijmons *et al.*, 1991). Seeds were kept at 4°C for 3 days prior to incubation in a growth chamber at 25°C, with a 16-h light and 8-h dark cycle.

Nematode infection

Heterodera schachtii was multiplied *in vitro* on mustard (*Sinapsis alba* cv. Albatros) roots growing on 0.2 concentrated Knop medium supplemented with 2% sucrose (Sijmons *et al.*, 1991). Hatching of L2 larvae was stimulated by soaking the cysts in sterile 3 mM $ZnCl_2$. The juveniles were washed four times in sterile water and resuspended in 0.5% (w/v) Gelrite for inoculation. Twelve-day-old roots of *A. thaliana* plants were inoculated with about 30 juveniles under axenic conditions.

RNA isolation

RNA was isolated from aspirated syncytia and root segments using the RNeasy Mini Kit (Qiagen, http://www.qiagen.com). The quality of all RNA samples was controlled by an Agilent 2100 Bioanalyzer (Agilent Technologies, http://www.home.agilent.com).

qPCR

RNA was transcribed into cDNA using random primers [oligo$(dN)_6$] and SuperScript III reverse transcriptase (Invitrogen, http://www.invitrogen.com), following the manufacturer's instructions. Gene-specific primers were selected using Primer Express v2.0 (Applied BioSystems, http://www.appliedbiosystems.com), and were checked for gene specificity within the Arabidopsis genome by a Blast search of the Arabidopsis gene data base. Primer sequences can be found in Appendix S1. *18S* RNA and *UBP22* were used as internal references, as described previously (Hofmann and Grundler, 2007).

Quantitative real-time PCR was performed in an ABI PRISM 7300 Sequence Detector (Applied BioSystems) using SYBR Green to monitor double-stranded DNA synthesis. The final PCR reaction

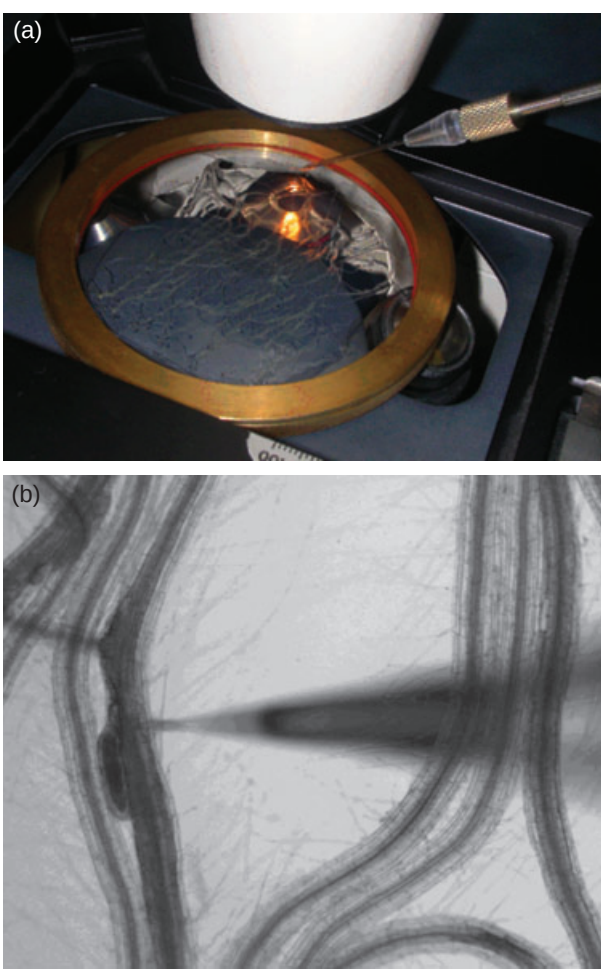

Figure 5. Experimental set-up for the microaspiration of infected Arabidopsis roots.
(a) A metal ring fixed under an inverse microscope (Zeiss, http://www.zeiss.com) holds a thin glass plate covered with medium enclosing the roots.
(b) A microcapillary is navigated towards the roots by a micromanipulator (Eppendorf, http://www.eppendorf.com) for piercing a single syncytium.

volume was 25 μl, containing 12.5 μl 2× Platinum SYBR Green qPCR SuperMix (Invitrogen), with UDG and ROX as reference dyes, primers and $MgCl_2$, dependent on primer pairs, water and 2 μl of cDNA template. Primer efficiencies and PCR conditions can be found in Appendix S1. cDNA was diluted 1:100 for *18S* RNA, and 1:2 for all other primers. As a control, water was added instead of cDNA, resulting in no detectable fluorescent signal. PCR was carried out at 50°C for 2 min and 95°C for 5 min, followed by 43 cycles at 95°C for 15 sec, at 60°C for 30 sec and at 72°C for 60 sec. Data analysis was carried out using the SEQUENCE DETECTION SOFTWARE (SDS) v2.0 (Applied BioSystems). Changes in transcript levels were related to the expression of *18S* RNA and *UBP22* using the formula $(1+E)^{-\Delta\Delta Ct}$ (Livak and Schmittgen, 2001).

In situ *RT-PCR*

In situ RT-PCR was performed exactly as described previously (Wieczorek *et al.*, 2006), using the same primers as for the real-time RT-PCR analysis (see Appendix S1).

Affymetrix GeneChip analysis

Arabidopsis plants were grown in Knop medium on thin glass plates, which were kept in Petri dishes under the conditions described above. They were inoculated with *H. schachtii* larvae after 12 days. The glass plates supporting the roots could then be removed from the Petri dishes for microscopy (Figure 5a). Cytoplasm from syncytia was obtained through microaspiration using an inverse microscope equipped with a microinjector (Figure 5b). The number of syncytia microaspirated was 346 for 5-dpi syncytia, and 191 for 15-dpi syncytia. These syncytia were collected from seven and five independent inoculations, respectively, but were pooled to obtain enough material for RNA amplification. Control root segments were cut from the elongation zone of uninfected roots, which were grown under the same conditions as described above. Special care was taken to avoid any root tips or lateral root primordia. Similarly as for infected material, uninfected root segments were collected as a pool from approximately 1000 plants that were grown in four independent batches.

RNA was isolated as described above. As the most variable part of the whole procedure is the amplification of the RNA using T7 RNA polymerase, we have performed at least three independent amplification experiments for each RNA pool, and have used each amplified copy RNA for the labeling and hybridization of one GeneChip. We hybridized four chips for 5-dpi samples, three chips for 15-dpi samples and four chips for control samples, with individual microarrays representing independent technical replicates. Biotin-labeled probes were prepared according to the Affymetrix protocol, with some modifications. For further details see Appendix S1.

Statistical analysis of microarray data

Affymetrix CEL files were read into the R statistical analysis environment (http://www.r-project.org) using the AFFY package of the BIOCONDUCTOR suite (http://www.bioconductor.org). As 10–40% of probe sets are affected by updated gene annotation, chips were processed with the current TAIR v8 probe-set annotation (Dai *et al.*, 2005). Probe sequence-specific 'background correction' (Wu *et al.*, 2004) was performed using routines available in the Bioconductor *gcrma* package. Using the 'affinity' model, although 'MM' probes were employed for the determination of affinity parameters, only 'PM' probes were used for the probe-specific background correction. An inspection of exploratory pairwise scatter and 'MA' plots confirmed the need for inter-chip normalization. Thus, the explicit normalization steps required made a subtraction of the heuristic estimate for optical instrument background, as offered in gcrma, unnecessary. Defaults were used for all other gcrma parameters. As an examination of pairwise quantile-quantile plots showed only random fluctuations, inter-chip normalization could be achieved using quantile-quantile normalization (Bolstad *et al.*, 2003). See the 'Low-level microarray analysis and diagnostic plots' section (Appendix S3) for diagnostic plots and figures.

After normalization, robust summaries of probe-set signals were obtained for each gene using an iterative weighted least-squares fit of a linear probe level model (Bolstad, 2004), through the *fitPLM* function of the Bioconductor package *affyPLM*. This process automatically identifies unreliable chip areas, and correspondingly downweights outlier probes. See Appendix S2 and S3.

The normalized data on a log2 scale were then fitted gene by gene with a linear model including hybridization batch effects, using the *lmFit* function (Smyth, 2004) of the BIOCONDUCTOR package *limma*. The result tables also include *q* values as indicators of significance of contrasts, after correction for multiple testing controlling the false discovery rate (Benjamini and Hochberg, 1995). For the statistical tests, individual gene variances have been moderated using an Empirical Bayes approach that draws strength from transferring variance characteristics from the set of all genes to the test for each individual gene (Smyth, 2004).

Full GO annotation was downloaded from TAIR on 6 Jan 2007 (http://www.arabidopsis.org). Annotation (including 'unknown' assignments) was available for almost all genes on the chip (99.6%, 21 053). To permit analyses of arbitrary GO categories, GO-IDs were processed resolving obsolete IDs (http://www.geneontology.org; rev. 1.287, 6 Jan 2007), secondary IDs/aliases (rev. 1.48, 5 Jan 2007), and annotation was revised for consistency by the fully recursive propagation of category membership to parent nodes. For each category, we then tested for relative enrichment of genes in the test set by comparison with the distribution of genes on the chip by Fisher's exact test and Bonferroni correction for multiple testing of the $N = 4279$ examined categories. This corresponds and is equivalent to the commonly employed tests using the hypergeometric distribution. Results are provided in the 'Analysis' section of Appendix S1.

To further characterize the nature of regulatory changes, in this paper we tested whether significantly regulated genes were preferentially up- or downregulated. In an assessment of the over-representation of upregulated genes in comparison with downregulated genes, we compared the distribution across GO categories of the 3885 annotated genes that were upregulated significantly for $q < 5\%$, with that of an equal number of the most significantly downregulated genes. Similarly, examining the over-representation of downregulated genes in comparison with upregulated genes, we compared the distribution across GO categories of the 3331 annotated genes that were downregulated significantly for $q < 5\%$ with that of an equal number of most significantly upregulated genes. *P* values for a significance assessment of the observed differences from the binomial distribution were Bonferroni corrected for testing of all GO categories ($N = 4279$), and are also provided in the 'Analysis' section of Appendix S1. Results for selected categories are presented in Figures 2(a,b) and 3.

The additional online material providing large, comprehensive tables and plots, and detailed technical analysis is archived at http://bioinf.boku.ac.at/pub/Szakasits2008/.

Principal component analysis

In total, 185 Affymetrix.CEL files from three different studies (Birnbaum *et al*., 2003; Schmid *et al*., 2005, this work) were directly loaded from the Affymetrix GeneChip Operating Software (GCOS) into GeneSpring v7.2 (Silicon Genetics; Agilent Technologies, http://www.home.agilent.com) applying the GeneSpring GCRMA probe summarization (robust multi-chip average, with GC-content background correction algorithm). After preprocessing the files, the following GeneSpring standard normalization steps for one-colour data were performed: (i) data transformation (set measurements from less than 0.01 to 0.01), (ii) per chip (normalized to the 50th percentile) and (iii) per gene (normalized to median).

In order to compare expression patterns of different tissue types, we performed a Principal Components Analysis of log-ratios for all of the different tissue samples. The data were then visualized by plotting samples in principal component space, utilizing the first two components, thereby explaining ~41% of the total expression variance. The relationship between the samples was then investigated by visually examining clusters in this reduced two-dimensional space.

Acknowledgements

This research was supported by grant QLK-CT-1999-01501 (NONEMA) from the European Union within the 5th Framework, FWF grant P16296-B06 and FWF grant P16897-B06. The WWTF Chair of Bioinformatics acknowledges funding by the Vienna Science and Technology Fund (WWTF), the Austrian Centre of Biopharmaceutical Technology (ACBT), Austrian Research Centres (ARC) Seibersdorf and Baxter AG.

Supporting Information

Additional Supporting Information may be found on the author's own website: http://bioinf.boku.ac.at/pub/Szakasits2008/:

Figure S1. MA plot for the syncytium versus the root. The 100 most significantly differentially expressed genes are marked.

Figure S2. MA plot for 5-dpi syncytium versus 15-dpi syncytium. All significantly differentially expressed genes are marked.

Table S1. Syncytium versus root. Expression of all genes.

Table S2. The 100 genes with the strongest significant increase in expression level compared with control roots.

Table S3. The 100 genes with the strongest significant decrease in expression level compared with control roots.

Table S4. Contingency tables and Fisher's exact test for the overrepresentation of the downregulated transcripts of major intrinsic proteins (MIPs) genes (a), and peroxidase genes (b).

Table S5. Syncytium versus root. Genes with a high expression level in syncytia.

Table S6. Genes with significant differences in expression level between 5- and 15-day-old syncytia, showing up- (a) and downregulation (b).

Table S7. 5- versus 15-dpi syncytium. Expression of all genes.

Table S8. Preferentially up- (a) and downregulated (b) gene ontology categories.

Table S9. Expression of the 100 strongest upregulated genes in Arabidopsis organs, according to Genevestigator.

Appendix S1. Methods.

Appendix S2. Archive of data and sample description tables.

Appendix S3. Low-level microarray analysis and diagnostic plots.

Please note: Wiley-Blackwell are not responsible for the content or functionality of any supporting materials supplied by the authors. Any queries (other than missing material) should be directed to the corresponding author for the article.

References

Alkharouf, N.W., Klink, V.P., Chouikha, I.B., Beard, H.S., MacDonald, M.H., Meyer, S., Knap, H.T., Khan, R. and Matthews, B.F. (2006) Timecourse microarray analyses reveal global changes in gene expression of susceptible *Glycine max* (soybean) roots during infection by *Heterodera glycines* (soybean cyst nematode). *Planta*, **224**, 838–852.

Benjamini, Y. and Hochberg, Y. (1995) Controlling the false discoveryrate: a practical and powerful approach to multiple testing. *J. R. Stat. Soc. Ser. B*, **57**, 289–300.

Birnbaum, K., Shasha, D.E., Wang, J.Y., Jung, J.W., Lambert, G.M., Galbraith, D.W. and Benfey, P.N. (2003) A gene expression map of the Arabidopsis root. *Science*, **302**, 1956–1960.

Böckenhoff, A. and Grundler, F.M.W. (1994) Studies on the nutrient uptake by the beet cyst nematode *Heterodera schachtii* by *in situ* microinjection of fluorescent probes into the feeding structures in *Arabidopsis thaliana*. *Parasitology*, **109**, 249–254.

Bolstad, B.M. (2004) *Low level analysis of high-density oligonucleotide array data: background, normalization and summarization*. PhD Dissertation. Berkeley: University of California.

Bolstad, B.M., Irizarry, R.A., Astrand, M. and Speed, T.P. (2003) A comparison of normalization methods for high density oligonucleotide array data based on bias and variance. *Bioinformatics*, **19**, 185–193.

Dai, M., Wang, P., Boyd, A.D. *et al.* (2005) Evolving gene/transcript definitions significantly alter the interpretation of GeneChip data. *Nucleic Acids Res.* **33**, e175.

Davis, E.L., Hussey, R.S. and Baum, T.J. (2004) Getting to the roots of parasitism by nematodes. *Trends Parasitol.* **20**, 134–141.

Debroy, S., Thilmony, R., Kwack, Y.B., Nomura, K. and He, S.Y. (2004) A family of conserved bacterial effectors inhibits salicylic acid-mediated basal immunity and promotes disease necrosis in plants. *Proc. Natl Acad. Sci. USA*, **101**, 9927–9932.

Galan, J.E. and Wolf-Watz, H. (2006) Protein delivery into eukaryotic cells by type III secretion machines. *Nature*, **444**, 567–573.

Gheysen, G. and Fenoll, C. (2002) Gene expression in nematode feeding sites. *Annu. Rev. Phytopathol.* **40**, 191–219.

Goellner, M., Wang, X. and Davis, E.L. (2001) Endo-beta-1,4-glucanase expression in compatible plant-nematode interactions. *Plant Cell*, **13**, 2241–2255.

Golinowski, W., Grundler, F.M.W. and Sobczak, M. (1996) Changes in the structure of Arabidopsis thaliana induced during development of females of the plant parasitic nematode *Heterodera schachtii*. *Protoplasma*, **194**, 103–116.

Gus-Mayer, S., Naton, B., Hahlbrock, K. and Schmelzer, E. (1998) Local mechanical stimulation induces components of the pathogen defense response in parsley. *Proc. Natl Acad. Sci. USA*, **95**, 8398–8403.

Hammes, U.Z., Schachtman, D.P., Berg, R.H., Nielsen, E., Koch, W., McIntyre, L.M. and Taylor, C.G. (2005) Nematode-induced changes of transporter gene expression in Arabidopsis roots. *Mol. Plant Microbe Interact.* **18**, 1247–1257.

Hofmann, J. and Grundler, F.M.W. (2006) Females and males of root-parasitic cyst nematodes induce different symplasmic connections between their syncytial feeding cells and the phloem in *Arabidopsis thaliana*. *Plant Physiol. Biochem.* **44**, 430–433.

Hofmann, J. and Grundler, F.M.W. (2007) Identification of reference genes for qRT-PCR studies of gene expression in giant cells and syncytia induced in *Arabidopsis thaliana* by *Meloidogyne incognita* and *Heterodera schachtii*. *Nematology*, **9**, 317–323.

Hofmann, J., Wieczorek, K., Blöchl, A. and Grundler, F.M.W. (2007) Sucrose supply to nematode-induced syncytia depends on the apoplasmic and the symplasmic pathway. *J. Exp. Bot.* **58**, 1591–1601.

Hofmann, J., Szakasits, D., Blöchl, A., Sobczak, M., Daxböck-Horvath, S., Golinowski, W., Bohlmann, H. and Grundler, F.M.W. (2008) Starch serves as carbohydrate storage in nematode-induced syncytia. *Plant Physiol.* **146**, 228–235.

Hoth, S., Schneidereit, A., Lauterbach, C., Scholz-Starke, J. and Sauer, N. (2005) Nematode infection triggers the de novo formation of unloading phloem that allows macromolecular trafficking of green fluorescent protein into syncytia. *Plant Physiol.* **138**, 383–392.

Ithal, N., Recknor, J., Nettleton, D., Hearne, L., Maier, T., Baum, T.J. and Mitchum, M.G. (2007a) Parallel genome-wide expression profiling of host and pathogen during soybean cyst nematode infection of soybean. *Mol. Plant Microbe Interact.* **20**, 293–305.

Ithal, N., Recknor, J., Nettleton, D., Maier, T., Baum, T.J. and Mitchum, M.G. (2007b) Developmental transcript profiling of cyst nematode feeding cells in soybean roots. *Mol. Plant Microbe Interact.* **20**, 510–525.

Jamir, Y., Guo, M., Oh, H.S., Petnicki-Ocwieja, T., Chen, S., Tang, X., Dickman, M.B., Collmer, A. and Alfano, J.R. (2004) Identification of *Pseudomonas syringae* type III effectors that can suppress programmed cell death in plants and yeast. *Plant J.* **37**, 554–565.

Jammes, F., Lecomte, P., Almeida-Engler, J., Bitton, F., Martin-Magniette, M.L., Renou, J.P., Abad, P. and Favery, B. (2005) Genome-wide expression profiling of the host response to root-knot nematode infection in Arabidopsis. *Plant J.* **44**, 447–458.

Jaubert, S., Ledger, T.N., Laffaire, J.B., Piotte, C., Abad, P. and Rosso, M.N. (2002) Direct identification of stylet secreted proteins from root-knot nematodes by a proteomic approach. *Mol. Biochem. Parasitol.* **121**, 205–211.

Jones, M.G.K. and Northcote, D.H. (1972) Nematode-induced syncytium-A multinucleate transfer cell. *J. Cell Sci.* **10**, 789–809.

Juergensen, K., Scholz-Starke, J., Sauer, N., Hess, P., van Bel, A.J.E. and Grundler, F.M.W. (2003) The companion cell-specific Arabidopsis disaccharide carrier AtSUC2 is expressed in nematode-induced syncytia. *Plant Physiol.* **131**, 61–69.

Kanter, U., Usadel, B., Guerineau, F., Li, Y., Pauly, M. and Tenhaken, R. (2005) The inositol oxygenase gene family of Arabidopsis is involved in the biosynthesis of nucleotide sugar precursors for cell-wall matrix polysaccharides. *Planta*, **221**, 243–254.

Klink, V.P., Overall, C.C., Alkharouf, N.W., MacDonald, M.H. and Matthews, B.F. (2007a) A time-course comparative microarray analysis of an incompatible and compatible response by *Glycine max* (soybean) to *Heterodera glycines* (soybean cyst nematode) infection. *Planta*, **226**, 1423–1447.

Klink, V.P., Overall, C.C., Alkharouf, N.W., MacDonald, M.H. and Matthews, B.F. (2007b) Laser capture microdissection (LCM) and comparative microarray expression analysis of syncytial cells isolated from incompatible and compatible soybean (*Glycine max*) roots infected by the soybean cyst nematode (*Heterodera glycines*). *Planta*, **226**, 1389–1409.

Kudla, U., Qin, L., Milac, A. *et al.* (2005) Origin, distribution and 3D-modeling of Gr-EXPB1, an expansin from the potato cyst nematode *Globodera rostochiensis*. *FEBS Lett.* **579**, 2451–2457.

Livak, K.J. and Schmittgen, T.D. (2001) Analysis of relative gene expression data using real-time quantitative PCR and the 2(-Delta Delta C(T)). *Methods*, **25**, 402–408.

Lorence, A., Chevone, B.I., Mendes, P. and Nessler, C.L. (2004) *myo*-Inositol oxygenase offers a possible entry point into plant ascorbate biosynthesis. *Plant Physiol.* **134**, 1200–1205.

Niebel, A., De Almeida Engler, J., Hemerly, A., Ferreira, P., Inzé, D., Van Montagu, M. and Gheysen, G. (1996) Induction of cdc2a and cyc1At expression in *Arabidopsis thaliana* during early phases of nematode-induced feeding cell formation. *Plant J.* **10**, 1037–1043.

Offler, C.E., McCurdy, D.W., Patrick, J.W. and Talbot, M.J. (2002) Transfer cells: cells specialized for a special purpose. *Annu. Rev. Plant Biol.* **54**, 431–454.

Okumoto, S., Schmidt, R., Tegeder, M., Fischer, W.N., Rentsch, D., Frommer, W.B. and Koch, W. (2002) High affinity amino acid transporters specifically expressed in xylem parenchyma and developing seeds of Arabidopsis. *J. Biol. Chem.* **277**, 45338–45346.

Puthoff, D.P., Nettleton, D., Rodermel, S.R. and Baum, T.J. (2003) Arabidopsis gene expression changes during cyst nematode parasitism revealed by statistical analyses of microarray expression profiles. *Plant J.* **33**, 911–921.

Schmid, M., Davison, T.S., Henz, S.R., Pape, U.J., Demar, M., Vingron, M., Scholkopf, B., Weigel, D. and Lohmann, J.U. (2005) A gene expression map of *Arabidopsis thaliana* development. *Nat. Genet.* **37**, 501–506.

Sijmons, P.C., Grundler, F.M.W., von Mende, N., Burrows, P. and Wyss, U. (1991) *Arabidopsis thaliana* as a new model host for plant-parasitic nematodes. *Plant J.* **1**, 245–254.

Smant, G., Stokkermans, J.P.W.G., Yan, Y. *et al.* (1998) Endogenous cellulases in animals: Isolation of beta-1,4-endoglucanase genes from two species of plant-parasitic cyst nematodes. *Proc. Natl Acad. Sci. USA*, **95**, 4906–4911.

Smyth, G.K. (2004) Linear models and empirical Bayes methods for assessing differential expression in microarray experiments. *Stat. Appl. Gene. Mol. Biol.* **3**, Article 3.

Sobczak, M., Golinowski, W. and Grundler, F.M.W. (1997) Changes in the structure of *Arabidopsis thaliana* roots induced during development of males of the plant parasitic nematode *Heterodera schachtii*. *Eur. J. Plant Pathol.* **103**, 113–124.

Thomma, B.P., Cammue, B.P. and Thevissen, K. (2002) Plant defensins. *Planta*, **216**, 193–202.

Vanholme, B., De Meutter, J., Tytgat, T., Van Montagu, M., Coomans, A. and Gheysen, G. (2004) Secretions of plant-parasitic nematodes: a molecular update. *Gene*, **332**, 13–27.

Vanholme, B., Mitreva, M., Van Criekinge, W., Logghe, M., Bird, D., McCarter, J.P. and Gheysen, G. (2006) Detection of putative secreted proteins in the plant-parasitic nematode *Heterodera schachtii*. *Parasitol. Res.* **98**, 414–424.

Wallace, I.S. and Roberts, D.M. (2004) Homology modeling of representative subfamilies of Arabidopsis major intrinsic proteins. Classification based on the aromatic/arginine selectivity filter. *Plant Physiol.* **135**, 1059–1068.

Wieczorek, K., Golecki, B., Gerdes, L. *et al.* (2006) Expansins are involved in the formation of nematode-induced syncytia in roots of *Arabidopsis thaliana*. *Plant J.* **48**, 98–112.

Wieczorek, K., Hofmann, J., Blöchl, A., Szakasits, D., Bohlmann, H. and Grundler, F.M.W. (2008) Arabidopsis endo-1,4-beta-glucanases are involved in the formation of root syncytia induced by *Heterodera schachtii*. *Plant J.* **53**, 336–351.

Williamson, V.M. and Kumar, A. (2006) Nematode resistance in plants: the battle underground. *Trends Genet.* **22**, 396–403.

Wu, Z., Irizarry, R.A., Gentleman, R., Martinez-Murillo, F. and Spencer, F. (2004) A model based background adjustment for oligonucleotide expression arrays. *J. Am. Stat. Assoc.* **99**, 909–917.

Wyss, U. and Grundler, F.M.W. (1992) *Heterodera schachtii* and *Arabidopsis thaliana*, a model host-parasite interaction. *Nematologica*, **38**, 488–493.

Yang, H., Matsubayashi, Y., Nakamura, K. and Sakagami, Y. (2001) Diversity of Arabidopsis genes encoding precursors for phytosulfokine, a peptide growth factor. *Plant Physiol.* **127**, 842–851.

Zimmermann, P., Hirsch-Hoffmann, M., Hennig, L. and Gruissem, W. (2004) GENEVESTIGATOR. Arabidopsis microarray database and analysis toolbox. *Plant Physiol.* **136**, 2621–2632.

CHAPTER 3

Expansins are involved in the formation of nematode-induced syncytia in roots of *Arabidopsis thaliana*

Wieczorek, K., Golecki, B., Gerdes, L., Heinen, P., Szakasits, D., Durachko, D.M., Cosgrove, D.J., Kreil, D.P., Puzio, P.S., Bohlmann, H. and Grundler, F.M.W.

The Plant Journal (2006) 48:98-112.

The Plant Journal (2006) **48**, 98–112 doi: 10.1111/j.1365-313X.2006.02856.x

Expansins are involved in the formation of nematode-induced syncytia in roots of *Arabidopsis thaliana*

Krzysztof Wieczorek[1], Bettina Golecki[2,†], Lars Gerdes[2,‡], Petra Heinen[1], Dagmar Szakasits[1], Daniel M. Durachko[3], Daniel J. Cosgrove[3], David P. Kreil[4], Piotr S. Puzio[2,§], Holger Bohlmann[1] and Florian M. W. Grundler[1,*]

[1]*Institute of Plant Protection, Department of Applied Plant Sciences and Plant Biotechnology, University of Natural Resources and Applied Life Sciences, Vienna, Austria,*

[2]*Institut für Phytopathologie, Christian-Albrechts-Universität Kiel, Germany,*

[3]*Department of Biology, 208 Mueller Lab, Pennsylvania State University, University Park, PA, 16870 USA, and*

[4]*Bioinformatics, Department of Biotechnology, University of Natural Resources and Applied Life Sciences, Vienna, Austria*

Received 1 April 2006; revised 26 May 2006; accepted 21 June 2006.

*For correspondence (fax +43 1 47654 3359; email florian.grundler@boku.ac.at).

†Present address: ALW Kiel, Germany.

‡Present address: Institute of Botany, Ludwig-Maximilian-University Munich, Germany.

§Present address: Metanomics GmbH, Berlin, Germany.

Summary

Parasitism of the cyst nematode *Heterodera schachtii* is characterized by the formation of syncytial feeding structures in the host root. Syncytia are formed by the fusion of root cells, accompanied by local cell wall degradation, fusion of protoplasts and hypertrophy. Expansins are cell wall-loosening proteins involved in growth and cell wall disassembly. In this study, we analysed whether members of the expansin gene family are specifically and developmentally regulated during syncytium formation in the roots of *Arabidopsis thaliana*. We used PCR to screen a cDNA library of 5–7-day-old syncytia for expansin transcripts with primers differentiating between 26 α- and three β-expansin cDNAs. *AtEXPA1*, *AtEXPA3*, *AtEXPA4*, *AtEXPA6*, *AtEXPA8*, *AtEXPA10*, *AtEXPA15*, *AtEXPA16*, *AtEXPA20* and *AtEXPB3* could be amplified from the library. In a semi-quantitative RT-PCR and a Genechip analysis *AtEXPA3*, *AtEXPA6*, *AtEXPA8*, *AtEXPA10* and *AtEXPA16* were found to be upregulated specifically in syncytia, but not to be transcribed in surrounding root tissue. Histological analyses were performed with the aid of promoter::GUS lines and *in situ* RT-PCR. Results from both approaches supported the specific expression pattern. Among the specifically expressed genes, *AtEXPA3* and *AtEXPA16* turned out to be of special interest as they are shoot-specific in uninfected plants. We conclude that syncytium formation involves the specific regulation of expansin genes, indicating that the encoded expansins take part in cell growth and cell wall disassembly during syncytium formation.

Keywords: expansins, cell wall, *Heterodera schachtii*, plant pathogens, Genechip, *in situ* RT-PCR.

Introduction

Sedentary plant-parasitic cyst nematodes of the genera *Heterodera* and *Globodera* cause substantial damage to a variety of crop plants such as soybean, potato, sugar beet and wheat. After root penetration the nematodes induce changes in the vascular cylinder and in the entire system of water, mineral and assimilate transport (Grundler and Böckenhoff, 1997). Infective second-stage juveniles invade the roots of host plants where they induce a syncytial feeding structure. Syncytium formation is supposed to be triggered by secretions released through the nematode stylet into a single initial root cell, which then fuses with neighbouring cells – a process that requires local cell wall dissolutions and subsequent fusion of the protoplasts (Golinowski *et al.*, 1996; Wyss and Grundler, 1992). In Arabidopsis, which has also been successfully established as a model plant also in plant nematology (Sijmons *et al.*, 1991), *Heterodera schachtii* induces syncytia within the root central cylinder. The cell walls of syncytia undergo remarkable changes, which were described by Golinowski *et al.* (1996) and Grundler *et al.* (1998). With syncytium formation the outer

syncytial cell walls are expanded and thickened, whereas at the interface to xylem vessels elaborate cell wall ingrowths are formed. Syncytia develop by the fusion of root cells through partial cell wall degradation. Openings between syncytial elements are formed via two different mechanisms: at the beginning of syncytium development, plasmodesmata between the initial cell and neighbouring cells are widened by gradual cell wall dissolution; in more advanced syncytia, the affected cell walls between two cells expand and become bent before being degraded without the involvement of plasmodesmata (Grundler *et al*., 1998). This process of cell fusion and cell expansion is suggested to be based on the activity of cell wall-modifying agents such as hydrolytic enzymes and expansins.

Grundler *et al*. (1998) gave indirect evidence for cell wall-degrading enzymes within developing syncytia by detecting the precipitations of liberated reducing sugars close to cell wall openings. Goellner *et al.* (2001) found five β-1,4-endoglucanases (*NtCel2*, *NtCel4*, *NtCel5*, *NtCel7* and *NtCel8*) to be upregulated in tobacco roots upon infection by both the tobacco cyst nematode (*Globodera tabacum*) and the root-knot nematode (*Meloidogyne incognita*). Root-knot nematodes induce giant cells as feeding structures within a root gall. Using differential display Vercauteren *et al.* (2002) identified DiDi 9C-12, a putative pectin acetylesterase homolog that was found to be upregulated in syncytia and giant cells. Mitchum *et al.* (2004) infected transgenic tobacco and Arabidopsis plants carrying an *AtCel1*::GUS construct with *H. schachtii* (Arabidopsis), *G. tabacum* (tobacco) and *M. incognita*, and found that the *AtCel1* promoter was activated only at the beginning of giant-cell formation. Using genome-wide expression profiling, Jammes *et al*. (2005) found seven EXPA and two EXPB to be upregulated in galls induced by *M. incognita* in the roots of Arabidopsis. Golecki *et al.* (2002) reported on the upregulation of the tomato expansin gene *LeEXP5* in syncytia induced by *Globodera rostochiensis*. Using microarray technology, quantitative RT-PCR and *in situ* localization *LeEXP5* was recently also found in gall cells adjacent to the feeding site induced by *Meloidogyne javanica* in the tomato (Gal *et al*., 2005).

Expansins were first identified more than a decade ago as the key cell wall factors responsible for 'acid growth' (McQueen-Mason *et al*., 1992). Characteristically, expansins induce cell wall extension at an acidic pH optimum *in vitro*, and enhance stress relaxation of isolated cell walls over a broad time range (Cosgrove, 2000a,b). They comprise two major gene families: α-expansins (EXPA) and β-expansins (EXPB) (Kende *et al*., 2004). EXPA proteins bind tightly to cellulose and hemicellulose, but they have no hydrolytic activity against these major polysaccharides of the cell wall (McQueen-Mason and Cosgrove, 1995). It has been proposed that expansins disrupt non-covalent bonding between cellulose microfibrils and matrix glucans, thereby allowing turgor-driven slippage of microfibrils relative to one another. Comparable studies of EXPB binding and hydrolytic activity have not yet been published, but their wall-loosening action is similar to that of EXPA (Cosgrove *et al*., 1997).

In Arabidopsis, EXPA proteins are encoded by a subfamily of 26 genes with 52–99% amino acid sequence identity. The EXPB subfamily is smaller, with five genes (six in some Arabidopsis ecotypes; http://www.bio.psu.edu/expansins). In addition, Arabidopsis has two related groups of genes that have been named expansin-like family A and B (EXPLA and EXPLB, respectively). Their functions, however, have not yet been ascertained.

Expansins are thought to be involved in the growth control of different cell types responding to different stimuli at different stages of a plant's life (Cosgrove, 2000a,b; Li *et al*., 2002). They play a role in cell enlargement, pollen tube invasion of the stigma, cell wall disassembly during fruit ripening and softening, organ abscission and leaf organogenesis. Knowledge about the regulation of expansin genes is still very limited, but in many cases expansin gene expression is regulated by plant hormones such as auxin, gibberellin and ethylene (Caderas *et al*., 2000; Cho and Cosgrove, 2002, 2004; Cho and Kende, 1997; McQueen-Mason and Rochange, 1999; Sánchez *et al*., 2004). Also, environmental triggers such as water stress (Wu *et al*., 2001), mycorrhizal infection (Balestrini *et al*., 2004) and rhizobium interaction (Giordano and Hirsch, 2004) were found to induce expansin gene expression.

Recently, it was shown that nematodes secrete proteins with sequence similarity to expansins (Kudla *et al*., 2005; Qin *et al*., 2004). Nematode secretions containing these and other cell wall-loosening proteins may assist the rapid penetration of the nematode into the root tissues. However, the highly orchestrated patterns of altered cell growth and syncytium formation would seem to require more subtle spatial and temporal control of cell wall loosening and growth processes that could not be achieved through nematode secretion alone.

In this study, we investigated whether the expression of members of the expansin gene family are specifically and developmentally regulated during syncytium formation in roots of *Arabidopsis thaliana*. In fact, our results demonstrate highly specific expression and implicate a substantial role of certain expansins in the cell wall re-organization occurring in the host response to cyst-forming nematodes.

Results

Expansins are differentially expressed in shoots and roots of uninfected control plants

In order to get a basic overview of the distribution of expansin gene expression in uninfected plants, shoots were separated from roots, and each sample was taken to perform

RT-PCR reactions. Primer pairs were designed for 26 *AtEXPA* genes (*AtEXPA1–26*) and three *AtEXPB* genes (*AtEXPB1–3*; see Supplementary Material). RT-PCR with total RNA isolated from shoots and roots of 21-day-old *A. thaliana* plants showed that most isoforms are expressed in both shoots and roots. Only *AtEXPA3*, *AtEXPA5* and *AtEXPA16* were found exclusively in the shoot, and *AtEXPA18* was found exclusively in the root. For *AtEXPA13*, *AtEXPA14*, *AtEXPA21*, *AtEXPA22*, *AtEXPA23*, *AtEXPA24*, *AtEXPA25*, *AtEXPA26* and *AtEXPB2* no products could be detected, suggesting that these isoforms are expressed neither in the shoot nor in the root at the selected plant developmental stage (Table 1).

Expansin genes are expressed in nematode-induced syncytia

Expansin gene expression in syncytia was determined using a syncytium-specific cDNA library from 5–7-day-old syncytia induced by *H. schachtii*. This library was made from microaspirated syncytial cytoplasm. The quality and specificity of this library has been evaluated with different genes (e.g. *Atpyk20*) known to be expressed specifically in syncytia (Jürgensen *et al.*, 2003; Puzio *et al.*, 2000). In PCR reactions with primers differentiating between the 26 *EXPA* and three *EXPB* genes, transcripts of nine different *AtEXPA* genes (*AtEXPA1*, *AtEXPA3*, *AtEXPA4*, *AtEXPA6*, *AtEXPA8*, *AtEXPA10*, *AtEXPA15*, *AtEXPA16* and *AtEXPA20*) and *AtEXPB3* were amplified (Table 1). Compared with the expression pattern in the uninfected plants, the expansin genes detected in the syncytium can be divided into two groups: *AtEXPA1*, *AtEXPA4*, *AtEXPA6*, *AtEXPA8*, *AtEXPA10*, *AtEXPA15*, *AtEXPA20* and *AtEXPB3* were found in syncytia, shoots and roots, whereas *AtEXPA3* and *AtEXPA16* were found in syncytia and shoots. Results obtained for uninfected plants are supported by Genechip data collected at Genevestigator (http://www.genevestigator.ethz.ch; Zimmermann *et al.*, 2004).

Table 1 Results obtained for PCR reactions with the syncytium-specific cDNA library and for RT-PCR reactions with total RNA isolated from Arabidopsis shoots and roots

Gene	cDNA library of syncytial cytoplasm	RT-PCR	
		Root	Shoot
AtEXPA1	+	+	+
AtEXPA2	–	+	+
AtEXPA3	+	–	+
AtEXPA4	+	+	+
AtEXPA5	–	–	+
AtEXPA6	+	+	+
AtEXPA7	–	+	+
AtEXPA8	+	+	+
AtEXPA9	–	+	+
AtEXPA10	+	+	+
AtEXPA11	–	+	+
AtEXPA12	–	+	+
AtEXPA13	–	–	–
AtEXPA14	–	–	–
AtEXPA15	+	+	+
AtEXPA16	+	–	+
AtEXPA17	–	+	+
AtEXPA18	–	+	–
AtEXPA19	–	+	+
AtEXPA20	+	+	+
AtEXPA21	–	–	–
AtEXPA22	–	–	–
AtEXPA23	–	–	–
AtEXPA24	–	–	–
AtEXPA25	–	–	–
AtEXPA26	–	–	–
AtEXPB1	–	+	–
AtEXPB2	–	–	–
AtEXPB3	+	+	+

+, PCR product was detected; –, no PCR product detected.

Several expansin genes are specifically expressed during syncytium formation

After having identified which expansin genes are expressed in syncytia, we compared the expression of these genes in root segments containing syncytia versus segments of coeval uninfected roots. The samples contained neither root tips nor primordia of secondary roots. Semi-quantitative RT-PCR (sqRT-PCR) was performed for all the expansin genes that had been detected in the syncytium-specific cDNA library and for *18S rRNA* and *UBQ1* as controls (Figure 1). According to the results the expressed expansin genes can be divided into two groups. Group one comprises *AtEXPA3*, *AtEXPA6*, *AtEXPA8*, *AtEXPA10* and *AtEXPA16*, which gave positive signals with syncytium material collected at 5, 10 and 15 days after infection (dai), whereas no products could be amplified from control root segments. Except for *AtEXPA16* the group-one signals were weak at 5 dai, strongest at 10 dai and slightly reduced at 15 dai. *AtEXPA16* gave the weakest signal at 5 dai, but gave a strong signal at both 10 and 15 dai. Group two consists of *AtEXPA1*, *AtEXPA4*, *AtEXPA15*, *AtEXPA20* and *AtEXPB3*, which could be detected in samples with and without syncytia. However, they are strongly upregulated in root segments with syncytia. *AtEXPA1* is generally expressed in all samples with syncytia, whereas its expression in uninfected roots is increased in older samples. Expression of *AtEXPA4* became weaker in older segments with syncytia, whereas it was detectable in control roots coeval to 5 dai, but reduced at the age coeval to 10 dai and no longer detectable in control roots corresponding to 15 dai. *AtEXPA15* is expressed at the same high level at all time points in root segments with syncytia. In the control roots a weak signal was detected only at the age corresponding to 5 dai, whereas at later time points no signal could be detected. Maximum expression of

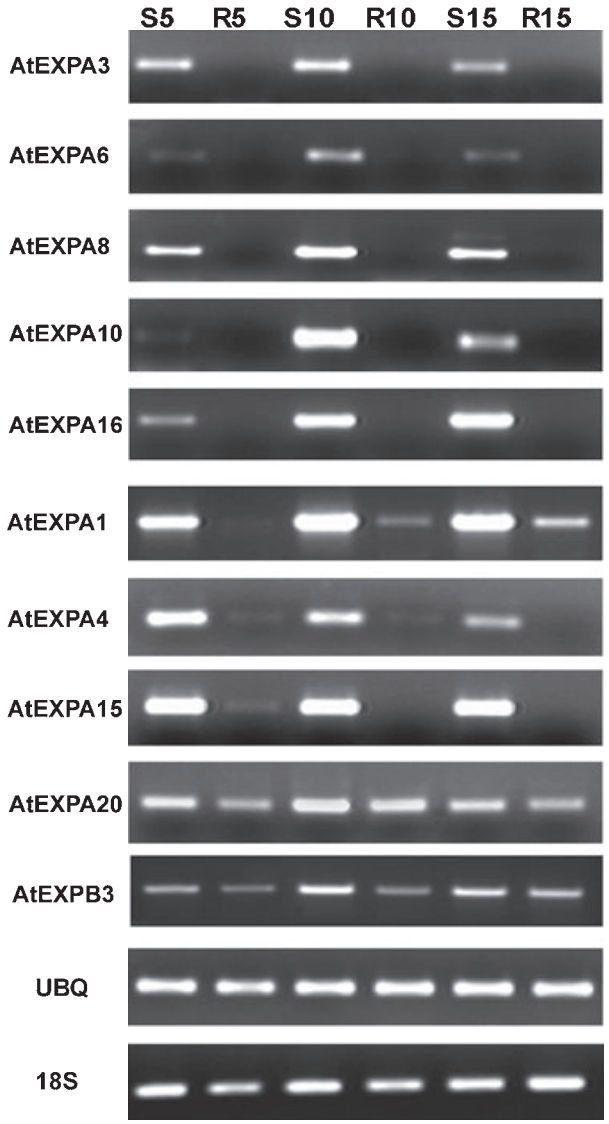

Figure 1. Semi-quantitative RT-PCR with specific primer pairs designed for 10 expansin genes. Syncytium samples (S) were collected at 5, 10 and 15 dai (S5, S10 and S15) and uninfected root segments (R) were collected at 5, 10 and 15 dai (R5, R10 and R15). *UBQ1* and *18S rRNA* were used as internal controls.

AtEXPA20 and *AtEXPB3* occurred in syncytium material collected at 10 dai. The signal of *AtEXPA20* was slightly stronger at 5 dai than at 15 dai, whereas for *AtEXPB3* it was slightly reduced at 5 dai compared with 15 dai. Signals for both expansin genes were weaker in uninfected root samples than in samples with syncytia.

The results clearly show that *AtEXPA3*, *AtEXPA6*, *AtEXPA8*, *AtEXPA10* and *AtEXPA16* are specifically expressed during syncytium formation, and are not transcribed in the corresponding parts of healthy roots. *AtEXPA1*, *AtEXPA4*, *AtEXPA15*, *AtEXPA20* and *AtEXPB3* are also upregulated during syncytium formation but are also expressed in control roots.

Analyses of expansin expression profiles in syncytia and uninfected roots were also made using Affymetrix Genechips. The basis material was again micro-aspirated syncytial cytoplasm sampled at 5 and 15 dai compared with corresponding uninfected root segments. These data confirmed the results of all other experiments (Table 2). Significant upregulation was detected for *AtEXPA1*, *AtEXPA3*, *AtEXPA5*, *AtEXPA6*, *AtEXPA8*, *AtEXPA10*, *AtEXPA16* and *AtEXPB3*. Upregulation of *AtEXPA3*, *AtEXPA6*, *AtEXPA8*, *AtEXPA16* and *AtEXPB3* was found in syncytia both at 5 and 15 dai, with either a similar level (*AtEXPB3*) or a higher level observed in the older samples. Increased expression of *AtEXPA1*, *AtEXPA5* and *AtEXPA10* was only detected at 15 dai. Upregulation of *AtEXPA4*, *AtEXPA15* and *AtEXPA20* was not detected with significance in this assay.

A highly significant reduction of expression was found for *AtEXPA7* and *AtEXPA18*, both at 5 and 15 dai. For all other expansin genes no significant changes in expression during syncytium development were detected.

Promoter::GUS studies support differential regulation of expansin genes in syncytia

For some expansin isoforms, promoter::GUS lines were studied (*AtEXPA1*, *AtEXPA3*, *AtEXPA4*, *AtEXPA6*, *AtEXPA10*, *AtEXPA15* and *AtEXPA16*). In order to analyse the specificity of expression of these genes during syncytium formation, plants were infected with nematodes and stained for GUS activity. In the context of this work we focused our attention to the roots, whereas a general expression analysis of uninfected plants will be presented elsewhere (Cosgrove and Durachko, in preparation).

GUS assays with uninfected roots gave the following results: in *AtEXPA1*, *AtEXPA4* and *AtEXPA15*::GUS plants, a generally strong staining was found mainly in the vascular cylinder of the primary and lateral roots, as well as in the root tips (Figure 2b,c,h,i,q,r). In *AtEXPA6*::GUS plants staining was restricted to root tips (Figure 2k), emerging primordia of lateral roots (Figure 2l) and young lateral roots. In the roots of *AtEXPA3*::GUS plants, no GUS activity could be observed (Figure 2e,f). The *AtEXPA10*::GUS line showed a faint expression in the root tips (Figure 2n). In *AtEXPA16*::GUS plants *gus* expression was detected at a very low level in lateral roots and root tips (Figure 2t,u).

Blue staining in syncytia was found in *AtEXPA1*, *AtEXPA3*, *AtEXPA4*, *AtEXPA6*, *AtEXPA10*, *AtEXPA15* and *AtEXPA16*::GUS plants (Figure 2). Syncytia in the lines with promoters of *AtEXPA1*, *AtEXPA4* and *AtEXPA15* showed a remarkably strong staining (Figure 2a,g,p). In the lines *AtEXPA3*::GUS, *AtEXPA10*::GUS and *AtEXPA16*::GUS activity was restricted to the syncytium, and was not observed in the root tissue above and below the feeding site (Figure 2d,m,s).

Genes	Controls	Syn 5d	Syn 15d	Ctl versus 5d	Ctl versus 15d	5d versus 15d
EXPA1	2.23	6.42	8.31	3.06	5.49*	2.43
EXPA2	2.88	2.93	3.10	0.21	0.27	0.05
EXPA3	2.40	5.86	8.73	3.05**	6.66***	3.61
EXPA4	2.73	5.70	6.64	1.40	4.31	2.90
EXPA5	3.15	3.45	4.28	0.51	1.38*	0.87
EXPA6	2.79	8.26	8.97	4.41**	5.77***	1.36
EXPA7	9.74	2.34	2.40	−7.30***	−7.32***	−0.02
EXPA8	2.90	6.18	9.83	2.86*	6.90***	4.05*
EXPA9	2.39	2.34	2.88	−0.04	0.55	0.60
EXPA10	3.20	4.64	6.41	1.12	2.85*	1.73
EXPA11	2.86	3.04	3.09	0.34	0.32	−0.02
EXPA12	3.64	3.74	3.99	0.13	0.43	0.30
EXPA13	5.68	6.10	5.79	0.15	0.00	−0.15
EXPA14	3.07	2.94	2.90	−0.30	−0.25	0.04
EXPA15	4.08	4.64	4.87	0.51	0.61	0.10
EXPA16	3.22	6.00	8.49	1.95*	4.79***	2.84*
EXPA17	3.46	2.90	2.84	−0.71	−0.80	−0.09
EXPA18	8.52	2.67	2.79	−5.89***	−5.86***	0.03
EXPA20	4.37	5.70	5.07	0.89	0.60	−0.29
EXPA21	2.82	2.76	2.68	0.06	−0.02	−0.07
EXPA22 & 26	2.67	2.69	2.85	0.26	0.10	−0.15
EXPA23 & 25	2.55	2.36	2.48	−0.03	0.03	0.06
EXPA24	2.18	2.17	2.26	−0.01	0.15	0.16
EXPB1	2.24	2.22	2.32	0.00	0.22	0.22
EXPB2	2.92	3.04	2.61	0.17	−0.55	−0.73
EXPB2 & 4	2.25	2.17	2.07	0.08	−0.13	−0.20
EXPB 3	3.64	7.25	5.95	2.68*	2.66*	−0.03
EXPB5	2.56	2.72	2.74	0.23	0.09	−0.14
	Raw group means			Pairwise contrasts in a batch detrending linear model		

Table 2 Genechip expression profiles of Arabidopsis expansin genes during the development of syncytia induced by *Heterodera schachtii*. Changes in gene expression were obtained in comparison between micro-aspirated syncytia content at 5 dai (5d) and 15 dai (15d) and coeval root fragments from the elongation zone without root tips and lateral root primordia (Ctl). Values displayed have been normalized and are on a $\log_2$ scale (see Experimental procedures for details). The differences shown are consequently $\log_2$ ratios, with values of $\pm$ 1 corresponding to either a twofold up- or downregulation

In the table, significance in a regularized Benjamini–Hochberg corrected test is indicated by asterisks (*q < 25%; **q < 10%; ***q < 5%; see Experimental procedures for details).

A time course analysis was performed with the *AtEXPA6:GUS* line because of its *gus* expression in syncytia and the background expression in both root tips and lateral root primordia (Figure 3j,k,l). Samples were taken at 3, 4, 5, 7, 12, 15 and 18 dai. At 3 and 4 dai GUS activity was located in a diffuse zone within and around the young syncytia (Figure 3a,b). It became stronger and more focused to syncytia at 5 dai (Figure 3c). The strongest *gus* expression was found in syncytia at 7 and 10 dai. At this stage GUS staining was restricted to the feeding site (Figure 3d,e). In syncytia at 12 and 15 dai expression decreased (Figure 3f,g) and was no longer detectable at 18 dai (Figure 3h), which is in contrast to our Genechip data showing a strong expression in syncytia at 15 dai. However, this phenomenon is explained by a general decrease of GUS staining in older syncytia (see Discussion).

In situ *analysis: expression of* AtEXPA3*,* AtEXPA6*,* AtEXPA8*,* AtEXPA10 *and* AtEXPA16 *is restricted to syncytia*

AtEXPA3, *AtEXPA6*, *AtEXPA8*, *AtEXPA10* and *AtEXPA16* mRNA localization within 7-dai syncytia was also investigated using *in situ* RT-PCR. Transcripts of *AtEXPA3* were mainly found in young and relatively small cells either freshly incorporated or being prepared for fusion with syncytium (Figure 4a). Results with specific primers for

Figure 2. Expression of *gus* driven by expansin promoters in syncytia and root tissue at 5 dai. *AtEXPA1*::GUS: staining in the syncytium and the surrounding root tissue (a), the root tip (b), the lateral root primordium and the vascular cylinder of the root (c). *AtEXPA3*::GUS: staining in the syncytium, no background in parts above and below the feeding site (d), no staining in the root tip (e), no *gus* expression in the lateral root primordium and in the vascular cylinder of the root (f). *AtEXPA4*::GUS: staining in syncytia and the surrounding root tissue (g), the root tip (h), the lateral root primordium and in the vascular cylinder (i). *AtEXPA6*::GUS: staining in the syncytium, no staining in neighbouring cells (j), faint *gus* expression in the root cap and the root elongation zone (k), *gus* expression in the lateral root primordium, no staining in the vascular cylinder (l). *AtEXPA10*::GUS: staining in the syncytium, no staining in neighbouring cells (m), faint GUS activity in the root tip (n), no *gus* expression in the lateral root primordium and the vascular cylinder (o). *AtEXPA15*::GUS: staining in the syncytium and surrounding cells (p), the root tip (q), young lateral roots and in the vascular cylinder of the root (r). *AtEXPA16*::GUS: staining in the syncytium, no background in the root tissue surrounding the feeding site (s), very faint *gus* expression in the root tip, elongation and differentiation zone (t), no GUS activity in the lateral root primordium and in the vascular cylinder (u). S, syncytium; N, nematode; scalebar = 200 μm.

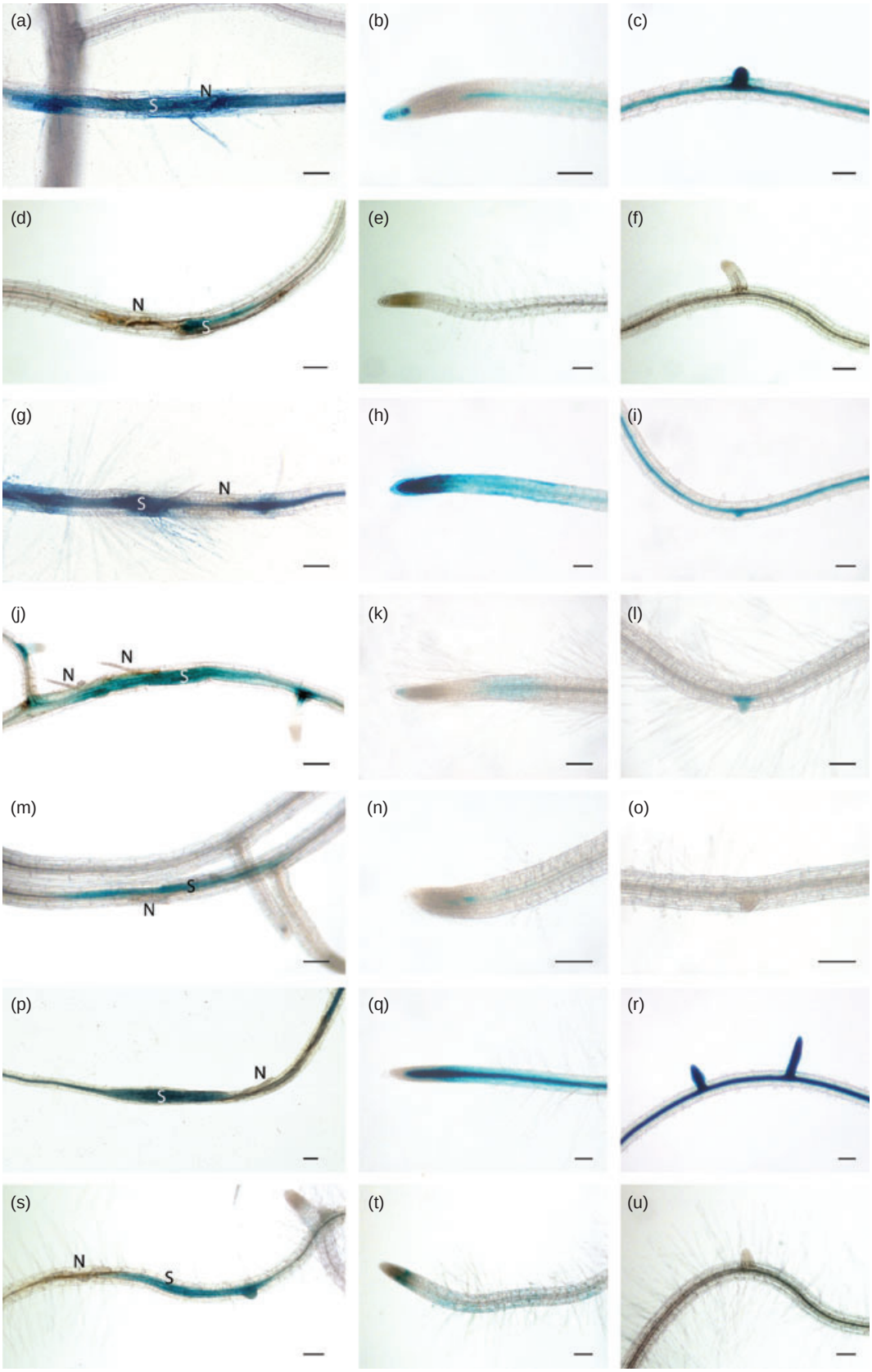

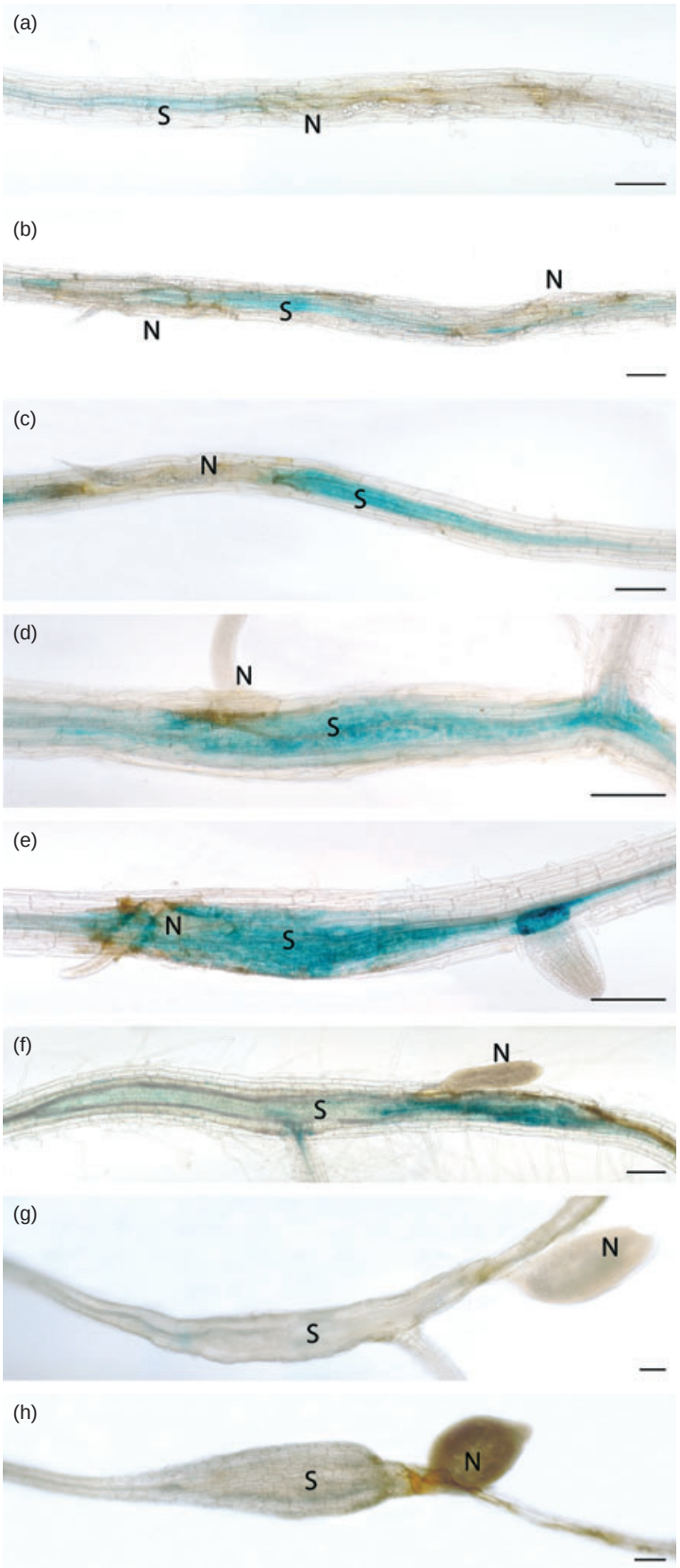

Figure 3. Time course analysis of *gus* expression in the nematode-infected line *AtEXPA6*::GUS.
(a) syncytium at 3 dai.
(b) syncytium at 4 dai.
(c) syncytium at 5 dai.
(d) syncytium at 7 dai.
(a–d) GUS activity occurs in the syncytium, no *gus* expression is visible in the surrounding root tissue.
(e) syncytium at 10 dai; GUS accumulates strongly within syncytium and in the base of a lateral root primordium.
(f) syncytium at 12 dai; strong *gus* expression is visible only in a part of the syncytium adjacent to the nematode.
(g) syncytium at 15 dai; weak *gus* expression is observable in the syncytium.
(h) syncytium at 18 dai; no *gus* expression is visible in the syncytium. S, syncytium; N, nematode; scalebar = 200 μm.

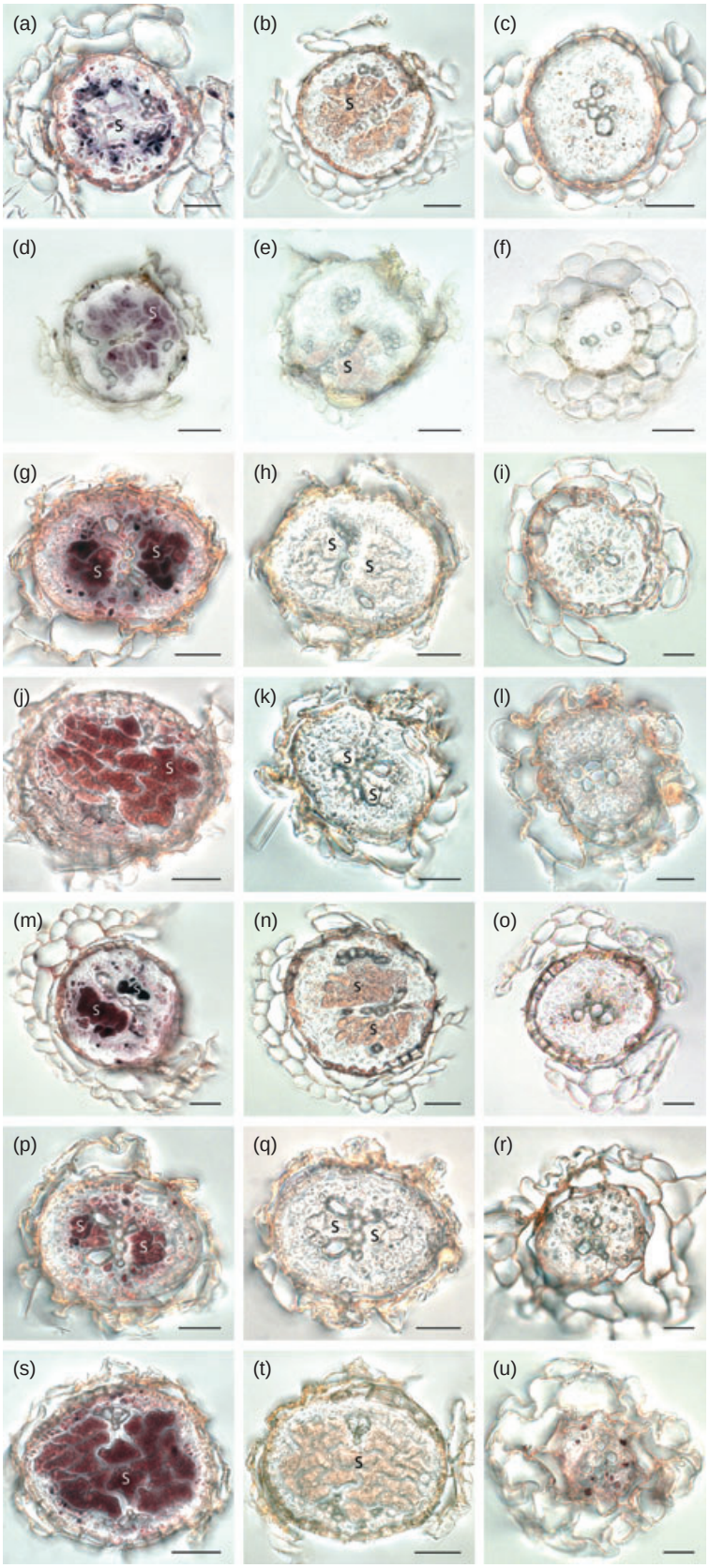

Figure 4. *In situ* RT-PCR analysis of *AtEXPA3*, *AtEXPA6*, *AtEXPA8*, *AtEXPA10* and *AtEXPA16* mRNA on a section of a nematode-infected Arabidopsis root.
(a) *AtEXPA3* transcripts are visible mainly in young small cells adjacent to the syncytium.
(b) Control reaction for A performed without *Taq* Polymerase: staining is neither visible in syncytium nor in the surrounding tissue.
(c) Control reaction for A on a root section above the syncytium. Transcripts of *AtEXPA3* were not detected.
(d) *AtEXPA6* mRNA is accumulated in the syncytium. No staining is visible in uninfected vascular cylinder cells surrounding the syncytium.
(e) Control reaction for D performed without *Taq* Polymerase on a section of an infected root. Staining is neither visible in syncytia nor in surrounding cells.
(f) Control reaction for D on a root section above the feeding site. Transcripts of *AtEXPA6* were not detected.
(g) *AtEXPA8* transcripts are visible mainly in syncytium and low background staining is visible in the central cylinder.
(h) Control reaction for G performed without *Taq* Polymerase, staining is neither visible in syncytium nor in the surrounding tissue.
(i) Control reaction for G on a root section above the syncytium. Transcripts of *AtEXPA8* were not detected.
(j) *AtEXPA10* transcripts accumulate in the syncytium, low background staining is visible in tissue surrounding the feeding site.
(k) Control reaction for J performed without *Taq* Polymerase, staining is neither visible in syncytium nor in the surrounding tissue.
(l) Control reaction for J on a root section above the syncytium. No transcripts of *AtEXPA10* are visible.
(m) Transcripts of *AtEXPA16* strongly accumulate in the syncytium. Low background staining is visible in tissue adjacent to the syncytium.
(n) Control reaction for M performed without *Taq* Polymerase. Lack of the *AtEXPA16* transcripts in the syncytium and adjacent root tissue.
(o) Control reaction for (m). No staining is visible in the root section above the syncytium. Scale-bar = 50 μm.

AtEXPA6 on sections of syncytia showed that *AtEXPA6* transcripts occurred in syncytial elements, but not in the surrounding tissue (Figure 4d). Reactions with primers for *AtEXPA8*, *AtEXPA10* and *AtEXPA16* showed specific accumulation of transcripts of these expansin genes in syncytia. Low background staining occurs in the surrounding root tissue (Figure 4g,j,m). No products of all these genes were detected with the control reactions without *Taq* Polymerase (Figure 4b,e,h,k,n). Control reactions on root sections above the syncytium gave no staining in the vascular cylinder and the surrounding root cell layers (Figure 4c,f,i,l,o).

Discussion

Expansins are known to play an important role in cell wall formation and modification. Therefore it can be anticipated that they are involved in plant–pathogen interactions that go along with major structural changes in cell wall architecture, such as the formation of hypertrophic and hyperplastic tissues.

In this paper we studied the expression of the expansin gene family in roots of Arabidopsis that were infected with the beet cyst nematode *H. schachtii*. A group of ten expansin genes were found to be expressed in the syncytia induced by the nematode. In uninfected plants the majority of these genes are expressed in roots, whereas two genes, *AtEXPA3* and *AtEXPA16*, are expressed mainly in the shoot. As far as uninfected control plants are concerned, these data match with gene expression profiles that are available in the Genevestigator database (http://www.genevestigator.ethz.ch; Table 3). For this comprehensive analysis we applied several methods that differ in their potential to detect, quantify and localize gene expression. Complementing each other, these methods gave a clear picture of expansin genes expression during syncytium development.

Table 3 Signal intensities of the expansin genes in Arabidopsis (Col-0). Data are taken from Genevestigator site (http://www.genevestigator.ethz.ch)

Anatomy	Cell suspension	Seedling	Inflorescence	Rosette	Roots
No. chips	42	320	139	577	187
AtEXPA1 ↑	7846	6563	4569	7009	1567
AtEXPA3 ↑	178	2981	1745	861	46
AtEXPA4 ↑	4695	2205	3323	1045	4259
AtEXPA6 ↑	1972	3215	5352	3614	877
AtEXPA7 ↓	81	606	136	145	913
AtEXPA8 ↑	200	3015	3272	2879	264
AtEXPA10 ↑	1380	2090	2420	2159	446
AtEXPA15 ↑	1130	1381	2081	725	2409
AtEXPA16 ↑	95	257	259	441	101
AtEXPA18 ↓	147	883	177	180	1242
AtEXPA20 ↑	668	357	488	168	343
AtEXPB3 ↑	439	1956	2311	951	3310

All listed genes are specifically either up- (↑) or downregulated (↓) in syncytia.

Specific expression of expansin genes in nematode-infected root tissue

Arabidopsis contains 26 *AtEXPA* and six *AtEXPB* expansin genes, and so far the advantage of this high number of isomers is not known. In general, there is not much information on the specific functions of single members of the expansin gene family. One may speculate that there is either a variability in function or a variability in regulation, but so far there is no experimental evidence in either the one or the other direction. However, as different functions have not yet been found, it is highly probable that variability is an approach to specify expression during either different developmental stages or under different environmental influences.

With the aid of the specific cDNA library and the Genechip, expression of ten expansin genes within syncytia could be clearly shown. However, as these analyses were based on micro-aspirated syncytium samples, they do not indicate whether or not there is additional expression in other areas of the root. This information was obtained by promoter::GUS lines, *in-situ* RT-PCR and sqRT-PCR with samples of infected and uninfected root segments. The analysed genes can be divided into four different categories according to their expression pattern (Figure 5).

Category I comprises five genes that are expressed in syncytia and the entire root system, including the tissue surrounding the syncytia. It comprises *AtEXPA1*, *AtEXPA4*, *AtEXPA15*, *AtEXPA20* and *AtEXPB3*. Durachko and Cosgrove (unpublished results) found that *AtEXPA1* is mainly expressed in the stomatal guard cells and very young vascular bundles, whereas the *AtEXPA4* promoter directs expression

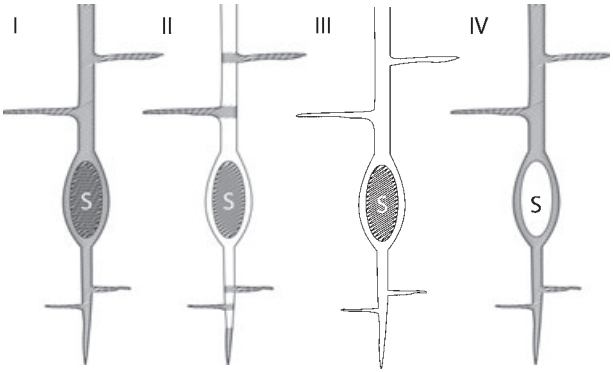

Figure 5. Expression patterns of up- and downregulated expansin genes in syncytia (S) at 5 dai induced by *H. schachtii*. Category I – *AtEXPA1*, *AtEXPA4*, *AtEXPA15*, *AtEXPA20* and *AtEXPB3*; category II – *AtEXPA6*, *AtEXPA8*, *AtEXPA10*; category III – *AtEXPA3* and *AtEXPA16*; category IV – *AtEXPA7* and *AtEXPA18*. For a description of these patterns see the main text.

in the vascular bundles throughout the plant. For *AtEXPA1*, *AtEXPA4* and *AtEXPA15* promoter::GUS lines were available and expression in the whole root including the area adjacent to syncytia could be shown clearly. Slight differences between the Genechip data and the results of the sqRT-PCR experiments (Figure 2) in the case of *AtEXPA4* and *AtEXPB3* can be explained with the different origin of the starting material. For sqRT-PCR, root segments containing syncytia were taken, whereas micro-aspirated syncytial cytoplasm without surrounding tissue was used for Genechip analysis.

Category II contains three genes that are expressed in syncytia and in other parts of the roots, but not in the surrounding root tissue. It includes *AtEXPA6*, *AtEXPA8* and *AtEXPA10*. Expression analyses of promoter::GUS lines indicate that *AtEXPA8* is expressed in specific cells in the root, whereas *AtEXPA10* occurred in leaf petioles and midribs and at the base of the pedicels (Cosgrove, 1998).

Category III consists of *AtEXPA3* and *AtEXPA16*, which are upregulated in syncytia and are otherwise expressed only in shoot tissue. Expression of *AtEXPA3* was found in the shoot apical meristem (Cosgrove and Durachko, unpublished results). Comparing Genechip data and the results of sqRT-PCR with *AtEXPA3* the same phenomenon occurred as explained with *AtEXPA4* and *AtEXPB3*.

Category IV contains two expansin genes, *AtEXPA7* and *AtEXPA18*, which are downregulated in syncytia. Expression data from Genevestigator for expansin genes belonging to all four categories are shown in Table 3.

Expression of expansin genes changes during the development of nematode feeding sites

Using GUS assays we performed a time-course analysis of the expression pattern of *AtEXPA6* during syncytium development. GUS activity was observed already in syncytia at 3 dai and reached its maximum in syncytia at 7–10 dai. These data were supported by results of the Genechip analysis at two time-points, where a significant increase of expression in syncytia at 5 and 15 dai was measured (Table 2). No blue staining was found in syncytia at 18 dai. This can be explained by earlier studies with this host-pathogen system, which revealed that GUS activity generally decreases in the syncytia of older plants independent of the used construct (Barthels *et al.*, 1997; Puzio *et al.*, 1998).

Jammes *et al.* (2005) performed similar gene expression profiling during the formation of galls induced by the root-knot nematode *Meloidogyne javanica* in roots of Arabidopsis. They identified seven *AtEXPA* and two *AtEXPB* genes upregulated in galls. Expression of six genes (*AtEXPA1*, *AtEXPA6*, *AtEXPA10*, *AtEXPA15*, *AtEXPB1* and *AtEXPB3*) continuously increased in galls from 7 to 14 dai. *AtEXPA7* is more strongly expressed in galls at 7 dai than in galls at 14 dai. For two genes (*AtEXPA11* and *AtEXPA16*) no changes in expression levels between 7 and 14 dai were measured. The observed signal intensities were generally much weaker than those reported here. However this is not surprising because they dissected the galls, so that mRNA from giant cells was diluted in the samples by contamination from other tissues, whereas either micro-aspirated or laser-captured cell contents (Ramsay *et al.*, 2004) are specifically sampled and therefore much less contaminated. Nevertheless, there are some clear differences in the expression dynamics of expansin genes in galls obtained by these authors (Jammes *et al.*, 2005), and in cyst nematode-induced syncytia as described in this paper (Table 2). Although the expression of *AtEXPA7* is strongly downregulated in syncytia, it is slightly upregulated in galls. In the case of *AtEXPA15* no difference was observed in younger and older syncytia, whereas in galls an increase of expression was observed. *AtEXPA16* is specifically upregulated in syncytia at 5 and 15 dai. Interestingly, there is no change in its expression at 5 dai, but a slight increase at 14 dai in galls. There are also differences in the expression of *AtEXPB* genes between syncytia and galls. In syncytia the expression of *AtEXPB1* is not changed significantly, whereas in galls this expansin gene is upregulated. *AtEXPB3* has its strongest expression in syncytia at 5 dai, whereas in galls the maximum of its expression occurs at 14 dai. Data for *AtEXPA3* were not provided by Jammes *et al.* (2005).

This comparison shows that root-knot and cyst nematodes differ in their influence on the expression of expansin genes (either activation or reduction) during feeding site development in Arabidopsis.

Another study with root-knot nematodes was recently performed in the tomato. Gal *et al.* (2005) described the expression of the tomato expansin gene *LeEXP5*, which was observed at a very low expression level in the uninfected root, but was upregulated in gall cells adjacent to the giant cells induced by the root-knot nematode *M. javanica*. Using *in situ* RT-PCR they could not detect the transcripts in giant cells. Furthermore, these authors have generated *LeEXP5*-antisense transgenic roots using *Agrobacterium rhizogenes* transformation. After nematode infection they observed a decrease of the egg mass per gall, the number of eggs per gall mass and the giant cell diameter in *LeEXP5*-antisense transgenic lines in comparison with the control plants. They concluded that expression of *LeEXP5* is required for gall cell expansion, and thus gall formation, and that a decrease of its transcription caused a reduced parasitism by the nematodes. However, there are several possible problems associated with the presented data. It is known that the use of rhizogenic roots can be problematic for studies of nematode infections because of their artificial hormone status (Plovie *et al.*, 2003). Furthermore, a conserved region of the *LeEXP5* gene was used for the antisense construct. Considering the high sequence homology among members of this large gene family, this means that also other expansin genes will be downregulated. To characterize a specific function of

the *LeEXP5* gene it would be necessary to use more specific parts of the sequence for RNAi constructs. Such experiments are underway in our laboratory for both Arabidopsis and tomato expansin genes.

Expansins may have specific functions in plant-microbe interactions

To date there are only a few reports showing plant expansin gene expression in plant–microbe interactions. Balestrini *et al.* (2004) found the cucumber expansins *CsEXPA1* and *CsEXPA2* to be more abundant in cell walls upon mycorrhizal infection. They proposed that these expansins are directly involved in the accumulation of *Glomus veriforme* in infected cortical cells, and may be cell wall-loosening agents that facilitate the penetration of the hyphae through the cell wall. Giordano and Hirsch (2004) studied the expression of expansin genes during nodule development induced by *Sinorhizobium meliloti* in the roots of *Melilotus alba* and found *MaEXP1* to be upregulated.

In other cases, expansin-like proteins of unknown function were found in plant-associated bacteria and fungi (Laine *et al.*, 2000; Saloheimo *et al.*, 2002). A gene with structural and putative functional similarities to plant expansins has recently been found in juveniles of the cyst nematode *G. rostochiensis*, which is related to *H. schachtii* (Kudla *et al.*, 2005; Qin *et al.*, 2004). The authors suggested that the protein is produced and secreted by the juvenile during the invasion through the root where it could help to soften cell walls and thus facilitate nematode migration through the root tissue.

On the plant side, future analyses will have to focus on the function of the different described expansins as well as on their regulation. The cell walls of nematode-induced syncytia undergo highly specific modifications that are necessary to meet the specific demands of the cell complex and the associated parasite. Therefore, it is essential to understand how these modifications are formed and controlled. Here we describe the expression pattern of an entire gene family in response to a nematode infection. We show that the different members of the expansin family are regulated in a highly specific manner that includes upregulation as well as downregulation of the single members. The type of expression pattern, in which shoot-specific genes are especially activated in roots during the formation of syncytia, is highly remarkable. Further studies have to be performed in order to clarify the basis of this expression pattern. A detailed promoter analysis and comparison with related genes might reveal specific regulatory elements leading to transcription in shoot organs and syncytia. On the other hand, the specific function of these genes in the shoot has to be studied in order to find out whether this relates to processes in syncytium development.

Experimental procedures

Plant cultivation

Seeds of *A. thaliana* were surface-sterilised for 10 min in 5% (w/v) calcium hypochlorite, submerged for 5 min in 70% (v/v) ethanol and subsequently three times in sterile dH_20 (Sijmons *et al.*, 1991). The sterilized seeds were placed into sterile Petri dishes (9 cm in diameter) on a modified 0.2 concentrated Knop medium supplemented with 2% sucrose (Sijmons *et al.*, 1991). Seeds were kept at 4°C for 3 days prior to incubation in a growth chamber at 25°C with a 16-h light and 8-h dark cycle.

DNA and RNA isolation from A. thaliana

Genomic DNA and total RNA were extracted from various organs of *A. thaliana* (ecotype Columbia) following the method of Gustincich *et al.* (1991) as modified by Clark *et al.* (1997). Genomic DNA was isolated from young leaves of *A. thaliana*. RNA was isolated from complete shoots and roots of 21-day-old *A. thaliana* plants.

Plasmid construction

DNA manipulation, including enzymatic digestions, agarose gel electrophoresis, ligation and transformation to *Escherichia coli* DH5α were performed according to Sambrook *et al.* (1989). Promoters of various Arabidopsis expansin genes were cloned into the binary vector pGPTV-HPT (Becker, 1992) in order to drive the expression of the β-glucuronidase reporter gene (*gus*). The promoters were from *AtEXPA1* (from −1610 to −70 bp before the ATG start codon), *AtEXPA4* (from −2299 to −82 bp), *AtEXPA10* (from −1561 to −70 bp) and *AtEXPA15* (−1635 to −38 bp). In most cases, genomic fragments containing whole promoter regions were first subcloned from appropriate BAC clones (Arabidopsis Stock Centre, Ohio State University, Columbus, OH, USA) by restriction and ligation into either pUC118 or pBSK plasmids. For *AtEXPA10* and *AtEXPA15*, promoter regions were first amplified by PCR using primers engineered with suitable restriction sites, then cloned into either pUC18 or pUC118. Promoters were then excised with appropriate restriction enzymes and ligated into the polylinker site of pGPTV-HPT (Cosgrove and Durachko, unpublished results). The pGPTV-HPT vectors were amplified in *E. coli* DH5α and then transformed into *Agrobacterium tumefaciens* strain C58C1.

A 1704-bp *AtEXPA6* promoter fragment was produced and cloned into the binary pMOG819 vector that contains *gus* and *nptII*, flanked by the T-DNA border sequences. This *AtEXPA6* promoter::GUS construct was transformed from *E. coli* DH5α into *A. tumefaciens* strain MOG101 (Goddijn *et al.*, 1993) by triparental mating, using the helper plasmid pRK2013 in *E. coli* DH5α.

The 953-bp *AtEXPA3* and the 577-bp *AtEXPA16* promoter fragments were amplified by PCR and cloned into pCambia 1304 vector. The vectors were amplified in *E. coli* DH10β and then electroporated into *A. tumefaciens* LBA 4404.

Plant transformation

In most cases, the *AtEXPA*::GUS chimeric constructs were inserted into the genome of *A. thaliana*, ecotype Columbia, by Agrobacterium-mediated transformation using the floral-dip method (Bechtold *et al.*, 1993; Bent *et al.*, 1994). For *AtEXPA10*, ecotype C24 was used. Transformants were identified by hygromycin

selection, selfed, and homozygous lines were characterized (Cosgrove and Durachko, unpublished results). *AtEXPA3*::GUS and *AtEXPA16*::GUS transformants were selected on kanamycin. In the case of the *AtEXPA6*::GUS construct, 51 transformants were regenerated from *A. thaliana* (ecotype C-24) root explants according to Valvekens *et al.* (1988).

Nematode infection

Cysts of *H. schachtii* cultures were harvested from *in vitro* stock cultures on mustard (*Sinapsis alba* cv. Albatros) roots growing on 0.2 concentrated Knop medium supplemented with 2% sucrose (Sijmons *et al.*, 1991). Hatching of juveniles was stimulated by soaking cysts in 3 mM $ZnCl_2$. The larvae were then washed four times in sterile H_2O and resuspended in 0.5% (w/v) Gelrite (Duchefa, Haarlem, The Netherlands) before inoculation. Twelve-day-old roots of *A. thaliana* plants were inoculated under axenic conditions with about 30 juveniles.

Histochemical localization of GUS activity

Histochemical detection of GUS activity was performed by staining, according to the method of Schrammeijer *et al.* (1990), using a solution of 2 mM 5-bromo-4-chloro-3-indolyl-β-D-glucuronic acid (X-gluc; Biomol, Hamburg, Germany) in 0.1 M sodium phosphate buffer pH 7.0, 0.1% Triton-X 100, 0.5 mM $K_3[Fe(CN)_6]$, 0.5 mM $K_4[Fe(CN)_6]$ and 10 mM Na_2EDTA incubated overnight at 37°C. After staining, chlorophyll was extracted from photosynthetic tissues with 70% (v/v) ethanol. The *gus* expression was detected microscopically by the distinct blue colouration resulting from the enzymatic cleavage of X-gluc. The GUS staining of roots of *AtEXPA1*::GUS, *AtEXPA4*::GUS, *AtEXPA6*::GUS, *AtEXPA10*::GUS and *AtEXPA15*::GUS lines containing syncytia was examined at 5 dai. Plants of line *AtEXPA6*::GUS used for the histochemical localization of GUS activity were additionally examined at 3, 4, 5, 7, 12, 15 and 18 dai.

RT-PCR

Oligonucleotide primers flanking the protein coding sequences of *A. thaliana* expansin genes (see Supplementary Material) were used for first-strand synthesis and amplification of mRNA templates. Control reactions were performed using the 5′ primer (5′-GGTGGTAACGGGTGACGGAGAAT-3′) and 3′ primer (5′-CGCCGACCGAAGGGACAAGCCGA-3′) designed from the sequence of *A. thaliana* 18S ribosomal cDNA. Total RNA (50 ng) was denatured for 3 min at 65°C and added to the RT reaction mix (final concentrations: 1 × RT buffer; 0.5 mM of each dNTP; 1 μM gene-specific 3′ primer; 10 U Rnasin, Promega, Mannheim, Germany; 1.0 μl Sensiscript Reverse Transcriptase, Qiagen, Helden, Germany; in a total volume of 20 μl). Samples were incubated at 37°C for 1 h, heated to 95°C for 5 min, and cooled to 10°C for 15 min. The cDNA was amplified by PCR using a PCR mix containing 1 × PCR buffer (Qiagen), 1.5 mM $MgCl_2$, 200 μM of each dNTP, 1.0 μM each of the gene specific primers, 2.5 U HotStar*Taq* DNA Polymerase (Qiagen). Two PCR protocols were used, PCR1 and PCR2. The cycle order for PCR1 was as follows: denaturation for 2 min at 94°C; cycles 1–20, 15 sec at 94°C, 0.7°C sec^{-1} to 65°C, 30 sec at 65°C, 1.5°C sec^{-1} to 72°C and 2 min at 72°C; cycles 21–40, 15 sec at 94°C, slope 0.7°C sec^{-1} to 45°C, 30 sec at 45°C, 1.5°C sec^{-1} to 72°C, 2 min at 72°C; 5 min at 72°C. The cycle order for PCR2 was as follows: denaturation for 2 min at 94°C; cycles 1–40, 40 sec at 94°C, 0.7°C sec^{-1} to 60°C, 1 min at 65°C, 1.5°C sec^{-1} to 72°C; 5 min 72°C. RT-PCR products (18 μl) were separated on a 1.0% agarose gel. The specificity of each primer pair was established by RT-PCR reactions from *A. thaliana* shoot RNA of a predicted unique fragment, the identity of which was confirmed by DNA sequencing.

Table 4 Number of cycles performed in semi-quantitative RT-PCR for *18S rRNA*, *UBQ1*, and expansin genes

	5 dai		10 dai		15 dai	
	Syncytia	Roots	Syncytia	Roots	Syncytia	Roots
18S rRNA/UBQ	20 +19	22 +19	20 +19	26 +19	24 +19	26 +19
Expansins	39	41	39	45	43	45

Semi-quantitative RT-PCR

Syncytia and corresponding uninfected root fragments without root tips and lateral root primordia were collected, and total RNA was isolated using the RNeasy Plant Mini Kit (Qiagen) according to the manufacturer's instructions, including DNA digestion with *DNaseI*. Syncytia were dissected at 5, 10 and 15 dai. cDNA was amplified using SuperScript III reverse transcriptase (Invitrogen, Carlsbad, CA, USA) and random primer [oligo$(dN)_6$]. For PCR experiments a 1:10 cDNA dilution and specific primer pairs were used (see Supplementary Material). PCR conditions were as described above. Because of the very limited quantity of the RNA isolated from syncytia samples, the measurement of the RNA concentration was not possible. Therefore, PCR conditions (number of cycles) were established for *18S rRNA* and *UBQ1* to give bands of similar intensity with each RNA sample. Because of the lower level of expansin transcripts, the number of cycles was increased for PCR reactions with expansin primers (Table 4). In this way the bands for all RNA samples can be compared directly. The PCR cycles for 18S rRNA and *UBQ1* controls were: 20 cycles for syncytia at 5 and 10 dai, 22 cycles for control roots at the age corresponding to 5 dai, 24 cycles for syncytia at 15 dai and 26 cycles for control roots at the age corresponding to 10 and 15 dai. For expansin genes, 39 cycles for syncytia at 5 and 10 dai, 41 cycles for control roots at the age corresponding to 5 dai, 43 cycles for syncytia at 15 dai and 45 cycles for control roots at the age corresponding to 10 and 15 dai, were performed.

RNA isolation from syncytia and cDNA library construction

The cytoplasm of syncytia was extracted with a microcapillary and a micromanipulator (Eppendorf AG, Hamburg, Germany) without contamination from either uninfected root cells or nematodes (Jürgensen *et al.*, 2003). Samples of cytoplasm were collected between 5 and 7 dai. Total RNA was isolated from 100 micro-aspirated syncytia by using the RNeasy Plant Mini Kit (Qiagen). An aliquot of approximately 15 syncytia was used for cDNA library construction. A syncytium-specific cDNA library, containing approximately 2.5×10^6 primary recombinants, was produced with the SMART™ cDNA library construction kit (Clontech Laboratories, Palo Alto, CA, USA), according to the manufacturer's instructions. The quality of the cDNA library was determined by PCR amplification of known nematode-responsive plant genes (P.S. Puzio, P. Voss, F.M.W. Grundler, Institut für phytopathologie, Universität

Kiel, Germany unpublished results). A sample of the primary non-amplified cDNA library (2 μl) was used as the template for PCR reactions.

PCR reactions with A. thaliana *gDNA and syncytium-specific cDNA library*

For PCR reactions 1 μg μl^{-1} gDNA from *A. thaliana* and 2 μl of syncytium-specific cDNA were used, respectively. The reactions were performed with HotStar*Taq* DNA Polymerase (Qiagen) as described above.

In situ *RT-PCR*

The *in situ* RT-PCR was performed according to the method described by Koltai and Bird (2000) and Urbanczyk-Wochniak *et al.* (2001). Infected and non-infected *A. thaliana* control roots were cut into small pieces and fixed at 4°C for 24 h in fixation solution (63% ethanol, v/v; 2% formalin v/v) at 5 dai. Fixed samples were washed three times for 10 min each in 63% (v/v) ethanol and once in phosphate-buffered saline (PBS; 10 mM Na_3PO_4 and 130 mM NaCl, pH 7.5). Samples were embedded into 5 % (w/v) low-melting point agarose in PBS. Small blocks of agarose containing root samples were attached to the block of a Vibratom (VT 1000, Leica, Wetzlar, Germany), sections (20–30 μm thick) were cut and then digested overnight at 37°C with 8 U of *DNase* (Fluka, Sigma-Aldrich, Seelze, Germany). Washing steps were always performed for 10 min at 37°C: once with 0.5 M EDTA, twice with 2 × SSC, once with 1 × SSC and 0.5 × SSC and finally with *RNase*-free water. Afterwards, about ten agarose-free root sections were transferred into 10 μl of RT mix per reaction tube. For in-well RT amplification the same conditions as described for normal RT-PCR were used. PCR was performed in a 50 μl reaction volume containing 0.25 μl of *Taq* polymerase (5 U μl^{-1}; BioTherm, GeneGraft, Lüdinghausen, Germany) and the appropriate 10 × buffer, 1 μl primer (10 μM), 1 μl each of dCTP, dGTP and dATP (10 mM), 2.36 μl dTTP (2 mM) and 0.5 μl digoxigenin-11-dUTP (DIG; 1 mM; Roche Diagnostics, Indianapolis, IN, USA). For PCR profiles see RT-PCR and Supplementary Material. Positive control reactions were performed using the 5′ and 3′ primers designed from the sequence of *A. thaliana* 18S ribosomal cDNA, as describe above. Three different negative controls reactions were performed, by omitting primers, *Taq* DNA polymerase or digoxigenin-11-dUTP, respectively. Afterwards cross sections were washed twice with 1 × PBS for 5 min, once with 0.1% (v/w) BSA (Roth, Karlsruhe, Germany) in PBS for 30 min and finally with anti-DIG antibodies (1:500; 150 U; Roche Diagnostics) in PBS containing BSA for 1 h at room temperature (25°C). Root sections were then washed twice for 15 min with washing buffer (0.1 M Tris-HCl, 0.15 M NaCl, pH 9.5). Staining reactions (5–10 min) with NBT/BCIP (Roche Diagnostics, Mannheim, Germany) were performed according to the manufacturer's recommendations. Sections with satisfactory signals were photographed under an inverse microscope (Axiovert 200M; Zeiss, Hallerbergmoos, Germany) containing an integrated camera (AxioCam MRc5; Zeiss).

Affymetrix Genechip analysis

Syncytia were aspirated and RNA isolated as described above. Root segments cut from the elongation zone were used as controls. Care was taken to avoid any either root tips or lateral root primordia. Biotin-labelled probes were synthesized according to the Affymetrix protocol with some modifications. Details will be published elsewhere. ATH1 genechips were hybridized by German Resource Centre for Genome Research GmbH (Berlin, Germany) according to the manufacturer's protocols.

Affymetrix CEL files were read into the R statistical analysis environment (http://www.r-project.org) using the affy package of the Bioconductor suite (http://www.bioconductor.org). Probe sequence-specific 'background correction' (Wu *et al.*, 2004) was performed using routines available in the Bioconductor gcrma package. Both 'PM' and 'MM' probes were employed for this correction. A heuristic estimate for optical instrument background as offered in gcrma, however, was not subtracted. An inspection of exploratory pairwise scatter and 'MA' plots confirmed the necessity for inter-chip normalization. As an examination of pairwise quantile–quantile plots showed only random fluctuations, inter-chip normalization could be achieved using quantile–quantile normalization (Bolstad *et al.*, 2003). See Supplementary Material.

After normalization, robust summaries of probe set signals were obtained for each gene using an iterative weighted least-squares fit of a linear probe level model (Bolstad, 2004) through the fitPLM function of the Bioconductor package affyPLM. This process automatically identifies unreliable chip areas and correspondingly downweights outlier probes. See Supplementary Material.

The normalized data on a $\log_2$ scale was then fitted gene by gene with a linear model, including hybridization batch effects, using the lmFit function (Smyth, 2004) of the Bioconductor package limma. The pairwise contrasts from this fit shown in Table 2 also include *q*-values as indicators of significance after the correction for multiple-testing controlling the False Discovery Rate (Benjamini and Hochberg, 1995). For the statistical tests, individual gene variances have been moderated using an Empirical Bayes approach that draws strength from transferring variance characteristics from the set of all genes to the test for each individual gene (Smyth, 2004).

Acknowledgements

We would like to thank Krzysztof Jeziorny for technical support in preparing the figures. This research was supported by grant QLK-CT-1999-01501 ('NONEMA') from the European Union within the 5th Framework, FWF grant P16296-B06, and by grant IBN-9874432 from the US National Science Foundation. DPK acknowledges funding by the Vienna Science and Technology Fund (WWTF), the Austrian Centre of Biopharmaceutical Technology (ACBT), Austrian Research Centres (ARC) Seibersdorf, and Baxter AG.

Supplementary Material

The following supplementary material is available for this article online:

Table S1. Sequences of primer pairs for Arabidopsis *AtEXPA* and *AtEXPB*. The numbers in brackets indicate the annealing temperature if different from given in original PCR protocol.

This material is available as part of the online article from http://www.blackwell-synergy.com

References

Balestrini, R., Cosgrove, D.J. and Bonfante, P. (2004) Differential location of α-expansin proteins during the accommodation of root cells to an arbuscular mycorrhizal fungus. *Planta*, **220**, 889–899.

Barthels, N., van der Lee, F.M., Klap, J. *et al.* (1997) Regulatory sequences of Arabidopsis drive reporter gene expression in nematode feeding structures. *Plant Cell*, **9**, 2119–2134.

Bechtold, N., Ellis, J. and Pelletier, G. (1993) In planta Agrobacterium mediated gene transfer by infiltration of adult *Arabidopsis thaliana* plants. *C. R. Acad. Sci. Paris*, **316**, 1194–1199.

Becker, D. (1992) New plant binary vectors with selectable markers located proximal to the left T-DNA border. *Plant Mol. Biol.* **20**, 1195–1197.

Benjamini, Y. and Hochberg, Y. (1995) Controlling the false discovery rate: a practical and powerful approach to multiple testing. *J. R. Stat. Soc. Ser. B* **57**, 289–300.

Bent, A., Kunkel, B.N., Dahlbeck, D., Brown, K.L., Schmidt, R., Giraudat, J., Leung, J. and Staskawicz, B.J. (1994) *Rps2* of *Arabidopsis thaliana* – a leucine-rich repeat class of plant-disease resistance genes. *Science*, **265**, 1856–1860.

Bolstad, B.M. (2004) Low Level Analysis of High-density Oligonucleotide Array Data: Background, Normalization and Summarization. PhD Dissertation. University of California, Berkeley.

Bolstad, B.M., Irizarry, R.A., Astrand, M. and Speed, T.P. (2003) A comparison of normalization methods for high density oligonucleotide array data based on bias and variance. *Bioinformatics*, **19**, 185–193.

Caderas, D., Muster, M., Vogel, H., Mandel, T., Rose, J.K.C., McQueen-Mason, S. and Kuhlmeier, C. (2000) Limited correlation between expansin gene expression and elongation growth rate. *Plant Physiol.* **123**, 1399–1413.

Cho, H.T. and Cosgrove, D.J. (2002) Regulation of root hair initiation and expansin gene expression in Arabidopsis. *Plant Cell*, **14**, 3237–3253.

Cho, H.T. and Cosgrove, D.J. (2004) Expansins as agents of hormone action. In *Plant Hormones: Biosynthesis, Signal Transduction, Action!* (Davies, P.J., ed.). Dordrecht: Kluwer, pp. 262–281.

Cho, H.T. and Kende, H. (1997) Expression of expansin genes is correlated with growth in deepwater rice. *Plant Cell*, **9**, 1661–1671.

Clark, A.M., Jacobsen, K.R., Dannenhoffer, J.M., Skaggs, M.I. and Thompson, G.A. (1997) Molecular characterisation of a phloem-specific gene encoding the filament protein, phloem protein 1 (PP1), from Cucurbita maxima. *Plant J.* **12**, 49–61.

Cosgrove, D.J. (1998) Cell wall loosening by expansins. *Plant Physiol.* **118**, 333–339.

Cosgrove, D.J. (2000a) New genes and new biological roles for expansins. *Curr. Opin. Plant Biol.* **3**, 73–78.

Cosgrove, D.J. (2000b) Loosening of plant cell walls by expansins. *Nature*, **407**, 321–326.

Cosgrove, D.J., Bedinger, P. and Durachko, D.M. (1997) Group I allergens of grass pollen as cell wall-loosening agents. *Proc. Natl Acad. Sci. USA*, **94**, 6559–6564.

Gal, T.Z., Aussenberg, E.R., Burdman, S., Kapulnik, Y. and Koltai, H. (2005) Expression of a plant expansin is involved in the establishment of root knot nematode parasitism in tomato. *Planta*, **224**, 155–162.

Giordano, W. and Hirsch, A.M. (2004) The expression of *MaEXP1*, a *Melilotus alba* expansin gene, is upregulated during the sweet-clover-*Sinorhizobium meliloti* interaction. *Mol. Plant Microbe Interact.* **17**, 613–622.

Goddijn, O.J., Lindsey, K., van der Lee, F.M., Klap, J.C. and Sijmons, P.C. (1993) Differential gene expression in nematode-induced feeding structures of transgenic plants harboring promoter-*gusA* fusion constructs. *Plant J.* **4**, 863–873.

Goellner, M., Wang, X. and Davis, E.L. (2001) Endo-β-1,4-Glucanase expression in compatible plant–nematode interaction. *Plant Cell*, **13**, 2241–2255.

Golecki, B., Fudali, S., Wieczorek, K. and Grundler, F.M.W. (2002) Identification and localisation of tomato expansin gene expression in nematode-induced syncytia. *Nematology*, **4**, 219.

Golinowski, W., Grundler, F.M.W. and Sobczak, M. (1996) Changes in the structure of *Arabidopsis thaliana* during female development of plant-parasitic nematode *Heterodera schachtii*. *Protoplasma*, **194**, 103–116.

Grundler, F.M.W. and Böckenhoff, A. (1997) Physiology of nematode feeding and feeding sites. In *Cellular and Molecular Aspects of Plant–Nematode Interactions* (Fenol, C., Grundler, F.M.W. and Ohl, S.A., eds). Dordrecht: Kluwer, pp. 107–119.

Grundler, F.M.W., Sobczak, M. and Golinowski, W. (1998) Formation of wall openings in root cells of *Arabidopsis thaliana* following infection by the plant–parasitic nematode *Heterodera schachtii*. *Eur. J. Plant Pathol.* **104**, 545–551.

Gustincich, S., Manfioletti, G., del Sal, G. and Schneider, C. (1991) A fast method for high quality genomic DNA extraction from whole human blood. *Biotechniques*, **11**, 298–302.

Jammes, F., Lecomte, P., de Almeida-Engler, J., Bitton, F., Martin-Magniette, M.L., Renou, J.P., Abad, P. and Favery, B. (2005) Genome-wide expression profiling of the host response to root-knot nematode infection in Arabidopsis. *Plant J.* **44**, 447–458.

Jürgensen, K., Scholz-Starke, J., Sauer, N., van Bel, A.J.E. and Grundler, F.M.W. (2003) The companion cell-specific Arabidopsis disaccharide carrier *AtSUC2* is expressed in nematode-induced syncytia. *Plant Physiol.* **131**, 1–9.

Kende, H., Bradford, K.J., Brummell, D.A. *et al.* (2004) Nomenclature for members of the expansin superfamily of genes and proteins. *Plant Mol. Biol.* **55**, 311–314.

Koltai, H. and Bird, D.M. (2000) High throughput cellular localization of specific plant mRNAs by liquid-phase in situ reverse transcription-polymerase chain reaction of tissue sections. *Plant Physiol.* **123**, 1203–1212.

Kudla, U., Qin, L., Milac, A. *et al.* (2005) Origin, distribution and 3D-modeling of GR-EXPB1, an expansin from the potato cyst nematode *Globodera rostochiensis*. *FEBS Lett.* **579**, 2451–2457.

Laine, M.J., Haapalainen, M., Wahlroos, T., Kankare, K., Nissinen, R., Kassuwi, S. and Metzler, M.C. (2000) The cellulase encoded by the native plasmid of *Clavibacter michiganensis* ssp. sepedonicus plays a role in virulence and contains an expansin-like domain. *Physiol. Mol. Plant Pathol.* **57**, 221–233.

Li, Y., Darley, C.P., Ongaro, V., Fleming, A., Schipper, O., Baldauf, S.L. and McQueen-Mason, S.J. (2002) Plant expansins are a complex multigene family with an ancient evolutionary origin. *Plant Physiol.* **128**, 854–864.

McQueen-Mason, S.J. and Cosgrove, D.J. (1995) Expansins mode of action on cell walls: analysis of wall hydrolysis, stress relaxation, and binding. *Plant Physiol.* **107**, 87–100.

McQueen-Mason, S.J. and Rochange, F. (1999) Expansins in plant growth and development: an update on an emerging topic. *Plant Biol.* **1**, 19–25.

McQueen-Mason, S.J., Durachko, D.M. and Cosgrove, D.J. (1992) Two endogenous proteins that induce cell wall extension in plants. *Plant Cell*, **4**, 1425–1433.

Mitchum, M.G., Sukno, S., Wang, X., Shani, Z., Tsabary, G., Shoseyov, O. and Davis, E. (2004) The promoter of the *Arabidopsis thaliana* cel1 endo-1,4-β glucanase gene is differentially expressed on plant feeding cells induced by root-knot and cyst nematode. *Mol. Plant Pathol.* **5**, 175–181.

Plovie, E., de Buck, S., Goeleven, E., Tanghe, M., Vercauteren, I. and Gheysen, G. (2003) Hairy roots to test for transgenic nematode resistance: think twice. *Nematology*, **5**, 831–841.

Puzio, P., Cai, D., Ohl, S., Wyss, U. and Grundler, F.M.W. (1998) Isolation of regulatory DNA region related to differentiation of nematode feeding structure in *Arabidopsis thaliana*. *Physiol. Mol. Plant Pathol.* **53**, 177–193.

Puzio, P.S., Lausen, J., Heinen, P. and Grundler, F.M.W. (2000) Promoter analysis of *pyk20*, a gene from *Arabidopsis thaliana*. *Plant Sci.* **22**, 245–255.

Qin, L., Kudla, U., Roze, E.H.A. *et al.* (2004) A nematode expansin acting on plants. *Nature*, **427**, 30.

Ramsay, K., Wang, Z.H. and Jones, M.G.K. (2004) Using laser capture microdissection to study gene expression in early stages of giant cells induced by root-knot nematodes. *Mol. Plant Pathol.* **5**, 587–592.

Saloheimo, M., Paloheimo, M., Hakola, S., Pere, J., Swanson, B., Nyyssönen, E., Bhatia, A., Ward, M. and Penttilä, M. (2002) Swollenin, a *Trichoderma reesei* protein with sequence similarity to the plant expansins, exhibits disruption activity on cellulosic materials. *Eur. J. Biochem.* **269**, 4202–4211.

Sambrook, J., Fritsch, E.F. and Maniatis, T. (1989) *Molecular Cloning: A Laboratory Manual*, 2nd edn. Cold Spring Habor, NY: Cold Spring Harbor Laboratory Press.

Sánchez, A.M., Mateos, I., Labrador, E. and Dopico, B. (2004) Brassinolides and IAA induce the transcription of four α-expansin genes related to development in *Cicer arietinum*. *Plant Physiol. Biochem.* **42**, 709–716.

Schrammeijer, P.C., Sijmons, P.C., van den Elzen, P.J.M. and Hoekema, A. (1990) Meristem transformation of sunflower via Agrobacterium. *Plant Cell Rep.* **9**, 55–60.

Sijmons, P.C., Grundler, F.M.W., von Mende, N., Burrows, P.R. and Wyss, U. (1991) *Arabidopsis thaliana* as a new model host for plant-parasitic nematodes. *Plant J.* **1**, 245–254.

Smyth, G.K. (2004) Linear models and empirical Bayes methods for assessing differential expression in microarray experiments. *Stat. Appl. Gene. Mol. Biol.* **3**, Article 3.

Urbanczyk-Wochniak, E., Filipecki, M. and Przybecki, Z. (2001) A useful protocol for *in situ* RT-PCR on plant tissues. *Cell. Mol. Biol. Lett.* **7**, 7–18.

Valvekens, D., van Montagu, M. and van Lijsebettens, M. (1988) Agrobacterium tumefaciens-mediated transformation of *Arabidopsis thaliana* root explants by using kanamycin selections. *Proc. Natl Acad. Sci. USA*, **85**, 5536–5540.

Vercauteren, I., de Almeida Engler, J., de Groodt, R. and Gheysen, G. (2002) An *Arabidopsis thaliana* pectin acetylesterase gene is upregulated in nematode feeding sites induced by root-knot and cyst nematodes. *Mol. Plant Microbe Interact.* **15**, 404–407.

Wu, Y., Meeley, R.B. and Cosgrove, D.J. (2001) Analysis and expression of the α-expansins and β-expansins gene families in maize. *Plant Physiol.* **126**, 222–232.

Wu, Z., Irizarry, R.A., Gentleman, R., Martinez-Murillo, F. and Spencer, F. (2004) A model based background adjustment for oligonucleotide expression arrays. *J. Am. Stat. Assoc.* **99**, 909–917.

Wyss, U. and Grundler, F.M.W. (1992) Feeding behavior of sedentary plant parasitic nematodes. *Neth. J. Plant. Pathol.* **98** (Suppl. 2), 165–173.

Zimmermann, P., Hirsch-Hoffmann, M., Hennig, L. and Gruissem, W. (2004) GENEVESTIGATOR. Arabidopsis microarray database and analysis toolbox. *Plant Physiol.* **136**, 2621–2632.

Accession numbers: *AtEXPA1*, At1g69530; *AtEXPA2*, At5g05290; *AtEXPA3*, At2g37640; *AtEXPA4*, At2g39700; *AtEXPA5*, At3g29030; *AtEXPA6*, At2g28950; *AtEXPA7*, At1g12560; *AtEXPA8*, At2g40610; *AtEXPA9*, At5g02260; *AtEXPA10*, At1g26770; *AtEXPA11*, At1g20190; *AtEXPA12*, At3g15370; *AtEXPA13*, At3g03220; *AtEXPA14*, At5g56320; *AtEXPA15*, At2g03090; *AtEXPA16*, At3g55500; *AtEXPA17*, At4g01630; *AtEXPA18*, At1g62980; *AtEXPA19*, At3g29365; *AtEXPA20*, At4g38210; *AtEXPA21*, At5g39260; *AtEXPA22*, At5g39270; *AtEXPA23*, At5g39280; *AtEXPA24*, At5g39310; *AtEXPA25*, At5g39300; *AtEXPA26*, At5g39290; *AtEXPB1*, At2g20750; *AtEXPB2*, At1g65680; *AtEXPB3*, At4g28250; *18S rRNA*, X16077; *UBQ1*, At3G52590

CHAPTER 4

Arabidopsis endo-1,4-β-glucanases are involved in the formation of root syncytia induced by *Heterodera schachtii*

Wieczorek, K., Hofmann, J., Blöchl, A., Szakasits, D., Holger Bohlmann, H. and Grundler, F.M.W.

The Plant Journal (2008) 53:336-351.

The Plant Journal (2008) **53**, 336–351 doi: 10.1111/j.1365-313X.2007.03340.x

Arabidopsis endo-1,4-β-glucanases are involved in the formation of root syncytia induced by *Heterodera schachtii*

Krzysztof Wieczorek[1], Julia Hofmann[1], Andreas Blöchl[2], Dagmar Szakasits[1], Holger Bohlmann[1] and Florian M. W. Grundler[1,*]
[1]*Institute of Plant Protection, Department of Applied Plant Sciences and Plant Biotechnology, University of Natural Resources and Applied Life Sciences, A-1190 Vienna, Austria, and*
[2]*Department of Chemical Ecology and Ecosystem Research, University of Vienna, A-1090 Vienna, Austria*

Received 16 August 2007; revised 25 September 2007; accepted 28 September 2007.
[*]For correspondence (fax +43 1 47654 3359; e-mail florian.grundler@boku.ac.at).

Summary

Cyst nematodes induce root syncytia with specific features such as hypertrophy, increased metabolic activity and fusion with adjacent cells. Cell walls of the syncytia undergo massive changes such as thickening, local dissolution and formation of ingrowths. Cell wall degrading and modifying proteins are apparently involved in syncytium formation but detailed knowledge of this is still limited. Therefore, we studied the regulation and function of the entire Arabidopsis endo-1,4-β-glucanase gene family in syncytia induced by *Heterodera schachtii*. Endo-1,4-β-glucanases hydrolyze the 1,4-β-glucosidic linkages between glucose residues. Using semi-quantitative and quantitative approaches we identified seven genes that are upregulated in syncytia. Two of these genes, coding for secreted AtCel2 and membrane-bound KOR3, are shoot-specific but show high expression in syncytia at different developmental stages. *In silico* analysis of the promoter regions of both genes compared with other genes with modified regulation in nematode feeding sites did not reveal specific *cis*-acting elements that could be related to specific transcription in syncytia. However, motifs responsive to sugar and different plant hormones were identified. Accordingly, treatments with sucrose, gibberellic acid and NAA induced upregulation of *AtCel2*, whereas ABA triggered downregulation of both *AtCel2* and *KOR3* in roots. As *AtCel2* is related to degradation of the cell wall matrix, we analysed the hemicellulose content in syncytia. The measured values resembled the expression pattern of *AtCel2*. A distinctly reduced number of females developed in *cel2* and *kor3* T-DNA mutants, and we therefore conclude that endo-1,4-β-glucanases play an important role in the formation and function of syncytia.

Keywords: cell wall, endo-1,4-β-glucanases, Genechip, *Heterodera schachtii, in situ* RT-PCR, plant pathogens.

Introduction

The interaction between plant-parasitic nematodes and their host plants is very complex and highly specific. The sedentary cyst nematode *Heterodera schachtii* serves as an ideal model system (Wyss and Grundler, 1992a). Infective juveniles invade the roots and trigger the formation of syncytial feeding sites in the host tissue, serving as a nutrition source for the nematode. The induction and formation of these structures is linked with substantial changes in the infected root tissue. In the central cylinder, the syncytium arises from a single initial cell which fuses with neighbouring cells through local cell wall dissolution and expands by fusion of the protoplasts within the root (Golinowski *et al.*, 1996; Wyss and Grundler, 1992b). In this complex process the syncytial cell wall is greatly modified as it has to withstand the high osmotic pressure inside the enlarging feeding site on the one side (Böckenhoff and Grundler, 1994) and to expand and be locally dissolved on the other side. Golinowski *et al.* (1996) and Grundler *et al.* (1998) presented detailed descriptions of the modifications of the cell wall during induction and further maintenance of syncytia. While the outer syncytial cell walls are expanded and thickened, along the borders with xylem elements cell wall ingrowths are formed which enlarge the plasma membrane surface and facilitate short-distance transport. All these processes are controlled by the host plant and it is obvious that the massive reorganisation of the syncytial cell wall is based on the activity of appropriate factors and enzymes. The involvement of expansins in this process is relatively well

described. These proteins are cell wall modifying factors without hydrolytic activity but with a function in turgor-driven slippage of cellulose microfibrils causing extension of the cell wall (Cosgrove, 2000). In tomato (*Lycopersicon esculentum*) it was shown by use of microarray data, quantitative (q)RT-PCR and *in situ* localisation that *LeEXP5* is expressed in gall cells surrounding the giant cells induced by *Meloidogyne javanica* (Gal *et al.*, 2005). Recently, Wieczorek *et al.* (2006) reported on the upregulation of several expansin genes in syncytia induced by *H. schachtii* in *Arabidopsis thaliana* roots. The increase of expression of *AtEXPA3* and *AtEXPA16* in infected root tissue indicates the important role of these proteins in the development of feeding sites.

Enzymes that seem to play a role during the development of nematode feeding sites are plant endo-1,4-β-glucanases (EGases; EC 3.2.1.4). They are cellulolytic proteins that hydrolyse the 1,4-β-glucosidic linkages between glucose residues. In Arabidopsis, the endo-1,4-β-glucanases form a relatively large gene family with 25 members that interestingly belong to just one sequence family of endo-1,4-β-glucanases, whereas in all other cellulolytic organisms these genes can be classified into 11 different families (Henrissat *et al.*, 2001). About half of all endo-1,4-β-glucanase genes can be classified as tandem duplication of genes or duplication of DNA segments. The general role of endo-1,4-β-glucanases is known, but the specific function of most of the members is still unclear. The general function is usually linked to processes such as cell wall biosynthesis and modifications, cell elongation and differentiation, organ abscission (Del Campillo and Bennett, 1996) and fruit ripening (Rose and Bennett, 1999). The family consists of two groups: enzymes with a putative signal peptide (α- and β-subfamily) coding for secreted proteins and enzymes with a membrane-anchoring domain (γ-subfamily) coding for non-secreted proteins (Del Campillo, 1999).

The secreted proteins act within the cell wall including its outermost layers. Their potential substrates are cellulose and xyloglucan. Ohmiya *et al.* (1995, 2000) analysed two endo-1,4-β-glucanases from poplar (*Populus alba*), PopCel1 and PopCel2, and suggested that these enzymes hydrolyse non-crystalline regions of cellulose and loosen cell walls by releasing xyloglucans from cellulose microfibrils. This irreversible modification is thought to promote cell wall expansion. Recently, it was shown that expression of *PopCel1* in transgenic Arabidopsis plants leads to an enhanced growth rate and stimulation of cellulose biosynthesis (Park *et al.*, 2003).

The membrane-bound proteins (KOR and homologues KOR2 and KOR3) function at the innermost layers of the cell wall and hydrolyse amorphous cellulose. They do not act on crystalline cellulose, xyloglucan or xylans (Master *et al.*, 2004; Molhoj *et al.*, 2001). Three hypotheses on their function are proposed: they are involved in (i) chain termination during cellulose biosynthesis, (ii) in the degradation of a β-D-glucans that are not properly crystallised into cellulose micro-fibrils and (iii) in hydrolysis of lipid-linked intermediates acting as primers for the elongation of β-glucan chains (Del Campillo, 1999; Libertini *et al.*, 2003; Peng *et al.*, 2002; Reiter, 2002; Robert *et al.*, 2004).

There are some reports on the expression of endo-1,4-β-glucanase genes during nematode infection. Goellner *et al.* (2001) found five endo-1,4-β-glucanases from tobacco (*Nicotiana tabacum*) to be upregulated upon infection with root-knot and cyst nematodes. One of these genes, *NtCel7*, was further characterised recently. Wang *et al.* (2007) isolated the *NtCel7* promoter and analysed the expression pattern of *NtCel7* in soybean (*Glycine max*), tomato and Arabidopsis by use of histochemical approaches and transgenic plants. Further, Mitchum *et al.* (2004) and Sukno *et al.* (2006) showed *AtCel1*-driven GUS expression in tobacco and Arabidopsis upon infection with *Meloidogyne incognita*. However, infection with *Globodera tabacum* or *H. schachtii* did not lead to expression of the *AtCel1* promoter.

The relevance of glucanases in nematode parasitism is indirectly supported by the fact that the nematodes themselves produce and secrete endo-1,4-β-glucanases. Rosso *et al.* (1999) cloned a *Mi-eng-1* from *M. incognita* and suggested that this enzyme is involved in cell wall softening during nematode parasitism. Endo-1,4-β-glucanases were also found to be secreted by cyst nematodes. *ENG-1* and *ENG-2* were found to be released during penetration and intracellular migration by the soybean cyst nematode (De Boer *et al.*, 1999; Wang *et al.*, 1999; Yan *et al.*, 2001) and the tobacco cyst nematode (Goellner *et al.*, 2001). Gao *et al.* (2004) showed that three endo-1,4-β-glucanases are secreted by *Heterodera glycines* during infection of soybean. Secretion of two other endo-1,4-β-glucanases was also shown for the migratory root-lesion nematode *Pratylenchus penetrans* (Uehara *et al.*, 2001).

Nematodes are thought to inject not only active proteins into infected tissue (e.g. glucanases) but also plant hormones or hormone-related compounds (De Meutter *et al.*, 2005). On the other hand, nematodes are able to alter the hormone homeostasis within feeding sites, as shown by Goverse *et al.* (2000) and later by Karczmarek *et al.* (2004). Both strategies may influence expression of essential genes and thereby support the change from healthy root tissue to a feeding site.

There are several publications dealing with regulation of plant endo-1,4-β-glucanase genes. Recently, Sukno *et al.* (2006) analysed the promoter region of *AtCel1*, which is upregulated in galls induced by root-knot nematode *M. incognita*, in comparison with several other promoters that are known to be activated or downregulated either in giant cells or syncytia. They found a set of putative *cis*-acting elements that are development- and organ-specific, and elicitor- and hormone-responsive that also occur in other nematode-induced promoters such as *Lemmi9*,

Hahsp17.7G4, *AtSuc2* and *AtPyk20*. With the aid of hormone treatments it was possible to clone hormone-regulated EGases from several plants. Nakamura *et al.* (1995) found endo-1,4-β-glucanase from poplar to be upregulated by 2.4-dichlorophenoxyacetic acid (2,4-D) and downregulated by gibberellic acid (GA3), 6-benzyladenine (BA) and abscisic acid (ABA). Wu *et al.* (1996) found about a 10-fold increased concentration of an EGase from pea (*Pisum sativum*) after treatment with 2,4-D. Catalá *et al.* (1997) cloned auxin-regulated endo-1,4-β-glucanase from tomato and in Arabidopsis, Nicol *et al.* (1998) described changes in the expression of *KOR* after hormone treatments. They show that naphthaleneacetic acid (NAA) causes increase of *KOR* mRNA levels, while the effect of GA3 is minor and results in only a slight increase of *KOR* expression. They also tested 1-aminocyclopropane-1-carboxylic acid (ACC) but did not find any changes in *KOR* transcript abundance. Del Campillo *et al.* (2004) analysed the effects of several hormones on *AtCel5* from Arabidopsis – ABA, indole-3-acetic acid (IAA) and *N*-1-naphthylphthalamic acid (NPA), an auxin transport inhibitor, cause reduction of *AtCel5* expression, whereas there was no change in *AtCel5* expression after treatments with ACC. An analysis made by Wang *et al.* (2007) revealed that the *NtCel7* promoter contains an auxin-responsive element and several *cis*-acting elements that are gibberellin responsive, as well as a W-BOX and other elements that are sucrose, stress and pathogen responsive. The authors showed that the *NtCel7* promoter responds to auxin, but did not respond to gibberellin, ethylene or sucrose.

Other studies revealed that expression of endo-1,4-β-glucanases depends on addition of sucrose as shown for *PopCel1* and *PopCel2* (Ohmiya *et al.*, 2000) and for *AtCel1* (Shani *et al.*, 2006). Based on these results the authors suggest that the EGases are involved in cellulose biosynthesis.

In this work we studied the role of the entire endo-1,4-β-glucanase family in the development of syncytia induced by *H. schachtii* in roots of Arabidopsis. By use of specific syncytial material and different methods we analysed the gene expression, regulation and involvement in syncytium formation. Considering all obtained results, we conclude that at least two endo-1,4-β-glucanases play an important role in the formation and maintenance of syncytial feeding sites.

Results

Expression patterns of endo-1,4-β-glucanase genes in shoots and roots of uninfected plants

The results of RT-PCR reactions with total RNA isolated from shoot and root of Arabidopsis show the expression of all 25 endo-1,4-β-glucanase genes in uninfected plants. Ten genes were found in both shoot and root of the 21-day-old plant, whereas five (*AtCel2*, At2g44540, At2g44550, At2g44560 and At4g23560) were found only in the shoot and three (*KOR2*, At1g19940 and At4g39000) exclusively in the root. Seven genes could not be amplified with RNA isolated from either shoot or root. These results suggest that these genes are not expressed at the stage when plants were sampled (Table 1). Genevestigator data confirm that some of these genes are expressed only in specific organs, e.g. At2g44570 and At4g09740 exclusively in pollen (http://https://www.genevestigator.ethz.ch; Zimmermann *et al.*, 2004).

Table 1 Results of RT-PCR with total RNA isolated from roots and shoots of Arabidopsis and PCR with the syncytium-specific cDNA library obtained by use of primers distinguishing between 25 Arabidopsis endo-1,4-β-glucanase genes

Endo-1,4-β-glucanases	RT-PCR		cDNA library of syncytial cytoplasm
	Root	Shoot	
AtCel1	–	–	–
AtCel2	–	++	++
AtCel3	++	+	+++
AtCel5	–	–	–
KOR	+++	+++	+++
KOR2	++	–	–
KOR3	+	++	+++
At1g19940	+	–	–
At1g23210	+	–	–
At1g48930	+++	++	–
At1g64390	++	++	++
At1g75680	+++	++	–
At2g32990	++	++	++
At2g44540, −50, −60	–	+	–
At2g44570	–	–	–
At3g43860	–	–	–
At4g02290	++	++	+++
At4g09740	–	–	–
At4g11050	–	–	–
At4g38990	–	–	–
At4g39000	++	–	–
At4g39010	+	+	–
At4g23560	–	+	–

+, weak signal; ++, moderate signal; +++, strong signal; –, no signal.

Endo-1,4-β-glucanase genes are differentially expressed in nematode-induced syncytia

In the next step, we used a syncytium-specific cDNA library to determine which genes are expressed in 5–7-day-old feeding sites of *H. schachtii*. Polymerase chain reactions with specific primers show that 7 of the 25 endo-1,4-β-glucanase genes are expressed in syncytia. Signals were obtained for *AtCel2*, *AtCel3*, *KOR*, *KOR3*, At1g64390, At2g32990 and At4g02290. The results of both RT-PCR and PCR reactions are summarized in Table 1.

Results of PCR with the syncytium-specific cDNA library, RT-PCR reactions with RNAs isolated from healthy plants and expression data from Genevestigator indicate that only

Table 2 Signal intensities of the endo-1,4-β-glucanase genes in different organs of Arabidopsis. Data are shown for genes which were detected in syncytia induced by *Heterodera schachtii*. Data for Arabidopsis (Col-0) are taken from Genevestigator site (http://https://www.genevestigator.ethz.ch)

Anatomy	Cell suspension	Seedling	Inflorescence	Rosette	Roots
No. of chips	91	711	460	828	259
AtCel2	43	135	1756	189	19
AtCel3	5780	165	181	132	214
KOR	7620	10448	6330	7778	8705
KOR3	922	355	625	347	309
At2g32990	91	811	838	737	1398
At4g02290	4466	1245	4971	559	2933
At1g64390	2598	3802	3142	2713	3842

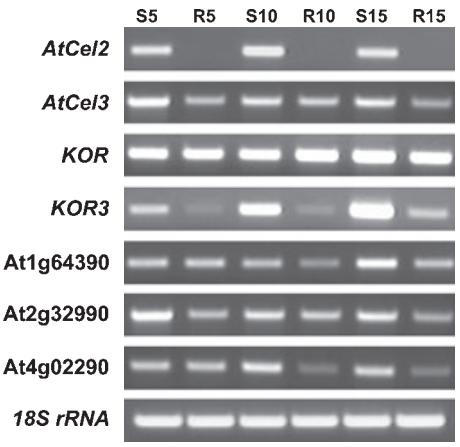

Figure 1. Semi-quantitative RT-PCR with specific primer pairs distinguishing between seven Arabidopsis endo-1,4-β-glucanase genes which were found in the syncytium-specific cDNA library.
Infected root fragments (S) were sampled at 5, 10 and 15 days after inoculation (dai) (S5, S10 and S15) and uninfected root pieces (R) corresponding to 5, 10 and 15 dai (R5, R10 and R15). *18S rRNA* was used as the control.

AtCel2 and *KOR3* are expressed in the infected root tissue and shoots, whereas in the uninfected control roots they are only weakly expressed and/or cannot be detected. Other genes upregulated in syncytia gave strong signals with the root as well as shoot samples. Data from Genevestigator are summarized in Table 2.

We performed semi-quantitative (sq)RT-PCR in order to determine a temporal expression profile of genes found to be upregulated in syncytia. We used RNA isolated from dissected root segments containing feeding sites and uninfected root fragments which served as a control. The samples were collected at three different time points: 5, 10 and 15 days after infection (dai). Primers for *18S rRNA* were used as an internal control.

The results show that most endo-1,4-β-glucanases are upregulated in feeding sites but are also present in uninfected root tissue. Two genes, *AtCel3* and At2g32990, gave the strongest signals with the infected tissue at 5 dai, whereas the strongest signal for At4g02290 was found at 10 dai. The strongest signals at 15 dai were obtained for *KOR3* and At1g64390. As an exception, *KOR* gave signals which were equal for all infected and uninfected samples.

AtCel2 has a different expression pattern and gave signals exclusively in infected samples. The strongest signals were obtained at 10 dai, whereas signals at 5 and 15 dai were equally extensive. Results of this analysis are presented in Figure 1.

With the aid of the techniques presented above we could detect whether transcripts of genes are present in the isolated infected root material (cDNA library, sqRT-PCR with root samples containing syncytia). By use of the very sensitive Affymetrix Genechip technology we were able to detect genes far below the detection level of the other methods. Genechip analysis also provided data on downregulated endo-1,4-β-glucanase genes in syncytia. Genechips for 5 dai, 15 dai and for uninfected root segments were made from micro-aspirated syncytial cytoplasm sampled without contamination from surrounding root tissue. Obtained results show that at 5 dai *AtCel1*, *AtCel2*, *AtCel3*, *KOR3*, At1g64390, At2g32990 and At4g02290 are significantly upregulated. Significant downregulation was observed in *AtCel5*, *KOR*, *KOR2*, At1g48930 (At1g19940, At4g09740 and At4g39000 at a lower level of significance, 25%<*q*-value>10%). At 15 dai only *AtCel2* and *KOR3* were found to be significantly upregulated (At2g32990 with 25%<*q*-value>10%), while downregulation of *KOR*, *KOR2* and At1g48930 could be detected (*AtCel5* and At4g39000 with 25%<*q*-value>10%). *AtCel2* and *KOR3* are significantly upregulated at both 5 and 15 dai, whereas *KOR*, *KOR2* and At1g48930 are downregulated at both time points. *AtCel2* and *KOR3* were the only genes found to be strongly upregulated at both time points. The results are shown in Table 3.

Gene expression of *AtCel2* and *KOR3* was further analysed by qRT-PCR, which, up to now, is the most sensitive and reliable quantification method. The same cDNA material taken for the semi-quantitative analysis was used for qRT-PCR, whereas primers for the genes were specifically designed. Both genes were found to be strongly upregulated at both 5 and 15 dai, thus confirming Genechip analysis.

The maximum expression level of *AtCel2* (indicated as $\log_2$) was detected at 10 dai. Values obtained for 5 and 15 dai were similar (Figure 2a). This result corresponds with the expression profile shown by sqRT-PCR. Expression values of *KOR3* increased continuously from 5 to 15 dai (Figure 2b). The highest value was obtained for the infected sample at 15 dai. Results resembled those of sqRT-PCR, while they differ slightly from those gained from Genechip analysis. This can be explained by the use of different materials taken for sqRT-PCR (dissected syncytia containing surrounding tissue)

Genes	Controls	Syn. 5 dai	Syn. 15 dai	Ctl versus 5 dai	Ctl versus 15 dai	5 dai versus 15 dai
AtCel1	5.64	7.63	5.60	1.89***	−0.20	−2.10*
AtCel2	2.74	6.82	6.95	3.94***	4.12***	0.19
AtCel3	2.90	5.03	3.01	2.07***	0.05	−2.03*
AtCel5	5.92	4.02	4.35	−1.88**	−1.63*	0.24
KOR	10.89	8.83	8.43	−2.21***	−2.51***	−0.30
KOR2	8.14	3.87	4.40	−4.20***	−3.68***	0.52
KOR3	5.37	9.02	8.71	3.56***	3.25***	−0.30
At1g19940	3.98	2.90	2.85	−0.95*	−0.96	0.00
At1g23210	2.11	2.21	2.34	0.04	0.13	0.09
At1g48930	9.53	2.54	2.86	−6.77***	−6.47***	0.30
At1g64390	4.97	6.84	5.72	1.88**	0.89	−0.99
At1g75680	9.74	9.93	9.64	0.16	−0.12	−0.28
At2g32990	7.13	9.27	9.00	2.27**	2.05*	−0.22
At2g44540	4.56	4.40	4.32	−0.27	−0.31	−0.04
At2g44560	4.57	4.55	4.75	−0.09	0.04	0.13
At2g44570	4.22	3.88	3.98	−0.55	−0.27	0.27
At3g43860	2.16	2.16	2.20	−0.07	0.00	0.07
At4g02290	6.00	8.44	5.67	2.33***	−0.37	−2.71***
At4g09740	4.20	3.51	3.72	−0.73*	−0.63	0.10
At4g11050	4.32	4.70	3.89	0.35	−0.38	−0.74
At4g38990	3.49	3.31	3.35	−0.28	−0.16	0.11
At4g39000	3.72	2.48	1.97	−1.17*	−1.53*	−0.35
At4g39010	3.88	3.76	3.59	−0.14	−0.29	−0.16

Ctl, control; Syn. syncytia; dai, days after inoculation.
*q < 25%; **q < 10%; ***q < 5%; see Experimental procedures for details.

Table 3 Genechip expression profiles of endo-1,4-β-glucanase genes in Arabidopsis roots during nematode infection. For three different time points the gene expression levels are shown as raw values on a $\log_2$ scale. After several normalization steps (see Experimental procedures for details) the changes between the two different conditions are shown as fold change $\log_2$ ratios, with values of ±1 corresponding to twofold up- or downregulation. Asterisks indicate significances determined by a Benjamini–Hochberg multiple correction test

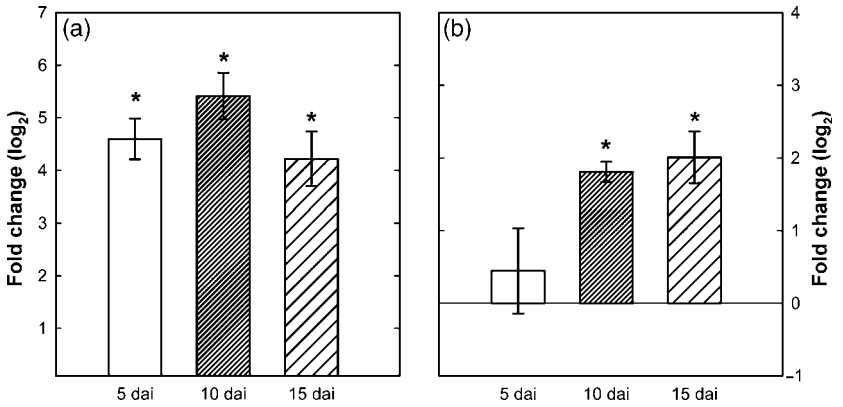

Figure 2. Changes in expression of *AtCel2* (a) and *KOR3* (b) in root samples containing syncytia at 5, 10 and 15 days after inoculation (dai).
The level of transcripts was measured by qRT-PCR relative to the expression of *AtUBP22* and *18S rRNA*. Asterisks indicate a significant difference between expression levels in infected and uninfected root samples ($P < 0.05$). $\log_2$ values are means ± SE, $n \geq 3$.

and Genechip hybridization (micro-aspirated syncytial cytoplasm).

All methods employed indicate the presence, absence or quantitative changes in expression of the genes but did not indicate the exact site of expression within the feeding sites and/or in the neighbouring root tissue. Therefore, *in situ* RT-PCR was used for the localisation of the transcripts of *AtCel2* and *KOR3* at the cellular level in fresh sections of syncytia at 10 dai. Specific staining of the mRNAs of these genes was found in feeding sites, while in the surrounding tissue only weak background staining could be observed. The localisation of specific PCR products of both genes in feeding sites is presented in Figure 3.

Analysis of AtCel2 *and* KOR3 *promoter regions*

In order to elucidate the possible regulatory mechanisms that trigger upregulation of *AtCel2* and *KOR3* in syncytia we performed an *in silico* analysis of their promoter regions. With the aid of plant-CARE, PLACE and MOTIF SAMPLER both promoter sequences were analysed for the most important *cis*-acting elements (Figure 4). In both promoters typical TATA boxes were found at the position −120 in *AtCel2* and −225 before ATG in *KOR3*.

According to the analysis of Sukno *et al.* (2006) we used a set of motifs (E-Box, EIRE, ERE, P-BOX, W-BOX, WUN-MOTIF) in order to compare promoters of *AtCel2* and *KOR3*

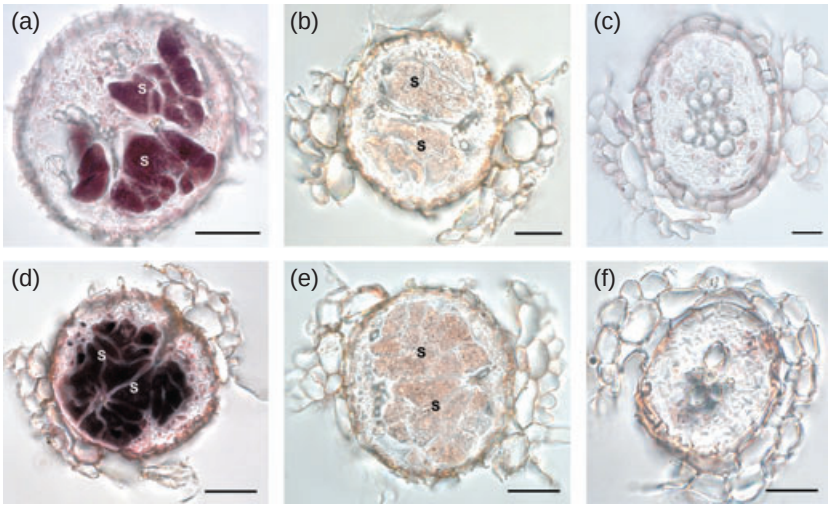

Figure 3. *In situ* RT-PCR analysis of *AtCel2* and *KOR3* on sections of syncytia induced by *Heterodera schachtii* at 10 days after inoculation (dai).
(a) *AtCel2* transcripts accumulate within syncytium.
(b) Control reaction for (a) performed without polymerase. Staining is not detected.
(c) Control reaction for (a) on a root section above the syncytium. Transcripts of *AtCel2* were not detected.
(d) Strong staining associated with transcripts of *KOR3* is visible in the syncytium.
(e) Control reaction to (d) performed without polymerase; no staining is visible.
(f) Control reaction for (d) on a root section above the syncytium. No transcripts of *KOR3* are visible.
(a), (b), (d) and (e) scale bar = 50 μm; (c) and (f) scale bar = 20 μm.

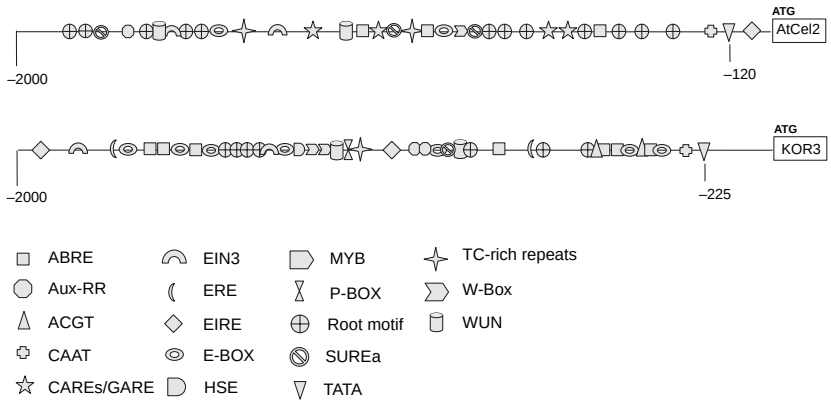

Figure 4. Promoter sequences of *AtCel2* and *KOR3* with predicted putative *cis*-acting elements.
Analysis performed with Plant-CARE (Lescot *et al.*, 2002), PLACE (Higo *et al.*, 1999) and MOTIF SAMPLER (Thijs *et al.*, 2001, 2002).

Table 4 *Cis*-acting elements according to Sukno *et al.* (2006) in promoter regions of genes upregulated (↑), downregulated (↓) or not regulated (↔) in syncytia induced by cyst nematode *Heterodera schachtii*

Gene	Accession numbers	Response to *H. schachtii*	Elements						Reference
			E-Box	EIRE	ERE	P-BOX	W-BOX	WUN-Motif	
AtCel2	At1g02800	↑	x			x	x	x	This publication
KOR3	At4g24260	↑	x	x	x		x	x	This publication
AtEXPA3	At2g37640	↑	x	x			x	x	Wieczorek *et al.* (2006)
AtEXPA16	At3g55500	↑	x	x			x	x	Wieczorek *et al.* (2006)
KOR2	At1g65610	↓	x	x	x		x	x	This publication
At1g48930	–	↓	x	x	x		x	x	This publication
AtEXPA7	At1g12560	↓	x	x	x	x	x	x	Wieczorek *et al.* (2006)
AtEXPA18	At1g62980	↓	x	x	x	x	x	x	Wieczorek *et al.* (2006)
At1g75680	–	↔	x				x	x	This publication

with each other and with genes known to be upregulated (*AtEXPA3*/At2g37640, *AtEXPA16*/At3g55500; Wieczorek *et al.*, 2006), downregulated (*KOR2*, At1g48930, *AtEXPA7*/At1g12560, *AtEXPA18*/At1g62980; Wieczorek *et al.*, 2006) and not regulated (At1g75680) in syncytia.

The occurrence of the motifs is presented in Table 4. All promoters share the occurrence of E-BOX, WUN-MOTIF and W-BOX. However, the analysis did not reveal a specific pattern in the occurrence of motifs that could be related to a syncytium-specific regulation. The downregulated genes *AtEXPA7* and *AtEXPA18* contain the complete set of the analyzed elements, while the upregulated *KOR3* contains exactly the same motifs as the downregulated genes *KOR2* and At1g48930. We performed the same analysis with

expression data of giant cells of root-knot nematodes but also could find no correlation (data not shown).

In a further analysis we looked for motifs that can be related to hormone and sugar responsiveness. In addition to AUX-RR (auxin-responsive), our analysis revealed the presence of several motifs such as ABRE (ABA-responsive), CAREs/GARE (gibberellin (GA)-responsive) and EIN3 (ethylene-responsive). Further, we identified three SURE motifs responsive to sugar in the promoter of *AtCel2* and one SURE element in the promoter of *KOR3*. In both promoters we identified stress- or pathogen-related motifs such as MYB or TC-rich repeats.

Sucrose affects expression of AtCel2 *but not* KOR3

The questions of how nematodes trigger the expression of shoot-specific endo-1,4-β-glucanase genes in the infected root tissue and how these genes are regulated are still open. Based on *in silico* analysis of promoter regions of *AtCel2* and *KOR3* that revealed the presence of several sugar-responsive motifs in promoters of both genes we performed an experiment with plants growing in media supplemented with additional sucrose. Its basis was the observation that syncytia are enriched with sucrose (Hofmann *et al.*, 2007) and some reports that indicated a sucrose-dependent regulation of endo-1,4-β-glucanase genes (Ohmiya *et al.*, 2000; Shani *et al.*, 2006). Quantitative RT-PCR with RNA isolated from 7-day-old root tissue growing on media with 6% sucrose shows that *AtCel2* is upregulated, while expression of *KOR3* does not change (Figure 5).

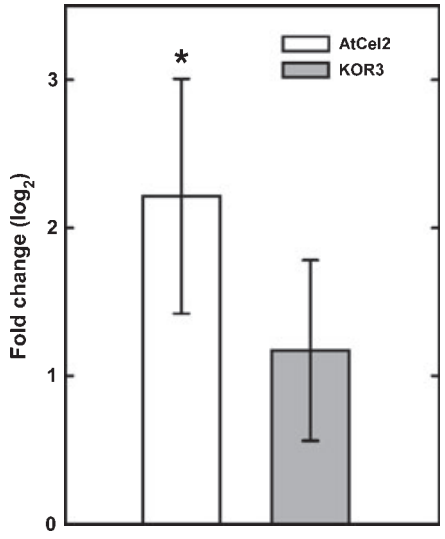

Figure 5. Results of quantitative RT-PCR obtained for *AtCel2* and *KOR3* showing changes in expression of both genes in 1-week-old roots growing on medium supplemented with 6% sucrose compared with 2%.
The level of transcripts was measured relative to the expression of *AtUBP22* and *18S rRNA*. Asterisks indicate a significant difference between expression levels in treated and untreated roots ($P < 0.05$). Log_2 values are means ± SE, $n \geq 3$.

Upregulation of *AtCel2* triggered by high sucrose concentration in the medium indicates its involvement in cellulose biosynthesis as previously suggested by Ohmiya *et al.* (2000) and Shani *et al.* (2006) for other endo-1,4-β-glucanases. Putative cell wall substrates of secreted endo-1,4-β-glucanases are non-crystalline cellulose and xyloglucans. Hence, we analysed the hemicellulose and its monosaccharide composition in infected and uninfected root tissue at 10 and 15 dai (Figure 6). The results show an increased abundance of rhamnose, arabinose, galactose, glucose, xylose and mannose at 10 dai in syncytium samples. There are no differences in fucose content between syncytia and uninfected roots at 10 dai. At 15 dai no difference could be detected.

Plant hormones regulate expression of AtCel2 *and* KOR3

Beside sucrose, plant hormones are thought to have a putative function as regulators of expression of endo-1,4-β-glucanase genes as shown by Nakamura *et al.* (1995), Wu *et al.* (1996), Catalá *et al.* (1997), Nicol *et al.* (1998) and Del Campillo *et al.* (2004). The analysis of promoter regions of *AtCel2* and *KOR3* showed several predicted motifs that can act as hormone-responsive *cis*-elements such as ABRE, ERE, EIN3, AUX-RR and CAREs/GARE. To determine if the expression of both genes is in fact dependent on ABA and ethylene, we grew plants on media supplemented with 100 μM ABA and 10 μM ACC, respectively, prior to harvesting root tissue. In the presence of a higher concentration of ABA we observed reduced expression of *AtCel2* and *KOR3*. In both cases ACC as an ethylene precursor did not show any effects on the expression. Similarly, NPA, an inhibitor of auxin basipetal transport causing an increase in concentration of endogenous auxin at the root tip (Casimiro *et al.*, 2001), did not significantly change the expression of *AtCel2* and *KOR3*. Gibberellic acid triggered upregulation in root tissue only for *AtCel2*; in the case of *KOR3* we did not observe any changes. A significant increase of expression of *AtCel2* was observed when roots were grown in media containing 10 μM NAA. Expression of *KOR3* after treatment with NAA was not significantly affected. Results are shown in Figure 7.

AtCel2 *and* KOR3 *mutants impair nematode development*

Based on the strong upregulation of the *AtCel2* and *KOR3* in syncytia induced by *H. schachtii* we decided to perform a functional analysis with mutants in the context of nematodes. Therefore, we ordered T-DNA insertion mutant lines for both genes from the SALK collection (Alonso *et al.*, 2003; http://signal.salk.edu/cgi-bin/tdnaexpress). In the *AtCel2* mutant line the T-DNA is integrated in the promoter region at the position –554 bp (Figure 8/1). In the *kor3* mutant T-DNA is

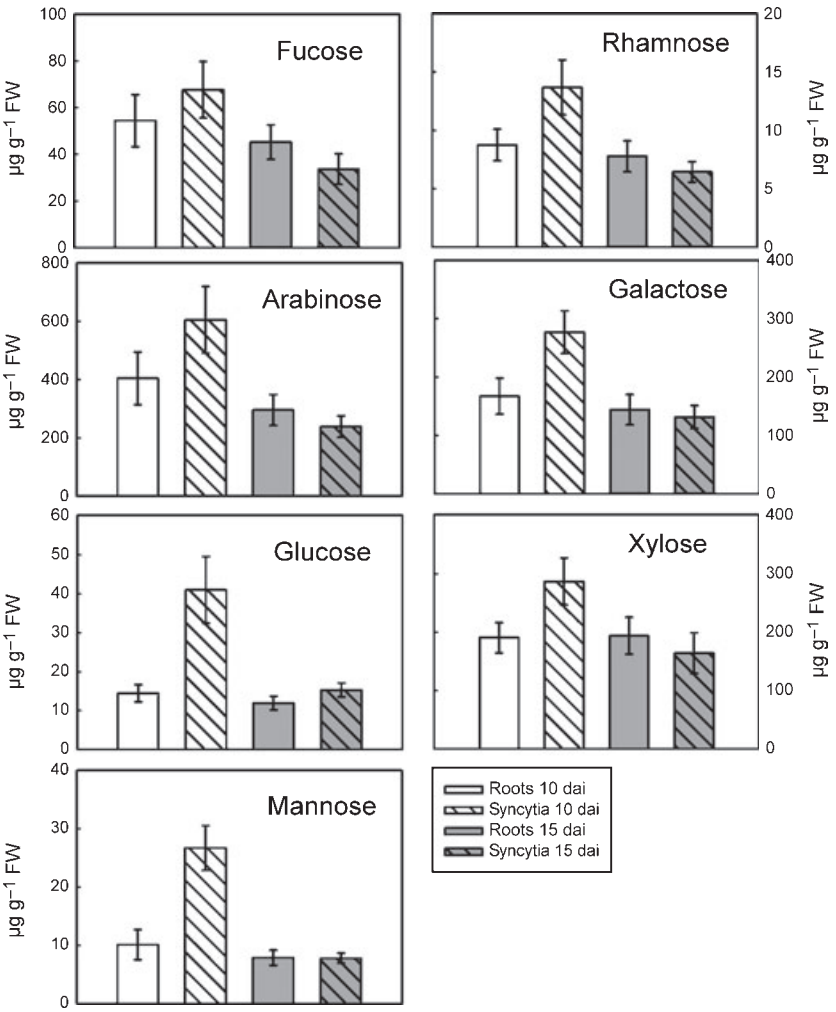

Figure 6. Monosaccharide composition of hemicellulose in syncytia induced by *Heterodera schachtii* and uninfected root tissue at 10 and 15 days after inoculation (dai). Values are means ± SE, $n = 3$.

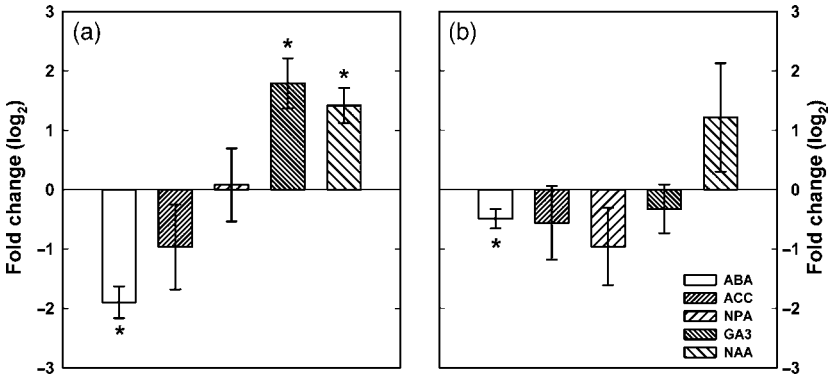

Figure 7. Results of quantitative RT-PCR obtained for *AtCel2* (a) and *KOR3* (b) showing changes in expression of both genes after several hormonal treatments.
The level of transcripts was measured relative to the expression of *AtUBP22* and *18S rRNA*. Asterisks indicate a significant difference between expression levels in treated and untreated roots ($P < 0.05$). Log_2 values are means ± SE, $n \geq 3$.

inserted in the coding region of the gene at the position 1935 bp in the last exon, which contains two catalytic domains typical for glycosyl hydrolases family 9 (Figure 8/2).

Homozygous plants of both lines were preselected on plates with modified Murashige and Skoog medium (MSM) supplemented with kanamycin (30 µg ml^{-1}). After isolation of total DNA and RNA, additional PCR and RT-PCR experiments were performed in order to confirm the homozygosity and the T-DNA insertion in the expected position. Homozygosity was tested in RT-PCR reactions by the use of two gene-specific primers flanking the T-DNA insertion site, while the position of the integrated T-DNA was analysed with the aid of a gene-specific primer and a T-DNA specific primer (Figure 8).

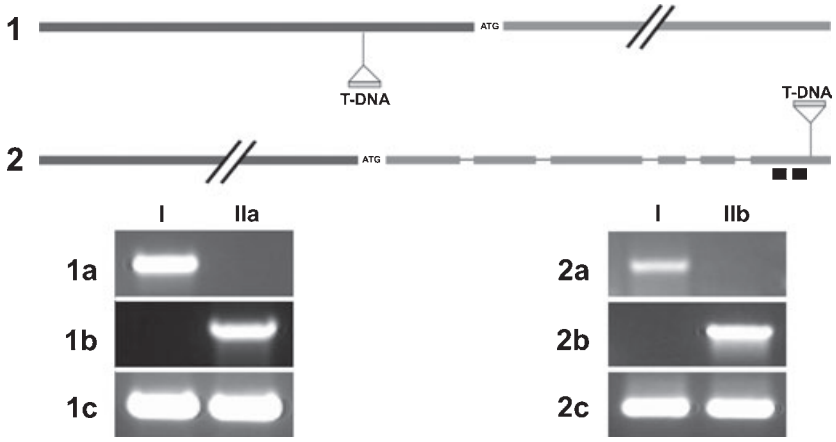

Figure 8. T-DNA insertion in *cel2* (1; Salk: N613404) and *kor3* (2; Salk: N516250).
(1a) Reverse transcription-PCR reaction with the *AtCel2*-specific primers. *AtCel2* transcript was detected only with the RNA isolated from the wild type.
(1b) Polymerase chain reaction with *AtCel2*-specific and T-DNA primer, signals amplified only with the homozygous *cel2* mutant.
(1c) *18S rRNA* primers were used as a control for RT-PCR reaction.
(2a) Reverse transcription-PCR reaction with the *KOR3*-specific primers flanking the T-DNA insertion position. *KOR3* transcript was detected only with the RNA isolated from the wild type.
(2b) Polymerase chain reaction with *KOR3*-specific and T-DNA primer, signals amplified only with the homozygous *kor3* mutant.
(2c) *18S rRNA* primers were used as a control for RT-PCR reaction. Squares indicate two catalytic domains within last exon of *KOR3*. Column I, wild type; column IIa, *cel2*; column IIb, *kor3*.

In the selected mutant line *cel2* no *AtCel2* transcript could be amplified with the RNA (Figure 8/1A), whereas a PCR product confirming the T-DNA insertion was obtained with DNA isolated only from this line (Figure 8/1B). A *KOR3* transcript was obtained only with RNA isolated from wild type (Figure 8/2A). A PCR product detecting the T-DNA could be amplified only with DNA isolated from *kor3* plants (Figure 8/2B). As a control, primers for *18S rRNA* were used for both wild type and the mutants (Figure 8/1C and 2C).

Although it could be shown that both *cel2* and *kor3* lines are homozygous and the T-DNA insertion occurs in the expected place, plants do not show any visible phenotype.

Nematode infection tests with the wild type and both mutants showed clear effects on nematode development. Three weeks after inoculation the number of females was determined and found to be reduced by 48% in *cel2* and 45% in *kor3*. The low proportion of females led to a significant decrease of the female:male ratio in both mutant lines (Col = 0.92, *cel2* = 0.57, *kor3* = 0.56). This phenomenon is common in poor host plants or resistant plant varieties (Lelivelt and Hoogendoorn, 1993; Sanft and Wyss, 1990). The results of the infection test are shown in Figure 9.

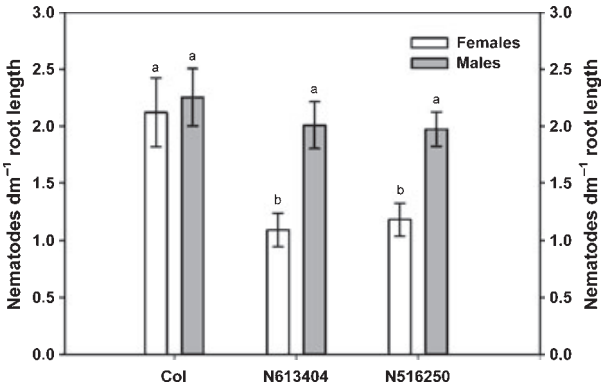

Figure 9. Number of female and male nematodes per root decimetre of *cel2* (Salk: N613404) and *kor3* (Salk: N516250) mutant lines and wild type (Col) determined 2 weeks after inoculation.
Columns represent the numbers of females and males. The statistical significance of the results was determined by a *t*-test of three independent replicates, letters indicate significances ($P < 0.05$; SPSS 12.0). Values are means ± SE, $n = 3$.

Discussion

Plant cell wall modifications in the interaction between host plants and parasitic nematodes are well described but the mechanisms, the genes involved and their regulation are still largely unknown. Recently, Wieczorek *et al.* (2006) presented an analysis of the involvement of the expansin gene family in the development and maintenance of syncytia induced by *H. schachtii*. Here, we report on another group of cell wall related proteins that may play an important role in this sophisticated relationship.

In earlier studies the role of single endo-1,4-β-glucanases was analysed in different plant–nematode interactions. These studies demonstrated that the regulation of endo-1,4-β-glucanases is specific for different plants and different nematode species. Goellner *et al.* (2001) found five tobacco endo-1,4-β-glucanases to be upregulated upon infection with root-knot and cyst nematodes. An analysis in Arabidopsis revealed *AtCel1* to be upregulated upon infection with

the root-knot nematode *M. incognita*. However, infection with *G. tabacum* or *H. schachtii* did not lead to its expression (Mitchum *et al.*, 2004; Sukno *et al.*, 2006*).* Whereas these studies were focused on single genes that were selected on the basis of single observations, our work monitors and analyses the expression of the entire endo-1,4-β-glucanase gene family in the roots of Arabidopsis upon infection with the cyst nematode *H. schachtii*. In this way we were able to identify genes with a regulation that closely correlates with feeding site development and which, therefore, play an important role in the host–parasite interaction.

Specific expression of endo-1,4-β-glucanase genes in nematode-infected root tissue

Using different approaches such as screening of a syncytium-specific cDNA library, sqRT-PCR, Affymetrix Genechip technology and qRT-PCR we could clearly show upregulation of seven endo-1,4-β-glucanase genes (*AtCel1*, *AtCel2*, *AtCel3*, *KOR3*, *At4g02290*, *At1g64390* and *At2g32990*). Downregulation was detected for *AtCel5*, *KOR*, *KOR2*, *At1g19940*, *At1g48930*, *At4g09740* and *At4g39000*.

Endo-1,4-β-glucanases can be sorted approximately into two groups: AtCel1, AtCel2, AtCel3, At4g02290, At1g64390 and At2g32990 are secreted and soluble EGases, whereas members of the KOR subfamily are not secreted and are located at the innermost layer of the plant cell wall.

AtCel1 is expressed in young expanding tissues mostly in xylem cells (Shani *et al.*, 2006) and plays a role in cell wall relaxation and during cell growth and expansion (Tsabary *et al.*, 2003). With promoter:GUS studies it was also found to be upregulated in giant cells induced by root-knot nematodes, but not in syncytia of cyst nematodes (Mitchum *et al.*, 2004). In our Genechip analysis, however, we found it to be moderately upregulated at 5 dai in syncytia, whereas it was not detectable by any of the other methods. We suppose that the observed discrepancies are due to different sensitivity levels of the methods employed.

AtCel2 was previously found to be expressed in flowers, i.e. in developing septum and ovule primordia during early stages of flower development (Yung *et al.*, 1999). The authors suggest that *AtCel2* is involved in cell wall extension during growth and division of the cells in these organs. *AtCel3* is known as a paralogue of *AtCel5*, and both genes play a role during sloughing of border cells from the root tip, as shown by Del Campillo *et al.* (2004). The other genes of this group are annotated but so far not described in detail.

The KOR subfamily consists of three genes *KOR*, *KOR2* and *KOR3* and all members are involved in cell wall assembly (Del Campillo, 1999; Molhoj *et al.*, 2001; Nicol and Höfte, 1998). *KOR* is strongly expressed throughout the whole plant, whereas *KOR2* has a more specific expression pattern (Molhoj *et al.*, 2001; Nicol and Höfte, 1998). Both genes are downregulated in syncytia as shown by the use of the GeneChip method. Semi-quantitative RT-PCR of *KOR* showing equal signals for all infected and uninfected samples was either not sensitive enough to detect the rather moderate downregulation of *KOR* in root segments containing syncytia or an upregulation of this gene takes place in the surrounding root tissue.

KOR3 is the only member of this family that is strongly upregulated in syncytia. In healthy plants its expression is restricted to specific cell types (Molhoj *et al.*, 2001). The *KOR3* promoter was found to be active in conductive tissue of cotyledons, rosette leaves and young roots. Staining was also observed in the trichome support cells and in the bundle sheath cells, which surround the vascular bundle mesophyll tissue.

Two genes, *AtCel2* and *KOR3*, both strongly upregulated in syncytia during the first 2 weeks of their development, share a specific expression pattern. Both were found mainly in the shoot and at very low level or not at all in the root tissue. Results of RT-PCR (Table 1) and sqRT-PCR (Figure 1) together with expression data from Genevestigator (Table 2) show that *AtCel2* must be expressed at a very low level in the uninfected root tissue, while *KOR3* is weakly expressed in the uninfected root.

The other endo-1,4-β-glucanase genes which we found to be upregulated in syncytia are genes with relatively strong background in the root tissue (see Table 2 and Figure 1) and they do not share the characteristic expression pattern of *AtCel2* and *KOR3*. Thus, we assume that they play a minor role in modifying the cell wall in syncytia. In cases of gene silencing, however, they might be activated and compensate the loss of function of the targeted gene.

It remains enigmatic how the expression of *AtCel2* and *KOR3* is activated in syncytia and which regulatory pathways are involved. To get a clue about this phenomenon we performed an *in silico* analysis of the promoter regions of *AtCel2* and *KOR3* in terms of putative *cis*-acting elements. We identified several motifs (EIRE, ERE, P-BOX, WUN-MOTIF) that were recently described as typical for promoters of genes that are upregulated in NFS (*AtCel1*, *Lemmi9*, *TobRB7*, *Hahsp17.7G4* – giant cells of root-knot nematodes; *AtPyk20*, *AtSuc2* – giant cells of root-knot nematodes and syncytia of cyst nematodes) and were absent in promoters of downregulated genes (*AtPal1*, *AtTip*; Sukno *et al.*, 2006). However, our analysis of other genes that are known to be strongly downregulated revealed that promoters of these genes contain nearly or exactly the same set of elements as upregulated genes, thus indicating that these *cis*-elements are not necessarily responsible for the upregulation in feeding sites.

Analyses of promoter regions or studies with deletions of particular elements have so far been insufficient to explain the specific expression patterns of nematode-responsive plant genes. However, identified promoter elements may provide hints for the pathways involved in gene regulation.

Hence, based on the results obtained in terms of elements responsive to sucrose and several plant hormones, we investigated the effects of these possible regulators on the root expression of *AtCel2* and *KOR3*.

Putative role of sucrose in regulation of AtCel2 *and* KOR3 *expression and in cell wall related processes in syncytia*

Jürgensen *et al.* (2003) and Hofmann *et al.* (2007) reported on two sucrose transporters from Arabidopsis, *AtSUC2* and *AtSUC4*, which are upregulated at 10 dai in syncytia induced by *H. schachtii*. Moreover, sucrose concentration in syncytia at this stage as well as at 15 dai is significantly increased compared to the uninfected roots (Hofmann *et al.*, 2007). In addition, Ohmiya *et al.* (2003) and Shani *et al.* (2006) showed that expression of endo-1,4-β-glucanase genes depends on sucrose. In the promoter regions of *AtCel2* and *KOR3* we identified *cis*-elements that are responsive to sugar. We found three SURE motifs in the *AtCel2* promoter and one in the *KOR3* promoter. Therefore, we tested the hypothesis that a higher concentration of sucrose in the medium has an effect on the expression of *AtCel2* and *KOR3* in the uninfected root and thus may explain the syncytium-specific expression of both genes. Our experiments clearly show that at least *AtCel2* is upregulated in roots growing on media supplemented with 6% sucrose, thus suggesting that an increased level of sucrose in the feeding site could be one of the factors that triggers the local expression of this gene. In fact, the maximum of *AtCel2* expression at 10 dai occurs at the same time as the highest sucrose concentration in the feeding site (Hofmann *et al.*, 2007). The extent of the sugar-induced response also correlates with the number of identified sugar-responsive elements in both *AtCel2* and *KOR3* promoter sequences, which in *AtCel2* is higher than in *KOR3*.

Based on the significant increase of xyloglucan compounds such as xylose, glucose, galactose and fucose (Figure 6) we assume that at 10 dai a maximum of hemicellulose biosynthesis is reached and presumably a high number of associated cell wall modifications in the rapidly expanding syncytia occur. AtCel2 might play an important role in modifying the cell wall structure by hydrolysing the hemicellulose produced, thus allowing cell wall extension and syncytium expansion. At 15 dai the syncytium ceases to expand and the amount of hemicellulose residue decreases to the level found in non-infected roots. At the same time the expression level of *AtCel2* is reduced.

The expression of *KOR3* increased gradually from 5 to 15 dai, suggesting that this EGase plays an important role in cell wall related processes in mature syncytia. However, *KOR3* with only one SURE motif in its promoter region does not show any upregulation in roots growing on medium supplemented with sucrose, suggesting that sucrose does not strongly influence the regulation of this gene in syncytia. Recently, the effect of sucrose on *NtCel7*::GUS expression was analysed. Although the promoter region contains a *cis*-acting sugar response element, the incubation of transgenic plants in 6% sucrose medium did not change GUS activity (Wang *et al.*, 2007).

Plant hormones affect expression of AtCel2 *and* KOR3

There are a few reports showing the effects of hormones on expression of EGases. Nicol *et al.* (1998) showed that NAA increases expression of *KOR*. Another Arabidopsis EGase *AtCel5* is downregulated by ABA and NAA, whereas the auxin transport inhibitor NPA leads to a reduction of its expression (Del Campillo *et al.*, 2004). Wang *et al.* (2007) found that the tobacco *NtCel7* promoter is induced by auxin, but not gibberellin and ethylene. Our promoter analysis revealed the presence of several motifs responsive to the different plant hormones, so we performed qRT-PCR experiments with roots treated with NAA, NPA, GA3, ABA and ACC. Our experiments show that expression of *KOR3* and *AtCel2* varies depending on the supplemented hormones. Both GA3 and NAA enhance expression of *AtCel2*. Indeed, we found four CAREs/GARE and one Aux-RR motif in the promoter region of *AtCel2*. In the promoter of *KOR3* we identified two motifs responsive to auxin but we did not observe significant upregulation of this gene after auxin treatment. Furthermore, although motifs responsive to ABA (ABRE) were found in both promoters, ABA leads to the reduction of the expression of both genes. Similar discrepancies were observed with the *NtCel7* promoter (Wang *et al.*, 2007). Although ethylene- (EIN3) and gibberellin-responsive boxes (CAREs/GARE) were identified in this promoter, treatments with ACC and GA did not trigger the induction.

It was shown by Goverse *et al.* (2000) and Karczmarek *et al.* (2004) that auxin plays a crucial role in the development of nematode feeding sites. They suggested that nematodes are able locally to increase auxin concentration, thus in turn enhancing ethylene production. Both events may locally activate plant cell wall degrading enzymes. However, our results show that only auxin enhances expression of both EGases, while ACC had no detectable effect on their regulation.

We conclude that the analyses of the possible factors influencing gene expression do not fully explain regulation of EGase, but we clearly show that a number of different regulatory pathways is involved, which must be orchestrated by the plant under the control of triggers from the nematode. In addition, the activity of nematode released effectors must be considered. As described recently, salivated compounds of *H. schachtii* and *M. incognita* contain auxin or auxin-like substances (De Meutter *et al.*, 2005). Therefore it is possible that nematodes influence hormone homeostasis during syncytium induction either indirectly by activating a shift in plant hormone homeostasis in affected

cells or directly through the release of hormone-active salivary compounds.

AtCel2 *and* KOR3 *function in nematode-induced syncytia*

One of the questions posed in this work concerns the functional relevance of EGases during syncytium development. Previously published reports dealing with the involvement of endo-1,4-β-glucanases in the development of syncytia and giant cells were restricted to expression and localization studies of single upregulated genes (Goellner *et al.*, 2001; Mitchum *et al.*, 2004; Sukno *et al.*, 2006). However, these studies did not provide evidence that these genes are functional in the formation and maintenance of feeding sites. The latter two papers showed that *M. incognita* and giant cells develop normally within the roots of an *AtCel1* antisense line. The authors suggest that there is a functional redundancy among endo-1,4-β-glucanases. In our study, using mutants we present proof for the function of AtCel2 and KOR3 in nematode-induced syncytia. Infection tests of both mutant lines with nematodes showed a significant decrease in the number of females (Figure 9). This causes a significant decrease of the female:male ratio, which indicates an impairment of syncytial development triggered by the loss of AtCel2 and KOR3 function. This phenomenon has been described frequently in resistant host plant cultivars (Lelivelt and Hoogendoorn, 1993; Sanft and Wyss, 1990) or as a response to certain plant treatments (Grundler *et al.*, 1991).

Another question that is more difficult to answer and exceeds the focus of this work is what is the biological function of the EGases identified as being involved in syncytium development? A detailed analysis of the mutant lines will be necessary to provide an answer. As a next step we intend to monitor the changes in expression of all active EGases in syncytia in the roots of both mutants using qRT-PCR and to analyse double or triple mutants of important genes and their effects on plant and nematode development. Here we can only state that *cel2* and *kor3* do not show any visible phenotype, suggesting that redundant genes, e.g. *KOR* that is strongly expressed throughout the whole plant (Nicol *et al.*, 1998), may complement to a certain extent the loss of function of both genes. A similar phenomenon was observed for a T-DNA mutant of another EGase gene from Arabidopsis, *AtCel5* (Del Campillo *et al.*, 2004), which did not show any impact on morphological traits. The authors suggest that abolishing *AtCel5* expression can be overcome by multiple redundant genes such as *AtCel3* as a paralogue of *AtCel5*. Both genes play a role in the process of sloughing of the root cap.

Our results suggest that two processes take place in the syncytial cell wall: on the one hand the cell wall is reorganized by secreted enzymes (AtCel2) and other factors (e.g. expansins) and on the other hand cellulose is increasingly synthesized (KOR3). Further research is in progress to analyse the observed effects in the mutants and to find out in what way the syncytial cell wall differs from walls of unaffected cells. This information will give a clue to help further understand the role of the cell wall and cell wall related processes in the unique physiology of nematode-induced syncytia.

Experimental procedures

Plant cultivation

Seeds of Arabidopsis were surface-sterilised for 10 min in 5% (w/v) calcium hypochlorite, submerged for 5 min in 70% (v/v) ethanol and subsequently three times in sterile distilled H_2O. The sterilised seeds were placed into sterile Petri dishes (9 cm in diameter) on a modified 0.2 concentrated Knop medium supplemented with 2% sucrose (Sijmons *et al.*, 1991). For hemicellulose sugar analysis plants were grown on soil/sand culture (1:2 v/v) in 24-well plates. Arabidopsis seedlings were grown in a growth chamber at 24°C with a 16-h photoperiod.

Isolation of DNA and RNA from Arabidopsis

Isolation of genomic DNA from various organs of Arabidopsis (ecotype Columbia) was done according to the method of Gustincich *et al.* (1991) as modified by Clark *et al.* (1997). Total RNA was isolated using an RNeasy Plant Mini Kit (Qiagen, http://www.qiagen.com/) according to the manufacturer's instructions, including DNA digestion with DNaseI. Genomic DNA was isolated from young leaves, whereas RNA was obtained from complete shoots and roots of 21-day-old Arabidopsis plants.

Nematode infection

Cysts of *H. schachtii* were harvested from *in vitro* stock cultures on mustard (*Sinapsis alba* cv Albatros) roots growing on 0.2 concentrated Knop medium supplemented with 2% sucrose (Sijmons *et al.*, 1991). Hatching of juveniles was stimulated by soaking cysts in 3 mM $ZnCl_2$. The juveniles were washed four times in sterile H_2O and resuspended in 0.5% (w/v) Gelrite (Duchefa, http://www.duchefa.com/) before inoculation. Twelve-day-old roots of Arabidopsis plants were inoculated under axenic conditions with approximately 50 juveniles per plant.

For nematode infection assays Arabidopsis plants were grown under sterile conditions and after 12 days inoculated with batches of about 50 freshly hatched juveniles as described. Before inoculation, total root length was estimated as described by Jürgensen (2001). After 2 weeks, the total number of females and males was counted and the female:male ratio was calculated. Experiments were repeated three times with approximately 100 plants per replicate and line. The significance of the results was determined statistically by three independent samples *t*-test ($P < 0.05$; SPSS 12.0; SPSS Inc., http://spss.com).

Reverse transcription-PCR (RT-PCR)

Primers flanking the protein coding sequences of Arabidopsis endo-1,4-β-glucanase genes (Supplementary Table S1) were used for first-strand synthesis and amplification of mRNA templates. For PCR and RT-PCR analysis of T-DNA insertion mutants following

additional primers were used: T-DNA-specific primer, 5′-TGGTTCACGTAGTGGGCCATCG-3′; *AtCel2*-specific primer used for T-DNA detection, 5′-ACGTTGAGAGCAGAGCCATCA-3′; *KOR3*-specific reverse primer flanking T-DNA insertion side, 5′-GTGCAGGTTTCTTTCATGTTCTTTGGAATTG-3′. Control reactions were performed with the 5′ primer (5′-GGTGGTAACGGGTGACGGAGAAT-3′) and 3′ primer (5′-CGCCGACCGAAGGGACAAGCCGA-3′) designed from the sequence of Arabidopsis 18S ribosomal cDNA. Fifty nanograms of total RNA was denatured for 3 min at 65°C and added to the reverse transcription (RT) reaction mix [final concentrations: 1 × RT buffer, 0.5 mM of each deoxyribonucleotide (dNTP), 1 μM gene-specific 3′ primer, 10 U RNasin (Promega, http://www.promega.com), 1.0 μl Sensiscript Reverse Transcriptase (Qiagen) in a total volume of 20 μl]. Samples were incubated at 37°C for 1 h, heated to 95°C for 5 min and cooled to 10°C for 15 min. The cDNA was amplified by PCR using a PCR mix containing 1× PCR buffer (GeneCraft; http://genecraft.de), 1.5 mM $MgCl_2$, 200 μM of each dNTP, 1.0 μM each of the gene-specific primers, 2.5 U BioTherm Polymerase (GeneCraft, http://www.genecraft.de/). The PCR was performed as follows: denaturation for 2 min at 94°C; cycles 1 to 35, 15 sec at 94°C, 30 sec at 55°C, 2 min at 72°C; 5 min at 72°C. Twenty microlitres of the RT-PCR products was separated on a 1.0% agarose gel.

Semi-quantitative RT-PCR

Syncytia and corresponding uninfected root pieces dissected without root tips and lateral root primordia were collected at 5, 10 and 15 dai. Total RNA was isolated using the RNeasy Plant Mini Kit (Qiagen) according to the manufacturer's instructions, including DNA digestion with DNaseI. Using SuperScript III reverse transcriptase (Invitrogen, http://www.invitrogen.com/) and random primer (oligo$(dN)_6$) cDNA was amplified. For PCR experiments a cDNA dilution and specific primer pairs were used (Supplementary Table S1). The PCR conditions were as described above. For details see Wieczorek *et al.* (2006).

RNA isolation from syncytia and cDNA library construction

The syncytial cytoplasm was extracted with a microcapillary and a micromanipulator (Eppendorf AG, http://www.eppendorf.com/) without contamination from uninfected root cells or nematodes (Jürgensen *et al.*, 2003). Samples were collected between 5 and 7 dai. Approximately 100 micro-aspirated syncytia were used for RNA isolation with the RNeasy Plant Mini Kit (Qiagen). A syncytium-specific cDNA library was produced by use of the SMART™ cDNA library construction kit (Clontech Laboratories, http://www.clontech.com/) according to the manufacturer's instructions. An aliquot of approximately 15 syncytia was taken for library construction. It contains approximately 2.5×10^6 primary recombinants. The quality of the cDNA library was tested by PCR amplification of known nematode-responsive plant genes (P. S. Puzio, P. Voss, F. M. W. Grundler, Institut für Phytopathologie, Universität Kiel, Germany, unpublished results).

PCR reactions with Arabidopsis genomic DNA and syncytium-specific cDNA library

For PCR reactions 1 μg μl^{-1} gDNA from Arabidopsis and 2 μl of syncytium-specific cDNA were used, respectively. The reactions were performed with Biotherm DNA Polymerase (GeneCraft) as described above.

In situ *RT-PCR*

The *in situ* RT-PCR was done according to Koltai and Bird (2000) and Urbanczyk-Wochniak *et al.* (2001). Syncytia at 10 dai were dissected from roots and immediately put into cold fixation solution (63% ethanol, v/v; 2% formalin, v/v). After 24 h, syncytia were embedded in 4% low-melting agarose and 25 μm thick sections were prepared using a vibratom (VT 100, Leica, http://www.leica.com/); afterwards RT-PCR with digoxigenin-labelled dUTP was carried out. After a staining reaction with nitro blue tetrazolium (NBT)/5-bromo-4-chloro-3-indolyl phosphate (BCIP) substrate, cross-sections were photographed under an inverted microscope (Axiovert 200M, Zeiss, http://www.zeiss.com/) with an integrated camera (AxioCam MRc5, Zeiss, http://www.zeiss.com/). For full details see Wieczorek *et al.* (2006).

Affymetrix Genechip analysis

Syncytial cytoplasm was aspirated and total RNA was isolated as described above. As controls, root pieces cut from the elongation zone without root tips or lateral root primordia were used. Biotin-labelled probes were synthesized according to the Affymetrix protocol with some modifications. Details will be published elsewhere. ATH1 Arabidopsis Genechips (Affymetrix, http://www.affymetrix.com/) were hybridized by RZPD (Deutsches Ressourcenzentrum für Genomforschung GmbH, Heubnerweg 6, 14059 Berlin, Germany) according to the manufacturer's protocols. For the control roots and 5 dai syncytia the experiment was repeated four times each and for 15 dai three times.

Affymetrix.CEL files (from GCOS 1.2) were imported into the software program GENESPRING version 7.2 (Silicon Genetics, Agilent Technologies, Inc. http://www.chem.agilent.com/) using the GC-RMA normalization pre-processor. The standard normalization for one-colour data was performed as follows: (i) data transformation (set measurements less than 0.01 to 0.01), (ii) per chip (normalized to 50th percentile) and (iii) per gene (normalized to median). As a default interpretation the data were set to the log of ratio mode, which was used for further analysis. To identify endo-1,4-β-glucanase genes that were differentially expressed during syncytia development, pairwise comparisons for the set of 23 genes present on the chip were made (*At2g44550* and *At4g23560* are not present on the chip), i.e. the three different time points were compared with each other (control roots versus syncytia at 5 dai, control versus 15 dai and 15 dai versus 5 dai).

We used a one-way ANOVA test (variances not assumed equal) coupled with the Benjamini and Hochberg multiple testing correction to control the false discovery rate (FDR). The significance *P*-value cut-off was set at 0.25.

For the calculation of the fold change of the gene expression levels between two conditions the geometric mean of the normalized ratios within each condition was used. The resulting fold change ratio values are shown (as $\log_2$ ratios) in Table 3 (with values of ±1 corresponding to either a twofold up- or downregulation).

Real time RT-PCR

Ribonucleic acid isolated from uninfected root samples and root fragments containing syncytia at 5, 10 and 15 dai was analysed and quantified by an Agilent 2100 bioanalyser (Agilent Technologies, http://www.agilent.com/). Complementary DNA was amplified by use of random primers (oligo$(dN)_6$) and the SuperScript III reverse transcriptase (Invitrogen) according to the manufacturer's instructions.

Primers for the quantitative RT-PCR were designed using the PRIMER EXPRESS v. 2.0 Software (Applied Biosystems, http://www.

appliedbiosystems.com/). The specificity of oligonucleotides was checked by PCR with cDNA isolated from Arabidopsis shoots. *18S rRNA* and *AtUBP22* were used as controls (Hofmann and Grundler, 2007). The following primers were used: for *AtCel2*, forward, 5′-TCCAATGGCTTCTCGTCCTC-3′, reverse 5′-ACGTTGAGAGCAG-AGCCATCA-3′; for *KOR3* forward 5′-GGAACAGGTCGGATCTGGA-3′, reverse 5′-AGCGTCTTAGCACCATGAACA-3′; for *18S rRNA*, forward 5′-GGTGGTAACGGGTGACGGAGAAT-3′, reverse 5′-CGC-CGACCGAAGGGACAAGCCGA-3′; for *AtUBP22*, forward 5′-ACA-ACATATGACCCGTTTATCGA-3′, reverse 5′-TGTTTAGGGGAAC-GGATACT-3′.

The efficiencies of all primers were tested by standard curves of four template dilutions (tested in triplicate) with the following results: *AtCel2* $E = 0.882$, $R^2 = 0.991$, *KOR3* $E = 0.882$, $R^2 = 0.993$, *18S rRNA* $E = 0.848$, $R^2 = 0.994$ and *AtUBP22* $E = 0.915$, $R^2 = 0.996$. Quantitative RT-PCR was performed using an ABI Prism 7300 Sequence Detector (Applied Biosystems). The reactions were performed in 25 μl final volume that contained: 1× SYBR Green Buffer (Karsai *et al.*, 2002), 0.5 U Biotherm Polymerase, 3 mM $MgCl_2$ (50 mM), dNTP (10 μM), forward and reverse primer (10 μM). For *AtCel2* and *KOR3* cDNA was diluted 1:2, whereas for *18S rRNA* 1:100 dilution was used. Experiments were repeated three times with RNA isolated from independent uninfected and infected samples. The PCR was as followed: 95°C for 10 min, next 40 cycles: 95°C for 15 sec, 60°C for 30 sec and 72°C for 1 min. Evaluation of the data was carried out using the SEQUENCE DETECTION Software SDS v2.0 (Applied Biosystems). Changes in expression of *AtCel2* and *KOR3* were related to the expression of *18S rRNA* and *AtUBP22* according to the $2^{-\Delta\Delta C_t}$ method (Livak and Schmittgen, 2001). The significance of the results was determined statistically by at least three independent sample *t*-tests ($P < 0.05$; SPSS 12.0).

In silico *analysis of promoter regions of* AtCel2 *and* KOR3

Promoter analysis was performed with the Plant-CARE (http://bioinformatics.psb.ugent.be/webtools/plantcare/html/; Lescot *et al.*, 2002), PLACE (http://www.dna.affrc.go.jp/PLACE/signalscan.html; Higo *et al.*, 1999) and MOTIF SAMPLER (http://homes.esat.kuleuven.be/~thijs/BioDemo/MotifSampler.html; Thijs *et al.*, 2001, 2002).

Hormone and sucrose treatments

Arabidopsis plants were grown under sterile conditions in vertical plates on MSM medium for 5 days and were transferred to the flasks containing liquid MSM medium supplemented with 100 μM ABA (Sigma, http://www.sigmaaldrich.com/), 10 μM ACC (Sigma), 1 μM NPA (Riedel-de Haën, Sigma-Aldrich), 0.1 mg l^{-1} GA3 (Sigma) and 10 μM NAA (synthetic auxin; Duchefa). Control plants were grown in liquid MSM medium without any supplements. Plants were incubated on a rotary shaker at 75 r.p.m. in a growth chamber at 24°C with a 16-h photoperiod. After 48 h, complete roots were harvested and immediately frozen in liquid nitrogen.

For treatments with sucrose, plants were grown for 7 days on vertical plates with MSM medium supplemented with 2% and 6% sucrose. Roots were harvested and frozen in liquid nitrogen. Total RNA was isolated, analysed and quantified by an Agilent 2100 bioanalyser (Agilent Technologies). Complementary DNA was synthesised as described above. Quantitative RT-PCR was performed using an ABI Prism 7300 Sequence Detector (Applied Biosystems) and the results were analysed as described above. Significance of the results was determined statistically by at least three independent sample *t*-tests ($P < 0.05$; SPSS 12.0).

Analysis of monosaccharide composition of syncytial hemicellulose

For hemicellulose sugar analysis, plants were grown on soil/sand culture (1:2 v/v) in 24-well plates. In each well 5–10 plants were grown that were inoculated after 12 days with approximately 500 juveniles per well.

Ten and 15 days after inoculation roots of infected and uninfected plants were washed from soil to dissect syncytia and control roots. Eighteen to 127 mg fresh root material was harvested, immediately shock frozen in liquid nitrogen and ground to a fine powder within the reaction tube using a pestle. To remove starch the powder was suspended in 500 μl of a heat stable α-amylase solution (Sigma-Aldrich) (500 U ml^{-1} in deionised water) from *Bacillus licheniformis* and incubated for 30 min at 85°C (Van Soest *et al.*, 1991). After centrifugation (20,000*g* for 10 min) 500 μl neutral detergent (Van Soest *et al.*, 1967) was added to the pellet and boiled for 60 min. To remove soluble proteins, sugars and lipids the supernatant was discarded after centrifugation (20,000*g* for 10 min) and the pellet was washed (3× distilled water and 2× acetone) and dried *in vacuo*. For hemicellulose extraction 500 μl acid detergent (Van Soest, 1963) was added to the remaining pellet and incubated for 60 min at 95°C. After centrifugation (20,000*g* for 10 min) aliquots of the supernatant were diluted 20-fold and hemicellulose sugars were analysed by pulsed amperometric HPLC on a Carbopac PA20 column (Dionex, http://www1.dionex.com/) using a Dionex ICS3000 chromatography system. To separate fucose, rhamnose and arabinose, the temperature of the column was thermostatically maintained at 30°C and sugars were eluted with 20 mM NaOH at a flow rate of 0.5 ml min^{-1}. Galactose, glucose, xylose and mannose were eluted with distilled water.

Accession numbers

Sequence data from this article can be found in the EMBL/GenBank data libraries under accession numbers At1g70710 (*AtCel1*), At1g02800 (*AtCel2*), At1g71380 (*AtCel3*), At1g22880 (*AtCel5*), At5g49720 (*KOR*), At1g65610 (*KOR2*), At4g24260 (*KOR3*), X16077 (*18S rRNA*), At5g10790 (*AtUBP22*).

Acknowledgements

This research was supported by grant QLK-CT-1999-01501 ('NONEMA') from the European Union within the 5th Framework and FWF grants P16296-B06 and P16897-B06. We gratefully acknowledge the technical support of Krzysztof Jeziorny, Petra Heinen and Piotr Puzio. We would like to thank Professor Roland Perry for helpful comments on the manuscript.

Supplementary Material

The following supplementary material is available for this article online:

Table S1. Sequences of primer pairs for Arabidopsis endo-1,4-β-glucanase genes.

This material is available as part of the online article from http://www.blackwell-synergy.com

Please note: Blackwell Publishing are not responsible for the content or functionality of any supplementary materials supplied by the

authors. Any queries (other than missing material) should be directed to the corresponding author for the article.

References

Alonso, J.M., Stepanova, A.N., Leisse, T.J. *et al.* (2003) Genome-wide insertional mutagenesis of *Arabidopsis thaliana*. *Science*, **301**, 653–657.

Böckenhoff, A. and Grundler, F.M.W. (1994) Studies on the nutrient uptake by the beet cyst nematode *Heterodera schachtii* by in situ microinjection of fluorescent probes into the feeding structures in *Arabidopsis thaliana*. *Parasitology*, **109**, 249–254.

Casimiro, I., Marchant, A., Bhalerao, R.P. *et al.* (2001) Auxin transport promotes *Arabidopsis* lateral root initiation. *Plant Cell*, **13**, 843–852.

Catalá, C., Rose, J.K.C. and Bennett, A.B. (1997) Auxin regulation and spatial localization of an endo-1,4-β-D-glucanase and a xyloglucan endotransglycosylase in expanding tomato hypocotyls. *Plant J.* **12**, 417–426.

Clark, A.M., Jacobsen, K.R., Dannenhoffer, J.M., Skaggs, M.I. and Thompson, G.A. (1997) Molecular characterisation of a phloem-specific gene encoding the filament protein, phloem protein 1 (PP1), from *Cucurbita maxima*. *Plant J.* **12**, 49–61.

Cosgrove, D.J. (2000) New genes and new biological roles for expansins. *Curr. Opin. Plant Biol.* **3**, 73–78.

De Boer, J.M., Yan, Y., Wang, X., Smant, G., Hussey, R.S., Davis, E. and Baum, T. (1999) Developmental expression of secretory beta-1,4-endoglucanase in the subventral esophageal glans of *Heterodera glycines*. *MPMI*, **12**, 663–669.

Del Campillo, E. and Bennett, A.B. (1996) Pedicel breakstrength and cellulase gene expression during tomato flower abscission. *Plant Physiol.* **111**, 813–820.

Del Campillo, E. (1999) Multiple endo-1,4-β-D-glucanase (cellulase) genes in *Arabidopsis*. *Curr. Top. Cev. Biol.* **46**, 39–61.

Del Campillo, E., Abdel-Aziz, A., Crawford, D. and Patterson, S.E. (2004) Root cap specific expression of an endo-1,4-β-D-glucanase (cellulase): a new marker to study root development in *Arabidopsis*. *Plant Mol. Biol.* **56**, 309–323.

De Meutter, J., Tytgat, T., Prinsen, E., Gheysen, G. and Van Onckelen, H. (2005) Production of auxin and related compounds by the plant parasitic nematodes *Heterodera schachtii* and *Meloidogyne incognita*. *Commun. Agric. Appl. Biol. Sci.* **70**, 51–60.

Gal, T.Z., Aussenberg, E.R., Burdman, S., Kapulnik, Y. and Koltai, H. (2005) Expression of a plant expansin is involved in the establishment of root knot nematode parasitism in tomato. *Planta*, **224**, 155–162.

Gao, B., Allen, R., Davis, E.L., Baum, T.J. and Hussey, R.S. (2004) Molecular characterisation and developmental expression of a cellulose-binding protein gene in the soybean cyst nematode *Heterodera glycines*. *Int. J. Parasitol.* **34**, 1377–1383.

Goellner, M., Wang, X. and Davis, E.L. (2001) Endo-β-1,4-glucanase expression in compatible plant–nematode interaction. *Plant Cell*, **13**, 2241–2255.

Golinowski, W., Grundler, F.M.W. and Sobczak, M. (1996) Changes in the structure of *Arabidopsis thaliana* during female development of plant-parasitic nematode *Heterodera schachtii*. *Protoplasma*, **194**, 103–116.

Goverse, A., Overmars, H., Engelbertink, J., Schots, A., Bakker, J. and Helder, J. (2000) Both induction and morphogenesis of cyst nematode feeding cells are mediated by auxin. *MPMI*, **13**, 1121–1129.

Grundler, F., Betka, M. and Wyss, U. (1991) Influence of changes in the nurse cell system (syncytium) on sex determination and development of the cyst nematode *Heterodera schachtii*: total amounts of protein and amino acids. *Phytopathology*, **81**, 70–74.

Grundler, F.M.W., Sobczak, M. and Golinowski, W. (1998) Formation of wall openings in root cells of *Arabidopsis thaliana* following infection by the plant-parasitic nematode *Heterodera schachtii*. *Eur. J. Plant Path.* **104**, 545–551.

Gustincich, S., Manfioletti, G., del Sal, G. and Schneider, C. (1991) A fast method for high quality genomic DNA extraction from whole human blood. *BioTechniques*, **11**, 298–302.

Henrissat, B., Coutinho, P.M. and Davies, G.J. (2001) A census of carbohydrate-active enzymes in the genome of *Arabidopsis thaliana*. *Plant Mol. Biol.* **47**, 55–72.

Higo, K., Ugawa, Y., Iwamoto, M. and Korenaga, T. (1999) Plant *cis*-acting regulatory DNA elements (PLACE) database. *Nucleic Acids Res.* **1**, 297–300.

Hofmann, J. and Grundler, F.W.M. (2007) Identification of reference genes for qRT-PCR studies of gene expression in giant cells and syncytia induced in *Arabidopsis thaliana*. *Nematology*, **9**, 451–458.

Hofmann, J., Wieczorek, K., Blöchl, A and Grundler, F.W.M. (2007) Sucrose supply to nematode-induced syncytia depends on the apoplasmic and the symplasmic pathway. *J. Exp. Bot.* **58**, 1591–1601.

Jürgensen, K. (2001) *Untersuchungen zum Assimilat- und Wassertransfer in der Interaktion zwischen Arabidopsis thaliana* and *Heterodera schachtii*. PhD thesis, Agrar- und Ernährungswissenschaftlichen Fakultät, Christian-Albrecht Universität, Germany.

Jürgensen, K., Scholz-Starke, J., Sauer, N., van Bel, A.J.E. and Grundler, F.M.W. (2003) The companion cell-specific *Arabidopsis* disaccharide carrier *AtSUC2* is expressed in nematode-induced syncytia. *Plant Physiol.* **131**, 1–9.

Karczmarek, A., Overmars, H., Helder, J. and Goverse, A. (2004) Feeding cell development by cyst and root-knot nematodes involves a similar early, local and transient activation of a specific auxin-inducible promoter element. *Mol. Plant Path.* **5**, 343–346.

Karsai, A., Müller, S., Platz, S. and Hauser, M.T. (2002) Evaluation of a home-made SYBR green I reaction mixture for real-time PCR quantification of gene expression. *BioTechniques*, **32**, 790–796.

Koltai, H. and Bird, D.M. (2000) High throughput cellular localization of specific plant mRNAs by liquid-phase in situ reverse transcription-polymerase chain reaction of tissue sections. *Plant Physiol.* **123**, 1203–1212.

Lelivelt, C.L.C. and Hoogendoorn, J. (1993) The development of juveniles of *Heterodera schachtii* in roots of resistant and susceptible genotypes of *Sinapis alba*, *Brassica napus*, *Raphanus sativus* and hybrids. *Eur. J. Plant Path.* **99**, 13–22.

Lescot, M., Dehais, P., Thijs, G., Marchal, K., Moreau, Y., Van de Peer, Y., Rouzé, P. and Rombauts, S. (2002) PlantCARE, a database of plant *cis*-acting regulatory elements and a portal to tools for *in silico* analysis of promoter sequences. *Nucleic Acids Res.* **1**, 325–327.

Libertini, E., Li, Y. and McQueen-Mason, S.J. (2003) Phylogenetic analysis of the plant endo-1,4- β-glucanase gene family. *J. Mol. Evol.* **58**, 506–515.

Livak, K.J. and Schmittgen, T.D. (2001) Analysis of relative gene expression data using real-time quantitative PCR and the $2^{-\Delta\Delta C_t}$ method. *Methods*, **25**, 402–408.

Master, E.R, Rudsander, U.J., Zhou, W., Henriksson, H., Divne, C., Denman, S., Wilson, D.B. and Teeri, T.T. (2004) Recombinant expression and enzymatic characterization of PttCel9A, a KOR homologue from *Populus tremula* × *tremuloides*. *Biochemistry*, **43**, 10080–10089.

Molhoj, M., Jorgensen, B., Ulvskov, P. and Borkhardt, B. (2001) Two *Arabidopsis thaliana* genes, *KOR* and *KOR3*, which encode membrane-anchored endo-1,4-β-D-glucanases, are differentially expressed in developing leaf trichomes and their support cells. *Plant Mol. Biol.* **46**, 263–275.

Mitchum, M.G., Sukno, S., Wang, X., Shani, Z., Tsabary, G., Shoseyov, O. and Davis, E. (2004) The promoter of the *Arabidopsis thaliana Cel1* endo-1,4-β glucanase gene is differentially expressed on plant feeding cells induced by root-knot and cyst nematode. *Mol. Plant Path.* **5**, 175–181.

Nakamura, S., Mori, H., Sakai, F. and Hayashi, T. (1995) Cloning and sequencing of a cDNA for poplar endo-1,4-beta-glucanase. *Plant Cell Physiol.* **36**, 1229–1235.

Nicol, F., His, I., Jauneau, A., Verhettes, S., Canut, H. and Höfte, H. (1998) A plasma membrane-bound putative endo-1,4-β-D-glucanase is required for normal wall assembly and cell elongation in *Arabidopsis*. *EMBO J.* **17**, 5563–5576.

Nicol, F. and Höfte, H. (1998) Plant cell expansion: scaling the wall. *Curr. Opin. Plant Biol.* **1**, 12–17.

Ohmiya, Y., Takeda, T., Nakamura, S., Sakai, F. and Hayashi, T. (1995) Purification and properties of wall-bound endo-1,4-beta-glucanase from suspension-cultured poplar cells. *Plant Cell Physiol.* **36**, 607–614.

Ohmiya, Y., Samejima, M., Shiroishi, M., Amano., Y., Kanda, T., Sakai, F. and Hayashi, T. (2000) Evidence that endo-1,4-β glucanases act on cellulose in suspension-cultured poplar cells. *Plant J.* **24**, 147–158.

Ohmiya, Y., Nakai, T., Park, Y.W., Aoyama, T., Oka, A., Sakai, F. and Hayashi, T. (2003) The role of PopCel1 and PopCel2 in poplar leaf growth and cellulose biosynthesis. *Plant J.* **33**, 1087–1097.

Park, Y.W., Tominaga, R., Sugiyama, J., Furuta, Y., Tanimoto, E., Samejima, M., Sakai, F. and Hayashi, T. (2003) Enhancement of growth by expression of poplar cellulase in *Arabidopsis thaliana*. *Plant J.* **33**, 1099–1106.

Peng, L., Kawagoe, Y., Hogan, P. and Delmer, D. (2002) Sitosterol-β-glucoside as primers for cellulose synthesis in plants. *Science*, **295**, 147–150.

Reiter, W.D. (2002) Biosynthesis and properties of the plant cell wall. *Curr. Opin. Plant Biol.* **5**, 536–542.

Robert, S., Mouille, G. and Höfte, H. (2004) The mechanism and regulation of cellulose synthesis in primary walls: lessons from cellulose-deficient *Arabidopsis* mutants. *Cellulose*, **11**, 351–364.

Rose, J.K.C. and Bennett, A.B. (1999) Cooperative disassembly of the cellulose-xyloglucan network of plant cell walls: parallels between cell expansion and fruit ripening. *Reviews*, **4**, 176–183.

Rosso, M.N., Favery, B., Piotte, C., Arthaud, L., De Boer, J.M., Hussey, R.S., Bakker, J., Baum, T.J. and Abad, P. (1999) Isolation of a cDNA encoding a beta-1,4-endoglucanase in the root-knot nematode *Meloidogyne incognita* and expression analysis during plant parasitism. *MPMI*, **12**, 585–591.

Sanft, U. and Wyss, U. (1990) Monoxenischer Resistenztest für Kartoffelgenotypen gegenüber dem Zystennematoden *Globodera pallida*. 3. Anwendung und Prüfung des Tests. *Patato Res.* **33**, 67–76.

Shani, Z., Dekel, M., Roiz, L. *et al.* (2006) Expression of endo-1,4-endoglucanase (cel1) in *Arabidopsis thaliana* is associated with plant growth, xylem development and cell wall thickening. *Plant Cell Rep.* **25**, 1067–1074.

Sijmons, P.C., Grundler, F.M.W., von Mende, N., Burrows, P.R. and Wyss, U. (1991) *Arabidopsis thaliana* as a new model host for plant-parasitic nematodes. *Plant J.* **1**, 245–254.

Sukno, S., Shimerling, O., McCuiston, J., Tsabary, G., Shani, Z., Shoseyov, C. and Davis, E.L. (2006) Expression and regulation of the *Arabidopsis thaliana* cel1 Endo 1,4 beta glucanase gene during compatible plant–nematode interactions. *J. Nematol.* **38**, 354–361.

Thijs, G., Lescot, M., Marchal, K., Rombauts, S., De Moor, B., Rouzé, P. and Moreau, Y. (2001) A higher order background model improves the detection of regulatory elements by Gibbs Sampling. *Bioinformatics*, **17**, 1113–1122.

Thijs, G., Marchal, K., Lescot, M., Rombauts, S., De Moor, B., Rouzé, P. and Moreau, Y. (2002) A Gibbs Sampling method to detect over-represented motifs in upstream regions of coexpressed genes. *J. Comp. Biol.* **9**, 447–464.

Tsabary, G., Shani, Z., Roiz, L., Levy, I., Riov, J. and Shoseyov, O. (2003) Abnormal 'wrinkled' cell walls and retarded development of transgenic *Arabidopsis thaliana* plants expressing endo-1,4-β-glucanase (*cel1*) antisense. *Plant Mol. Biol.* **51**, 213–224.

Yan, Y., Smant, G. and Davis, E. (2001) Functional screening yields a new beta-1,4-endoglucanase gene from *Heterodera glycines* that may be the product of recent gene duplication. *MPMI*, **14**, 63–71.

Yung, M.H., Schaffer, R. and Putterill, J. (1999) Identification of genes expressed during early *Arabidopsis* carpel development by mRNA differential display: characterisation of ATCEL2, a novel endo-1, 4-beta-D-glucanase gene. *Plant J.* **17**, 203–208.

Van Soest, P.J., Robertson, J.B. and Lewis, B.A. (1991) Symposium: carbohydrate methodology, metabolism, and nutritional implications in dairy cattle. *J. Diary Sci.* **74**, 3583–3597.

Van Soest, P.J., Wine, R.H. and Lewis, B.A. (1967) Use of detergents in the analysis of fibrous feeds. IV. Determination of plant cell-wall constituents. *JAOAC*, **50**, 50–55.

Van Soest, P.J. (1963) Use of detergents in the analysis of fibrous feeds. II. A rapid method for the determination of fiber and lignin. *JAOAC*, **46**, 829–835.

Uehara, T., Kushida, A. and Momota, Y. (2001) PCR-based cloning of two β-1,4-endoglucanases from the root-lesion nematode *Pratylenchus penetrans*. *Nematology*, **3**, 335–341.

Urbanczyk-Wochniak, E., Filipecki, M. and Przybecki, Z. (2001) A useful protocol for *in situ* RT-PCR on plant tissues. *Cell. Mol. Biol. Lett.* **7**, 7–18.

Wang, X., Meyers, D., Yan, Y., Baum, T., Smant, G., Hussey, R. and Davis, E. (1999) In planta localization of beta-1,4-endoglucanase secreted by *Heterodera glycines*. *MPMI*, **12**, 64–67.

Wang, X., Replogle, A., Davis, E.L. and Mitchum, M.G. (2007) The tobacco Cel7 gene promoter is auxin-responsive and locally induced in nematode feeding sites of heterologous plants. *Mol. Plant Path.* **8**, 426–436.

Wieczorek, K., Golecki, B., Gerdes, L. *et al.* (2006) Expansins are involved in the formation of nematode-induced syncytia in roots of *Arabidopsis thaliana*. *Plant J.* **48**, 98–112.

Wu, S.C., Blumer, J.M., Darvill, A.G. and Albersheim, P. (1996) Characterization of an Endo-1,4-β-glucanase gene induced by auxin in elongating pea epicotyls. *Plant Physiol.* **110**, 163–170.

Wyss, U. and Grundler, F.M.W. (1992a) *Heterodera schachtii* and *Arabidopsis thaliana*, a model host–parasite interaction. *Nematologica*, **38**, 488–493.

Wyss, U. and Grundler, F.M.W. (1992b) Feeding behaviour of sedentary plant parasitic nematodes. *Neth. J. Pl. Path.* **98** (Suppl.), 2, 165–173.

Zimmermann, P., Hirsch-Hoffmann, M., Hennig, L. and Gruissem, W. (2004) GENEVESTIGATOR. Arabidopsis microarray database and analysis toolbox. *Plant Physiol.* **136**, 2621–2632.

CHAPTER 5

Myo-inositol oxygenase genes are involved in the development of syncytia induced by *Heterodera schachtii* in Arabidopsis roots

Siddique, S., Endres, S., Atkins, J.M., Szakasits, D., Wieczorek, K., Hofmann, J., Blaukopf, C., Urwin, P.E., Tenhaken, R., Grundler, F.M.W., Kreil, D.P. and Bohlmann, H.

The New phytologist (2009) 184:457-472

.

Myo-inositol oxygenase genes are involved in the development of syncytia induced by *Heterodera schachtii* in Arabidopsis roots

Shahid Siddique[1], Stefanie Endres[2], Jamie M. Atkins[3], Dagmar Szakasits[1], Krzysztof Wieczorek[1], Julia Hofmann[1], Claudia Blaukopf[1], Peter E. Urwin[3], Raimund Tenhaken[2], Florian M. W. Grundler[1], David P. Kreil[4] and Holger Bohlmann[1]

[1]Institute of Plant Protection, Department of Applied Plant Sciences and Plant Biotechnology, University of Natural Resources and Applied Life Sciences, Peter-Jordan-Strasse 82, A–1190 Vienna, Austria; [2]University of Salzburg, Plant Physiology, Hellbrunnerstrasse 34, A–5020 Salzburg, Austria; [3] Centre for Plant Sciences, Faculty of Biological Sciences, University of Leeds, Leeds, LS2 9JT, UK; [4]Chair of Bioinformatics, Department of Biotechnology, University of Natural Resources and Applied Life Sciences, Vienna, Austria

Author for correspondence:
Holger Bohlmann
Tel: +43 1 47654 3360
Email: Holger.bohlmann@boku.ac.at

Received: *5 May 2009*
Accepted: *2 June 2009*

New Phytologist (2009) **184**: 457–472
doi: 10.1111/j.1469-8137.2009.02981.x

Key words: Arabidopsis, *Heterodera schachtii*, MAPMAN, myo-inositol oxygenase, syncytium, roots.

Summary

• In plants, UDP-glucuronic acid is synthesized by the oxidation of UDP-glucose by UDP-glucose dehydrogenase or the oxygenation of free myo-inositol by myo-inositol oxygenase (MIOX). In Arabidopsis, myo-inositol oxygenase is encoded by four genes. Transcriptome analysis of syncytia induced by the cyst nematode *Heterodera schachtii* in Arabidopsis roots revealed that *MIOX* genes are among the most strongly upregulated genes.

• We have used β-glucuronidase (GUS) analysis, *in situ* reverse transcription polymerase chain reaction (RT-PCR), and real-time RT-PCR to study the expression of all four *MIOX* genes in syncytia induced by *H. schachtii* in Arabidopsis roots. All these methods showed that *MIOX* genes are strongly induced in syncytia. GeneChip data were analysed for the expression of genes related to the MIOX pathway (MAPMAN).

• Two complementary double mutants were used to study the importance of *MIOX* genes. Results of the infection assay with double mutants in two combinations (Δ*miox1+2*, Δ*miox4+5*) showed a significant reduction ($P < 0.05$) in the number of females per plant when compared with the wild-type. Furthermore, syncytia in double mutants were significantly smaller than in wild-type plants.

• Our data demonstrate an important role of the *MIOX* genes for syncytium development and for the development of female nematodes.

Introduction

Nematodes are a group of animals that include free-living bacterial feeders such as the intensively studied worm *Caenorhabditis elegans* as well as many pathogens of animals and plants. Plant-parasitic nematodes attack mainly the roots of a variety of plants, often causing severe damage to crop plants either directly or as virus vectors. Some of the most economically important species are the cyst and root-knot nematodes within the family Heteroderidae. The worldwide crop losses caused by nematode damage have been estimated at over $100 billion yr^{-1} (Sasser & Freckman, 1987). Cyst nematodes (genera *Heterodera* and *Globodera*) (Hussey & Grundler, 1998) enter the plant roots as second stage juveniles (J2) and establish a specialized feeding structure (Jones & Northcote, 1972), which is initiated from a single root cell and then expands by incorporating up to several-hundred neighbouring cells by local cell wall dissolution. The nematode feeds only from this syncytium which is thus a severe nutrient sink for the plant. Adult male cyst nematodes leave the root to mate with females. After mating, the female cyst nematode continues to feed but dies once egg development

is completed, leaving several-hundred eggs contained within its enlarged body. This subsequently hardens to form a cyst, which protects the eggs until infective J2 hatch in favourable conditions. Root-knot nematodes (genus *Meloidogyne*) induce a different feeding structure which is composed of several giant cells (Jones & Payne, 1978).

The development of the syncytium from the initial syncytial cell inside the central cylinder is probably initiated through secretions from the nematode and a coordinated expression of plant genes. Such plant genes include, for example, expansins and cellulases that are important for the degradation of cell walls leading to incorporation of new cells into the growing syncytium (Goellner *et al.*, 2001; Wieczorek *et al.*, 2006, 2008). Syncytial cell walls also undergo modification – a process that requires synthesis of new cell wall polysaccharides. Protuberances are produced at the interface between syncytia and xylem vessels and these are thought to be important for the transport of water and solutes (Jones & Northcote, 1972). The outer cell walls of the syncytium are strengthened, which also requires the synthesis of new cell wall polysaccharides. The cells that are incorporated into the syncytium undergo drastic changes in structure and activity. This includes fragmentation of the central vacuole into many small ones, accumulation of mitochondria and ribosomes in a dense granular cytoplasm and proliferation of the endoplasmic reticulum (Golinowski *et al.*, 1996; Sobczak *et al.*, 1997). To cope with this high metabolic activity, the nuclei and nucleoli are enlarged and contain endoreduplicated DNA (Niebel *et al.*, 1996).

These drastic changes in cell morphology imply an underlying global change in gene expression and a variety of methods have been used to identify genes that are specifically induced in nematode feeding sites (reviewed by Gheysen & Fenoll, 2002). During recent years microarrays have become the methodology of choice to allow a global view of the changes in gene expression in nematode feeding sites. The transcriptome of dissected galls induced by the root-knot nematode *Meloidogyne javanica* on tomato roots was studied using microarrays containing 12 500 cDNAs (Bar-Or *et al.*, 2005). A similar approach has been used to analyse whole root tips of soybean infected with the cyst nematode *Heterodera glycines* (Alkharouf *et al.*, 2006). Recently, Laser Capture Microdissection has been used to study gene expression in syncytia induced by *H. glycines* in soybean roots (Ithal *et al.*, 2007a; Klink *et al.*, 2007).

The sugar beet cyst nematode *Heterodera schachtii* completes its life cycle on *Arabidopsis thaliana* roots *in vitro* within 6 wk (Sijmons *et al.*, 1991) and this interaction has been established as a model system. The translucent Arabidopsis roots growing on artificial media facilitate study of the development of this and other nematode species inside the root (Wyss & Grundler, 1992).

We have recently analysed the transcriptome of syncytia induced by *H. schachtii* in roots of Arabidopsis at 5 and 15 d postinfection (dpi) (Szakasits *et al.*, 2009) and it was observed that two myo-inositol oxygenase (*MIOX*) genes were among those most strongly upregulated. MIOX converts myo-inositol to glucuronic acid which can be further phosphorylated to produce glucuronic acid-1-phosphate which is then converted to UDP-glucuronic acid (UDP-GlcA). The gene/s coding for the glucuronokinase which phosphorylates glucuronic acid in Arabidopsis is/are not known yet. However, the UDP-glucuronic acid pyrophosphorylase has recently been identified as UDP-sugar pyrophosphorylase (USP, *At5g52560*). This is probably a single gene and knockouts do not produce viable pollen (Schnurr *et al.*, 2006, R. Tenhaken, unpublished).

UDP-GlcA is an important precursor for several nucleotide sugars which are used for the synthesis of cell wall polysaccharides. In addition to the MIOX pathway, UDP-GlcA can also be produced from UDP-glucose by UDP-glucose dehydrogenase (UGD) that is encoded by four genes in Arabidopsis (Klinghammer & Tenhaken, 2007). The regulation and importance of these different pathways for the production of UDP-GlcA is largely unknown (Seifert, 2004).

A strong indication for the role of the MIOX pathway in providing nucleotide sugars for cell-wall polymers comes from the analysis of Arabidopsis mutant lines for *MIOX1* and *MIOX2*. Both MIOX knockout lines showed a drastic reduction of ^{3}H-inositol incorporation into cell walls when grown in liquid MS medium containing ^{3}H-inositol. This effect was not seen with the *MIOX5* knock-out line, which is not surprising because the *MIOX5* gene is expressed in seedlings only at a very low level (Kanter *et al.*, 2005). Similarly, overexpression of *MIOX4* resulted in increased incorporation of MIOX-derived sugars into cell walls (Endres & Tenhaken, 2009). In addition to producing UDP-GlcA, MIOX might also be involved in the production of ascorbate (Lorence *et al.*, 2004). Overexpression of the flower-specific *MIOX4* gene in Arabidopsis plants resulted in elevated ascorbate levels, suggesting a role for glucuronic acid and the myo-inositol oxygenase pathway in vitamin C biosynthesis in plants. However, Endres & Tenhaken (2009) were unable to repeat these experiments.

The finding that two *MIOX* genes were strongly upregulated in syncytia prompted us to further investigate the role of *MIOX* genes in the interaction with cyst nematodes. Our results showed that all Arabidopsis *MIOX* genes were expressed in syncytia and that they play an important role in syncytium development and in the development of female cyst nematodes.

Materials and Methods

Plant cultivation

Arabidopsis thaliana (L.) Heynh. seeds were surface sterilized for 20 min in 6% (w : v) sodium hypochlorite and subsequently washed three times with sterile H_2O. Seeds were placed into sterile Petri dishes (9 cm) on a modified Knop medium with 2% sucrose (Sijmons *et al.*, 1991). Seeds were grown in a growth chamber at 25°C in a 16 h light : 8 h dark cycle.

RNA isolation for quantitative real time reverse transcription polymerase chain reaction (qRT-PCR) analysis

Root segments containing syncytia were excised at 15 dpi and immediately frozen in liquid nitrogen. Control root segments were collected and frozen as described for Affymetrix analysis (described in the next section). Two biological replicates were done, each consisting of approx. 60 syncytia or a corresponding number of root segments. Total RNA was isolated using an RNeasy Plant Mini Kit (Qiagen) according to the manufacturer's instructions, including DNaseI (Qiagen) digestion. Quality and quantity of the RNA was assessed using an Agilent 2100 bioanalyser (Agilent Technologies, Palo Alto, CA, USA). Reverse transcription was performed with a SuperScript III reverse transcriptase (Invitrogen) and random primers (oligo$(dN)_6$) according to the manufacturer's instructions.

Affymetrix GeneChip analysis

Syncytial samples were collected at 5 dpi and 15 dpi by microaspiration. Root segments cut from the elongation zone of 12-d-old uninfected plants were used as controls. Care was taken to avoid any root tips or lateral root primordia. RNA was isolated as described above. Biotin-labelled probes were prepared according to the Affymetrix protocol with some modifications (for details see Szakasits *et al.*, 2009).

Statistical analysis of microarray data

Affymetrix CEL files were analysed using packages of the Bioconductor suite (http://www.bioconductor.org). Details are provided in Szakasits *et al.* (2009) and in the Supporting Information (Methods S1; the additional online material provides large, comprehensive tables and plots and detailed technical analysis of the results is archived at http://bioinf.boku.ac.at/pub/Siddique2008/).

Quantitative RT-PCR of gene expression in syncytia

Quantitative real time RT-PCR of *MIOX* gene expression in syncytia was performed with an ABI PRISM 7300 Sequence Detector (Applied BioSystems) as follows. Each qRT-PCR sample contained 12.5 µl Platinum SYBR Green qPCR SuperMix with UDG and ROX (Invitrogen), 2 mM $MgCl_2$, 0.5 µl forward and reverse primer (10 µM), 2 µl cDNA and water to make a 25 µl total reaction volume. The primers used were as described by Kanter *et al.* (2005): *MIOX1* (5′-CACACCAACTCTTTTGGTCGC-3′; 5′-GTACGA-TTTAGCTTCTCGTATTCTTC-3′; $E = 0.88$; $R^2 = 0.990$), *MIOX2* (5′-TGATATGAATTTCTTGGGCCATT-3′; 5′-ATCTTGTTAAGTTT TCCATACTCTTTCC-3′; $E = 0.83$; $R^2 = 0.995$), *MIOX4* (5′-GAGATGAATGCATTTGGCCG-3′; 5′-TTTATCTAATTTTCCATATTCAGCCC-3′; $E = 0.92$; $R^2 = 0.993$), and *MIOX5* (5′-GAGATGAACGCATTTGG-TCGT-3′ 5′-CTTGTCCAATTTTCCATACTCACTT-3′; $E = 0.87$; $R^2 = 0.990$). All samples were diluted 1 : 3 and were analysed in three technical replicates. Control reactions with no cDNA template ruled out false positives and dissociation runs were performed to assess the possible formation of primer dimers. The *UBP22* gene was used as an internal reference as described previously (Hofmann & Grundler, 2007). Results were obtained using the Sequence Detection Software SDS v2.0 (Applied BioSystems). Relative expression was calculated by the $(1+E)^{-\Delta\Delta Ct}$ method.

β-glucuronidase (GUS) reporter analysis

Promoter regions immediately upstream of the initiation codon of *MIOX4* (2185 bp) and *MIOX5* (1188 bp) were amplified by PCR using 50 ng Arabidopsis Col-0 genomic DNA as template. Primer pairs used for *MIOX4* (5′-ATAAAGCTTTATTTAACCAAAAATGGCATC-3′; 5′-ATACCATGGCTTTTCGAAGAAAGGTTTTTA-3v) and *MIOX5* (5′-ATATAAGCTTGGAGGAAGATGAGACTGA-3′; 5′-ATATCCATGGCATCTTCCAAAAAAAAACAAAGT-3′) included *Hin*d III and *Nco*I restriction sites (underlined) for subsequent cloning into the vector pCAMBIA1303. Promoter::GUS constructs were introduced into *Agrobacterium tumefaciens* GV3101 for transformation of Arabidopsis Col-0 plants by the floral dip method (Clough & Bent, 1998). Transformed plants were selected on half-strength Murashige and Skoog (MS) medium (Murashige & Skoog, 1962) containing 50 µg ml^{-1} hygromycin, then transferred to soil for seed collection.

For analysis of GUS expression, *Arabidopsis* seeds were surface-sterilized for 5 min in 95% ethanol followed by 5 min in 10% (v : v) commercial bleach and subsequently washed three times in sterile H_2O. Seedlings were grown vertically on half-strength MS medium supplemented with 1% (w : v) sucrose and 0.6% (w : v) plant agar (Duchefa, Haarlem, the Netherlands) in 10-cm square Petri dishes. Roots of 12-d-old plants were inoculated with *c.* 35 sterile *H. schachtii* J2 applied to 1 cm^2 pieces of GF/A paper (Whatman, Maidstone, Kent, UK) at each of three infection points per plant.

The GUS expression was analysed at 5, 7, 10, 15 and 20 dpi. Four plants from each of four transgenic lines per construct were analysed at each time-point. Root systems were separated from aerial tissue and submerged in 100 mM $NaPO_4$ buffer (pH 7.0) containing 10 mM EDTA, 0.01% Triton X-100, 0.5 mM $K_3(Fe(CN)_6)$, 0.5 mM $K_4(Fe(CN)_6)$ and 1 mg ml^{-1} 5-bromo-4-chloro-3-indolyl glucuronide (X-gluc; Melford Laboratories Ltd, Ipswich, UK). Tissue was vacuum-infiltrated for 5 min then incubated in the dark for 16 h at 37°C. Stained tissue was mounted in glycerol and viewed using bright field optics on a Leica DMRB microscope. Images were captured with an Olympus C-5050 digital camera.

Table 1 Primer pairs used for screening of single and double mutants

Allele	Forward primer	Reverse primer
Δ*miox1*	GTCCGCGTAAACGTTGAGGAAGTG	GGTATCTGGGAATGGCGAAATC
Wild type *MIOX1*	GTCCGCGTAAACGTTGAGGAAGTG	CTGGTTCGGGTGTATCATTGAG
Δ*miox2*	CATTTTCAGATCTTGGCAAGGTTC	ACTCAACCCTATCTCGGGCTATTC
wt *MIOX2*	CATTTTCAGATCTTGGCAAGGTTC	CCAGCGAGAGGAAGGGTCG
Δ*miox4*	GGTGGTGGCTAATTCACAAC	ACTCAACCCTATCTCGGGCTATTC
Wild type *MIOX4*	GGTGGTGGCTAATTCACAAC	TAGGGTAATCTTTGCGGATGGC
Δ*miox5*	ACGTACACCACAAGGTACAT	ACTCAACCCTATCTCGGGCTATTC
Wild type *MIOX5*	ACGTACACCACAAGGTACAT	AAGAGACATGTAGTACGGCTTAAC

In situ RT-PCR

In situ RT-PCR was carried out according to Koltai & Bird (2000) and Urbanczyk-Wochniak *et al*. (2002). Syncytia at 10 dpi were dissected from roots and immediately put into cold fixation solution (63% ethanol, v : v; 2% formalin, v : v). After 24 h, syncytia were embedded in 4% low-melting agarose and 25 μm thick sections were prepared using a vibratome (VT 100; Leica, http://www.leica.com/). A RT-PCR was then carried out using digoxigenin-labelled dUTP. After a staining reaction with nitro blue tetrazolium (NBT)/5-bromo-4-chloro-3-indolyl phosphate (BCIP) substrate, cross-sections were photographed under an inverted microscope (Axiovert 200M; Zeiss, http://www.zeiss.com/) with an integrated camera (AxioCam MRc5; Zeiss). For full details see Wieczorek *et al*. (2006).

Mutant screening

Single knockout mutants of all four alleles of MIOX were obtained from the GABI-KAT stock centre (450D10 for Δ*miox1*) and the SALK institute (040608 for Δ*miox2*, 018395 for Δ*miox4*, 112535 for Δ*miox5*). To obtain the Δ*1+2* and Δ*4+5* double mutants, the respective homozygous lines were crosspollinated and the resulting heterozygous generation was analysed via PCR for the presence of each intact and disrupted wild-type allele. This generation was allowed to self-pollinate to produce a generation in which the desired genotype of a homozygous double knockout will appear with a frequency of 1/16. A PCR analysis (primer pairs used for screening of single and double mutants are shown in Table 1) was used to identify these individuals. To verify true-breeding, six to eight individuals of their offspring were confirmed as homozygous double knockouts.

Quantitative RT-PCR of *MIOX* gene expression in mutants

Seedlings were grown on wet filter paper or on MS medium. Seven-day-old seedlings were harvested for extraction of RNA. Real time PCR was performed on a Stratagene MX3000 real-time cycler using the SybrGreen method. One reaction (30 μl) consisted of 1× PCR-buffer, a 1:200 000 dilution of SybrGreen stock (Roche), 200 nmol each primer, betaine at a final concentration of 0.6 M, and 1 U *Taq* polymerase (recombinant wild type). Primers were 5′-CATGTACCTTGTTGCGAAGGAG-3′ (forward); 5′-ACCATTTTAGCTTGGACGGA-3′ for *MIOX1*; 5′-GCTGTCGTTGGCGATACATTTC-3′; 5′-AGGGTCGTGCCATTCTTCTTAG-3′ for *MIOX2*; 5′-GGCTGTTGTTGGTGACACATTC-3′; 5′-CGTGTAGCCACTTCAGATTCTC-3′ for *MIOX4*; 5′-GGCTGTTGTTGGTGACACATTTC-3′; 5′-TAAGCTCCAGCCTTGTGCAATG-3′; for *MIOX5*, and 5′-GTAACAAGATGGATGCCACCACC-3′; 5′-CCTCTTGGGCTCGTTGATCTG-3′ for *EF1α* (used for internal normalization). Relative expression was calculated by the ΔΔCt method.

Analysis of cell wall sugars

Leaf material (100–150 mg) was frozen in liquid nitrogen, homogenized and suspended in 70% ethanol. Subsequent extractions with methanol–chloroform and acetone resulted in a cell wall pellet, which was dried and suspended in 800 μl 0.25 M sodium acetate (pH 4.0). The sample was incubated at 80°C for 20 min, chilled on ice, adjusted to a pH of 5.0 with 1 M NaOH, and incubated with α-amylase and pullulanase at 37°C overnight with 0.01% NaN_3. The following day, the sample was boiled for 10 min in a water bath, centrifuged at 18 000 ***g*** for 5 min, and the supernatant discarded. To remove all residual free sugars, the pellet was washed four times with 1 ml water. After two more washing steps with acetone, the pellet was dried. The weight of the sample was determined and the sample was hydrolysed by autoclaving for 2 h in 250 μl 2 M TFA (Trifluoroacetic acid) and 10 μl 0.5% inositol. Once again the sample was dried and redissolved in 1 ml distilled water per 3 mg of dry sample; 200 μl were then diluted with 300 μl water and analysed via HPLC on a Dionex ICS 3000 system with a PA 20 column. Peak identity was verified with authentic standards.

Nematode infection

Heterodera schachtii (Schmidt) cysts were harvested from *in vitro* stock cultures on mustard (*Sinapis alba* cv. Albatros)

roots growing on Knop medium supplemented with 2% sucrose (Sijmons *et al.*, 1991). Hatching of J2 was stimulated by adding 3 mM $ZnCl_2$. The J2 were resuspended in 0.5% (w : v) Gelrite (Duchefa) and 12-d-old Arabidopsis roots were inoculated under sterile conditions with *c.* 80–90 J2 per plant. Ten plants per plate were used and experiments were repeated at least three times with *c.* 40 plants per replicate per line.

The number of males and females per plant were counted at 14 dpi. The data were analysed using single factor ANOVA ($P < 0.05$). As the *F*-statistic was greater than *F*-critical, a Fisher LSD test was applied.

Syncytium size measurement

The size of syncytia (longitudinal sections) was measured at 10 dpi and 14 dpi with *H. schachtii.* For each line, 10 female syncytia were randomly selected and photographed by an Axiovert 200M (Zeiss) using a Zeiss Axiocam digital camera. The syncytia were outlined using the Axiovision Kontour tool and the area of longitudinal sections was calculated by the software. These individual measurements were used to calculate the average size of syncytia. Data were further statistically analysed using single factor ANOVA ($P < 0.05$) and LSD.

Results

GeneChip analysis of genes related to the MIOX pathway

We recently performed a transcriptome analysis of syncytia induced by *H. schachtii* in Arabidopsis roots (Szakasits *et al.*, 2009). This analysis revealed that the genes *MIOX4* and *MIOX5* were among the most strongly upregulated genes (Tables 2 and S1). *MIOX2* was also significantly upregulated in syncytia but had a much higher basal expression level in roots than *MIOX4* and *MIOX5*. *MIOX1*, the fourth *MIOX* gene (*MIOX3* is a pseudogene) cannot be measured with the Affymetrix ATH1 GeneChip. Because the GeneChip data indicated an important role for the *MIOX* genes, we studied the expression of all four *MIOX* genes in detail by using GUS analysis, qRT-PCR and *in situ* RT-PCR.

Promoter::GUS analysis

A GUS expression analysis was performed for *MIOX4* and *MIOX5* (Fig. 1). The general GUS expression pattern was assessed for seven Arabidopsis lines transformed with the *MIOX4*::GUS construct and 12 lines transformed with the *MIOX5*::GUS construct. For all lines, expression in uninfected plants was localized to floral tissues with the strongest expression in pollen grains and the stigma. Lower expression was observed in petals, sepals and filament (Fig. 1c). There was generally no expression in other plant tissues, although GUS activity was occasionally observed in < 1% of lateral root bases of *MIOX5*::GUS lines (Fig. 1b).

Four representative promoter::GUS lines for each gene were infected with nematodes and stained for GUS activity at different time-points after infection, i.e. 5 dpi, 7 dpi, 10 dpi, 15 dpi and 20 dpi. No *MIOX4*::GUS expression was seen in the vicinity of nematode infections at 5 dpi (Fig. 1a). However, at 7 dpi, expression was switched on in most of the feeding sites and nearly all of the syncytia showed staining at 10 dpi, which became very intense at 15 dpi (Fig. 1a). The GUS staining was localized to the syncytium. No expression was seen in the roots of *MIOX5*::GUS plants until 10 dpi, when every syncytium showed some degree of GUS expression (Fig. 1b). Similarly, there was strong GUS expression within *c.* 50% of syncytia at 15 dpi (Fig. 1b). In some cases the GUS staining extended beyond the syncytium into the surrounding root tissue. Representative pictures are shown for all time points. Additional pictures are available in Figs S3 and S4.

qRT-PCR

The regulation of all four *MIOX* genes in syncytia was further studied by using qRT-PCR. For this analysis, syncytia were excised at 15 dpi. For comparison with the GeneChip results, the same control roots were used as in that study (see the Materials and Methods section). For *MIOX4* and *MIOX5* no transcripts could be detected in control roots and it was therefore impossible to formally calculate a fold-change value for these genes (Table 3). *MIOX2* was shown to be upregulated in syncytia compared with controls, although the signal intensity was weak compared with GeneChip data. While no chip data were available for *MIOX1*, qRT-PCR revealed a strong upregulation in syncytia.

Localization of MIOX gene expression by *in situ* RT-PCR

Localization of *MIOX1*, *MIOX2*, *MIOX4* and *MIOX5* mRNA was investigated by *in situ* RT-PCR using fresh sections from syncytia at 10 dpi. Transcripts of all four genes were clearly detected in syncytia (Fig. 2a,d,g,j). In control roots, *MIOX1*, *MIOX2* and to a lesser degree *MIOX4* transcripts were detected while there was no detectable expression of *MIOX5* (Fig. 2c,f,i,l). No products were observed in controls using syncytium root sections without *Taq* polymerase (Fig. 2b,e,h,k). Thus, all four *MIOX* genes were expressed in syncytia.

Transcriptional analysis of genes involved in UDP-GlcA synthesis

The role for myo-inositol oxygenase in plants is still unclear. One proposed function is in the synthesis of UDP-GlcA, which is converted to sugar nucleotides as precursors for cell wall polysaccharides. However, UDP-GlcA can also be produced

New Phytologist

Table 2 GeneChip expression profiles of Arabidopsis genes involved in UDP-glucuronic acid (UDP-GlcA) formation during the development of syncytia induced by *Heterodera schachtii*

Gene ID	Gene	Control	Syncytium (5 + 15 dpi)	Control vs syncytium	*q*-value	Enzyme function
At1g12780	*UGE1*	6.7	8.3	1.6*	0.04	UDP-glucose 4-epimerase
At4g23920	*UGE2*	4.6	4.5	–0.1	0.64	UDP-glucose 4-epimerase
At1g63180	*UGE3*	5.5	4.6	–0.9	0.12	UDP-glucose 4-epimerase
At1g64440	*UGE4*	4.5	4.	0.0	0.90	UDP-glucose 4-epimerase
At4g10960	*UGE5*	4.9	4.7	–0.2	0.50	UDP-glucose 4-epimerase
At3g53520	*UXS1*	6.3	6.9	0.6	0.23	UDP-xylose synthase
At3g62830	*UXS2*	n.a.	n.a.	n.a.	n.a.	UDP-xylose synthase
At5g59290	*UXS3*	7.3	8.1	0.8	0.28	UDP-xylose synthase
At2g47650	*UXS4*	n.a.	n.a.	n.a.	n.a.	UDP-xylose synthase
At3g46440	*UXS5*	8.5	11.0	2.6*	0.03	UDP-xylose synthase
At2g28760	*USX6*	7.2	7.0	–0.2	0.38	UDP-xylose synthase
At1g30620	*UXE1*	4.8	6.0	1.3*	0.01	UDP-xylose 4-epimerase 1
At4g20460	*UXE2*	9.0	4.7	–4.3*	5.10 e-05	UDP-xylose 4-epimerase 1
At2g34850	*UXE3*	4.0	4.3	*0.3*	0.29	UDP-xylose 4-epimerase 1
At5g44480	*UXE4*	11.2	3.6	–7.7	2.31 e-06	UDP-xylose 4-epimerase 1
At4g30440	*GAE1*	6.8	7.9	1.1*	0.02	UDP-glucuronic acid 4-epimerase
At1g02000	*GAE2*	6.7	5.7	–1.0	0.03	UDP-glucuronic acid 4-epimerase
At4g00110	*GAE3*	4.7	4.6	–0.1	0.70	UDP-glucuronic acid 4-epimerase
At2g45310	*GAE4*	3.0	2.9	0.0	0.84	UDP-glucuronic acid 4-epimerase
At4g12250	*GAE5*	4.9	4.6	–0.3	0.40	UDP-glucuronic acid 4-epimerase
At3g23820	*GAE6*	11.1	11.0	0.0	0.90	UDP-glucuronic acid 4-epimerase
At5g39320	*UGD1*	6.3	4.3	–2.0*	0.00	UDP-glucose dehydrogenase
At3g29360	*UGD2*	5.7	5.3	–0.4	0.71	UDP-glucose dehydrogenase
At5g15490	*UGD3*	5.7	6.3	0.5	0.65	UDP-glucose dehydrogenase
At1g26570	*UGD4*	3.7	5.0	1.2*	0.01	UDP-glucose dehydrogenase
At1g78570	*RHM1*	6.5	5.2	–1.3	0.06	Rhamnose synthase
At1g53500	*RHM2*	5.9	6.0	0.1	0.69	Rhamnose synthase
At3g14790	*RHM3*	5.5	7.0	1.5	0.00	Rhamnose synthase
At5g66280	*GMD1*	4.9	4.1	–0.8*	0.01	GDP-mannose dehydrogenase
At3g51160	*GMD2/MUR1*	6.0	6.3	0.2	0.40	GDP-mannose dehydrogenase
At1g73250	*GER1*	5.5	6.1	0.6	0.05	GDP-4-keto-6-deoxy-mannose-3, 5-epimerase-4-reductase
At1g17890	*GER2*	5.5	6.3	0.8	0.06	GDP-4-keto-6-deoxy-mannose-3, 5-epimerase-4-reductase
At2g39770	*GMP1*	7.3	7.7	0.4	0.58	GDP-mannose pyrophosphorylase
At3g55590	*GMP*	3.4	3.1	–0.3	0.30	GDP-mannose pyrophosphorylase
At5g20830	*SUS1*	6.8	6.5	*–0.3*	0.71	Sucrose synthase
At5g49190	*SUS2*	2.9	3.0	*0.0*	0.71	Sucrose synthase
At4g02280	*SUS3*	4.2	5.4	*1.2*	0.00	Sucrose synthase
At3g43190	*SUS4*	5.7	5.1	–0.6	0.09	Sucrose synthase
At5g37180	*SUS5*	5.0	4.0	–1.0*	0.00	Sucrose synthase
At1g73370	*SUS6*	6.5	4.7	–1.8	0.00	Sucrose synthase
At1g63000	*UER1*	7.2	6.3	–0.9	0.13	Epimerase reductase
At1g70820	*PGM*	4.8	4.4	–0.4	0.23	Phospho-glucomutase
At5g51820	*PGM*	4.8	8.4	3.6*	0.00	Phospho-glucomutase
At1g23190	*PGM*	9.4	12.0	2.6	0.04	Phospho-glucomutase
At1g70730	*PGM*	8.4	10.7	2.4*	0.01	Phospho-glucomutase
At5g17530	*PGM*	6.8	6.6	–0.2	0.46	Phospho-glucomutase
At4g30570	*GMP*	4.5	4.2	–0.3	0.29	GDP-mannose pyrophosphorylase
At3g03250	*UGP*	7.6	9.7	2.2*	0.02	UDP-glucose pyrophsohporylase
At5g17310	*UGP*	4.3	9.1	4.8*	0.00	UDP-glucose pyrophsohporylase
At5g42740	*PGIC*	5.2	6.7	1.6	0.17	Glucose-6-phosphate isomerase, cytosolic
At4g24620	*PGI1*	10.8	11.8	1.0	0.10	Phospho-glucose (Glc) isomerase
At3g02570	*PMI*	5.4	5.8	0.4	0.58	Phosphomannose isomerase
At1g67070	*PMI*	3.1	3.0	0.0	0.83	Phosphomannose isomerase
At2g45790	*ATPMM*	8.6	10.3	1.7*	0.00	Phosphomannomutase
At3g01010	*UGD/GMD*	2.6	2.6	0.0	0.90	UDP-glucose dehydrogenase
At5g52560	*USP*	6.0	7.4	1.5	0.05	UDP-sugar pyrophosphorylase

Table 2 *continued*

Gene ID	Gene	Control	Syncytium (5 + 15 dpi)	Control vs syncytium	*q*-value	Enzyme function
At1g14520	*MIOX1*	na	na	na	na	Myo-inositol oxygenase
At2g19800	*MIOX2*	6.4	9.3	2.9*	0.0	Myo-inositol oxygenase
At4g26260	*MIOX4*	2.4	7.7	5.3*	5.10e-05	Myo-inositol oxygenase
At5g56640	*MIOX5*	2.1	10.9	8.8*	5.09e-07	Myo-inositol oxygenase
At3g07130	*ATPAP15*	9.4	7.3	–2.1*	0.00	Purple acid phosphatase
At2g32770	*ATPAP13*	2.5	3.0	0.6*	0.02	Purple acid phosphatase
At4g13700	*ATPAP23*	2.9	2.8	0.1	0.61	Purple acid phosphatase
At2g22240	*IPS2*	3.8	5.3	1.5*	0.00	Inositol phosphate synthase
At4g39800	*IPS1*	4.4	6.1	1.7*	0.00	Inositol phosphate synthase
At5g10170	*IPS3*	4.8	4.2	–0.6	0.06	Inositol phosphate synthase
At1g31190	*IMP*	5.7	6.2	0.6	0.10	Inositol monophosphatase
At3g02870	*IMP*	7.7	10.0	2.3*	0.00	Inositol monophosphatase
At4g39120	*IMP*	3.4	3.8	0.4	0.10	Inositol monophosphatase
At1g34120	*IP5P1*	6.8	4.8	–2.0*	0.00	Inositol polyphosphatases
At1g71710	*IP5P*	4.8	3.7	–1.0*	0.01	Inositol polyphosphatases
At4g18010	*IP5P2*	6.1	5.3	–0.9	0.08	Inositol polyphosphatases
At2g27860	*AXS1*	8.3	10.4	2.1*	0.01	UDP-apiose
At1g08200	*AXS2*	8.3	10.4	2.1*	0.01	UDP-apiose

Data for microaspirated syncytia at 5 d postinfection (dpi) and 15 dpi were combined and compared with control roots. Elongation zone without root tip was used as control. All expression values have been normalized and are on a $\log_2$ scale (third and fourth column) and the differences (fold changes) between the pairwise samples displayed (fifth column) are accordingly normalized $\log_2$ ratios (see the Materials and Methods section for details).
q-values indicate significance after correction for multiple testing controlling the false discovery rate.
*, Significant upregulation or downregulation (false discovery rate < 5%).
Data for *MIOX1*, *UXS2* and *UXS4* are not available because the probe sets are ambiguous.

Table 3 Change in expression of *MIOX* genes as measured by quantitative real-time reverse transcription polymerase chain reaction (qRT-PCR) relative to the expression of *At*UBP22

	GeneChip data (syncytium vs root)		qRT-PCR 15 dpi		
Gene	M value ($\log_2$)	Fold Change	Ct value ($\log_2 \pm$ SE)	Fold change	Name
At1g14520	na	na	5.9* ± 1.1	59.8	*MIOX1*
At2g19800	2.9*	7.64	2.50* ± 0.3	5.71	*MIOX2*
At4g26260	5.3*	39.5	∞	∞	*MIOX4*
At5g56640	8.8*	445.7	∞	∞	*MIOX5*

Transcripts were measured from root segments containing syncytia at 15 d postinfection (dpi) and compared with those from control root segments as used for GeneChips. Asterisks indicate significant difference in expression level between infected and noninfected roots. For both *MIOX4* and *MIOX5* no RNA was detected in the control, making it impossible to calculate a fold change value (indicated as ∞).
SE, standard error.

from UDP-glucose by UDP-glucose dehydrogenase (UGD), which is also encoded by four genes in Arabidopsis. We have therefore calculated normalized expression values for 71 genes involved in UDP-GlcA and myo-inositol metabolism (Tables 2 and S1) using GeneChip data for syncytia provided by Szakasits *et al.* (2009) and visualized these data using the MAPMAN program (Thimm *et al.*, 2004; http://gabi.rzpd.de/projects/MapMan/). For this analysis we combined the 5 dpi and 15 dpi syncytium data and compared them with the controls (Fig. 3a,b).

It is again clearly evident that the *MIOX* genes are strongly upregulated in syncytia while the single gene for USP is expressed in control roots and syncytia at approximately the same level. This is also the case for all four *UGD* genes (see also Table 2), although one (*UGD1*) is rather downregulated. Similarly, UDP-xylose synthase (UXS) is largely not regulated at the transcript level, except for *UXS5,* which is upregulated. The upregulation of the *MIOX* genes in syncytia could have resulted from a higher level of the substrate myo-inositol. We therefore extended our analysis to the expression of genes involved in myo-inositol synthesis from glucose-6-phosphate. Genes leading to the synthesis of myo-inositol were preferentially upregulated: One of two genes for inositol phosphate

New Phytologist

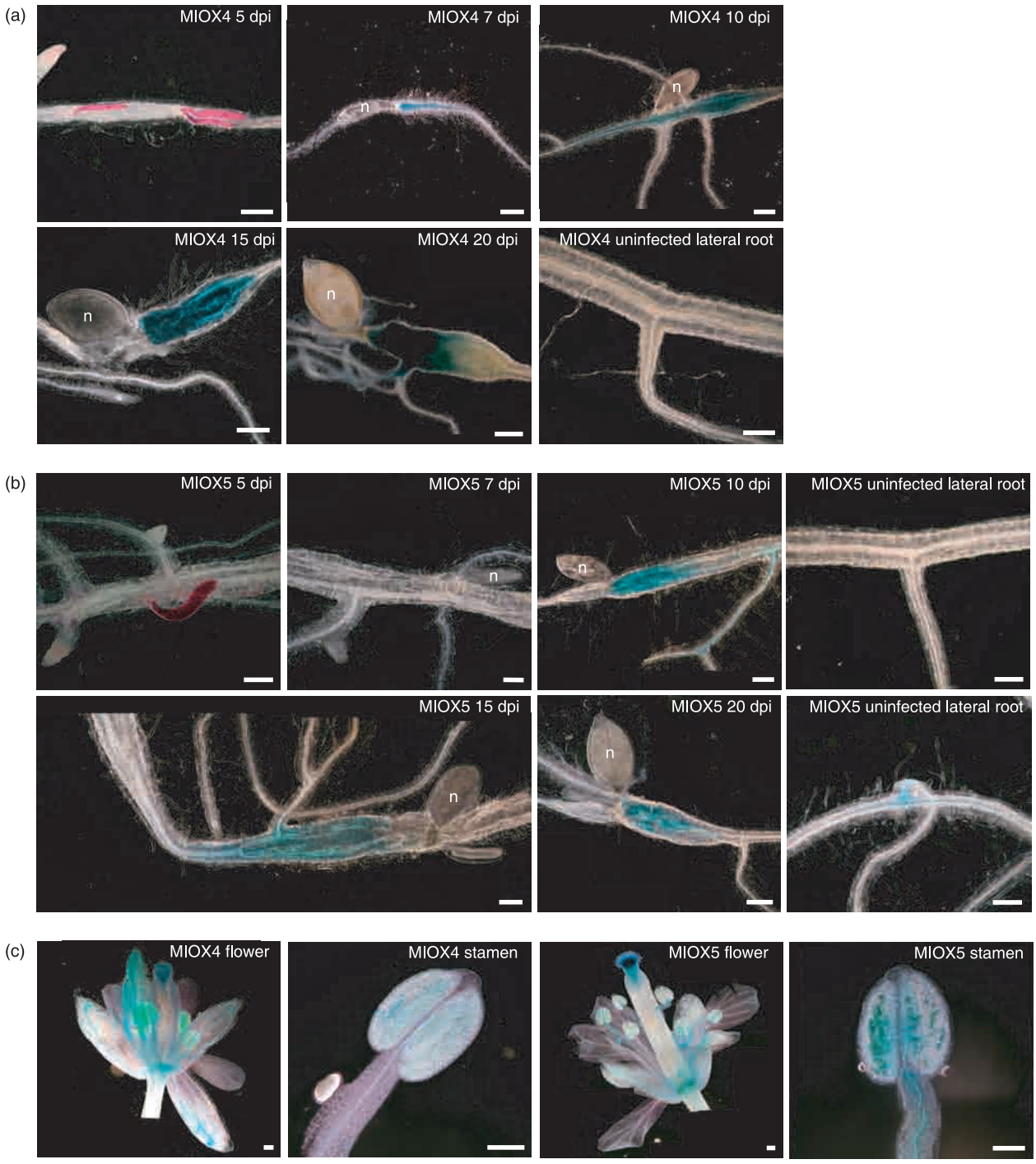

Fig. 1 Expression of glucuronidase (GUS) driven by *MIOX4* and *MIOX5* promoters in infected and uninfected Arabidopsis lines. (a) GUS expression for *MIOX4* in infected and uninfected roots. No expression was seen for *MIOX4* in uninfected roots or at 5 d postinfection (dpi) in syncytia, however, expression was turned on at 7 dpi, and intense GUS staining for *MIOX4* was observed in syncytia at 10, 15 and 20 dpi. (b) Expression of GUS for *MIOX5* in infected and uninfected roots. No expression was observed for *MIOX5* at 5 and 7 dpi in syncytia; however, strong expression was observed at 10, 15 and 20 dpi; GUS expression was very occasionally observed at the base of uninfected lateral roots. (c) Expression of GUS was observed in sepals, petals, stigma and pollen grains of *MIOX4*::GUS lines and in the filaments of *MIOX5*::GUS lines. At 5 dpi nematodes were stained pink with acid fuchsin to aid visualization. Bar, 100 μm.

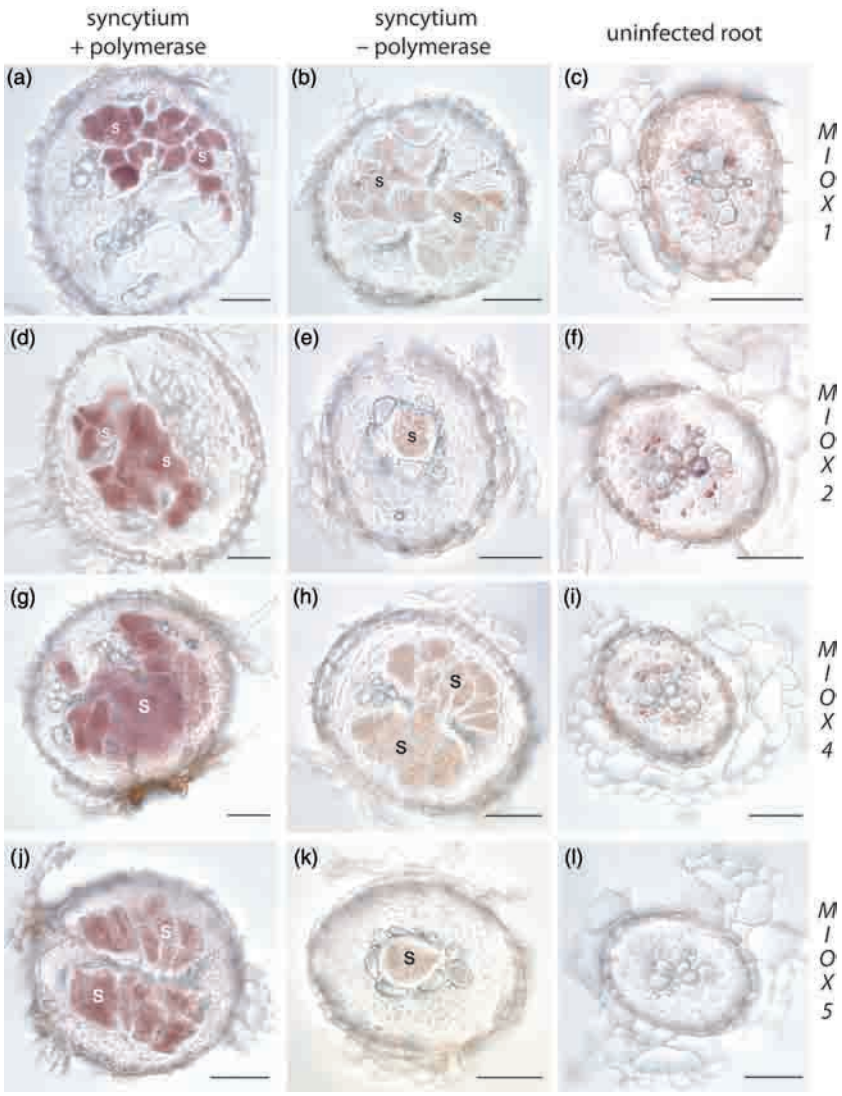

Fig. 2 *In situ* reverse transcription polymerase chain reaction (RT-PCR) of *MIOX* gene expression in syncytia (s). (a–c) *MIOX1*; (d–f) *MIOX2*; (g–i) *MIOX4*; (j–l) *MIOX5*. (a,d,g,j) specific reaction; (b, e, h and k) control without polymerase; (c,f,i,l) uninfected roots. Bar, 50 μm.

synthase and one of three genes for inositol monophosphatase were upregulated, while one of three genes for inositol polyphosphatase was downregulated (Table 2, Fig. 3b). This would indicate a preferential production of myo-inositol as a substrate for myo-inositol oxygenase.

Analysis of *MIOX* mutants

Kanter *et al*. (2005) have recently described single T-DNA mutants for all four *MIOX* genes. These mutants were crossed to produce a set of corresponding double mutants (see the Materials and Methods section). The PCR characterization of the double mutants is shown in Fig. 4.

The double mutants were indistinguishable from wild-type plants. Flowers and pollen developed normally, the siliques were filled, and seeds were fertile, and germinated readily.

We have used qPCR to test the expression of the *MIOX* genes in seedlings of the double mutants (Table 4). *MIOX1* and *MIOX2* were not detectable or at the limit of detection in the *miox1+2* mutants. The same is true for *MIOX4* and *MIOX5* in the *miox4+5* mutants. In the *miox1+2* mutants an increase in *MIOX4* expression and a decrease in *MIOX5* expression was observed.

In agreement with previous data (Kanter *et al*., 2005), a substantial loss of *MIOX* activity was seen in incorporation experiments for the *miox1+2* mutant (data not shown). The same experiment cannot serve to assay the decreased activity of m*iox4+5* because its level in seedlings is negligible. Root anatomy in the double mutants was studied by embedding roots in LR White and staining sections for cellulose with Calcofluor white. No difference between wild-type and the double mutants was observed in uninfected roots and in roots infected with *H. schachtii* (Fig. S5).

It has also been shown previously that the single mutants had no differences in cell wall sugars compared with wild type (Kanter *et al*., 2005). We have similarly tested the double

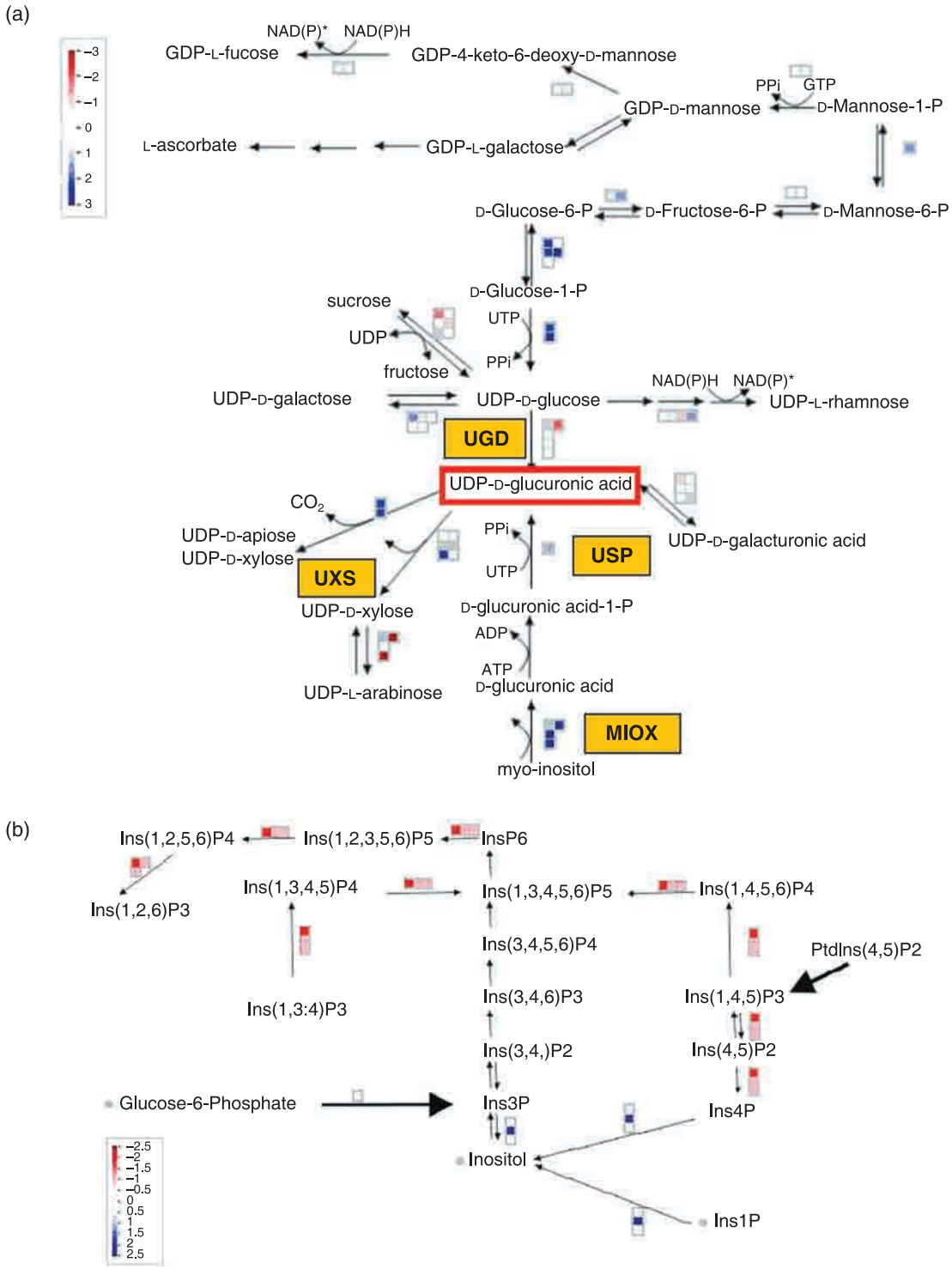

Fig. 3 (a) MAPMAN visualization of expression of genes involved in synthesis of the cell wall precursor UDP-GlcA in syncytia (syncytium vs control root). Red or blue colour indicates downregulation or upregulation at $\log_2$ scale, respectively. Genes whose expression cannot be measured with GeneChips are indicated by grey squares. MIOX, myo-inositol oxygenase; UGD, UDP-glucose dehydrogenase; USP, UDP-sugar pyrophosphorylase; UXS, UDP-xylose synthase. (b) MAPMAN visualization of expression of genes involved in synthesis of myo-inositol (syncytia (5 and 15 days postinfection (dpi) vs control root). Both *IMP* and *IPS* are upregulated, which might lead to accumulation of inositol in the syncytium. Red or blue colour indicates downregulation or upregulation at $\log_2$ scale, respectively. Genes whose expression cannot be measured with GeneChips are indicated by grey squares. IMP, inositol monophosphatase; IPS, inositol phosphate synthase; IP5P, inositol polyphosphatases.

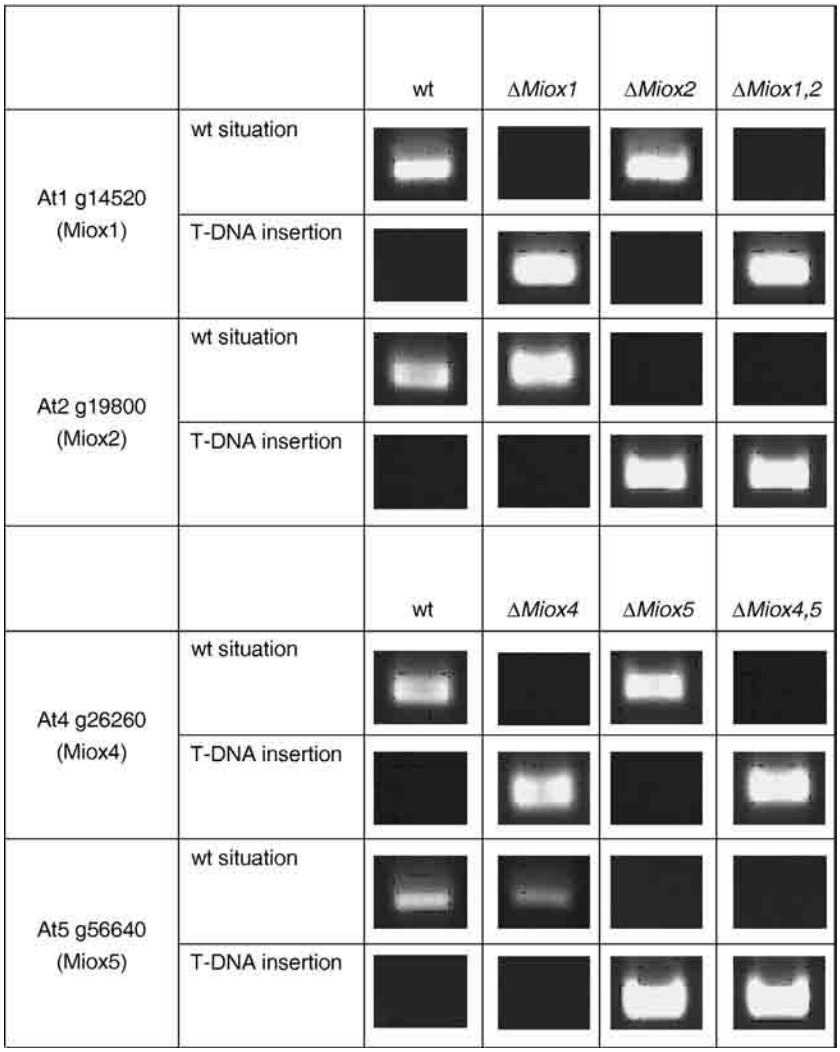

Fig. 4 Genomic DNA of wild-type and knockout lines was PCR amplified using the appropriate primers as introduced in Table 1. Horizontally, the presence or absence of the intact or disrupted wild-type allele in the respective *MIOX* gene loci is shown, while the different plant lines tested are arranged vertically.

Table 4 Expression of *MIOX* genes in Arabidopsis seedlings of double mutants (*miox1+2;* m*iox4+5*) as measured by quantitative real-time reverse transcription polymerase chain reaction (qRT-PCR) relative to the expression of *EF1α*

Locus	Δ*miox1+2* (ΔΔCt($\log_2$) ± SE, *n* = 3)	Δ*miox4+5* (ΔΔCt($\log_2$) ± SE, *n* = 3)	Name
At1g14520	∞	–0.38 ± 0.46	*MIOX1*
At2g19800	∞	0.01 ± 0.01	*MIOX2*
At4g26260	4.65 ± 0.40	∞	*MIOX4*
At5g56640	–2.39 ± 0.23	∞	*MIOX5*

Transcripts were measured from 7-d-old seedlings in double mutants compared with those from the wild type. It was not reasonable to calculate a fold change (indicated as ∞) for *MIOX1* and *MIOX2* in *miox1+2* and *MIOX4* and *MIOX5* in *miox4+5* as the respective transcripts were either absent or at the detection limit.
SE, standard error; *n*, number of biological replicates.

mutants (Fig. 5) but both double mutants again showed no significant differences in cell wall composition compared with the wild type.

Although we did not find any difference between the double mutants and the wild-type plants beyond the expression level of the *MIOX* genes, the strong expression of all *MIOX* genes in syncytia pointed to an important role for myo-inositol oxygenase in syncytium development. In that case, a strong downregulation of *MIOX* genes should severely impair syncytium development and lead to enhanced resistance against

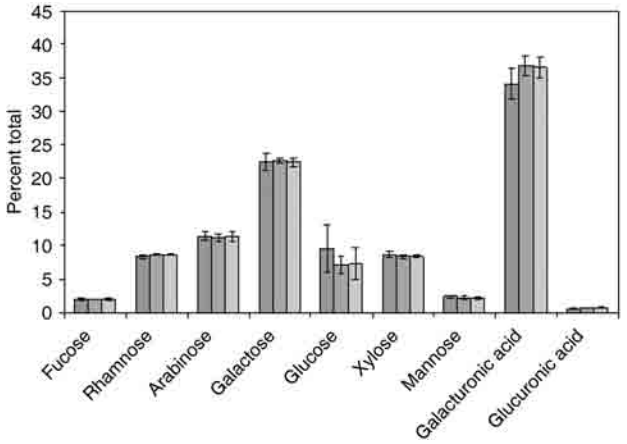

Fig. 5 Cell wall sugars in leaves of 4-wk-old Arabidopsis plants. Cell wall sugars were analysed via high-pressure liquid chromatography (HPLC) on a Dionex ICS 3000 system with a PA 20 column. Dark tinted bars, wild type; mid-tint bars, Δ*miox1+2*; light tinted bars, Δ*miox4+5*. Peak identity was verified with authentic standards. Values are means ± SE, $n = 3$.

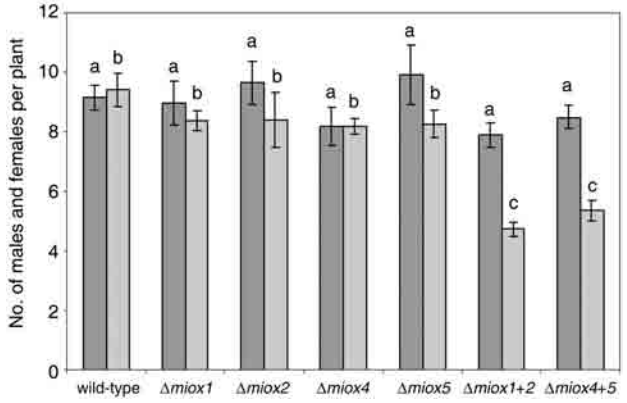

Fig. 6 Infection assay of single and double knockout mutants for *MIOX* genes compared with wild-type Arabidopsis plants. Numbers of males and females were counted at 14 d postinfection (dpi). Columns represent number of males (dark tinted bars) and females (light tinted bars) with letters indicating significant differences ($P < 0.05$; ANOVA and LSD). The statistical significance was determined by three independent replicates. Values are means ± SE, $n = 3$.

H. schachtii. To test this hypothesis, the functional role of the *MIOX* genes in syncytia was evaluated in a nematode infection assay using T-DNA insertion lines. Plants were grown on Knop medium and infected with *H. schachtii* J2 larvae as described in the Materials and Methods section. Two weeks after inoculation, when females and males could be clearly distinguished, the number of males and females was counted. From that, the infection rate per plant and the ratio of males to females was calculated. No significant difference was observed (Fig. 6) between wild-type plants and any of the single mutants (*miox1*, *miox2*, *miox4*, and *miox5*). However, because all four

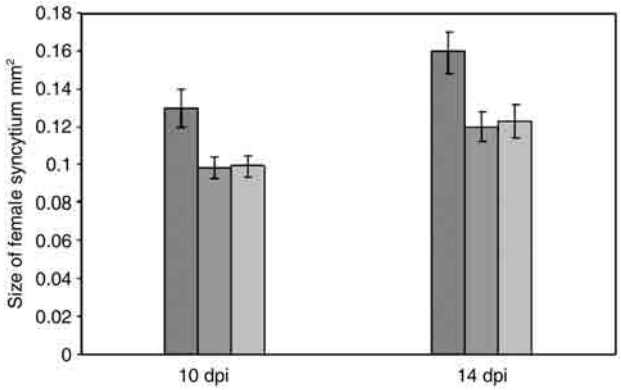

Fig. 7 Size of female syncytia at 10 and 14 d postinfection (dpi). Ten syncytia were selected randomly and their size was determined. Dark tinted bars, wild-type; mid-tint bars, Δ*miox1+2*; light tinted bars, Δ*miox4+5*. Data were analysed for significance difference using ANOVA ($P < 0.05$) and LSD. Values are means ± SE.

MIOX genes were strongly upregulated in syncytia, we reasoned that single mutants might not show a significant effect, because the three remaining genes might compensate for the loss of one gene. Indeed, when we tested the double mutants in the nematode infection assay described above, both double mutants (*miox1+2* and m*iox4+5*) showed a significant reduction ($P < 0.05$) in the number of females per plant compared with the wild type (Fig. 6) while the number of males per plant was not significantly different from the wild type in any of the mutants.

In addition to the number of males and females we measured the size of syncytia at 10 dpi and 14 dpi in the double mutants. Syncytia in the roots of both double mutants were significantly smaller than syncytia in wild-type roots at both time-points (Fig. 7).

Discussion

Expression of MIOX genes in response to nematode infection

Arabidopsis contains a total of four active genes in the *MIOX* gene family, *MIOX1*, *MIOX2*, *MIOX4* and *MIOX5* (*MIOX3* is a pseudogene). According to GeneChip data available at Genevestigator (http://www.genevestigator.ethz.ch; Zimmermann *et al.*, 2004), *MIOX4* and *MIOX5* are only strongly expressed in pollen under normal growth conditions while *MIOX2* is, in addition, expressed in roots and seedlings. The single *USP* gene is expressed in pollen but also in all other tissues. The *UGD* genes are also expressed in almost all tissues but with varying strength (Table S2).

In this paper, we studied the expression of all four *MIOX* genes in syncytia induced by the beet cyst nematode *H. schachtii* in roots of Arabidopsis using different techniques. Three of the four *MIOX* genes are unambiguously represented

on the Affymetrix ATH1 GeneChip (*MIOX1* is also included but the probes for this gene are not specific) and according to our GeneChip data, *MIOX*4 and *MIOX*5 were strongly upregulated in syncytia with barely detectable expression in uninfected roots. The *MIOX2* gene is expressed in control roots but its expression was also eightfold upregulated in syncytia. The GeneChip results were supported by GUS analysis, qPCR and *in situ* RT-PCR. The discrepancy between GeneChip data and qPCR data for *MIOX2* can be attributed to the fact that different syncytium material was used in the two cases. For the transcriptome analysis we used aspirated syncytial cell contents while qPCR analysis was carried out with syncytia that were excised from infected roots and thus contained additional root tissue that would cause a dilution effect in the expression of syncytium specific genes. However, obtaining syncytium material by microaspiration is very time-consuming and was therefore not used for the qRT-PCR analysis. *MIOX4* and *MIOX5* expression was not detected in control roots, which is in agreement with expression data for different Arabidopsis tissues available at Genevestigator (Zimmermann *et al*., 2004) and the expression data provided by Kanter *et al*. (2005).

Expression of *MIOX4* and *MIOX5* in syncytia was also confirmed by promoter::GUS analysis. The expression in roots was generally confined to the syncytium with only a few instances of GUS expression in lateral roots of some *MIOX5*::GUS lines. In addition, *in situ* RT-PCR confirmed a strong expression of all four *MIOX* genes in syncytia while control roots showed weak expression in the central cylinder for *MIOX1* and *MIOX2*, a very weak expression for *MIOX4*, and no expression for *MIOX5*. In conclusion, our expression analysis has shown a strong expression of all four *MIOX* genes in syncytia by a variety of different methods.

Jammes *et al*. (2005) performed a gene expression analysis of galls induced by the root-knot nematode *Meloidogyne incognita* in roots of Arabidopsis. Only two *MIOX* (*MIOX1* and *MIOX5*) genes were included on the microarray that was used in that study and the observed signal intensities were generally much weaker than those reported here. This could be attributed to the fact that they dissected the galls, so that mRNA from giant cells was diluted in the samples by other tissues. Nothing is known about the expression of the other two *MIOX* genes in response to *Meloidogyne* species and it is therefore not clear if the MIOX pathway is also important for gall formation and the development of giant cells.

Ithal *et al*. (2007a) have recently reported the use of Laser Capture Microdissection to collect material for transcriptome analysis of syncytia induced by *H. glycines* in soybean roots. According to the Unigene database (http://www.ncbi.nlm.nih.gov/sites/entrez?db=unigene), there are five known *MIOX* clusters in soybean. Two of these have sequence similarity to *MIOX4* and one each to *MIOX1*, *MIOX2* and *MIOX5* of Arabidopsis (Table S3). Examination of the online supplemental data showed that out of 12 *MIOX* probesets present on the chip (Table S3) one of them was upregulated in syncytia (Gma.3888.2.S1_at) showing that it might play a role in development and maintenance of the syncytium. Although Ithal *et al*. (2007a) annotated the ProbesetID Gma.3888.2.S1_at as representing a gene involved in tRNA processing, Unigene and Affymetrix data identify it as a *MIOX* gene. However, a more detailed study is needed to assess the exact function of this gene. An earlier study by the same authors (Ithal *et al*., 2007b) which used excised syncytia, showed that Gma.17873.1.S1_s_at, which corresponds to the *MIOX2* gene of Arabidopsis, was 20 times upregulated in syncytia compared with controls at 5 dpi.

Characterization of *MIOX* double mutants

The single mutants used to develop the double mutants were characterized by Kanter *et al*. (2005). These authors could not find any phenotypic differences between the single mutants and wild-type Arabidopsis plants. The same is true for the double mutants described in this paper under the growth conditions used. We used qPCR to verify lack of *MIOX* expression in the respective double mutants, This showed that expression of *MIOX1* and *MIOX2* dropped to the detection limit in the *miox1+2* mutant just as did *MIOX4* and *MIOX5* in the *miox4+5* mutant. The increase in *MIOX4* expression that was observed in the *miox1+2* mutant could indicate the possibility that some of the *MIOX* isoforms can replace each other. However, this needs to be further investigated in different tissues.

As UDP-glucuronic acid, the final metabolite of the MIOX pathway, is a precursor for cell wall polysaccharides, we tested the cell wall composition in double mutants. As has been found for single mutants (Kanter *et al*., 2005), we could not find any difference between double mutants and wild-type plants in the cell wall contents for nine different sugars. Furthermore, we looked at the root anatomy of double mutants, either uninfected or infected with *H. schachtii*. Again, there was no difference between the double mutants and the wild type.

MIOX genes are important for syncytium development

To test the importance of the *MIOX* genes for syncytium function, we used a set of *MIOX* T-DNA insertion mutants. As expected, infection of single knock-out mutants compared with wild-type plants showed no significant differences in the number of males and females per plant. This can be explained by the fact that all four *MIOX* genes are strongly expressed in syncytia allowing the other three genes to compensate for the loss of one gene function. By contrast, double mutants showed a significant reduction in the number of females per plant compared with wild-type plants, showing an important role of *MIOX* genes for the development of female nematodes. Both double mutants gave similar results, indicating that a high level of MIOX enzymes is necessary for optimal syncytial

development and function. A poorly developed syncytium will not provide enough nutrients to support the development of an adult female nematode (Müller *et al.*, 1981). In line with this, we found that the size of female syncytia was significantly smaller in both double mutants compared with the wild type. The MIOX level in single mutants seems to be sufficient for normal function of the syncytium. These results also suggest that all four *MIOX* genes have most likely the same function, at least in syncytia. Thus, *MIOX* genes are important for the normal development of syncytia and for the development of female *H. schachtii* nematodes.

All Arabidopsis *MIOX* genes are strongly expressed in pollen in addition to syncytia (Kanter *et al.*, 2005). This is confirmed by publicly available microarray data at Genevestigator (Zimmermann *et al.*, 2004) for *MIOX2*, *MIOX4*, and *MIOX5*. By contrast, *UGD* genes are only expressed at a low level in both tissues, which suggests that UDP-GlcA might be predominantly produced via the MIOX pathway in both tissues and only at a lower level via the UGD pathway. The importance of the MIOX pathway for pollen development is supported by analysis of a knockout mutant in the *USP* gene that does not produce viable pollen (Schnurr *et al.*, 2006; R. Tenhaken, unpublished).

In Arabidopsis, the major central intermediate for precursors of cell-wall polymers is UDP-GlcA based on polymer analysis of cell walls (Zablackis *et al.*, 1995). Myo-inositol oxygenase (MIOX) is generally supposed to play a role in UDP-GlcA synthesis although other roles (e.g. ascorbic acid synthesis) cannot be ruled out. If we assume that the MIOX pathway in syncytia is important for the production of UDP-glucuronic acid and, ultimately, cell-wall polysaccharides – although we cannot exclude other functions of *myo*-inositol oxygenase in syncytia – one might speculate that the alternative UDP-glucose dehydrogenase pathway is for some reason blocked, and that UDP-glucuronic acid has to be produced mainly through the MIOX pathway. This is indeed supported by work on UDP-glucose dehydrogenase from soybean nodules, indicating that this enzyme is subject to feedback inhibition by UDP-xylose, one of the nucleotide sugars produced from UDP-glucuronic acid (Stewart & Copeland, 1998). Biochemical feedback inhibition of the UGD enzymes by UDP-xylose (Hinterberg *et al.*, 2002) is superimposed on the transcriptional control of *UGD* gene expression (Seitz *et al.*, 2000). This mechanism might explain why no explicit changes in the mRNA levels of the *UGD* genes were detected in syncytia. In addition, one of the *UXS* genes is upregulated, hinting at an accumulation of UDP-Xylose, a prerequisite for feedback inhibition of UGDs.

Upregulation of the MIOX pathway would require an increased pool of the substrate *myo*-inositol in syncytia. Indeed, expression analysis of the genes involved in *myo*-inositol synthesis (Table 2, Fig. 3b) showed that there was a slight transcriptional upregulation of *IPS1* (inositol phosphate synthase 1) and *IPS2* and downregulation of *IPSP* (inositol polyphosphatases). Similarly, there was an upregulation of one of the *IMP* (inositol monophosphatase) genes. Dephosphorylation of $Ins(3)P_1$ by IMP is probably the major route to free *myo*-inositol in plants. Smart & Flores (1997) generated transgenic Arabidopis plants overexpressing $Ins(3)P_1$ synthase encoded by a TUR1 cDNA from *Spirodela polyrrhiza* and found these plants to contain elevated $Ins(3)P_1$ synthase activity with a concomitant fourfold increase in endogenous myo-inositol. Recently, Torabinejad *et al.* (2009) have shown that knocking out an *IMP* gene results in decreased levels of myo-inositol (and ascorbic acid) in Arabidopsis.

Osuna *et al.* (2007) have recently shown that *MIOX* genes are induced during carbon starvation (while *IPS1* and *IPS2* are repressed) to scavenge alternative carbon sources. These changes are reversed after the addition of sucrose. This regulation of *MIOX* and *IPS* genes is in agreement with a decreasing amount of myo-inositol during carbon starvation and its gradual recovery after the addition of sucrose. According to these data, the expression of *MIOX* genes might be related to the level of sucrose. However, syncytia have been show to contain high amounts of sucrose (Hofmann *et al.*, 2007) which would rather indicate an induction of *MIOX* genes by sucrose. Thus, the regulation of *MIOX* genes in syncytia might not be simply correlated with the level of sucrose.

Is the MIOX pathway in syncytia involved in ascorbate synthesis?

In plants, ascorbic acid (AsA) biosynthesis proceeds mainly via the GDP-Man pathway (Wheeler *et al.*, 1998) and most of the available data on the AsA biosynthesis pathway are consistent with this hypothesis. However, there is growing evidence indicating the existence of other pathways operating in plants that contribute to the AsA pool. Conversion of methyl-D-galacturonate and D-glucuronolactone to AsA in detached leaves of several plant species (Loewus, 1963) and Arabidopsis cell cultures (Davey *et al.*, 1999) have been shown by tracer and feeding studies. Lorence *et al.* (2004) have recently shown that constitutive expression of *MIOX4* resulted in an elevated level of AsA, suggesting a role for the MIOX pathway in AsA synthesis. Single knockout lines for *MIOX2* and *MIOX5* do not have a lower ascorbate level (Kanter *et al.*, 2005) but this could be explained by the redundancy in the *MIOX* gene family with *MIOX1* and *MIOX2* and *MIOX4* and *MIOX5*, respectively, having a very similar expression pattern (Kanter *et al.*, 2005). However, Endres & Tenhaken (2009) have recently measured the AsA level of two *MIOX4* overexpression lines by high-pressure liquid chromatography (HPLC) and concluded that although *MIOX* controls the levels of inositol in plants, it does not increase AsA.

Degradation of phytate by purple acid phosphatase (*PAP*) results in production of free *myo*-inositol and free Pi which might also lead to AsA synthesis. Recently, it has been shown that overexpression or knockout of a phytase gene (*AtPAP15*)

resulted in an increase or decrease of foliar ascorbic acid levels, respectively (Zhang *et al.*, 2008). However, examination of our transcriptome data showed that there was a downregulation in the expression of *AtPAP15* and only a slight upregulation of *AtPAP13* (Table 2). To further investigate the role of ascorbic acid in syncytium development, it would be important to compare ascorbate and phytate levels in wild-type plants and *MIOX* quadruple mutants in relation to nematode infection.

Conclusion

Our studies have shown that all (four) *MIOX* genes are expressed in syncytia induced by the cyst nematode *H. schachtii* in Arabidopsis. Knocking out pairs of Arabidopsis *MIOX* genes in combination resulted in plants that had smaller syncytia and that could only support a reduced number of female nematodes. To further study the function of the *MIOX* genes it will be important to develop Arabidopsis lines with a significant downregulation of all four *MIOX* genes in syncytia. Such lines would also facilitate study of the role of the MIOX pathway at the biochemical level (such as inositol and ascorbic acid measurements). This approach could potentially lead to the development of engineered nematode-resistant crops in the future. In this regard, it would also be interesting to knock down the *USP* gene in syncytia of Arabidopsis using RNAi as it is not possible to raise homozygous lines because the homozygous state is pollen lethal. The two pollen grains in the pollen tetrad that carry the mutated gene atrophy.

Acknowledgements

We thank Drs Axel Nagel and Björn Usadel for help with the MAPMAN program and Dr Georg Seifert for helpful discussions. We appreciate the excellent technical assistance of Sabine Daxböck-Horvath. This research was supported by grants P16296-B06, P16897-B06, and P20471-B11 of the Austrian Science Fund (FWF). S.S. was supported by Higher education commission (HEC) of Pakistan. D.P.K. gratefully acknowledges support by the Vienna Science and Technology Fund (WWTF), Baxter AG, Austrian Research Centres (ARC) Seibersdorf and the Austrian Centre of Biopharmaceutical Technology (ACBT).

References

Alkharouf NW, Klink VP, Chouikha IB, Beard HS, MacDonald MH, Meyer S, Knap HT, Khan R, Matthews BF. 2006. Timecourse microarray analyses reveal global changes in gene expression of susceptible *Glycine max* (soybean) roots during infection by *Heterodera glycines* (soybean cyst nematode). *Planta* **224**: 838–852.

Bar-Or C, Kapulnik Y, Koltai H. 2005. A broad characterization of the transcriptional profile of the compatible tomato response to the plant parasitic root knot nematode *Meloidogyne javanica*. *European Journal of Plant Pathology* **111**: 181–192.

Clough SJ, Bent AF. 1998. Floral dip: a simplified method for *Agrobacterium*-mediated transformation of *Arabidopsis thaliana*. *Plant Journal* **16**: 735–743.

Davey MW, Gilot C, Persiau G, Ostergaard J, Han Y, Bauw GC, Van Montagu MC. 1999. Ascorbate biosynthesis in *Arabidopsis* cell suspension culture. *Plant Physiology* **121**: 535–543.

Endres S, Tenhaken R. 2009. Myoinositol oxygenase controls the level of myoinositol in Arabidopsis, but does not increase ascorbic acid. *Plant Physiology* **149**: 1042–1049.

Gheysen G, Fenoll C. 2002. Gene expression in nematode feeding sites. *Annual Review of Phytopathology* **40**: 191–219.

Goellner M, Wang X, Davis EL. 2001. Endo-beta-1,4-glucanase expression in compatible plant-nematode interactions. *Plant Cell* **13**: 2241–2255.

Golinowski W, Grundler FMW, Sobczak M. 1996. Changes in the structure of *Arabidopsis thaliana* induced during development of females of the plant parasitic nematode *Heterodera schachtii*. *Protoplasma* **194**: 103–116.

Hinterberg B, Klos C, Tenhaken R. 2002. Recombinant UDP-glucose dehydrogenase from soybean. *Plant Physiology and Biochemistry* **40**: 1011–1017.

Hofmann J, Grundler FMW. 2007. Identification of reference genes for qRT-PCR studies of gene expression in giant cells and syncytia induced in *Arabidopsis thaliana* by *Meloidogyne incognita* and *Heterodera schachtii*. *Nematology* **9**: 317–323.

Hofmann J, Wieczorek K, Blöchl A, Grundler FMW. 2007. Sucrose supply to nematode-induced syncytia depends on the apoplasmic and symplasmic pathways. *Journal of Experimental Botany* **58**: 1591–1601.

Hussey RS, Grundler FM. 1998. Nematode parasitism of plants. In: Perry RN, Wright DJ, eds. *Physiology and biochemistry of free-living and plant-parasitic nematodes*. Wallingford, UK: CAB International, 213–243.

Ithal N, Recknor J, Nettleton D, Hearne L, Maier T, Baum TJ, Mitchum MG. 2007b. Parallel genome-wide expression profiling of host and pathogen during soybean cyst nematode infection of soybean. *Molecular Plant–Microbe Interactions* **20**: 293–305.

Ithal N, Recknor J, Nettleton D, Maier T, Baum TJ, Mitchum MG. 2007a. Developmental transcript profiling of cyst nematode feeding cells in soybean roots. *Molecular Plant–Microbe Interactions* **20**: 510–525.

Jammes F, Lecomte P, Almeida-Engler J, Bitton F, Martin-Magniette ML, Renou JP, Abad P, Favery B. 2005. Genome-wide expression profiling of the host response to root-knot nematode infection in Arabidopsis. *Plant Journal* **44**: 447–458.

Jones MGK, Northcote DH. 1972. Nematode-induced syncytium-A multinucleate transfer cell. *Journal of Cell Science* **10**: 789–809.

Jones MGK, Payne HL. 1978. Early stages of nematode-induced giant-cell formation in roots of *Impatiens balsamina*. *Journal of Nematology* **10**: 70–84.

Kanter U, Usadel B, Guerineau F, Li Y, Pauly M, Tenhaken R. 2005. The inositol oxygenase gene family of Arabidopsis is involved in the biosynthesis of nucleotide sugar precursors for cell-wall matrix polysaccharides. *Planta* **221**: 243–254.

Klinghammer M, Tenhaken R. 2007. Genome-wide analysis of the UDP-glucose dehydrogenase gene family in Arabidopsis, a key enzyme for matrix polysaccharides in cell walls. *Journal of Experimental Botany* **58**: 3609–3621.

Klink VP, Overall CC, Alkharouf NW, MacDonald MH, Matthews BF. 2007. Laser capture microdissection (LCM) and comparative microarray expression analysis of syncytial cells isolated from incompatible and compatible soybean (*Glycine max*) roots infected by the soybean cyst nematode (*Heterodera glycines*). *Planta* **226**: 1389–1409.

Koltai H, Bird DM. 2000. High throughput cellular localization of specific plant mRNAs by liquid-phase *in situ* reverse transcription polymerase chain reaction of tissue sections. *Plant Physiology* **123**: 1203–1212.

Loewus FA. 1963. Tracer studies on ascorbic acid formation in plants. *Phytochemistry* **2**: 109–128.

Lorence A, Chevone BI, Mendes P, Nessler CL. 2004. Myo-inositol oxygenase offers a possible entry point into plant ascorbate biosynthesis. *Plant Physiology* **134**: 1200–1205.

Müller J, Rehbock K, Wyss U. 1981. Growth of *Heterodera schachtii* with remarks on amounts of food consumed. *Revue Nématologie* **4**: 227–234.

Niebel A, De Almeida EJ, Hemerly A, Ferreira P, Inze D, Van Montagu M, Gheysen G. 1996. Induction of cdc2a and cyc1At expression in *Arabidopsis thaliana* during early phases of nematode-induced feeding cell formation. *Plant Journal* **10**: 1037–1043.

Murashige T, Skoog F. 1962. A revised medium for rapid growth and bioassays with tobacco tissue cultures. *Physiol Plant* **15**: 473–497.

Osuna D, Usadel B, Morcuende R, Gibon Y, Blasing OE, Hohne M, Gunter M, Kamlage B, Trethewey R, Scheible WR *et al.* 2007. Temporal responses of transcripts, enzyme activities and metabolites after adding sucrose to carbon-deprived Arabidopsis seedlings. *Plant Journal* **49**: 463–491.

Sasser JN, Freckman DW. 1987. A world perspective on Nematology: the role of the society. In: Veech JA, Dickson DW, eds. *Vistas on nematology*. Hyatssville, MD, USA: Society of Nematologists, 7–14.

Schnurr JA, Storey KK, Jung HJ, Somers DA, Gronwald JW. 2006. UDP-sugar pyrophosphorylase is essential for pollen development in Arabidopsis. *Planta* **224**: 520–532.

Seifert GJ. 2004. Nucleotide sugar interconversions and cell wall biosynthesis: how to bring the inside to the outside. *Current Opinion in Plant Biology* **7**: 277–284.

Seitz B, Klos C, Wurm M, Tenhaken R. 2000. Matrix polysaccharide precursors in Arabidopsis cell walls are synthesized by alternate pathways with organ-specific expression patterns. *Plant Journal* **21**: 537–546.

Sijmons PC, Grundler FMW, von Mende N, Burrows PR, Wyss U. 1991. *Arabidopsis thaliana* as a new model host for plant-parasitic nematodes. *Plant Journal* **1**: 245–254.

Smart CC, Flores S. 1997. Overexpression of D-myo-inositol-3-phosphate synthase leads to elevated levels of inositol in Arabidopsis. *Plant Molecular Biology* **33**: 811–820.

Sobczak M, Golinowski W, Grundler FMW. 1997. Changes in the structure of *Arabidopsis thaliana* roots induced during development of males of the plant parasitic nematode *Heterodera schachtii*. *European Journal of Plant Pathology* **103**: 113–124.

Stewart DC, Copeland L. 1998. Uridine 5′-diphosphate-glucose dehydrogenase from soybean nodules. *Plant Physiology* **116**: 349–355.

Szakasits D, Heinen P, Wieczorek K, Hofmann J, Wagner F, Kreil DP, Sykacek P, Grundler FMW, Bohlmann H. 2009. The transcriptome of syncytia induced by the cyst nematode *Heterodera schachtii* in Arabidopsis roots. *Plant Journal* **57**: 771–784

Thimm O, Blasing O, Gibon Y, Nagel A, Meyer S, Kruger P, Selbig J, Muller LA, Rhee SY, Stitt M. 2004. MAPMAN: a user-driven tool to display genomics data sets onto diagrams of metabolic pathways and other biological processes. *Plant Journal* **37**: 914–939.

Torabinejad J, Donahue JL, Gunesekera BN, Allen-Daniels MJ, Gillaspy GE. 2009. VTC4 is a bifunctional enzyme that impacts myo-inositol and ascorbate biosynthesis in plants. *Plant Physiology* **150**: 951–961.

Urbanczyk-Wochniak E, Filipecki M, Przybecki Z. 2002. A useful protocol for in situ RT-PCR on plant tissues. *Cellular and Molecular Biology Letters* **7**: 7–18.

Wheeler GL, Jones MA, Smirnoff N. 1998. The biosynthetic pathway of vitamin C in higher plants. *Nature* **393**: 365–369.

Wieczorek K, Golecki B, Gerdes L, Heinen P, Szakasits D, Durachko DM, Cosgrove DJ, Kreil DP, Puzio PS, Bohlmann H *et al.* 2006. Expansins are involved in the formation of nematode-induced syncytia in roots of *Arabidopsis thaliana*. *Plant Journal* **48**: 98–112.

Wieczorek K, Hofmann J, Blöchl A, Szakasits D, Bohlmann H, Grundler FM. 2008. Arabidopsis endo-1,4-beta-glucanases are involved in the formation of root syncytia induced by *Heterodera schachtii*. *Plant Journal* **53**: 336–351.

Wyss U, Grundler FMW. 1992. Feeding behaviour of sedentary plant parasitic nematodes. *Netherlands Journal of Phytopathology* **98**: 165–173.

Zablackis E, Huang J, Muller B, Darvill AG, Albersheim P. 1995. Characterization of the cell-wall polysaccharides of *Arabidopsis thaliana* leaves. *Plant Physiology* **107**: 1129–1138.

Zhang W, Gruszewski HA, Chevone BI, Nessler CL. 2008. An Arabidopsis purple acid phosphatase with phytase activity increases foliar ascorbate. *Plant Physiology* **146**: 431–440.

Zimmermann P, Hirsch-Hoffmann M, Hennig L, Gruissem W. 2004. GENEVESTIGATOR. Arabidopsis microarray database and analysis toolbox. *Plant Physiology* **136**: 2621–2632.

Supporting Information

Additional supporting information may be found on the following web page accompanying the article (http://bioinf.boku.ac.at/pub/Siddique2008/).

Fig. S1 The MA plot (syncytium vs root) for 71 genes involved in UDP-GlcA and myo-inositol metabolism.

Fig. S2 The MA plot (5 dpi syncytium vs 15 dpi syncytium) for 71 genes involved in UDP-GlcA and myo-inositol metabolism.

Fig. S3 *MIOX4*::GUS expression in uninfected Arabidopsis lines.

Fig. S4 *MIOX5*::GUS expression in uninfected Arabidopsis lines.

Fig. S5 Anatomy of root sections of wild-type and double mutants (Δ*miox1+2*; Δ*miox4+5*)

Table S1 Provides normalized expression values for 71 genes involved in UDP-GlcA and myo-inositol metabolism (http://bioinf.boku.ac.at/pub/Siddique2008/sub.data_rounded.txt)

Table S2 Relative expression of *MIOX, UGD* and *USP* genes according to GENEVESTIGATOR (http://www.genevestigator.ethz.ch)

Table S3 GeneChip expression profiles of *MIOX* transcripts in syncytia induced by *Heterodera glycines* in soybean

Please note: Wiley-Blackwell are not responsible for the content or functionality of any supporting information supplied by the authors. Any queries should be directed to the corresponding author.

CHAPTER 6

An Improved pPZP Vector for Agrobacterium-mediated Plant Transformation

Szakasits, D., Siddique, S. and Bohlmann, H.

.

Plant molecular biology reporter (2007) 25:115-120.

Plant Mol Biol Rep
DOI 10.1007/s11105-007-0013-4

An Improved pPZP Vector for *Agrobacterium*-mediated Plant Transformation

Dagmar Szakasits · Shahid Siddique · Holger Bohlmann

Abstract We report a new and improved pPZP vector (pPZP3425) for efficient plant transformation. This vector is derived from the widely used pPZP100 series of binary *Agrobacterium* vectors. One disadvantage of these vectors is the use of chloramphenicol resistance for selection in *Escherichia coli* and Agrobacteria. We have therefore included a kanamycin resistance gene for selection in *Agrobacterium*. Furthermore, the strong 35S CaMV promoter driving the plant resistance gene has been replaced by the weaker *nos* promoter because it has been shown that the 35S promoter driving the plant resistance marker can lead to ectopic expression of the transgene. During replacement of the 35S promoter, the NcoI site within the plant resistance gene has been removed, and NcoI can now be used for cloning purposes within the expression cassette which consists of an intron-containing *gus* gene driven by a strong constitutive promoter (35S promoter with doubled enhancer plus omega-element as translational enhancer). Thus, a single vector can conveniently be used for two purposes: (1) for overexpression of proteins by replacing the *gus* gene by the coding sequence of choice and (2) for creation of promoter:*gus* fusions by substituting the constitutive promoter by any other promoter. We demonstrate the usefulness of this vector for cloning a promoter:*gus* fusion and in planta transformation of Arabidopsis.

Keywords *Agrobacterium tumefaciens* · *Arabidopsis thaliana* · Binary vector · Chloramphenicol · Kanamycin · Plant transformation

D. Szakasits · S. Siddique · H. Bohlmann (✉)
Institute of Plant Protection, Department of Applied Plant Sciences and Plant Biotechnology,
University of Natural Resources and Applied Life Sciences,
Peter-Jordan-Str. 82, 1190 Vienna, Austria
e-mail: holger.bohlmann@boku.ac.at

Introduction

Agrobacterium tumefaciens is able to transform a variety of plant and fungal species by transferring its T-DNA into the host cell. The use of this transformation system has benefited very much from the development of binary vectors such as pBIN19 (Bevan 1984). This once very popular vector has now been largely replaced by a variety of different vector systems. One widely used group of vectors is the pPZP vectors (Hajdukiewicz et al. 1994). They are smaller and have a higher copy number as compared to pBIN19. However, the CaMV 35S promoter to drive the plant selectable marker is problematic, as it has been shown that the 35S promoter can affect the expression of the transgene (Yang et al. 2005; Yoo et al. 2005). Furthermore, chloramphenicol is used as a selectable marker for *Escherichia coli* and Agrobacteria in the pPZP100 series, but many *Agrobacterium* strains (including C58 and its derivative GV3101 which is routinely used for Arabidopsis transformation) have an inducible resistance mechanism against this antibiotic (Rogers et al. 2002; Tennigkeit and Matzura 1991). Additionally, the *Nco*I restriction site between 35S promoter and plant selectable marker excluded the use of this enzyme in the expression cassette. *Nco*I is one of a few enzymes that contain the ATG start codon in the recognition sequence, and can therefore conveniently be used to connect promoters and coding sequences. For all these reasons, we decided to construct an improved pPZP vector without these limitations. Furthermore, we inserted a *gus*-intron reporter driven by a strong constitutive promoter to create a vector which could be used for two applications: for promoter:*gus* fusions and for the overexpression of genes.

Materials and Methods

Construction of pPZP3425

The 35S promoter of the vector pPZP111 (Hajdukiewicz et al. 1994) was replaced by a *nos* promoter which also removed the *Nco*I site. We digested the vector pPZP111 with the two restriction enzymes *Nco*I and *Bst*XI and the large vector fragment corresponding to the vector without the 35S promoter was isolated from an agarose gel. The *nos* promoter was amplified by polymerase chain reaction (PCR) from the vector pPE13 (Epple et al. 1997) with the primer pNOSfor [5′-tgttcaatcatgagaaacgatccagatc-3′] to introduce a new *Bsp*HI restriction site and pNOSrev [5′-gaaacgaccaccatgttgggagcggagaat-3′] to replace the *Bsp*HI restriction site with a *Bst*XI site. The PCR fragment was cut with *Bsp*HI and *Bst*XI and ligated into the vector backbone from pPZP111 to yield the intermediate vector pPZP141. Sequencing confirmed the replacement of the *Nco*I site by the *Bsp*HI site and the presence of the *nos* promoter.

Next, we removed the *Bam*HI site in the MCS of the pPZP141 clone by digestion with *Bam*HI and filling up with Klenow enzyme. After purification and religation, the vector was transformed into *E. coli* and selected on chloramphenicol plates (25 μg/ml) to yield pPZP142. We introduced the high-level constitutive promoter of the expression vector pPE14 which has already been used successfully (Epple et al.

1997). For that, we transferred the complete expression cassette from the vector pPE14 (including thionin cDNA and *nos* terminator) into pPZP142 using *Hin*dIII. After transformation into *E. coli* and selection via chloramphenicol, we also checked the orientation of the cassette via digestion at the *Eco*RI site (within the pPZP backbone sequence) and *Bam*HI (within the cassette). The resulting intermediate vector pPZP1424 was digested with *Nco*I and *Bam*HI to substitute the thionin cDNA with the intron containing *uidA* gene derived from the pSH4GUS vector (Holtorf et al. 1995) which was cut with the same restriction enzymes. The intermediate vector pPZP1425 was again confirmed by sequencing.

Finally, we introduced the kanamycin resistance gene from pBIN19. The gene was amplified with the primers KAN_Rfor (5′-cagcatcatgcataattgtggtttca-3′) and KAN_Rrev (5′-gttgcgatgcatctaggtactaaaacaat-3′), which each introduced a Mph1103I restriction site. The PCR fragment was cut with Mph1103I and introduced into the single Mph1103I site of the pPZP backbone. The transformation into *E. coli* was now selected on medium containing kanamycin (50 μg/ml) and yielded positive clones of the final vector pPZP3425 shown in Fig. 1.

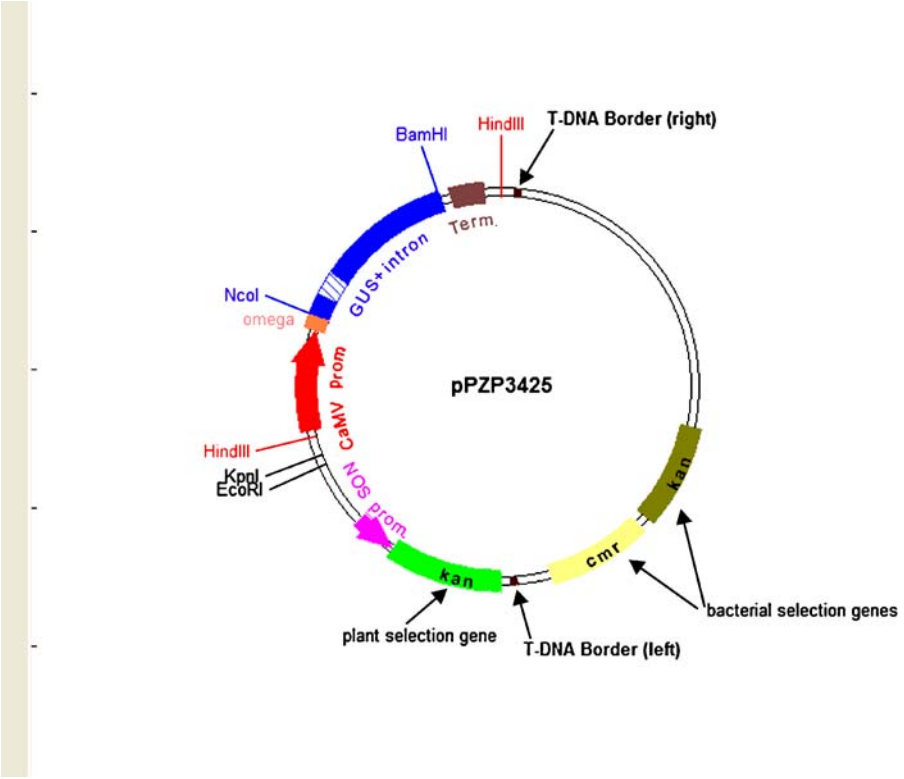

Fig. 1 Scheme of the new binary cloning vector pPZP3425

Fig. 2 **a** Selection plate containing transformed Arabidopsis seeds on MS medium supplemented with kanamycin. **b** GUS staining of the kanamycin-resistant seedlings from **a**

Cloning of At5g05340promoter: Gus Fusion

The vector pPZP3425 was digested with the restriction enzymes *Kpn*I and *Nco*I to cut out the constitutive CaMV promoter. The vector backbone was isolated from a 1% agarose gel. The promoter sequence (800 pb) of At5g05340 was amplified by using the following primer pair: At5g05340for (5′-caaaccttgggtaccaacaa-3′) containing a *Kpn*I restriction site and At5g05340rev (5′-gtatcaatgataaagccatggcgata-3′) containing an *Nco*I site. The PCR product was digested with *Kpn*I and *Nco*I and inserted upstream of the *uidA* gene into the purified backbone of pPZP3425. One isolate containing an insert for the predicted size was confirmed by sequencing and was transformed into *A. tumefaciens* strain GV3101.

Arabidopsis Transformation and Histochemical Assay

Arabidopsis plants (Columbia) where grown in short day conditions at 23°C and induced to flowering by shifting to long day conditions (16:8 h). Transformation was performed as described by Vignutelli et al. (1998), and transformants were selected on Murashige and Skoog (MS) agar including kanamycin (30 μg/ml) and timentin (250 μg/ml) to prevent bacterial overgrowth. After approximately 2 weeks, GUS staining of the putative transgenic seedlings was conducted essentially as described earlier (Jefferson et al. 1987).

Results and Discussion

The vector pPZP3425 (Fig. 1) provides an expression cassette consisting of an intron containing *gus* gene driven by a strong constitutive promoter. This vector can be used for two applications: for the overexpression of proteins, the *gus* gene is replaced by the coding sequence of choice, and for promoter:*gus* fusions, the constitutive promoter is substituted by the promoter of choice. pPZP3425 is a derivative of the pPZP100 series of binary vectors (Hajdukiewicz et al. 1994), but has several improvements. The strong 35S CaMV promoter driving the plant resistance gene has been replaced by the weaker *nos* promoter because it has been shown that the 35S promoter driving the plant resistance marker can lead to ectopic expression of the transgene (Yang et al. 2005; Yoo et al. 2005). During replacement of the 35S promoter, the *Nco*I site within the plant resistance gene has been removed, and *Nco*I can now be used for cloning purposes within the expression cassette. As discussed in the "Introduction", chloramphenicol selection is not possible with many *Agrobacterium* strains (Rogers et al. 2002; Tennigkeit and Matzura 1991). We have therefore included a kanamycin resistance gene for selection in *Agrobacterium*. Finally, we have introduced an expression cassette consisting of an intron-containing *gus* gene driven by a strong constitutive promoter (35S promoter with doubled enhancer plus omega-element as translational enhancer). The designation of the new pPZP vector follows that for the original pPZP vectors with pPZP3xxx now indicating that the bacterial resistance is based on kanamycin and pPZPx4xx indicating plant selectable kanamycin resistance driven by the *nos* promoter.

The vector pPZP3425 is routinely used in our lab for both applications, and we have already produced dozens of transgenic Arabidopsis lines via the in planta transformation method with some alterations (Bechtold et al. 1993; Vignutelli et al. 1998) using the *Agrobacterium* strain GV3101. We usually obtain at least approximately ten transformants per plant. An example containing a promoter:*gus* fusion for the gene At5g05340 is shown in Fig. 2. From approximately 100 seeds that were plated on kanamycin containing MS medium, two seedlings survived (Fig. 2a) and both stained positive for GUS (Fig. 2b).

It should be mentioned that although the vector does not contain extensive multi-cloning sites, we have always been able to clone the desired constructs using the available restriction sites. If the promoter or the coding sequence that is to be cloned contains an restriction site that is used in the vector (*Kpn*I or *Eco*rRI, *Nco*I, *Bam*HI), it is usually possible to select an enzyme that provides cohesive ends which are compatible with the enzyme used in the vector. *Nco*I for instance is producing cohesive ends that are compatible with those produced by *Bsp*HI, *Fat*I, and *Pci*I.

Acknowledgments The authors thank the Austrian Science Fund (FWF) for the financial support for this research project under grant number P16296-B06. We also thank Sabine Daxböck-Horvath and Sabrina Köllner for their assistance in the lab.

References

Bechtold N, Ellis J, Pelletier G. In planta *Agrobacterium*-mediated gene transfer by infiltration of adult *Arabidopsis thaliana* plants. C R Acad Sci Paris Life Sci 1993;316:1194–9.

Bevan M. Binary *Agrobacterium* vectors for plant transformation. Nucleic Acids Res 1984;12:8711–21.

Epple P, Apel K, Bohlmann H. Overexpression of an endogenous thionin enhances resistance of Arabidopsis against *Fusarium oxysporum*. Plant Cell 1997;9:509–20.

Hajdukiewicz P, Svab Z, Maliga P. The small versatile pPZP family of *Agrobacterium* binary vectors for plant transformation. Plant Mol Biol 1994;25:989–94.

Holtorf S, Apel K, Bohlmann H. Comparison of different constitutive and inducible promoters for the overexpression of transgenes in *Arabidopsis thaliana*. Plant Mol Biol 1995;29:637–46.

Jefferson RA, Kavanagh TA, Bevan MW. Related Articles, links GUS fusions: beta-glucuronidase as a sensitive and versatile gene fusion marker in higher plants. EMBO J 1987;6:3901–7.

Rogers EJ, Rahman MS, Hill RT, Lovett PS. The chloramphenicol-inducible catB gene in *Agrobacterium tumefaciens* is regulated by translation attenuation. J Bacteriol 2002;15:4296–300.

Tennigkeit J, Matzura H. Nucleotide sequence analysis of a chloramphenicol-resistance determinant from *Agrobacterium tumefaciens* and identification of its gene product. Gene 1991;89:113–6.

Vignutelli A, Wasternack C, Apel K, Bohlmann H. Systemic and local induction of an Arabidopsis thionin gene by wounding and pathogens. Plant J 1998a;14:285–95.

Yang W, Jefferson RA, Huttner E, Moore JM, Gagliano WB, Grossniklaus U. An egg apparatus-specific enhancer of Arabidopsis, identified by enhancer detection. Plant Physiol 2005;139:1421–32.

Yoo SY, Bomblies K, Yoo SK, Yang JW, Choi MS, Lee JS, et al. The 35S promoter used in a selectable marker gene of a plant transformation vector affects the expression of the transgene. Planta 2005;221:523–30.

CHAPTER 7

Summary and final Conclusions

Plant-parasitic nematodes mainly attack the root organ and cause disease by decreasing the water and nutrient absorbing area by malforming the vital organ. The major purpose of this thesis was to investigate gene expression in the feeding site of the cyst nematode *H. schachtii*, one of the most severe pathogens of crop plants worldwide, at a global level via GeneChip technology by specifically extracting pure infected cell material taken from infected roots of the model plant *Arabidopsis thaliana.*

When the J2 larva selects via its stylet a competent single cell within the vascular cylinder of the root it triggers the development of a syncytium that enlarges by means of hypertrophy of syncytial elements and incorporation of up to hundreds of adjacent cells. This NFS formation involves a series of cellular and subcellular changes including morphological and gene expression modifications so that the highly active syncytium serves the nutrient demands of the nematode being totally dependent on its host during its (mainly) sessile developmental stages. For a thorough analysis we put main emphasis on isolating pure syncytial material for our experiments, i.e. in contrast to previous gene expression studies on NFS in Arabidopsis we did not include any tissue outside the feeding cells. To this end, we enabled microaspiration (inverse microinjection) as a technique to accurately pierce the small transparent Arabidopsis roots under a light microscope and suck the cell content of syncytia in order to rule out confounding effects due to dilution or systemic expression in the plant when extracting RNA. In order to get insight to the time course of nematode infection, we collected samples at several time points after infection, i.e. as soon as 3 days past infection when the syncytium has reached a dealable size, at 5 dpi when the enlargement is ongoing, at 15 dpi when the syncytium has reached its maximum size and finally at 21 dpi. Due to an analogous size problem with the ISC we considered root segments cut from the elongation zone from 12-day-old uninfected plants (0 dpi) as most convenient control for RNA extraction; i.e. without any root tips or lateral root primordia. Among the diverse platforms available on the market we

chose the most current chip ATH1 (a 25mer oligonucleotide microarray covering the majority of the Arabidopsis genome) from Affymetrix, one of the first commercial microarray companies whose GeneChip technology became the most popular platform for genome-wide expression profiling, for hybridization that was performed in collaboration with the RZPD, the German Resource Center for Genome Research (Berlin, Germany, a non-profit service center for genomics and proteomics research).
We hybridized in total 11 chips, four chips for 5 dpi and control samples each and three technical replicates for 15 dpi; however, the extracted RNA of 3 dpi and 21 dpi samples was only sufficient for one and two hybridizations, respectively, and thus these time points both were excluded from our further analyses. The hybridization data were processed in several ways by employing two software tools. On the one hand, the Affymetrix CEL files were processed via the commercial GeneSpring software package that includes several clustering tools such as for example PCA. On the other hand, detailed analytical procedures were carried out in cooperation with the Department of Biotechnology at our university by using the freely distributed and frequently recommended Bioconductor suite with its wide range of powerful statistical applications. Together with the most current release (v8) of TAIR's probe-set annotation available we were able to monitor the expression of 21,138 Arabidopsis genes over time during nematode infection.
However, it turned out, that at a global view the expression profiles did not differ greatly between 5 and 15 dpi samples and they therefore were not treated as a time serious but taken together for pairwise comparisons with control roots. This analysis revealed the transcriptome of syncytia to be very modified because a total of 7,231 genes, corresponding to 34.2 %, were differentially expressed (for a FDR cut-off of $q < 5$ %), whereof 3,893 genes, i.e. 18.4 %, had a higher expression level and the remaining 3,338 genes, i.e. 15.8 %, had a lower expression level as compared to controls. For the detection of potential candidate genes that are supposed to be required or at least contributing to any biological differences between compared conditions with differential expression we prepared two lists encompassing 100 genes that have the strongest increase and decrease of syncytial expression level, respectively. Among these upregulated genes we found several coding for proteins with a putative cell wall-modulating function such as pectate lyase family proteins and expansins (e.g. *AtEXPA6* with a M value of $2^{5.9}$ corresponding to ~ 62fold upregulagtion).

To characterize the nature of the regulatory changes, we employed a gene ontology (as an international standard to annotate functions) analysis by looking at the preferential regulation in a collection of gene ontology categories that were selected with regard to syncytial relevance, i.e. related to metabolic activity and to response to external stimuli. In GO categories such as ‘defense response’ and responses to chemical and hormone stimulus within the main domain ‘biological process’, downregulation was significantly over-represented, which may suggest an active suppression of defense response by the nematode. On the other hand, unsurprisingly, we found significantly more genes upregulated than downregulated for GO categories like ‘translation’, ‘biosynthetic process’, ‘cellular biosynthetic process’, ‘cellular metabolic process’ etc.; similarly, within the GO domain ‘cellular component’ genes of the categories ‘ribosome’ and ‘chromosome’ e.g. were preferentially upregulated, which are all together clear trends reflecting the high metabolic activity imposed on NFS.

When we investigated the tissue-specific expression of the subset of 100 most strongly induced genes by consulting the publicly available reference expression database of Genevestigator we noted that under natural conditions several genes are only specifically expressed in reproductive organs like seeds (e.g. the plant defensine gene *Pdf2.1*) or pollen, both of them being important sinks for the plant, similar to the NFS. Examples for the pollen-specific transcription are the two *myo*-inositol oxygenase (*MIOX)* genes *MIOX4* and *MIOX5*, the latter representing the highest measured induction ($2^{8,8}$ i.e. ~ 446fold) coupled with a high rank of differential expression.

For a more global comparison of the whole syncytial transcriptome with the transcriptome of other tissue types of roots and also of other Arabidopsis organs (flower, leaf, pollen, root and seed) we further performed a PCA analysis (for a total of 185 Affymetrix.CEL files including samples from other studies) by reducing the data into two dimensions for better visualization of global trends. While the transcriptome of our root control samples clustered together with the transcriptomes of all other types of root tissues, the transcriptome of the syncytial samples were clearly distinct from them (which agrees with the global expression differences (34.2 % in total) between syncytia and the controls), as well as from all other organs. This therefore indicates that a syncytium, through its formation within the root organ,

shows a characteristic expression profile that is different from that of any other organ including root.

To improve the limited knowledge about the processes occurring within the syncytial call wall that undergoes intense morphological changes during feeding site development - local cell wall dissolutions inside the enlarging syncytium on the one hand and development of cell wall ingrowths and thickening of outer cell walls on the other hand - we focussed on expression profiles of cell wall-related genes supposed to be involved in the formation and maintenance of syncytia; i.e. genes belonging to the two relatively large gene families of expansins (26 α- and five to six β-expansins depending on the *A.t.* ecotype) and endo-1,4-β-glucanase (25 members) genes that are coding for primary and secondary cell wall modulating agents, respectively.
Expansins are extracellular cell wall-loosening proteins that induce long-term, irreversible extension (creep) of plant cell walls in a pH-dependent manner and are supposed to function in plant cell growth and wall disassembly control and thus probably play a role in NFS formation as well. In concordance with results of diverse other approaches such as semi-quantitative RT-PCR and histochemical techniques using promoter:*gus* lines and *in situ* RT-PCR, the chip data showed in pairwise contrasts out of ten pre-screened syncytial expressed expansin genes (in a cDNA library from microaspirated 5–7-dpi syncytia) the following six genes to be significantly upregulated in syncytia (5 dpi and/or 15 dpi) as compared to non-infected root tissue: *AtEXPA3, AtEXPA6, AtEXPA8, AtEXPA10, AtEXPA16* and also *AtEXPB3*, that, however, was also found to be transcribed in tissue surrounding the syncytia in contrast to the α-expansin genes; remarkably, among them *AtEXPA3* and *AtEXPA16* are shoot-specifically expressed in uninfected plants. An opposite expression pattern of a highly significant down-regulation at both syncytial time points in comparison to control roots was found in case of the two α-expansin genes *AtEXPA7* and *AtEXPA18.*
Analogously, inspecting the expression values of all 23 endo-1,4-β-glucanase genes represented on the GeneChip at the three times points of infection (control - 0 dpi, 5 dpi and 15 dpi) via pairwise tests comparing two conditions each, revealed again a mixed expression pattern within the gene family. *KOR*, *KOR2* and *At1g48930* were found to be highly significantly down-regulated at both infection time points, whereas

the two genes *AtCel2* (coding for a secreted enzyme) and *KOR3* (coding for a membrane-bound protein) were the only ones showing strong induction in comparison to the control (fold change ratios of $2^{3,25}$ – $2^{4,12}$). These two syncytial highly up-regulated genes that are usually shoot specifically expressed were selected as candidates for detailed further analyses beyond expression profiling, i.e. investigating their functional role by including *in silico* promoter analyses, sucrose and hormone treatments, measurements of the hemicellulose content in syncytia and infection tests with T-DNA mutants that resulted in an impairment of the growth conditions for nematodes.

Finally, we demonstrated a highly diverse altered expression pattern of expansin genes transcribed within the syncytium, implicating (some) family members to be involved in call-wall-reorganization as response to cyst nematode infection. Similarly, an altered expression profile was shown for genes belonging to the second gene family coding for EGases and we thus conclude that our experiments show strong evidence that endo-1,4-β-glucanase genes are involved in syncytium development and maintenance.

The function of *MIOX* gene family is not yet totally known, however, they are probably involved in the production of UDP-glucuronic acid (UDP-GlcA), an important precursor for cell wall polysaccharides, which indicates an involvement of *MIOX* genes in cell wall biosynthesis. In Arabidopsis there are four *MIOX* genes, i.e. *MIOX1, MIOX2, MIOX4, MIOX5 (MIOX3* being a pseudogene) encoding the enzyme *myo*-inositol oxygenase. All of them represented on the GeneChip (except *MIOX1* due to its ambiguous probe sets) turned out to be upregulated, including the relatively weaker induced *MIOX2* that is also expressed in pollen like *MIOX4* and *MIOX5* which were among the 100 most strongly upregulated genes. After validation of the chip data by GUS analysis and qRT-PCRs the potential role of the induced *MIOX* genes for syncytium formation was evaluated by an infection assay, where double mutants (Δ*miox1+2* and *miox4+5)* resulted in a significant reduced number of females per plant.

Hence, all three investigated gene families (expansin, EGases and *MIOX* genes) and their encoded proteins and enzymes are supposed to function in syncytial cell wall assembly and disassembly processes.

For taking further steps towards functional genomics with our host genes of interest we considered *Agrobacterium*-mediated genetic transformation, the most widely used means for the production of genetically modified plants, a useful technique of reverse genetics. The T-DNA binary systems where the 'disarmed' T-DNA region (without tumor genes) and the virulence (*vir) genes* are split on two separate plasmids (on the 'binary vector' and 'helper plasmid', repectively) have greatly simplified the manipulation of *Agrobacterium,* that is naturally able to transfer its T-DNA into numerous plant species, since theoretically any sequence of interest can be introduced between the left and the right T-DNA border. A variety of both, vectors and disarmed *Agrobacterium vir* helper strains have become more sophisticated over the years, however, several commonly used binary vectors such as pBIN19 and the pPZP series are still suffering from some deficiencies. Therefore, we have developed an improved vector called 'pPZP3425' on the basis of the pPZP family that is widely used because of the relative small size and stable maintenance of their T-DNA in bacteria; i.e. the vector pPZP111 was modified as followed:

Since many *Agrobacterium* strains are known to show inducible resistance against the antibiotic chloramphenicol, we additionally introduced kanamycin as bacterial selection gene. Due to potential expression of transgenes the strong 35S CaMV promoter driving the plant selectable marker has been replaced by the weaker *nos* promoter. Thereby the *Nco*I restriction site was removed at that site but instead was newly introduced within a new inserted expression cassette consisting of an intron-containing *gus* gene and a strong constitutive promoter (35S promoter including enhancers). The resulting new vector 'pPZP3425' follows the designation for the original pPZP vectors, i.e. 'pPZP3xxx' indicates that the bacterial resistance is based on kanamycin and 'pPZPx4xx' refers to kanamycin being the plant selectable resistance that is newly driven by the *nos* promoter. Thus, our improved binary vector is applicable to basically two purposes. Firstly, for promoter:*gus* fusions the constitutive promoter can be replaced with any other promoter and secondly for specific (over)expression the *gus* can be replaced with any gene or sequence (e.g. micro RNA) of interest. The pPZP3425 is intensively used in our lab in several regards (and was already internationally requested as well). Achieving at least approx. ten transgenic plants in case of Arabidopsis transformation (via the *in planta* method using the *Agrobacterium* strain GV3101 after replication in *E. coli*) we believe that this new vector shows high capability in illuminating functional aspects of gene

expression in general, as for example during nematode-plant-interactions, and may finally also serve to engineer resistance plants.